A HANDBOOK ON

ELECTRICAL FILTERS

SYNTHESIS, DESIGN AND APPLICATIONS

WHITE ELECTROMAGNETICS, INC.

wei

A HANDBOOK ON ELECTRICAL FILTERS

By
White Electromagnetics, Inc.
670 Lofstrand Lane
Rockville, Maryland

Library Of Congress Catalog Card Number
63-23232

Printed in the United States of America

PREFACE

While electrical filters are presented in the literature from many points of view, no single comprehensive text yet exists despite the need. On the other hand, a comprehensive discussion of filters, especially if encompassing synthesis, design, physical realizability, and applications of both lumped-element and transmission line filters, would represent an horrendous undertaking. Thus, rather than attempt to embrace the entire subject here, it was decided to close a gap in an area where significant need exists; viz, provide useful and extensive filter design data which are easily understood by both engineers and technicians. To enhance the usefulness of this handbook, many illustrative examples are given on low-pass, high-pass, band-pass, and band-rejection filters.

Regarding the subject of the image-parameter method of filter design vs. modern network synthesis techniques, Chapter 3 is devoted to the former, and the remainder of the handbook emphasizes the latter. The classical image-parameter theory or Zobel filters are better known in their constant-k and m-derived form. This method of filter design is considered obsolete in many circles since it does not lend itself well to predicting or controlling the amplitude and phase characteristics of filters developed by this technique. Thus, nearly all the synthesis, design, and application techniques and data in this handbook stress modern network filters having Butterworth (maximally-flat) and Tchebycheff (equal-ripple) responses.

To satisfy the curious mind, it was believed that a design handbook of this type should also contain some pertinent derivations and analytical material. Therefore, Chapter 2 is devoted to the complex-frequency plane and network behavior, and some sections in Chapter 4 cover the subject of synthesis of the desired prototype transfer functions. Parts of other chapters are devoted to such derivations as time delay and insertion loss. Thus, this handbook will also be useful for other applications such as text or supplementary course reading material for undergraduate electrical or electronics engineering students. These sections are identified by footnotes in the table of contents and throughout the

text, and may be omitted by the technologist who is only interested in the design and realization of filters.

To further enhance the usefulness of this text, many suppliers and manufacturers of filter components were contacted. While it is impractical to use all of their data, representative component characteristics have been used together with acknowledgments where applicable.

In the original manuscript, both lumped-element (R's, L's, and C's) and distributed-element (coaxial, strip line, and waveguide) filters were covered. However, since the background and experience of both the engineer and technician are generally very different in terms of the two filter types and since the methods of physical realizability and fabrication are dramatically different, this handbook addresses itself to lumped-element filters. Thus, the emphasis here is on the design and physical realizability of passive LC filters from power frequencies of 30 cps to about 500 mc in the lower UHF band. Active filters (filters containing a tube or transistor), electro-mechanical resonators (rods, disks, reeds, magnetostrictive, quartz crystals and the like), and lattice networks are also reserved for the subject of another handbook in this series.

Since the principal objective of this handbook is to stress usefulness by providing many design charts, tables, graphs, and illustrative examples, only the test of time will prove the extent to which this objective has been successfully achieved. Thus, educators, engineers, and technicians who use this handbook are encouraged to write the authors and inform us of your experience. We shall be especially grateful to learn about your ideas of how we may improve this handbook prior to preparation of the second edition.

August 1963

The Authors
White Electromagnetics, Inc.
Rockville, Maryland

CONTENTS

ILLUSTRATIONS

TABLES

ILLUSTRATIVE EXAMPLES

CHAPTER 1

INTRODUCTION TO ELECTRICAL FILTERS

This chapter presents a brief survey of the more useful filter classes or types available to the design engineer throughout the frequency spectrum of eleven decades; viz, from about 1 cps to 100 gc (10,000 mc). This filter handbook covers lumped-element filters of the passive LC ladder type, which meet most of the filter needs below about 500 mc. To accommodate those whose interest in filters is beyond the LC ladder type, the references in this chapter have been expanded to identify many references on microwave filters, electromechanical resonators, active R-C, and acoustical filters.

It is recognized that a collection of many techniques does not necessarily permit an engineer or technician to gainfully capitalize upon them; especially since he may become confused by various alternatives or since he may not necessarily remember the circumstances or conditions under which certain techniques may be more fruitfully used than others. Therefore, a section of this chapter has been reserved for the subject of how to use this handbook best in achieving the reader's objectives.

1.1 A DEFINITION OF ELECTRICAL FILTERS

The term "electrical filters" is used here to mean devices which may be placed between the terminals of an electrical network, electronic circuit, black box, or equipment in order to emphasize, to deemphasize, or to control the frequency components of either a desired or undesired signal which would otherwise be present. The term "signal" is used here in both the communications and power engineering sense. Electrical filters surveyed in the following section include those devices which accept an electrical signal at their input terminals and deliver an electrical signal at their output terminals regardless of the internal physical means of achieving the filtering action. This admits the use of intervening electromechanical transducers in which the filter action may be achieved by mechanical, piezoelectric,

magnetostrictive, or acoustic means. While the handbook deals with passive LC filters only, a knowledge that these other types exist and a few of their principal properties are considered useful.

Filters are ordinarily classified as:

(1) *Low-pass filters* allow electrical energy having frequency components from dc up to a specified frequency (the cut-off frequency) to pass with no or little attenuation and allow electrical energy having frequencies beyond this to be rejected by at least 6 db per octave more attenuation.

(2) *High-pass filters* accept energy above the cut-off frequency, and substantially reject it below this frequency.

(3) *Band-pass filters* accept energy within a defined band or spectrum and significantly reject it outside of the band.

(4) *Band-rejection filters* reject electrical energy within a defined band and accept or pass it outside the band.

Fig. 1.1 illustrates the four classes of electrical filters and typical frequency responses.

Since nothing in real life performs perfectly, the notion of energy acceptance or rejection is one of degree only, and the filter "transition zone" between energy acceptance and rejection exists in the region of the cut-off frequency, as shown in Fig. 1.2. Thus, this degree of both energy acceptance and rejection, and the frequency rate of crossover are three of several properties which define the characteristics of filter performance.

The principal characteristics commonly used to specify the desired performance[1] of an electrical filter are (cf: Fig. 1.2):

(1) *Insertion Loss* is the ratio of the amplitude of the desired signal before filter insertion to that value at the filter output terminals after insertion. Ordinarily, it is desired that this value be held at a minimum, especially for filters whose main signal of interest carries significant power, since a substantial amount of heat dissipation or undesired loss may be involved. For many low-power communication filters, conducting main

[1]Performance characteristics such as cost, size and weight, and packaging form factors, all of which are important properties, are not discussed in this handbook, but are reserved for the topic of another text in this series.

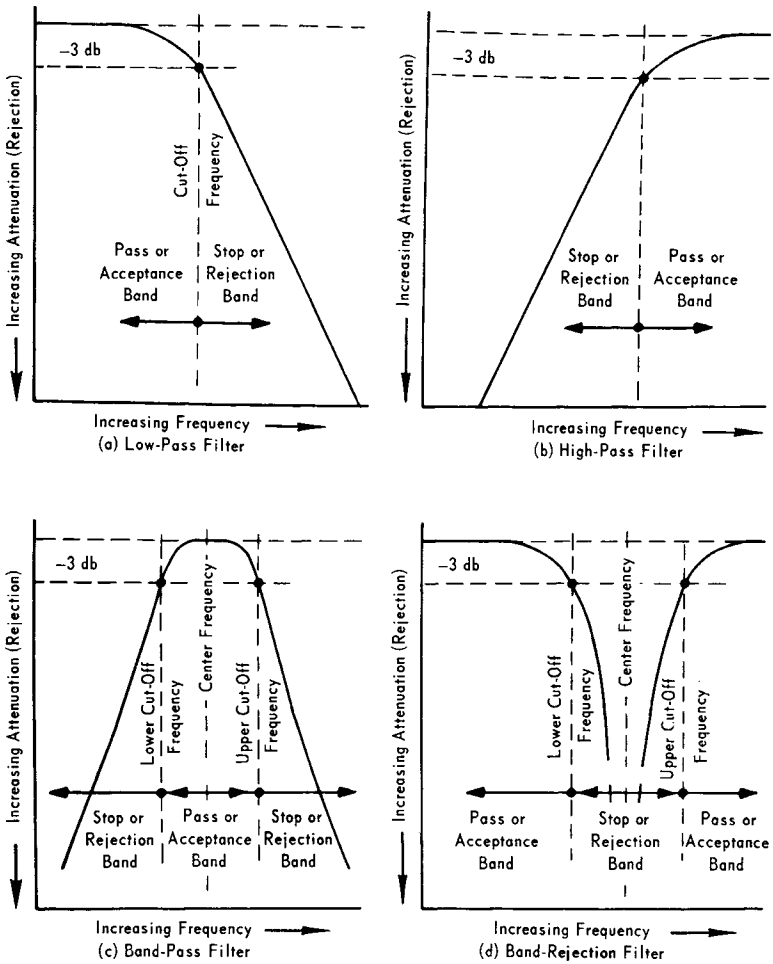

Figure 1.1. Typical Frequency Responses of the Four Filter Types

signal power of less than about one watt, an insertion loss of a decibel[1] or two is generally adequate. For filters passing high power in the acceptance band, such as those used for 60- or 400-cycle ac power mains, or radar or communications transmitters,

[1]See Appendix A for decibels vs. voltage and power ratios.

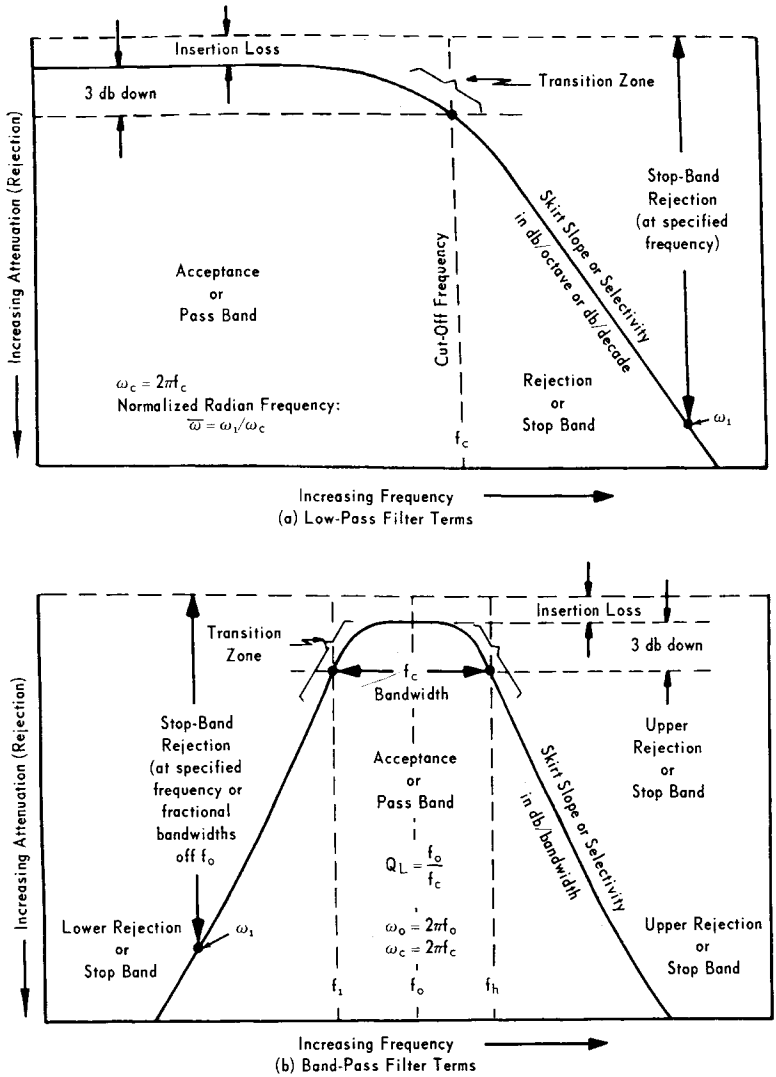

Figure 1.2. Terminology Used to Describe Filter Characteristics

it is often desired to keep insertion losses to about 0.1 db or less.

(2) *Stop-Band Rejection* is the ratio of the amplitude of unwanted frequency components before filter insertion to the

amplitude existing after filter insertion. This is the principal property of a filter in the sense that it is a measure of the extent to which it rejects unwanted energy. Typical values may range from a modest 20 db for certain harmonic-rejecting, high-power transmitter filters to more than 100 db for some preselector or tunable filters used to protect the front end of sensitive receivers. The degree of rejection will vary over the stop-band frequency and beyond some frequency the rejection may degrade or fail altogether; such as at VHF[1] where parasitic properties may cause a filter to degenerate into one having the opposite characteristics (see Chapter 6). Thus, a specification of the frequency band over which the minimum rejection must be maintained is of paramount importance.

(3) *Cut-Off Frequency* is the frequency between the signal acceptance and rejection bands corresponding to an attenuation of 3 db below the insertion loss. Although this characteristic is often specified by the application engineer who is designating a filter, it is sometimes better to allow the designer to choose the cut-off frequency (see Chapter 4) as long as the insertion loss and rejection bands are properly specified. The reason for this is that in the parameter trade-off design of filters, the choice of the type of frequency response and the number of stages affecting skirt selectivity in the transition zone allow an optimum exchange to be made in achieving or approaching the desired insertion loss and rejection.

(4) *Bandwidth* is the frequency acceptance window or band measured in cps, kc, or mc between the 3-db cut-off frequencies in a band-pass filter. Sometimes this is used in describing low-pass filters in which case it is the same as the band between zero frequency and the cut-off frequency or simply the cut-off frequency.

(5) *Q Factor* is the ratio of the center frequency to the bandwidth in describing band-pass filters. The center frequency is the geometric mean frequency between the 3-db cut-off frequencies and may be approximated by the arithmetic mean when the Q factor is higher than about 10; viz

$$Q = \frac{f_o}{f_c} = \frac{\sqrt{f_h f_L}}{f_h - f_L} \tag{1.1}$$

[1]VHF = very high frequency or 30 to 300 mc (10 to 1 meter wavelengths).

$$\approx \frac{(f_h + f_L)1/2}{f_h - f_L} = \frac{1}{2} + \frac{f_L}{f_c} = \frac{f_h}{f_c} - \frac{1}{2} \text{ for } Q \geq 10 \qquad (1.2)$$

where, f_o = the band-pass filter center frequency

f_c = the 3-db filter bandwidth (see Fig. 1.1)

f_h = the upper 3-db cut-off frequency.

f_L = the lower 3-db cut-off frequency.

The term Q-factor, used in specifying band-pass filters, is in reality the loaded Q-factor, Q_L, and is loaded in the sense that driving and terminating impedance loads are connected to the filter when inserted in a network. This is to be distinguished from the term unloaded Q-factor, Q_u, which is a measure of the performance of the components which are used in fabricating the filter (see Sec. 1.2 and Chap. 6). Thus, the ratio Q_L/Q_u becomes a measure of the expected insertion loss of the filter and degradation of the skirt slope or selectivity achievable in the 3-db transition zone. The unloaded Q-factor is not needed in specifying filter characteristics since the term is implicit in the other characteristics. However, Q_u is very important in specifying filter components by the filter design engineer.

(6) *Shape Factor* for band-pass filters is the ratio of the bandwidth at the 60-db points below insertion loss to the bandwidth at the 6-db points below insertion loss; viz,

$$\text{Shape Factor} = \frac{f_{60db}}{f_{6db}} \text{ (Conventional definition).} \qquad (1.3)$$

Unfortunately, the 6-db bandwidth is not often specified in contrast to the 3-db bandwidth. Thus, this paradox suggests that the shape factor definition should be changed to the more useful definition; viz,

$$\text{Suggested definition of Shape Factor} = \frac{f_{60db}}{f_{3db}} = \frac{f_{60db}}{f_c}. \qquad (1.4)$$

If the definition for Shape Factor in Eq. (1.4) is used, it should be accompanied by an explanation. It would appear that no new information exists in either of the definitions of the Shape Factor; i.e., why reference the skirt slope in terms of the 60-db bandwidth?

Yet, convention has made this term useful on occasion especially where specification of intermediate-frequency amplifier filters are concerned. The authors discourage the use of the shape factor term altogether and encourage, instead, the use of the terms "stop-band rejection" and "bandwidth" in its place.

(7) *Impedance Level* is the value, specified in ohms, of both the filter source (driving or input) impedance and the terminating (load or output) impedance. Generally, the input and output impedance levels specified are the same, especially for communication filters where 50-, 73-, and 300-ohm transmission lines are frequently used. On the other hand, power filters, especially those used in 60- and 400-cps generator lines to reject harmonics, rarely have equal input and output impedances since the internal voltage drop at the generator should be small. Also where filters are driven or terminated by an electron tube or transistor, the input and output impedances generally differ.

(8) *Power Handling Capacity* is the rated average power in watts beyond which the performance of the filter may degrade or fail altogether due to burn out. Occasionally, peak power is used to specify power handling capacity, especially where a breakdown of components or a gas inside a hollow transmission line is involved. This specification generally becomes important for filters handling more than about one watt.

1.2 A BRIEF SURVEY OF FILTERS

This section summarizes the different filter types available to the design engineer over the broad spectrum from 1 cps to 100 gc. The principal parameters used in this survey are frequency range, Q-factors, and methods of physical realization such as passive LC, mechanical resonators, microwave, and the like. See Fig. 1.3.

1.2.1 Lumped Elements, Electrical

Lumped-element electrical filters, consisting of inductors and capacitors, are usable from dc up to approximately 500 mc. Parasitic capacitance and lead length inductance make higher frequency applications impractical since the component performance behaves very differently and often unpredictably. Below about 100 cps, inductance and capacitance values of tuned circuits

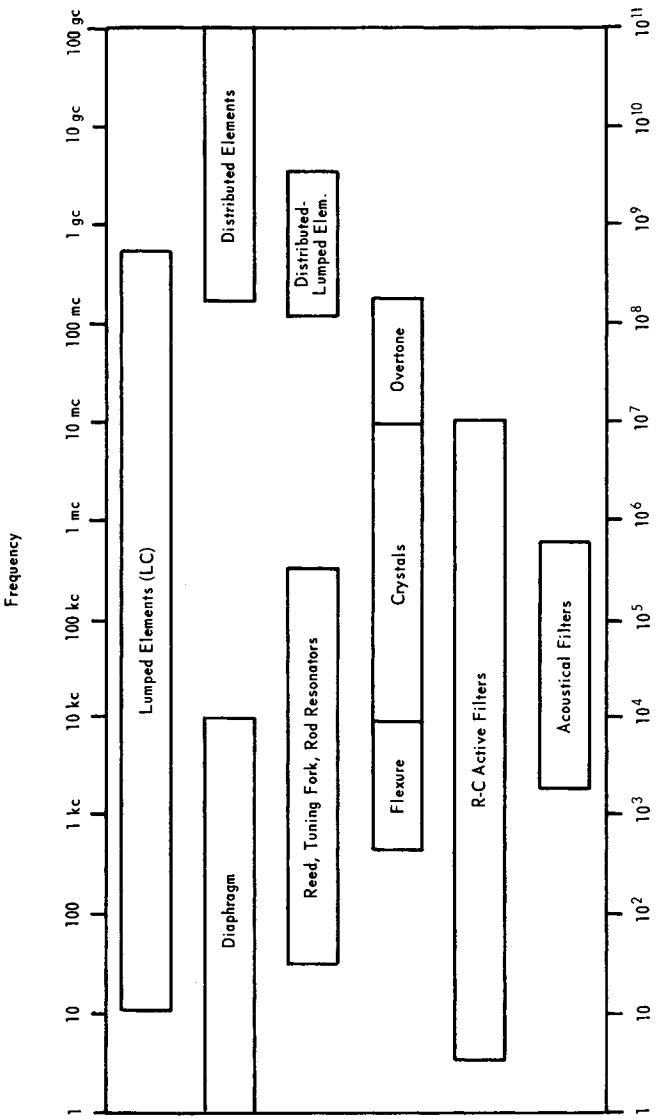

Figure 1.3. Filter Types vs. Operational Frequency Spectrum

become so large that they render impractical most packaging problems except where size and weight are less important.

Substantial progress, however, has been made in the past decade in the development of ferrite materials used in inductors and dielectrics used in capacitors. This permits realizing inductor, Q_u factors of the order of 300 at low frequencies and in comparatively small physical sizes, generally of the toroidal shape. Capacitor Q_u factors are significantly higher than their inductor counterparts with a ratio of capacitor to inductor Q_u factors of five to ten being typical. Cryogenic techniques or supercooling can be used in some situations to significantly reduce the dissipative resistance losses and hence improve the Q_u factors.

1.2.2 Distributed Elements, Electrical

Distributed-element or transmission-line filters are useful from about 200 mc to 100 gc or higher. The filters in these lines contain a wide variety of types such as open and shorted sections of branch transmission lines, tuned irises and posts in waveguides or coaxial lines, re-entrant cavities, ring filters, and direct and quarter-wave coupled chambers. Slow-wave structures such as helical and serrated lines used in traveling-wave tubes provide additional design flexibility. Gyromagnetic resonance and gaseous absorption effects are sometimes used to realize certain filter characteristics. Additionally, mode generators and suppressors are useful to respectively transfer energy to a waveguide or coaxial mode providing better filtering properties or to eliminate undesired energy in certain modes.

Hollow pipe and ridge waveguide, coaxial and strip line, and open dual-conductor lines are the more common transmission media. Their sizes may vary in cross section from as big as 200 square inches in P-band (300 mc) waveguide to perhaps 0.05 square inches for X-band strip line or 0.01 square inches for 70 gc waveguides. Unloaded Q_u factors in the order of 30,000 are obtainable with L-band (1 gc) waveguide; Q_u reduces to about 8,000 at X-band (10 gc). Coaxial or air-dielectric strip lines of about one square inch in cross section will have Q_u factors of about 600 at 100 mc and 1500 at L-band.

1.2.3 Hybrid Lumped-Distributed Elements

Lumped-distributed element filters are regarded as hybrid types employing the advantages of both lumped and distributed

elements particularly in the "awkward frequency spectrum" between about 100 mc and 1 gc. In this range, lumped-element parasitics become objectionable and the wavelength is comparatively long. Hollow waveguide pipes, operated well beyond cutoff frequency, for example, may use magnetic coupling between a series of axially-supported, resonant metallic loops. Another hybrid version uses stub-supported transmission lines to realize the equivalent of individual LC elements in a filter in which the remaining elements are of the lumped type. A third hybrid may use lumped capacitors in a coaxial or strip line as the series interface elements of direct-coupled chambers.

1.2.4 R-C Active Filters

R-C active filters, originally prompted by the large physical size limitations imposed by inductors in designing filter networks below about 100 cycles, are widely used. With increasingly stringent requirements for microminiaturization, R-C transistor network filters are currently used from a few cycles up to about 1 mc. As a feedback four-pole network, transistors with bridge R-C networks, such as parallel or twin-tee circuits, provide moderate Q factors of the order of 100. Employed as negative-impedance converters, sometimes called Q multipliers, in a two-pole network, controllable Q factors as high as 10,000 are obtainable.

1.2.5 Mechanical Resonators

Mechanical resonators suitable for filter construction and use appear in many shapes and forms. They may be used over the frequency spectrum from a fraction of a cycle to approximately 200 mc. Diaphragm resonators are useful at the lowest frequencies; i.e., below 1 cps to about 1 kc. Resonators in the form of vibrating reeds, tuning forks, or bender type crystals afford high Q factors of 100 to 10,000 and a frequency coverage from approximately 30 cps to 20 kc. From a few hundred cycles to about 300 kc, rod-type longitudinal resonators are used; they reduce to the form of plates at the higher frequencies. The plate structure exists primarily in quartz crystals which are used from about 10 kc to 10 mc (up to 200 mc on overtones). Q factors in the order of several thousand are realizable (as previously mentioned, crystals are frequently used with LC elements to obtain high

loaded Q factors because of the practical upper limit on the Q factors of inductance).

Mechanical filters cover the frequency spectrum from approximately 50 to 500 kc and exist in three major forms employing rod, disk, and plate type resonators. Loaded Q factors of 1000 are realizable.

Other than the crystal filter, all mechanical resonators discussed above require electromechanical transducers, such as magnetostrictive or quartz devices, for electrical applications. Apart from certain advantages, one significant penalty here is that the resulting insertion losses of the order of 10 to 30 db are typical.

1.2.6 Acoustical Networks

Acoustical networks with electromechanical transducers such as quartz crystals, have been used principally as delay lines for MTI radar, sonar, and circulating volatile computer memory devices. For other than electronic filter and delay line applications, acoustical lines appear to have received little use. By applying wave propagation phenomena, as used in the design of microwave distributed-element filters, to acoustical filter design (where respective wavelengths are comparable), the latter type filter will be useful from approximately a few kc to about 1 mc.

1.3 HOW TO USE THIS HANDBOOK

This handbook covers a broad range of filter subjects from techniques of network synthesis to the application and testing of filters. It follows, then, that the different chapters in this handbook would not be of equal interest to most engineers; viz, some will be more interested in the academic aspects while others will be more concerned about the practical problems of design and physical realization. With the exception of Chap. 2 on "The Frequency Plane and Network Behavior," the theoretical and practical aspects of electrical LC filters are treated sequentially in each section under the chapters in which they appear. Thus, at the end of each theoretical development, useful graphs, charts, tables, and the like are presented so that engineers and technicians who are interested only in applications, design, fabrication, tuning and/or performance measurements can identify their sections of interest.

One of the quickest ways to find a subject of interest in a handbook or text is through the use of the index. To make it especially useful and fast in finding the desired subject, the index has several redundant entries under different headings. Thus, because of the comprehensiveness of the index, the table of contents is broken down into chapter sections only. The list of figures and tables, located on Page vii has been prepared for those individuals who prefer this route of identifying the desired material. If there develops any question on the use of symbols, which may result when the user enters the handbook in the middle of a chapter or section and after symbols have been previously defined, a glossary of symbols is summarized on Page 245. Finally, the appendices have been provided for those engineers and technicians who are interested in referring to such general information as the voltage and power ratio to db conversion chart and the names and suppliers of filter components.

The following flow diagram has been prepared to lead the filter engineer to some of the appropriate information, design charts, and figures in the handbook. The use of this diagram in certain ways permits even greater flexibility than that offered by the index in rapidly getting to the information sought. Thus, the user begins at the "start" circle in Fig. 1.4 and answers the questions posed until a branch point is reached which ends in the identification of the desired material. The exception to this is in the answer to the first question which involves design; viz, turning to Page 13 or the next flow diagram, Fig. 1.5, on the following page.

Regarding the topic of how to design filters, there are so many facts that a generalization, such as depicted in Fig. 1.5, may not be the best approach for certain situations. A complete flow diagram, on the other hand, would be so comprehensive that it would become hard to use. Nevertheless, certain general procedures may be followed. The first step involves identifying which of the four filter types are to be designed (block 1, Fig. 1.5). Fortunately, modern network synthesis makes it possible to translate low-pass, high-pass (block 2), band-pass (block 3), and band-rejection (block 4) into the common denominator of a low-pass prototype or response.

Since most useful low-pass prototype responses are of the Butterworth (maximally-flat) or Tchebycheff (equal-ripple) type, a distinction of which to use in the design is required next. To

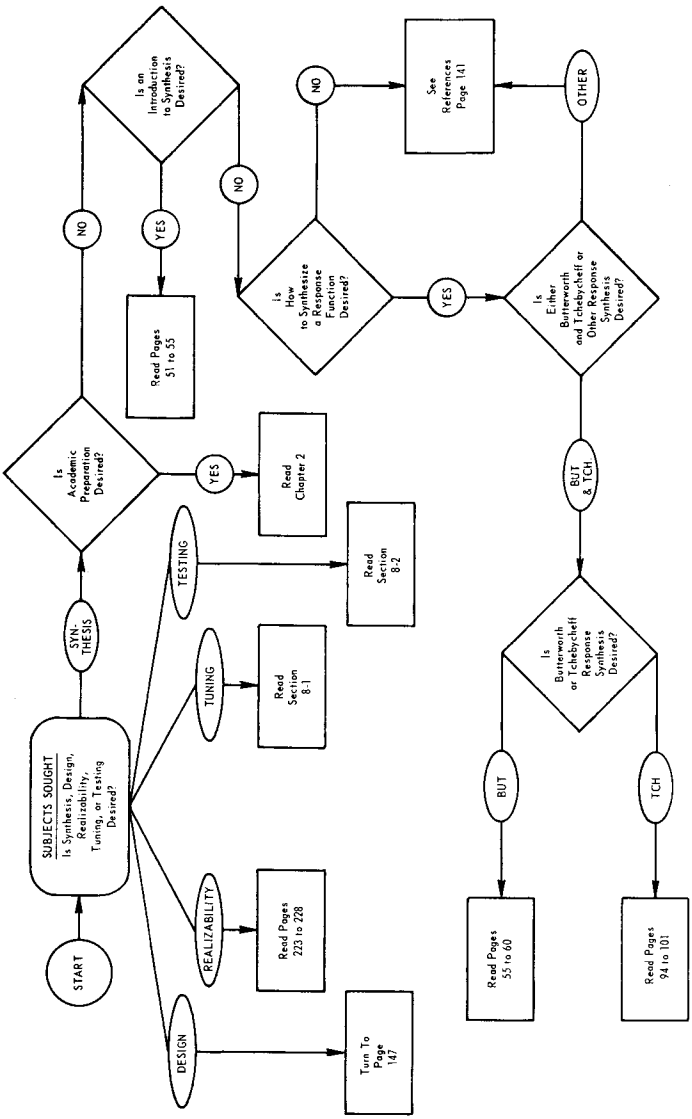

Figure 1.4. Flow Diagram on "How to Use This Filter Handbook"

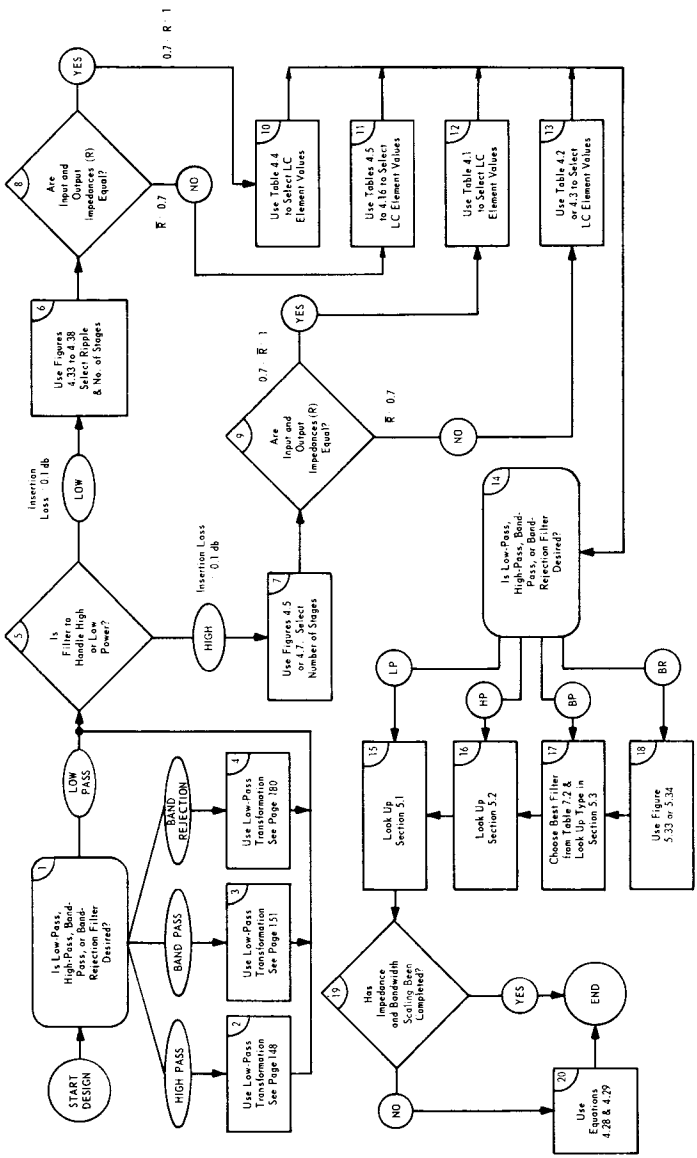

Figure 1.5. Flow Diagram of How to Design Filters With This Handbook (See Text for explanations and exceptions)

simplify the decision, these two responses are identified with high power (lower insertion loss associated with a Butterworth response) and low power (higher allowable insertion loss associated with a Tchebycheff response) respectively (diamond 5, Fig. 1.5). Again, such a decision basis is certainly not the only criterion nor necessarily a sound one, but for most applications it is a reasonable one. Blocks 6 and 7 steer the reader to the respective response design tables in the handbook where he can determine the required number of filter stages.

The next decision is based on whether or not the driving and terminating impedances are approximately equal (diamonds 8 and 9). Blocks 10 to 13 guide the designer to the respective low-pass filter prototype LC element values corresponding to the response type and number of filter stages. Finally, the element values of the desired filter are used in a low-pass type or are modified; i.e., they are translated back to values corresponding to a high-pass, band-pass, or band-rejection if the desired filter is one of these three types (block 14). Thus, blocks 15 to 18 guide the reader to the proper filter configuration.

Since the final LC element values of some of the filter configurations (emphasis low-pass filters) are given in terms of a one-ohm impedance and a one-radian per sec bandwidth, impedance and bandwidth scaling may be required (diamond 19). Where this is required, block 20 directs the designer to the appropriate rules.

Again, there are several other considerations which should be checked in the design of filters, but Fig. 1.5 provides a reasonable general approach. As the corresponding sections of this handbook become more familiar to the filter designer, these other considerations will become firmly implanted in his mind.

1.4 REFERENCES

1. Bechmann, R., "Quartz AT-Type Filter Crystals for the Frequency Range 0.7 to 60 Mc," *Proc. of the IRE,* Vol. 49, No. 2, pp. 523–524, February 1961.
2. Bechman, R., "High Frequency Quartz Filter Crystals," *Proc. of the IRE,* Vol. 46, No. 3, pp. 617–618, March 1958.
3. Bower, J. L. and Ardung, P. F., "The Synthesis of Resistor-Capacitor Networks," *Proc. of the IRE,* Vol. 38, pp. 263–269, March 1960.
4. Bower, J. L., "R-C Band-Pass Filter Design," *Electronics 20,* pp. 131–133, April 1947.
5. Brown, J. S. and Theyer, W., Jr., "High-Q Low-Frequency Resonant Filters," *Proc. Nat'l Electronics Conf.,* Vol. 7, 1951.
6. Burns, L. L., Jr., "A Band-Pass Mechanical Filter for 100 kc," *RCA Review,* No. 1, pp. 31–46, March 1952.
7. Chi Lung Kang, "Circuit Effects on Q," *The Boonton Radio Corp., Notebook,* No. 8, Winter 1956.
8. Cohn, S. B., "Microwave Filter Design for Interference Suppression," *Proceedings of the Symposium Electromagnetic Interference,* Asbury Park, N. J., June 1958.
9. Cohn, S. B., "Direct-Coupled-Resonator Filters," *Proc. IRE, 45, 2,* pp. 187–196, February, 1957.
10. Cowles, L. G., "The Parallel-T, R-C Networks," *Proc. IRE,* 40, pp. 1712–1717, December 1952.
11. Curran, D. R. and Gerber, W. J., "Piezoelectric Ceramic IF Filters, *Proc. 1959 Electronic Components Conference.*
12. DeWitz, G. H., "Consideration of Mechanical and LC Type Filters," *Trans. IRE,* Vol. CS-4, No. 2, Comms. System, May 1956.
13. Dishal, M., "Modern-Network-Theory Design of Crystal Filter for Communications & Navigation," (Federal Telecommunication Labs., Inc.), *Aeronautical Electronics Digest,* pp. 381–382, 1955.
14. Ergul, "Miniaturized High-Efficiency R-F Filters," AD-43261, ASTIA Tab. U-79, p. 29.

15. Falkow, A.D. and Gerst, I., "RLC Lattice Transfer Functions," *Proc. of the IRE*, pp. 462–469, April 1955.

16. Farkas, F.F., Hollenbeck, F.J., and Stenhlik, F.E., "Bandpass Filters, Band Elimination Filter and Phase Simulating Network for Carrier Program," *The Bell Systems Technical Journal*, p. 176, April 1949.

17. Fano, R.M. and Lawson, A.W., "The Theory of Microwave Filters," *Radiation Laboratory Series*, Chapter 9, Vol. 9, Microwave Transmission Circuits, McGraw-Hill Book Company, Inc., 1948.

18. George, S.F. and Zamanakos, A.S., "Comb Filters for Pulsed Radar Use," *Proc. IRE*, pp. 1159–1165, July 1954.

19. Geza, Zelinger, "Tunable Audio Filters," *Electronics*, pp. 173–175, November 1954.

20. Gitzendanner, Louis G., "Resistance and Capacitance Twin-T Filter Analysis," *Tele-Tech.*, pp. 46–48, February and April 1951.

21. Guillemin, E.A., "Communication Networks," Vol. 1 & 2, John Wiley & Sons, Inc., New York, 1935.

22. Hastings, A.E., "Analysis of a R-C Parallel-T Network and Application," *Proc. IRE*, 34, pp. 126–129, March 1946.

23. Jensen, G.K. and McGeogh, "An Active Filter," *NRL Report 4630*, Library of Congress PB111787, November 10, 1955.

24. Karakash, J.J., "Transmission Lines and Filter Networks," The MacMillan Co., N.Y., 1950.

25. Lawson, A.W. and Fano, R.M., "The Design of Microwave Filters," Chapter 10, Vol. 9, *Radiation Laboratory Series*, McGraw-Hill Book Co., New York, 1948.

26. Levy, M., "The Impulse Response of Electrical Networks with Special Reference to Use of Artificial Lines in Network Design," *Jour. IEE*, Vol. 90, Part III, pp. 153–164, December 1943.

27. Linvill, J.G., "A New RC Filter Employing Active Elements," *Proc. Nat'l Electronics Conf.*, Vol. IX, p. 342, 1953.

28. Longmire, C.L., "An RC Circuit Giving Over Unity-Gain," *Tele-Tech*, Vol. 6, pp. 40–41, April 1947.

29. Lungo, A. and Sauerland, F., "A Ceramic Band-Pass Transformer and Filter Element," *Proc. of the IRE National Convention Record,* 1961.

30. Lungo, A., "Ceramic Filters Aid Miniaturization," *Electronic Industries,* November 1959.

31. Mason, W. P., "Resistance Compensated Band-Pass Filters for Use in Unbalanced Circuits," *Bell Systems Technical Journal,* 16.4, 423, October 1937.

32. McCaughan, H. S., "Variation of an R-C Parallel-T Null Network," *Tele-Tech,* pp. 48–51, and 95, August 1947.

33. Met, V., "Absorptive Filters for Microwave Harmonic Power," *Proc. IRE,* Vol. 47, No. 10, pp. 1762–1769, October 1959.

34. "Microwave Engineers' Handbook;" Filter Design, pp. T-85–T-100, 1963.

35. "Microwave Engineers' Handbook;" Filters, Cavities, pp. TD-72–TD-84, 1961–1962.

36. Mingens, C. R., Frost, A. D., Howard, L. A., and Perry, R. W., "An Investigation of the Characteristics of Electromechanical Filters," Contr. No. DA36-039-sc-5402, February 1, 1951 through February 10, 1954.

37. Oono, Yoriro, "Design of Parallel-T Resistance-Capacitance Networks," *Proc. of the IRE,* pp. 617–619, May 1955.

38. Peterson, Arnold, "Continuously Adjustable Low and High-Pass Filters for Audio Frequencies, *Proc. Nat'l Electronics Conf.,* Vol. 5, p. 550, 1949.

39, Reza, F. M. and Lewis, P. M., III, "A Note on the Transfer Voltage Ratio of Passive RLC Networks," *Elect. Engr. Abstracts,* Vol. 58, No. 687, p. 163, March 1955, No. 1143.

40. Roberts, W. V. B. and Burns, L. L., Jr., "Mechanical Filters for Radio Frequency, *RCA Review,* No. 3, pp. 348–365, September 1949.

41. Sauerland, F. L., "Transient Response of Ceramic Filters," *Electronic Industries,* Vol. 22, No. 1, pp. 106–110, January 1963.

42. Sauerland, F. L., "Ceramic Band-Pass Filter with Unsymmetric-Tuned Hybrid Lattice Structure," *Proc. National Electronic Conference,* October 1961.

43. Savant, C. J., Jr., "Designing Notch Networks," *Electronics Buyers' Guide,* Twin-T Networks, Mid-Month, p. R-14, June 1955.

44. Shea, T. E., "Transmission Networks and Wave Filters," D. Van Nostrand Company, Inc., New York, 1957.

45. Shumard, C. C., "Design of High-Pass, Low-Pass and Band-Pass Filters using R-C Networks and Direct-Current Amplifiers with Feedback," *RCA Review,* p. 534, Vol. XI, December 1950, No. 4.

46. Southworth, G. C., "Principles and Applications of Waveguide Transmission," D. Van Nostrand Company, Inc., New York, 1950.

47. Stanton, L., "Theory and Application of Parallel-T, T-C Frequency-Selective Networks," *Proc. IRE,* 34, pp. 447–457, July 1946.

48. Storch, L., et al, "Crystal Filter Design from the Perspective of the Filter Design Literature," *Trans. IRE on Circuit Theory,* Vol. CT-7, No. 1, p. 67, March 1960.

49. Sykes, R. A., "A New Approach to the Design of HF Crystal Filters," *1958 IRE National Convention Record.*

50. Tuttle, W. N., "Bridged-T & Parallel-T Null Circuits for Measurements at Radio Frequencies," *Proc. IRE,* Vol. 28, pp. 23–29, 1940.

51. Urkowitz, H., "Filters for Detection of Small Radar Signals in Clutter," *Jour. Appl. Phys.,* Vol. 24, pp. 1024–1031, August 1953.

52. Vergara, Wm. C., "Design Procedure for Crystal Lattice Filters," *Tele-Tech,* pp. 86–87, September 1953

53. Weinberg, L., "New Synthesis Procedure for Realizing Transfer Functions of RLC and RC Networks," *Technical Report No. 201, MIT,* 1951.

54. White, Charles F., "Synthesis of RC Shunted High-Pass Networks," *Proc. Nat'l Electronics Conf.,* Vol. IX, 1953, p. 711.

55. White Electromagnetics, Inc., "RF Delay Line Filters," Final Report under NOLC Contract No. N123(62738)-29779A, June 30, 1962.

56. Wyndrum, R. W., "Distributed RC Notch Networks," *Proc. of the IEEE,* Vol. 51, No. 2, pp. 374, February 1963.

CHAPTER 2[1]

THE FREQUENCY PLANE AND NETWORK BEHAVIOR

This chapter discusses: (1) the "s-plane" or complex-frequency plane; (2) the manifestation and behavior of networks by the s-plane location of their characteristic zeros (roots of the numerator) and their poles (roots of the denominator); (3) the Laplace transform as a tool for going from the time-domain of an excitation function to the frequency domain (spectral characteristics and frequency response of networks to signals) and back to the time domain (steady-state and transient network response); and (4) some applications to RLC networks. This chapter then establishes most of the required background for an orderly treatment of the synthesis of filter networks presented in Chap. 4 and the deviation of band-pass prototypes discussed in Chap. 5.

2.1 THE COMPLEX-FREQUENCY PLANE

The following definitions involving the terms "frequency" and "impedance" are established.

(1) A voltage of peak amplitude, E, and frequency, f, is written as Ee^{st}, where e is the phasor of unit length, $s = j\omega = j2\pi f$, and t is time. Physically, this expression is interpreted by using only its real part, R_e:

$$R_e\,(Ee^{st}) = R_e\,(E\cos\omega t + jE\sin\omega t) = E\cos\omega t. \quad (2.1)$$

If E is a complex variable, it then amounts to a shift in the phase of the physical voltage as is readily seen by forming the real component of $(E_1 + jE_2)e^{st}$.

(2) The current in any loop is the quantity which satisfies the differential equations of the circuit having the voltage Ee^{st} as the driving source. The current appears in the form Ie^{st},

[1]This chapter may be omitted by the technologist who is only interested in design and realization of filters.

where I is another complex value. The physical voltage is the real component of this expression. For brevity, the constants E and I alone are sometimes called "voltage" and "current."

(3) Either the self- or transfer-impedance, depending upon whether the current and voltage are in the same or different loops respectively, is defined as the ratio, E/I, of the constants in the voltage and current expressions of definitions (1) and (2).

(4) The impedance is an algebraic quantity obtained from the solution of the set of linear equations which result when the differential operator, d/dt, or integral operator, $\int dt$, is replaced by s or 1/s respectively.

The definition of frequency and impedance presented above assumes that the driving source (input signal or excitation function) is a simple sine wave. The frequency, f, is then a real quantity and the new variable, $s = j2\pi f$, is a pure imaginary quantity. The definitions, however, can be extended to situations in which both f and s are complex variables. The physical meaning of this is easily determined. Suppose, for example, that Ee^{st} is an excitation voltage in which E and s are $E_1 + jE_2$ and $\sigma + j\omega$ respectively. The voltage can then be written as:

$$\begin{aligned} Ee^{st} &= (E_1 + jE_2)e^{(\sigma + j\omega)t} \\ &= (E_1 \cos \omega t - E_2 \sin \omega t)e^{\sigma t} + j(E_1 \sin \omega t + E_2 \cos \omega t)e^{\sigma t}. \end{aligned} \tag{2.2}$$

By the definitions established above, the physical voltage is the real component of Eq. (2.2), namely, $(E \cos \omega t - E \sin \omega t)e^{\sigma t}$ It is a sinusoidal oscillation having either positive gain or negative damping with time depending upon whether the real exponent, σ, is positive or negative. The physical current corresponding to this voltage is obtained by dividing the complex voltage by the impedance and taking the real component of the result. It is a damped sinusoid with the same frequency and damping as the driving voltage.

Frequency is considered hereafter as a complex quantity, $s = \sigma + j\omega$; $s = j\omega$ corresponds to a special case in which $\sigma = 0$, or the so-called steady-state condition with no damping. This can conveniently be represented on a complex-frequency plane such as that shown in Fig. 2.1. The horizontal axis represents real values of s, namely σ, in which positive values of

σ correspond to a function exponentially increasing in amplitude with time and negative values of σ correspond to a function exponentially decreasing in value with time. As discussed subsequently, there is a close connection between the steady-state response characteristics of a network and its transient characteristics (situations in which $\sigma = 0$). Since a network whose

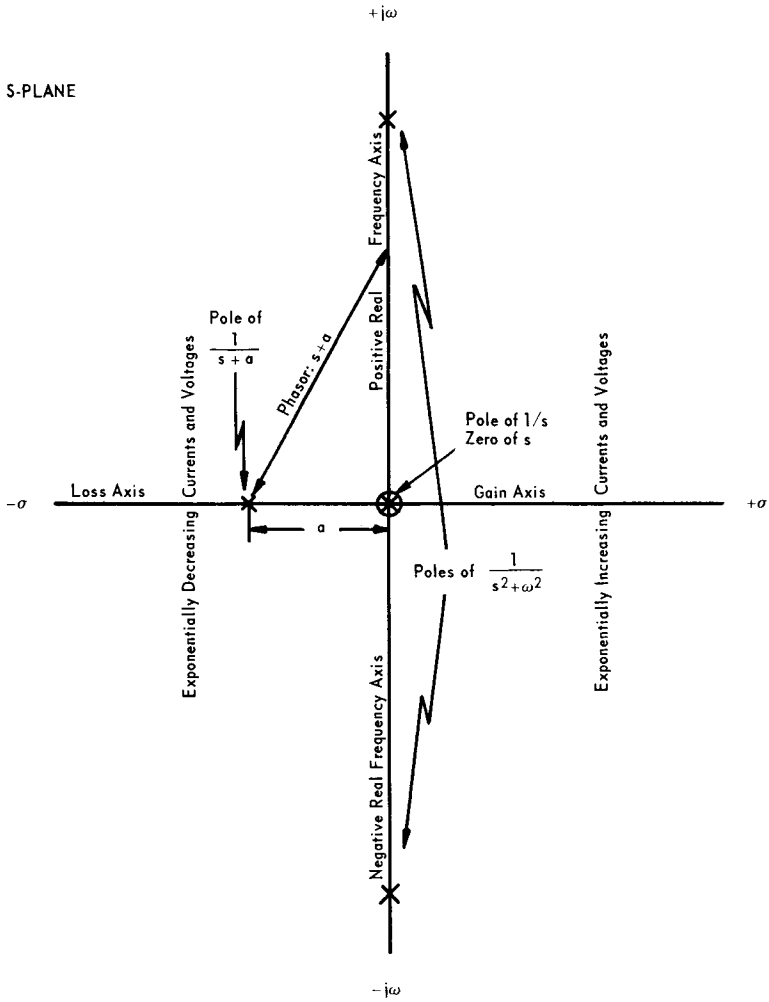

Figure 2.1. The Complex-Frequency Plane (S-PLANE)

transients increase in time is unstable, i.e., is nonphysical, the characteristics of physical networks in the right-half plane corresponding to exponentially increasing functions are severely limited.

The vertical axis of Fig. 2.1 represents imaginary values of s, namely $j\omega$, or real values of frequency. The upper half plane corresponds to the treatment of positive real frequencies. The lower half of the plane, in which negative values of frequency are found, is seldom of significant concern in network synthesis although it is used in the development of desirable filter networks. Its main advantage is in simplifying the associated mathematics.

In any physical circuit, the real component of impedance is an even function of frequency, and the imaginary component is an odd function. In other words, the real component of impedance at a negative frequency is the same as the corresponding positive frequency, while the imaginary component at a negative frequency is the negative of the imaginary component at the corresponding positive frequency. Thus, simple relations of symmetry connect the upper and lower halves of the s-plane.

2.2 ZEROS AND POLES OF IMPEDANCE AND ADMITTANCE

The functions whose behavior in the complex-frequency plane are of principal interest are the driving-point or input impedance (ratio of input voltage to input current), Z_{11}; the transfer impedance (ratio of output voltage to input current), Z_{12}; and the corresponding admittances, Y_{11} and Y_{12}. If the resistance termination or load in the output network equals one ohm, the output current and voltage are equal and a transfer function is defined: $Z_T = E_o/E_i$.

Each of the above impedances, admittances, and transfer functions is expressed in terms of determinants whose elements are relatively simple functions of frequency. In a loop analysis, for example, the general impedance coefficient of an RLC circuit is written as: $Z_{mn} = E_m/I_n = sL_{mn} + R_{mn} + 1/sC_{mn} = (s^2L_{mn} + sR_{mn} + 1/C_{mn})/s$. Since any of the determinants used in the definition of Z_{11} and Z_{12} can be expressed as the sum of products of this type, the cleared fraction expression must be polynominals in s divided by some power of s. The same result, of course, holds for determinants based on a nodal analysis.

The individual functions, Z_{11}, Z_{12}, Y_{11}, and Y_{12} are each expressed as the ratio of two determinants. It follows, therefore, that they must each appear, in general, as the ratio of two polynominals; viz,

$$H = \frac{N_m s^m + N_{m-1} s^{m-1} + \ldots + N_1 s + N_o}{D_n s^n + D_{n-1} s^{n-1} + \ldots + D_1 s + D_o}. \tag{2.3}$$

Such an expression is called a rational function of s.

In studying the behavior of a function described by Eq. (2.3), special attention is directed to its "zeros" and "poles," which are respectively the points located in the s-plane at which the function becomes zero and infinite. This is easily expressed by rewriting both numerator and denominator of Eq. (2.3) as a product of factors; viz,

$$H = \frac{N_m(s - s_{z_1})(s - s_{z_2}) \ldots (s - s_{zm})}{D_n(s - s_{p_1})(s - s_{p_2}) \ldots (s - s_{pn})} \tag{2.4}$$

where, $s_{z_1} \ldots s_{zm}$ are the zeros, and $s_{p_1} \ldots s_{pn}$ are the poles. Ordinarily, the s_z's and s_p's will all be different, so that the zeros and poles are all of the first order, or "simple." In special cases, however, two or more zeros or poles may coincide to give a multiple zero or pole. In filter networks, zeros and poles are the analogs of resonances and anti-resonances which are familiar in purely reactive circuits. By contrast, the principal difference in a general network is the fact that most resonances and anti-resonances occur at complex frequencies due to finite loss or dissipation (negative σ) in the network. This subject is discussed further in Chap. 4 under the subject of uniform dissipation and Chap. 6 under the heading of insertion loss and Q factors.

Zeros and poles are important for two reasons. The first is that, except for the constant multiplier N_m/D_n, they uniquely specify Eq. (2.4). Assuming, then, that H represents a driving-point impedance or admittance, it is concluded that two driving-point impedances or admittances having the same zeros and poles differ only by an ideal transformer. Similarly, if H is a transfer impedance or admittance having the same zeros and poles, they can differ only by a constant gain or loss.

The location of zeros and poles in the s-plane is of especial value in filter synthesis since it provides a powerful design tool as discussed in Chap. 4. Additionally, unless zeros and poles

meet certain restrictions, the impedance functions which they specify cannot be physically realized by a network.

2.3 THE LAPLACE TRANSFORM

Transformations of a wide variety of types exist in engineering. Perhaps the most familiar is the simple logarithm and inverse logarithm in which exponentials in the real number domain carry over to the operation of mutiplication and division in the logarithm domain. After suitable computations are carried out, the answer is obtained by the inverse logarithm. Table 2.1 illustrates this for the solution of $(17.5)^{2.2}$

Table 2.1
REAL NUMBER/LOGARITHM TRANSFORMS

Real Number		Logarithm
17.5	⟶	1.243
exp (2.2)	⟶	$2.2 \times 1.243 = 2.74$
550	⟵	Antilog (2.74)

Laplace transformations are convenient mathematical tools which are used for the solution of integro-differential equations that describe the behavior of RLC networks. To be useful, transforms, of course, must significantly simplify the mathematics in both extent and depth of complexity. The Laplace transform, per se, carries the more difficult operation of differentiation and integration from the time domain into multiplication and division respectively in the frequency domain. Computations are then executed in the frequency domain and the final answer is again transferred back to the time domain through inverse Laplace transformations. Table 2.2 represents the more frequently used Laplace transform pairs in which f(t) corresponds to the time domain and F(s) corresponds to the frequency domain.

A unit step function, whose value is zero up to time equal zero, but then jumps to a value of one thereafter, is defined as u(t). As indicated in the third entry in Table 2.2, the Laplace transform of the unit step function is $1/s$. In terms of real frequency then, the value of $1/s$ may be replaced by $1/j\omega = 1/j2\pi f$. This says that the spectral amplitude distribution of a step

Table 2.2
ELEMENTARY TRANSFORM PAIRS

Time Domain		Frequency Domain
$f(t)$	$\longleftrightarrow$	$F(s)$
$\frac{d}{dt}$	(1)	s
$\int dt$	(2)	$\frac{1}{s}$
1 or $u(t)$	(3)	$\frac{1}{s}$
e^{-at}	(4)	$\frac{1}{s+a}$
$\sin \omega t$	(5)	$\frac{\omega}{s^2+\omega^2}$
$\cos \omega t$	(6)	$\frac{s}{s^2+\omega^2}$
$e^{-at} \sin \omega t$	(7)	$\frac{\omega}{(s+a)^2+\omega^2}$
$e^{-at} \cos \omega t$	(8)	$\frac{s+a}{(s+a)^2+\omega^2}$
t	(9)	$\frac{1}{s^2}$
$\frac{t^{n-1}}{(n-1)!}$	(10)	$\frac{1}{s^n}$
te^{-at}	(11)	$\frac{1}{(s+a)^2}$
$\frac{t^{n-1}e^{-at}}{(n-1)!}$	(12)	$\frac{1}{(s+a)^n}$
$u(t-a)$	(13)	$\frac{e^{-as}}{s}$

function is inversely proportional to frequency; as the frequency is increased, the amplitude becomes less. This indicates that step functions of zero rise-time yield their greatest amplitude in the frequency domain at lower frequencies but that significant levels may still exist higher in the frequency spectrum even though the amplitude is hyperbolically related to frequency. This is a classical transient problem associated with radio-frequency interference or electromagnetic compatibility, for example.

The fourth entry in Table 2.2 indicates that a time-decaying function, e^{-at}, yields a pole in the frequency domain at $s = a$ (denominator of $1/(s + a)$ goes to zero here). Since $s = \sigma + j\omega = -a$, this pole exists at zero frequency and has an amplitude, σ, of $-a$ in the left-half plane, as identified on the σ axis in Fig. 2.1. Physically, this says that $1/(s + a)$ behaves as $1/s$ for large values of s compared to "a" as in the case of the unit step function where "a" would equal zero. Analytically, this may be seen:

$$\left|\frac{1}{s+a}\right| = \left|\frac{1}{a+j\omega}\right| = \sqrt{\frac{1}{a^2+\omega^2}} \approx \frac{1}{\omega} \text{ for } \omega \gg a. \qquad (2.5)$$

For very low frequencies:

$$\left|\frac{1}{s+a}\right| \approx \frac{1}{a} \text{ for } \omega \ll a. \qquad (2.6)$$

Eq. (2.6) says that the amplitude in the frequency domain of an exponentially decaying function at low frequencies is constant with frequency. By way of comparison, therefore, the time-decaying function yields the same amplitude as the unit step function at high frequencies, but levels off and becomes finite at any arbitrarily low frequency.

In a similar vein, the transform of the time function, sin ωt yields an expression which has two poles at $s^2 + \omega^2 = 0$ or $s = \pm j\omega$. Fig. 2.1 identifies these two poles on the real-frequency or $j\omega$ axis and only the one corresponding to the positive or upper-half plane has physical meaning. In terms of the s-plane interpretation, this example indicates that a discrete frequency only exists at ω and that there is no exponential damping or increase in time as is the case for a discontinuous sine wave.

Similar explanations exist for each of the other entries in Table 2.2. The following section describes a real RLC circuit

with emphasis being placed on its arrangement as a band-pass filter (cf. Chap. 5). This will serve to clarify some of the applications of Laplace transforms to the solution of both the steady-state and transient response of filter networks to any kind of driving function.

2.4 APPLICATION OF LAPLACE TRANSFORMS TO RESONANT CIRCUITS

Fig. 2.2 depicts an LC band-pass filter inserted between the driving source or generator (battery) resistance, R_g, and the terminating load resistance, R_L. The following discussion addresses itself to two aspects of the problem: (1) the steady-state, filter transfer function, Z_T, and (2) the transient response of the network to a unit step function which in this case applies to an input battery voltage existing upon the closing of a switch at time $t = 0$.

Based on the nodal method of analysis, the integro-differential equation describing the network shown in Fig. 2.2 is:

$$\frac{E_o}{R_L} + \frac{1}{L}\int E_o dt + C\frac{dE_o}{dt} + \frac{E_o - E}{R_g} = 0. \tag{2.7}$$

When $R_L = R_g = R$, Eq. (2.7) may be rewritten as:

$$\frac{2E_o}{R} + \frac{1}{L}\int E_o dt + C\frac{dE_o}{dt} = \frac{E}{R}. \tag{2.8}$$

Remembering from Table 2.2 that all integrals are replaced with $1/s$ and all differentials with s,[1] and the right hand term is a unit step function, Eq. (2.8) may be represented in its Laplace format as:

$$\frac{2E_o}{R} + \frac{E_o}{sL} + E_o sC = \frac{E}{sR} \tag{2.9}$$

$$= \frac{E_o}{s}\left(\frac{2s}{R} + \frac{1}{L} + s^2C\right) = \frac{E}{sR}. \tag{2.10}$$

[1]No previous charge on capacitor or current in inductor is assumed.

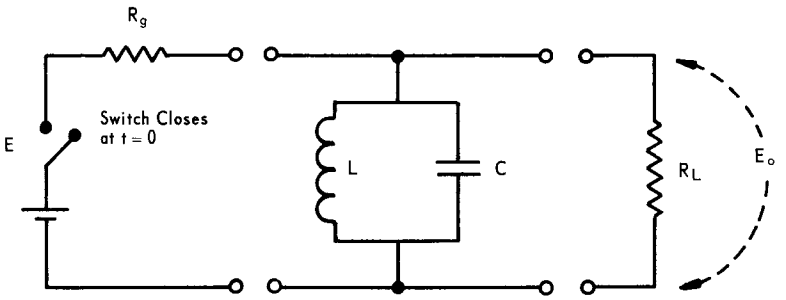

Figure 2.2. Doubly Loaded ($R = R_g = R_L$) Band-Pass Filter

As previously defined, the transfer function is the ratio of the output voltage, E_o to the input voltage, E. Thus, Eq. (2.10) is rearranged accordingly:

$$Z_T = \frac{E_o}{E} = \frac{1}{RC\left(s^2 + \frac{2s}{RC} + \frac{1}{LC}\right)} \tag{2.11}$$

Eq. (2.11) is a quadratic in s and can be represented by the product of two terms each of which represents the poles of the expression:

$$Z_T = \frac{1/RC}{(s - s_{p_1})(s - s_{p_2})} \tag{2.12}$$

where,
$$s_{p_1} \text{ and } s_{p_2} = -\frac{1}{RC} \pm \sqrt{\left(\frac{1}{RC}\right)^2 - \frac{1}{LC}}. \tag{2.13}$$

The poles of Eq. (2.12) are shown in Fig. 2.3. The location of these poles depends upon the two quantities, 1/RC and 1/LC. It is of interest to study the possible locations of s_{p_1} and s_{p_2} when 1/RC is varied in amplitude while 1/LC is fixed. If 1/RC is small compared to 1/LC, which corresponds to a resonant circuit with small damping, the quantity under the square root sign of Eq. (2.13) will be negative, and s_{p_1} and s_{p_2} will be conjugate complex numbers, viz: $-1/RC \pm j\sqrt{1/LC} = 1/RC \pm j\omega_o$. Typical locations for s_{p_1} and s_{p_2} are represented by the indicated poles, s_1 and s_2 in Fig. 2.3.

It is easily shown that, as 1/RC varies, s_{p_1} and s_{p_2} move along the circular paths indicated in Fig. 2.3. At the extreme

points A and A', for which 1/RC vanishes, s_{p1} and s_{p2} exist on the real-frequency axis. This corresponds to the resonance of a nondissipative resonant circuit in which the impedance of a parallel-tuned circuit such as shown in Fig. 2.2, goes to infinity at a real frequency. This is also evident in Eq. (2.12) since one of the two terms in the denominator goes to zero at a frequency equal to its pole.

At point B in Fig. 2.3, $(1/RC)^2$ equals 1/LC and the two poles therefore become equal. In other words for that situation, the radical in Eq. (2.13) goes to zero, and the impedance has a double pole at this point, viz: $-1/RC$. This is known as critically damping. Since B is found on the negative real axis, the corresponding physical voltages and current are non-oscillatory, exponentially decreasing functions.

Finally, if 1/RC becomes even larger, s_{p1} and s_{p2} are found respectively to diverge to the right and left of B on the real σ

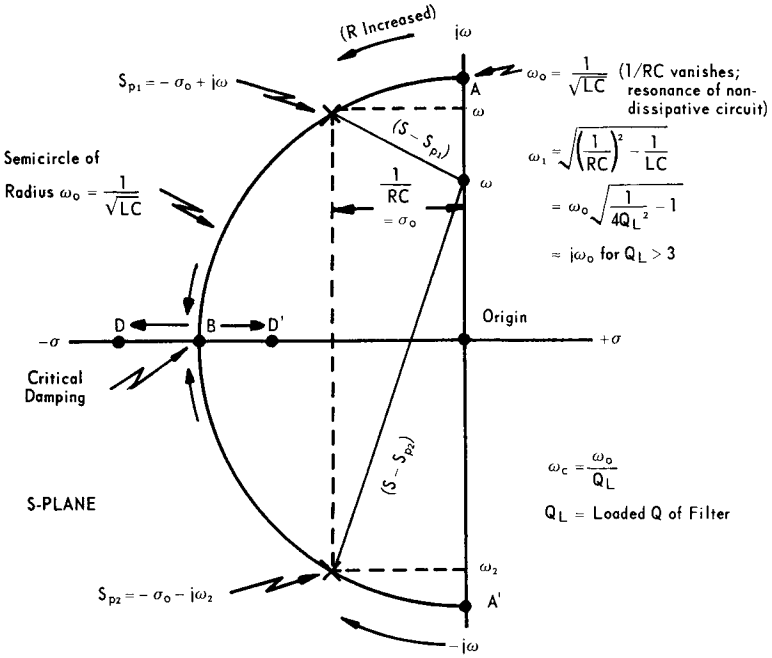

Figure 2.3. S-PLANE Pole Distribution of a Band-Pass Filter

axis as illustrated by D and D' in Fig. 2.3 and by Eq. (2.13). Although the poles can be assigned a great variety of positions by varying the relations among the R, L, and C, it is noticed that they are always found in the left-half of the s-plane.

Fig. 2.4 is a plot of the steady-state frequency response of the transfer functions shown in Eq. (2.12). For a finite driving and terminating resistance, the loaded Q_L factor is defined as the ratio of the center radian frequency, ω_o, to the bandwidth, ω_c (cf. Chap. 1). As seen in Figs. 2.3 and 2.4, and from Eqs. (2.12) and (2.13), the steepness of resonance and hence bandwidth narrowing becomes more pronounced as the values of the terminating resistance become greater (1/RC moves closer to the $j\omega$ axis). It is apparent, therefore, that the network zero and pole distribution or location uniquely describe the behavior of the transfer function except for a multiplier and provide a sound basis for understanding what is taking place in the design of desired circuits.

Before applying the inverse Laplace transform to Eq. (2.12) for obtaining the time response, it is first put in a format consistent with one of the pairs (fourth) listed in Table 2.2. Expanding by partial fractions yields:

$$Z_T = \frac{E_o}{E} = \frac{1}{RC}\left[\frac{1}{(s-s_{p1})(s_{p1}-s_{p2})} + \frac{1}{(s-s_{p2})(s_{p2}-s_{p1})}\right] . \quad (2.14)$$

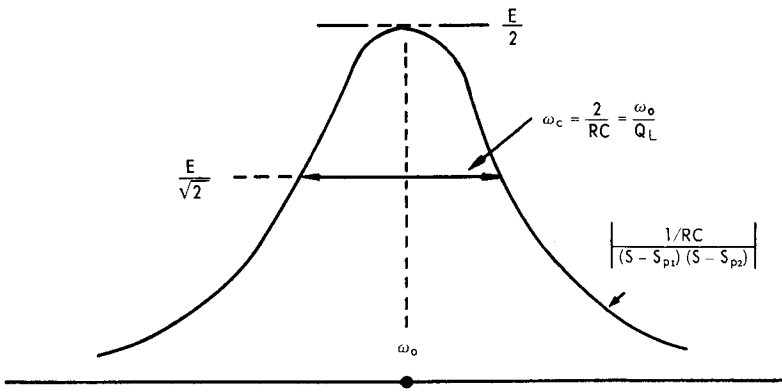

Figure 2.4. Steady-State Frequency Response

To obtain the transient response of the network to the unit step function caused by closing the battery switch, the inverse Laplace transform is now applied and yields:

$$E_o = \frac{E}{RC}\left[\frac{e^{s_{p1}t}}{(s_{p1} - s_{p2})} + \frac{e^{s_{p2}t}}{(s_{p2} - s_{p1})}\right] \tag{2.15}$$

where, $$s_{p1} - s_{p2} = 2\sqrt{\left(\frac{1}{RC}\right)^2 - \frac{1}{LC}} \approx 2\omega_o\sqrt{\frac{1}{4Q_L{}^2} - 1}. \tag{2.16}$$

For most resonant circuits, the dissipation is small ($Q_L{}^2 \gg 1$) and the radical in Eq. (2.16) may be approximated by $\sqrt{-1} = j$. For this situation the values of the poles in Eq. (2.13) become:

$$s_{p1} \approx -\frac{1}{RC} + j\omega_o = -\frac{\omega_o}{2Q_L} + j\omega_o \tag{2.17}$$

$$s_{p2} \approx -\frac{1}{RC} - j\omega_o = -\frac{\omega_o}{2Q_L} - j\omega_o. \tag{2.18}$$

With this approximation substituted in Eq. (2.15), the inverse Laplace transform becomes:

$$E_o = \frac{E\omega_o}{2Q_L} \times \frac{1}{2j\omega_o} \times e^{-\omega_o t/2Q_L}\left(e^{j\omega_o t} - e^{-j\omega_o t}\right) \tag{2.19}$$

$$E_o(t) = \frac{E}{2Q_L}e^{-\omega_o t/2Q_L} \sin \omega_o t. \tag{2.20}$$

At $t = 0$, the exponential damping term in Eq. (2.20) is equal to unity and the envelope of the maximum starting amplitude of this time response is reduced to $1/2Q_L$ times the amplitude of the excitation function E. The transient response of the shock-excited filter to the closing of the switch as described analytically in Eq. (2.20) is depicted in Fig. 2.5.

It is noted that the amplitude of the decayed oscillations has been reduced to $1/e$ of its value in the time required to make the exponent in Eq. (2.20) equal to unity; viz,

$$\frac{\omega_o t}{2Q_L} = 1, \text{ or } t = \frac{2Q_L}{\omega_o} = \frac{2}{\omega_c}. \tag{2.21}$$

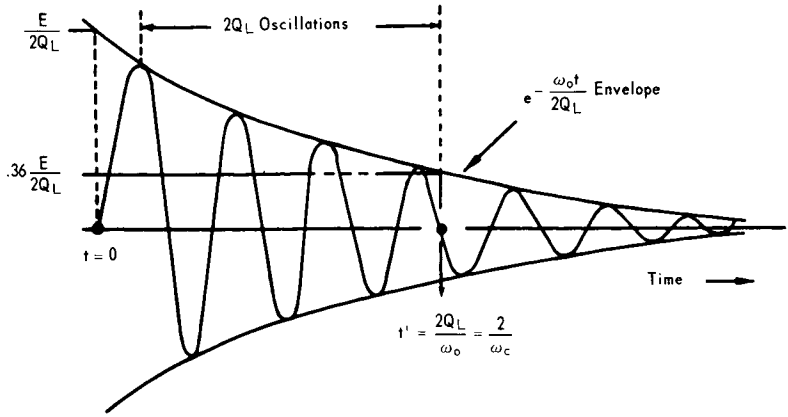

Figure 2.5. Transient Response of Network Shown in Figure 2.2

Eq. (2.20) indicates that the ringing time of the network becomes arbitrarily long as the bandwidth becomes very narrow or as the Q_L factor of the filter becomes very high. However, Eq. (2.20) also indicates that the maximum amplitude would become correspondingly less so that whether or not electromagnetic interference damage due to closing of switch or relay contacts, for example, may be expected would depend upon the actual circuit coupled into the filter.

Chap. 4 applies much of the material developed here to that part which has to do with network synthesis. Where a more thorough treatment of the above material is desired, the reader is referred to the following references.

2.5 REFERENCES

1. Bode, Hendrik W., "Network Analysis and Feedback Amplifier Design," D. Van Nostrand Company, Inc., New York, 1945.
2. Culp, S., "Step Function Charts Speed Filter Transient Analysis," *Electronic Design*, Vol. 11, No. 12, pp. 58–62, June 7, 1963.
3. Gardner and Barnes, "Transients in Linear Systems," Vol. I, John Wiley & Sons, Inc., New York, 1947.
4. Gottier, R. L., "The Node Method of Circuit Analysis," *Electronic Industries*, Vol. 22, No. 3, pp. 102–104, March 1963.
5. Guillemin, Ernst A., "Introductory Circuit Theory," John Wiley & Sons, Inc., New York, 1953.
6. Moses, A., "Finding the Laplace Transform from Frequency Response Data," *Electronic Equipment Engineering*, Vol. 11, No. 10, pp. 54–55, October 1963.
7. Rosenbrock, H. H., "An Approximate Method For Obtaining Transient Response from Frequency Response," *Proc. Inst. Elect. Engrs.*, Part B, Vol. 102, No. 6, pp. 744–752, November 1955.
8. Van Valkenburg, M. E., "Introduction to Modern Network Synthesis," John Wiley & Sons, Inc., New York, 1960.
9. Weinberg, L., "Network Analysis and Synthesis," McGraw-Hill Book Company, New York, 1962.
10. White, D. R. J., "Transient Testing Techniques," *Electronics Industries*, Vol. 19, No. 12, December 1960.

CHAPTER 3

CONSTANT-K AND M-DERIVED NETWORKS

This chapter discusses image-parameter or constant-k and m-derived filter responses. Responses obtained by the image-parameter method are generally inferior and less efficient per reactive element than those of either the maximally-flat Butterworth or equal-ripple Tchebycheff types discussed in Chap. 4. In fact, the image-parameter method of filter design, developed by G. A. Campbell, O. J. Zobel, and others in the 1920's, while a creditable achievement in its time, is rapidly becoming passé because of the difficulties of predicting and controlling the amplitude and phase characteristics. This method is being replaced with modern synthesis techniques for developing desired transfer functions.

Where sharp-skirt selectivity is required, however, certain advantages may be gained by adding "wave traps" (m-derived sections) just outside the stop band. Again, this method is not as sound as the use of elliptic-functions discussed in Chap. 4. Since so much of the (older) literature is based on the image-parameter method, it will suffice here to summarize the technique and design equations. Thus, this chapter is included in this handbook for those engineers who have been trained in the image-parameter technique and who do not have the inclination or time to acquaint themselves with the superior methods provided by modern network techniques.

Filter action is based upon the fact that an inductance represents a low impedance ($jX_L = j2\pi fL$) to low frequencies and a high impedance to high frequencies, whereas the opposite condition ($-jX_C = -j/2\pi fC$) occurs with a capacitance. When inductances are connected in series and capacitances are connected in shunt, as shown in Fig. 3.1, then direct current will flow without opposition and will be limited only by small finite series resistance losses associated with inductors and shunt leakage conductance associated with capacitors. As the frequency increases from dc, the series inductive reactances increase and the shunt

capacitive reactances decrease. If the magnitudes of the inductances and capacitances are properly chosen, then frequencies above a critical frequency, ω_c (bandwidth of network), will be attenuated and the network will form a low-pass filter. Fig. 3.2 shows the response of the filter depicted in Fig. 3.1.

3.1 CONSTANT-K FILTERS

A constant-k filter prototype is, in fact, a three-stage, low-pass filter, and as such, is limited to the maximum stop-band rate

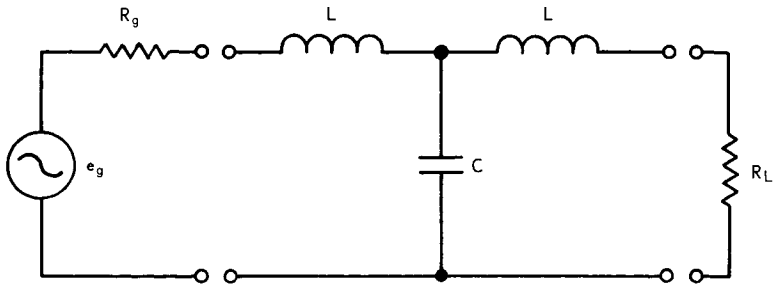

Figure 3.1. Typical Low-Pass Filter

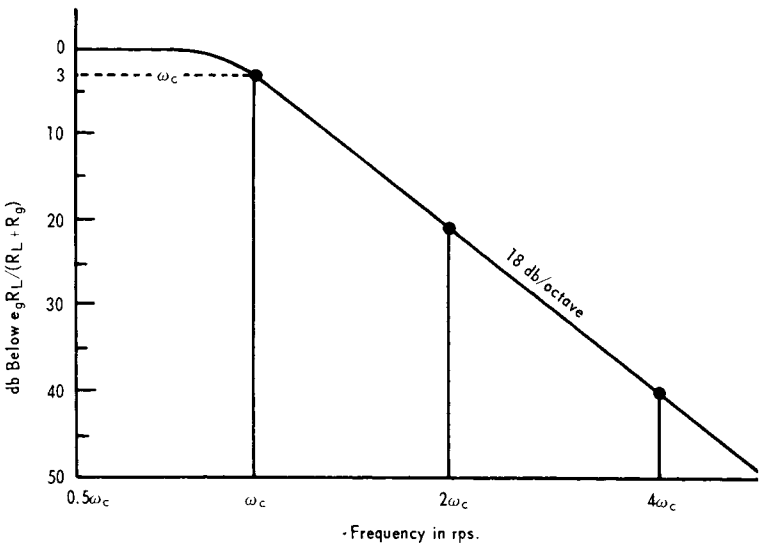

Figure 3.2. Response of Low-Pass Filter Shown in Figure 3.1

of attenuation of 18 db (3 stages × 6 db per reactive element) per octave. The term "constant-k" refers to the fact that the product of the series and shunt arm impedances is a constant:

$$Z_{series} \times Z_{shunt} = j\omega L\left(-j\frac{1}{\omega C}\right) = \frac{L}{C} = k^2. \qquad (3.1)$$

The prototype filter may be represented as either a T-section or its dual, a π-section, as illustrated in Figs. 3.3 and 3.4[1].

A network dual is formed by: (1) replacing all series inductances with shunt capacitances of the same value (e.g., 1/2 henry becomes 1/2 farad) and vice versa, and (2) replacing all resistances with conductances of the same value (e.g., 5 ohms becomes

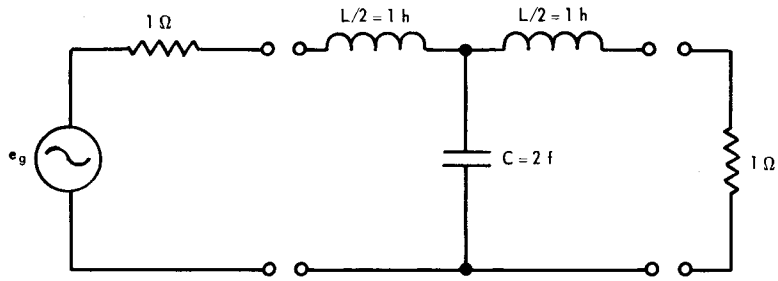

Figure 3.3. Constant-k (3 element), T-Section, Low-Pass Prototype

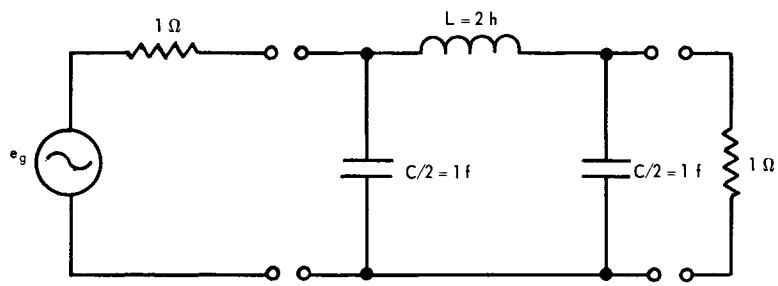

Figure 3.4. π-Section or Dual of Figure 3.3, Low-Pass Prototype

[1]This prototype is exactly the same as the three-stage, balanced Butterworth prototype discussed in the next chapter, Sec. 4.1.2.

5 mhos or 0.2 ohm). A network and its dual have a 3-db cut-off frequency, ω_c, of 1 radian/sec when the source and terminating resistances are each one ohm and the inductances and capacitances have the values shown in Figs. 3.3 and 3.4. This low-pass prototype filter may be impedance leveled and frequency scaled by applying the following rules.

Impedance Leveling–To change the source and terminating resistances from one to R ohms, multiply all resistances and inductances by R and divide all capacitances by R.

Frequency Scaling–To change the cut-off frequency, f_c, from one radian/sec to ω_c radian/sec ($\omega_c = 2\pi f_c$), divide all inductances and capacitances by ω_c. However, do not alter the values of the resistances.

Illustrative Example 3.1

Suppose a 50-ohm, constant-k, π-section, low-pass filter having a 3-db cut-off frequency of 10 kc is desired (cf. Fig. 3.4).

Then,
$$C_1' = C_3' = \frac{C/2}{R\omega_c} = \frac{1}{50 \times 2\pi \times 10^4} = 0.318\ \mu f \qquad (3.2)$$

$$L_2' = \frac{RL}{\omega_c} = \frac{50 \times 2}{2\pi \times 10^4} = 1.594\ \text{mh.} \qquad (3.3)$$

The filter and its frequency response are shown in Figs. 3.5 and 3.6. Note that the rate of attenuation in the stop band is 18 db per octave since each reactive element yields 6 db per octave.

Interestingly enough, the constant-k prototype is exactly equal to the 3-stage Butterworth or maximally-flat, low-pass prototype discussed in Chap. 4. If greater skirt selectivity is desired, however, constant-k networks cannot simply be connected in tandem as shown in Fig. 3.7. The reason for this is that predicable filter action depends upon the load resistance being maintained constant or nearly constant with frequency. Fig. 3.8 shows the amplitude of the input impedance variation of a constant-k network over the range from $0.1 \leq \omega \leq 10$ radians/sec. The source impedance is matched to the input impedance only at low frequencies ($\omega \ll 1.0$ radian; the apparent match at $\omega = 1.4$ rps is misleading since it is mostly reactive). Thus, since the input impedance of the last stage of a tandem-connected constant-k filter becomes the load impedances of the second to

last stage, it is apparent that the filtering action may result in nearly any kind of performance due to load variation of the second-to-last stage with frequency.

Associated with the problem of response degeneration for tandem-connected constant-k filters is the lower efficiency in terms of gain-bandwidth product reduction. For example, two

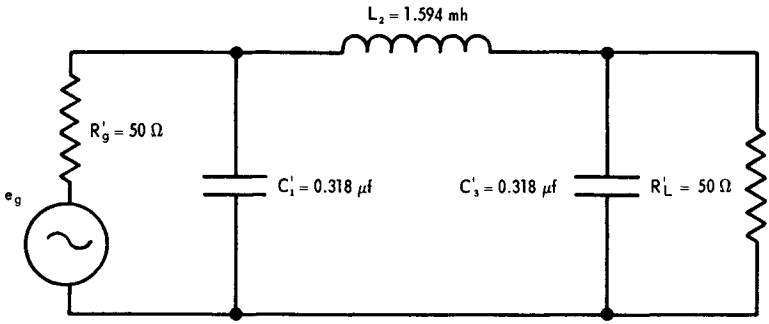

Figure 3.5. Constant-k, Low-Pass Filter with 10-kc Cut-Off Frequency (See Illustrative Example No. 3.1)

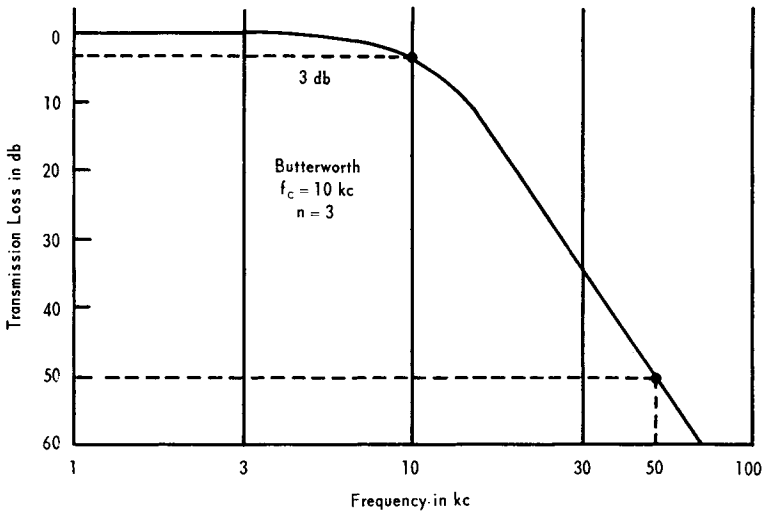

Figure 3.6. Transmission Response of Three-Stage Filter Depicted in Figure 3.5

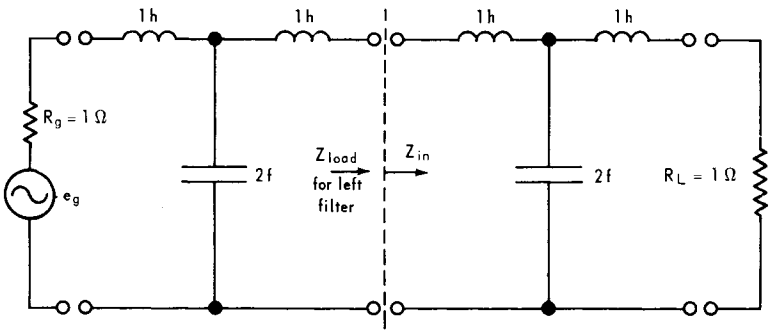

Figure 3.7. Two Tandemly Connected, Constant-k Filters

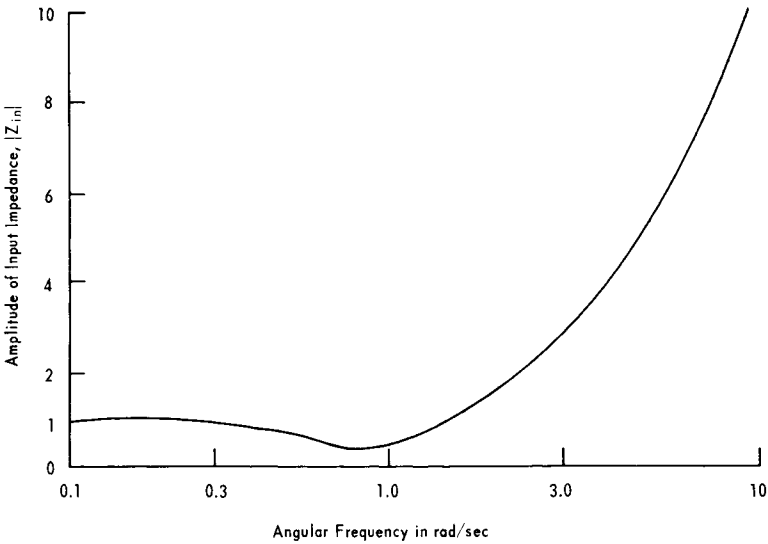

Figure 3.8. Input Impedance of Constant-k Filter with Frequency

tandemly connected filters having equal 3-db response characteristics will now collectively exhibit a 6-db attenuation (modified by the interaction effects) at the same cut-off frequency. It is shown below that the combined 3-db cut-off frequency has been reduced to 0.644 of the original value. The relation for the gain-bandwidth, or simply bandwidth, reduction of n-isolated, tandemly connected (synchronous), constant-k lossless filters is:

$$\frac{\omega_n}{\omega_1} = \sqrt{2^{1/n} - 1}. \tag{3.4}$$

Eq. (3.4) is plotted in Fig. (3.9) for n equals 1 through 20 tandem connections.

3.2 M-DERIVED FILTERS

Constant-k filters have two serious limitations:

(1) the impedance matching of source to termination is not a constant over the pass band.

(2) the attenuation provided just outside the pass band, but near the cut-off frequency in the transition zone, is often insufficient for many applications.

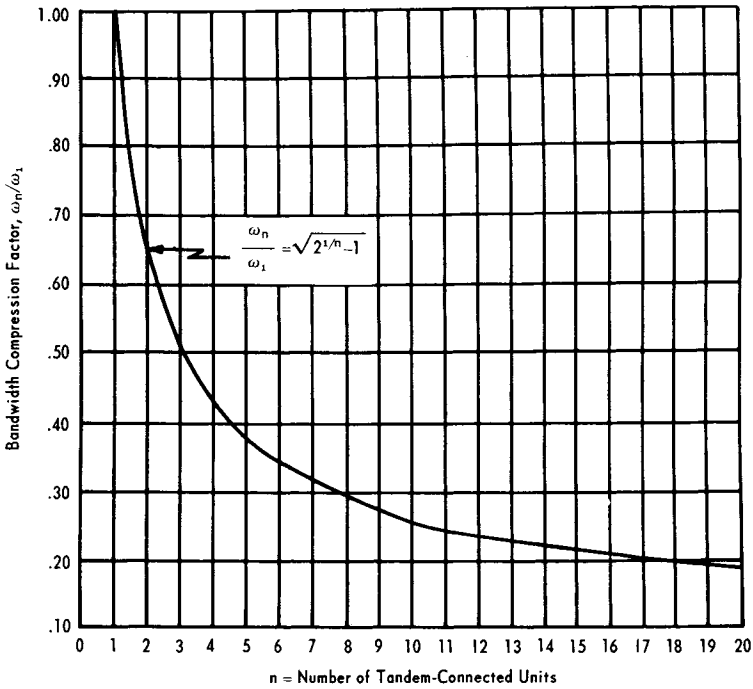

Figure 3.9. Bandwidth Compression Factor For Synchronous or Equal Tandemly-Connected Isolated Filter Units

Modern network synthesis provides sound answers to these limitations as discussed in Chap. 4; however, the older filter art employed the m-derived and terminating half sections as the answer for its time.

In order to eliminate the need for a large number of tandemly connected, constant-k filters to yield sharp skirt selectivity, an m-derived section can be added which will have a zero (cf. Chap. 2), i.e., an attenuation peak at a selected frequency in the stop band. This notch frequency can be placed wherever desired and, when a high attenuation near the cut-off frequency is required, it can be positioned very near the cut-off frequency. This m-derived section must be such, however, that it can be connected in tandem with other derived sections, and, of course, with the constant-k filter itself. Among other things, this means that the impedance of the derived section must be the same as that of the prototype.

Figs. 3.10 and 3.11 are the low-pass, m-derived prototypes which have been derived from the constant-k prototypes depicted in Figs. 3.3 and 3.4. The value of m is chosen from:

$$m = \sqrt{1 - (\omega_c/\omega_\infty)^2} \tag{3.5}$$

where, ω_c = 3-db cut-off radian frequency

ω_∞ = radian frequency where high attenuation is desired ($\omega_\infty > \omega_c$).

Eq. (3.5) is plotted in Fig. 3.13 in terms of the normalized infinite attenuation frequency.

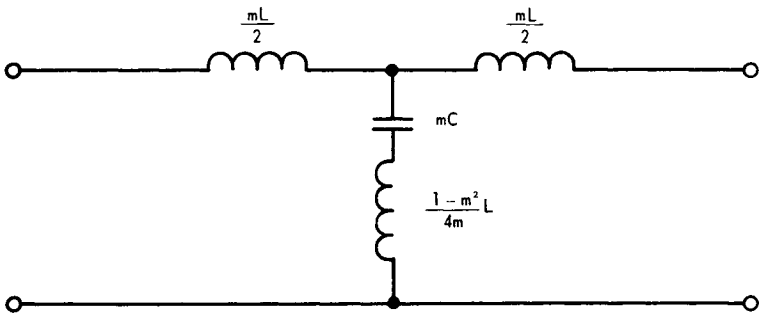

Figure 3.10. T-Section, M-Derived Filter

It develops that for m = 0.6 a degenerate form of the m-derived filter, viz, a terminating half-section, can be used to match the impedance of the source and terminating resistance with tandemly connected filters. This will reduce reflection loss, or power not realized due to mismatch, to a small amount within the pass band since the entire filter combination will now exhibit a practically constant resistance. The half-sections are obtained by splitting the m-derived, π-section shown in Fig. 3.11 to yield the networks shown in Fig. 3.12 for m = 0.6.

Illustrative Example 3.2

Suppose the previous filter (see Fig. 3.5) having a 50-ohm source and terminating resistance and a 10 kc cut-off frequency is desired; but it is necessary to provide a very high attenuation at 15 kc instead of the 15 db offered there by the attenuation characteristics of the constant-k alone. The low-pass filter, therefore,

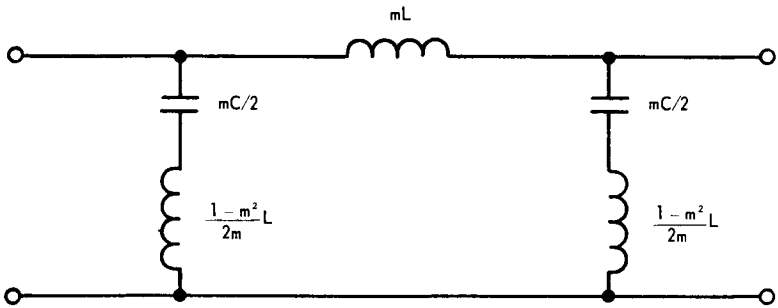

Figure 3.11. π-Section, M-Derived Filter

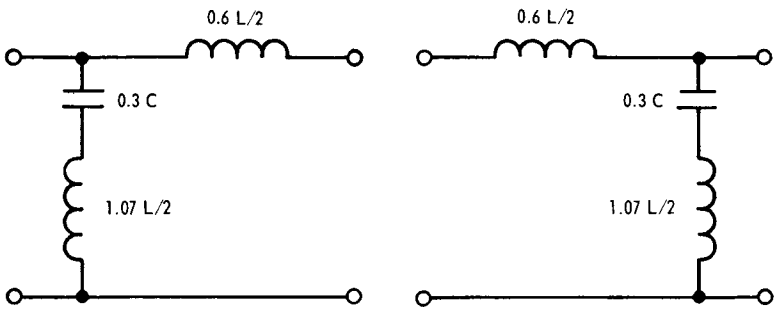

Figure 3.12. Terminating Half-Sections (m = 0.6)

will consist of one constant-k section, one m-derived section, and two terminating half-sections. The constant-k, T-section, filter (see Fig. 3.3) is:

$$L_3' = L_4' = \frac{RL/2}{\omega_c} = \frac{50 \times 1}{2\pi \times 10^4} = 0.797 \text{ mh} \tag{3.6}$$

$$C_2' = \frac{C}{R\omega_c} = \frac{2}{50 \times 2\pi \times 10^4} = 0.636 \ \mu\text{f.} \tag{3.7}$$

From either Eq. (3.5) or Fig. 3.13, the value of m is:

$$m = \sqrt{1 - \left(\frac{2\pi \times 10^4}{2\pi \times 1.5 \times 10^4}\right)^2} = 0.746.$$

From Fig. 3.10, the element values of the m-derived T-section are:

$$L_5' = L_7' = mL_3' = 0.746 \times 0.797 \text{ mh} = 0.595 \text{ mh} \tag{3.8}$$

$$L_6' = \frac{(1 - m^2)L_3'}{2m} = \frac{0.444 \times 0.797 \text{ mh}}{2 \times 0.746} = 0.237 \text{ mh} \tag{3.9}$$

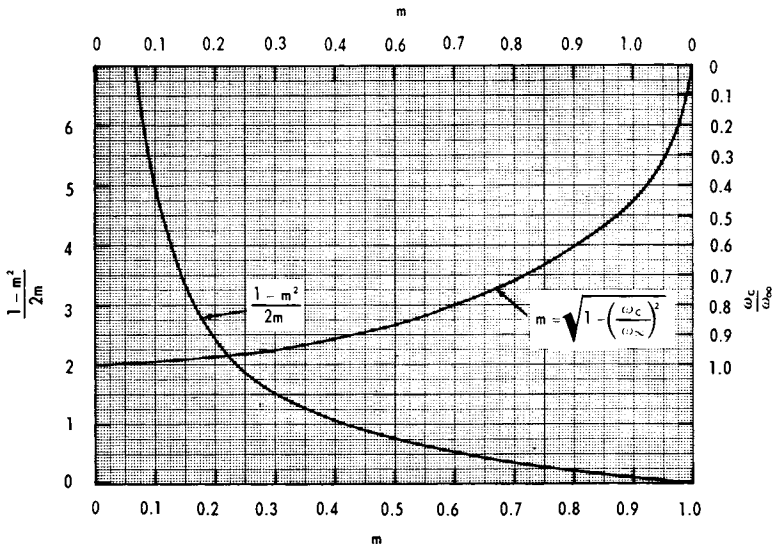

Figure 3.13. M-Derived Terms Used in Filter Design

$$C_3' = mC_2' = 0.746 \times 0.636\ \mu f = 0.475\ \mu f \qquad (3.10)$$

Finally, the terminating half-sections, corresponding to m = 0.6 are (see Fig. 3.12):

$$L_2' = L_8' = 0.6L_3' = 0.6 \times 0.797\ \text{mh} = 0.478\ \text{mh} \qquad (3.11)$$

$$L_1' = L_9' = 1.07L_3' = 1.07 \times 0.797\ \text{mh} = 0.850\ \text{mh} \qquad (3.12)$$

$$C_1' = C_4' = 0.3C_2' = 0.3 \times 0.636\ \mu f = 0.191\ \mu f. \qquad (3.13)$$

The complete low-pass filter is shown in Fig. 3.14. The series inductance values are combined to yield the network shown in Fig. 3.15. The frequency response is shown in Fig. 3.16.

Since the filter used up ten reactive elements, a 10-stage Butterworth, low-pass filter response (cf. Chap. 4, Sec. 4.1.1) with f_0 = 10 kc is also shown for comparison purposes. Note that the only region outside the pass band where the hybrid constant-k and m-derived filter is better (provides more attenuation) than the Butterworth response is in the region between about 13.5 and 15.5 kc. If a 10-stage, 0.5-db ripple Tchebycheff filter (cf. Sec. 4.2.1) had been shown in Fig. 3.16, it would have been superior to both of the above filters. In fact, except for the 0.5-db ripple, the Tchebycheff filter would have provided less attenuation just inside the stopband and sharper selectivity outside the pass band. For a 50-db rejection at 15 kc, only eight stages of the Tchebycheff would have been required and it would again have been superior to the constant-k and m-derived filters everywhere.

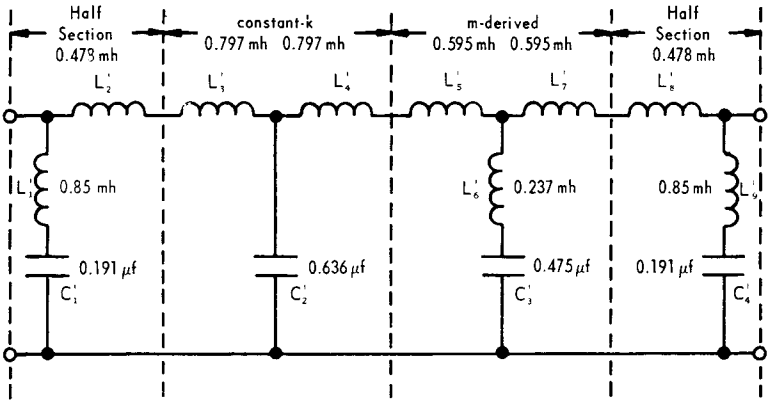

Figure 3.14. Low-Pass Filter Before Element Combination

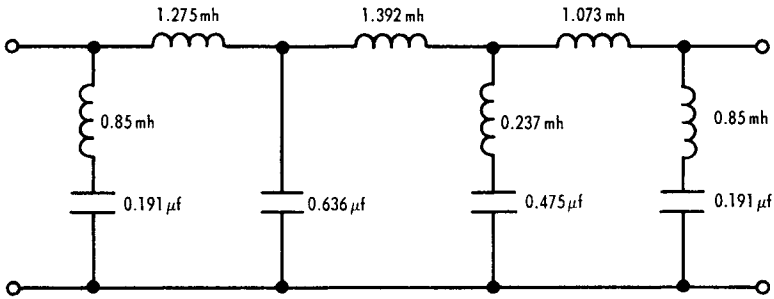

Figure 3.15. Final Low-Pass Filter with f_c = 10 kc and f_∞ = 15 kc

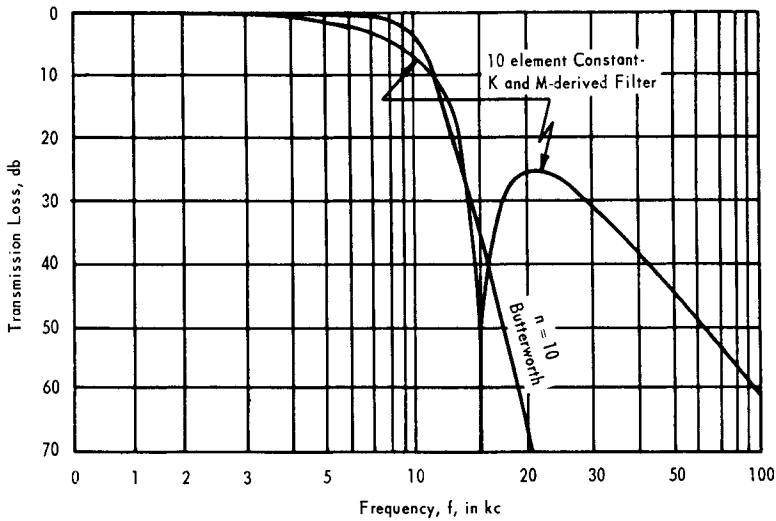

Figure 3.16. Frequency Response of Circuit Shown in Figures 3.14 and 3.15

Because the constant-k and m-derived image parameter techniques provide limited flexibility in filter design in general and almost none in the design of band-pass filters in particular, the subject will not be carried beyond this point. The reader is encouraged to develop a working knowledge of the application of modern network synthesis to the design of low-pass, high-pass, band-pass, and band-rejection filters as discussed in the next two chapters.

3.3 REFERENCES

1. Campbell, G. A., "Physical-Theory On The Electric Wave-Filter," *Bell System Technical Journal,* Vol. 1, p. 2, November 1922.
2. Guillemin, E. A., "Introductory Circuit Theory," John Wiley & Sons, Inc., New York, 1953.
3. IT&T, "Reference Data for Radio Engineers," Fourth Edition, International Telephone and Telegraph Corp., pp. 164–185, New York, 1956.
4. Landee, R. W., et al, "Electronic Designers Handbook," McGraw-Hill Book Co., pp. 16.1–16.20, New York, 1957.
5. LePage, W. R. and Seely, S., "General Network Analysis," McGraw-Hill Book Co., Inc., 1952.
6. Lubkin, Y. J., "The Fickle Constant-K Filter," *Electronic Design,* Vol. 11, No. 11, pp. 71–72, May 24, 1963.
7. Lubkin, Y. J., "The m-Derived Filter," *Electronic Design,* Vol. 11, No. 13, pp. 73–74.
8. Ulinkhamer, J. F., (1), "Empirical Determination of Wave-Filter Transfer Functions with Specified Properties," *Philips Research Reports,* No. 3 and No. 5(1948).
9. Ware, L. A. and Reed, H. R., "Communication Circuits," John Wiley & Sons, Inc., New York, 1944.
10. Zobel, O. J., "Theory and Design of Uniform and Composite Electric Wave-Filters," *Bell System Technical Journal,* Vol. 2, p. 1, January 1923.

CHAPTER 4

MODERN NETWORK SYNTHESIS AND RESPONSE FUNCTIONS

The realization of a desired network performance may be divided into four steps: (1) selecting the desired frequency and/or time response to one or more excitation functions; (2) synthesizing a network which will yield transformation of the desired response (a prototype) in terms of the electrical analog of resistors, inductors, and capacitors to form a two-terminal pair network; (3) transforming the prototype to the final network configurations; and (4) the physical realization of the electrical network, including component realizability, filter fabrication, and tuning and measurements. The first two steps are treated in the remainder of this chapter, and the last two steps are presented in subsequent chapters.

The synthesis approach used here is based on Cauer's extension of Foster's theorem (see References at end of Chapter). This requires that either the driving-point impedance[1] or admittance of the desired network be known. Therefore, the synthesis process will be to go from the desired transfer function[1] to the reflection coefficient and thence to the driving-point impedance of a terminated, non-dissipative network.

The power-loss ratio of a network, $|t(j\omega)|^2$, is:

$$|t(j\omega)|^2 = \frac{P_L}{P_a} \tag{4.1}$$

where, P_L is the power delivered to the terminating load of the network from the generator

[1]The technologist who is interested in the design of filters and not in the synthesis should start reading Sec. 4.12 on page 56.

[2]cf. Sec. 2.2, Chap. 2. Driving-point impedance is the input impedance, Z_{11} or ratio, E_1/I_1 of source voltage to input current. It is the impedance of the terminated network looking from the generator to the network. The transfer function is the ratio of the network output voltage (or current) to the source or input voltage (or current).

P_a is the available power from the source or generator; viz, the power delivered to a load whose impedance is the conjugate of that of the source.

The power loss ratio describes the transfer behavior of the network and therefore is more frequently called the power transfer function or simply the transfer function. It specifies the transmission loss of a two-terminal pair network for a steady-state operating condition.

The power reflection coefficient, $|p(j\omega)|^2$, of a lossless network is the fractional power not delivered to the load. Thus, it is the fractional power reflected or returned to the generator. Since the network has been specified as lossless (no network absorption or insertion loss), the sum of the power reflection coefficient and the transfer function must equal the incident unity fractional power; viz,

$$|p(j\omega)|^2 + |t(j\omega)|^2 = 1. \tag{4.2}$$

The power delivered to the load and the available power may be substituted into the transfer function relation of Eq. (4.1):

$$|t(j\omega)|^2 = \frac{E_L^2/R_L}{E_g^2/4R_g} \tag{4.3}$$

where the voltage and resistance terms are identified in Fig. 4.1. It now remains to replace the right side of Eq. (4.3) in terms of the driving-point impedance, $Z_{11}(j\omega)$, where $Z_{11}(j\omega) = R_{11} + jX_{11}$, the input resistance and reactance. Thus, since the network is lossless, the power entering the network from the generator is equal to that dissipated in the load; viz,

$$I_g^2 R_{11} = \frac{E_L^2}{R_L} \tag{4.4}$$

where,

$$I_g = \frac{E_g}{R_g + Z_{11}}. \tag{4.5}$$

Substituting Eq. (4.5) into (4.4) and the result into the numerator of the right side of Eq. (4.3), yields:

$$|t(j\omega)|^2 = \frac{R_{11}E_g^2/(R_g + Z_{11})^2}{E_g^2/4R_g}. \tag{4.6}$$

Eq. (4.6) may be rewritten through completion of squares by adding and subtracting R_{11}^2 and X_{11}^2:

$$|t(j\omega)|^2 = \frac{4R_{11}R_g}{|R_g + Z_{11}|^2} = \frac{(R_g + R_{11})^2 + X_{11}^2 - (R_g - R_{11})^2 - X_{11}^2}{|R_g + Z_{11}|^2}$$

$$= \frac{|R_g + Z_{11}|^2 - |R_g - Z_{11}|^2}{|R_g + Z_{11}|^2} = 1 - \frac{|R_g - Z_{11}|^2}{|R_g + Z_{11}|^2}. \tag{4.7}$$

Finally, Eq. (4.7) may be substituted into Eq. (4.2) to yield:

$$|p(j\omega)|^2 = p(j\omega) \cdot p(-j\omega) = \frac{|R_g - Z_{11}|^2}{|R_g + Z_{11}|^2} \tag{4.8}$$

where $p(j\omega)$ is the voltage reflection coefficient.

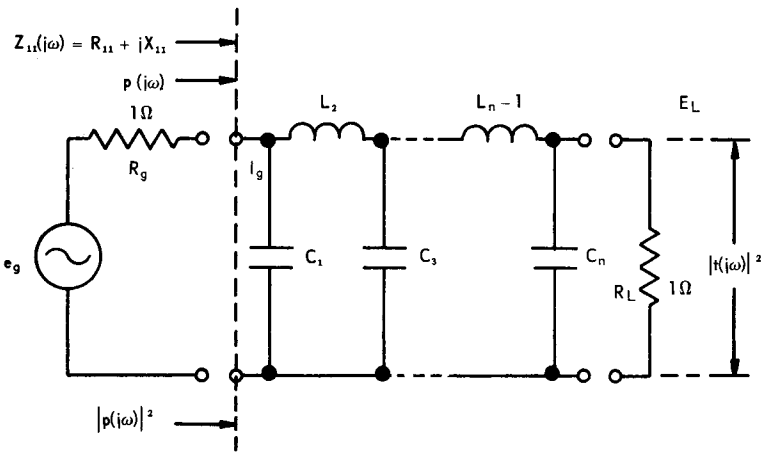

Figure 4.1. Low-Pass Prototype Filter Showing the Transfer Function on a Power Basis, $|t(j\omega)|^2$; The Reflection Coefficient, $p(j\omega)$; and the Input Impedance, $Z_{11}(j\omega)$.

The voltage reflection coefficient for a network which has a driving-point (input) impedance of Z_{11}, and is fed from a normalized source impedance of 1 ohm is obtained from Eq. (4.8) by setting $R_g = 1$:

$$p(j\omega) = \frac{1 - Z_{11}}{1 + Z_{11}} . \tag{4.9}$$

Therefore, the driving-point impedance is:

$$Z_{11} = \frac{1 - p(j\omega)}{1 + p(j\omega)} . \tag{4.10}$$

In order to obtain $p(j\omega)$ from the expression given in Eq. (4.2), certain restrictions exist regarding physical realizability. Although the zeros and poles of $|p(j\omega)|^2$ may lie anywhere on the complex frequency plane (they occur with quadrantal symmetry), the poles of $p(j\omega)$ must lie in the left-half s-plane in order for the amplitude and phase parts of $p(j\omega)$ to be uniquely related; i.e., $p(j\omega)$ must be a minimum-phase function. Therefore, the zeros of $p(j\omega)$ must either lie in the left-half s-plane[1] or on the real-frequency axis. Summarizing, this may be expressed:

$$p(j\omega) = \frac{\prod_{k=1}^{n} (s - s_{zm})}{\prod_{k=1}^{n} (s - s_{pk})} \tag{4.11}$$

where s_z and s_p are the left-half, complex-frequency plane zeros and poles[1] of $|p(j\omega)|^2$ respectively.

The driving-point impedance may now be expressed in terms of the voltage reflection coefficient (implicitly in terms of the transfer function) by substituting Eq. (4.11) into (4.10). The resulting network may then be synthesized by a continuous fraction expansion of Z_{11}, as shown in the following section.

There exists a large number of transfer functions which will yield desirable responses from a given set of excitation functions. Since the mathematics tends to become quite tedious, it is natural that relatively simple transfer functions (in the sense of

[1] cf. Chap. 2 regarding the complex frequency or s-plane.

their pole locations) have first been explored for the least difficult excitation functions; viz, those existing at positive real frequencies. And so it has been that the Butterworth functions (maximally-flat amplitude), the Tchebycheff functions (equal-ripple amplitude) of the first and second kind, the Bessel polynomial functions (maximally-flat time delay), and the Butterworth-Thompson functions (compromise between maximally-flat, steady-state and transient characteristics) have found wide popularity. As previously remarked, these transfer functions are almost always expressed in terms of their low-pass prototype because of the relative simplicity of the mathematics. This chapter emphasizes the first two functions only, because of their extensive use today. A brief discussion on the Butterworth-Thompson is presented in Sec. 4.3.

4.1 BUTTERWORTH (Maximally-Flat) PROTOTYPE

4.1.1[1] Synthesis of Butterworth Function

The transfer function describing a maximally-flat, steady-state response ($s = j\omega$) in the complex-frequency plane is the Butterworth, low-pass prototype function:

$$|t_B(j\omega)|^2 = \frac{1}{1 + \omega^{2n}} \tag{4.12}$$

where n is the number of frequency-sensitive elements in the low-pass prototype (cf. Fig. 4.1).

By substituting Eq. (4.12) into Eq. (4.2), the power reflection coefficient of the Butterworth function is obtained:

$$|p(j\omega)|^2 = p(j\omega) \cdot p(-j\omega) = 1 - \frac{1}{1 + \omega^{2n}} = \frac{\omega^{2n}}{1 + \omega^{2n}} . \tag{4.13}$$

The zeros[2] of Eq. (4.13) occur at zero frequency and are of multiplicity 2n. Only the zeros of multipicity n are retained for $p(j\omega)$. The poles of Eq. (4.13) are obtained by substituting $s = j\omega$ and solving for the roots of the denominator; viz,

[1] This section may be omitted by the technologist who is only interested in the design and realization of filters.

[2] cf. Chap. 2, Sec. 2.2 for discussion of location of zeros and poles in the complex-frequency plane.

$$\omega^{2n} = -1 \text{ or } s^{2n} = (-j)^{2n} = -(-1)^n. \tag{4.14}$$

The roots of Eq. (4.14) are equally spaced on the periphery of a unit circle and are located at:

$$e^{j\frac{(n+1)\pi}{2n}}, \ldots e^{j\frac{(2k-1+n)\pi}{2n}}, \ldots e^{j\frac{(5n-1)\pi}{2n}}, \tag{4.15}$$

where k is a positive integer from 1 to 2n. Only the poles of $|p(j\omega)|^2$ in the left-half s-plane are retained in order to make $p(j\omega)$ physically realizable (cf. Chap. 2). Therefore, the poles, s_{pk}, of $p(j\omega)$ are:

$$s_{pk} = e^{j\frac{(2k-1+n)\pi}{2n}}, \quad k = 1,2, \ldots, n. \tag{4.16}$$

Eq. (4.16) is generally expressed in trigonometric form; viz,

$$s_{pk} = -\sin\frac{(2k-1)\pi}{2n} + j\cos\frac{(2k-1)\pi}{2n}, \quad k = 1,2, \ldots n. \tag{4.17}$$

Eqs. (4.15) to (4.17) are depicted in Fig. 4.2 for the three cases of n = 1,2, and 3.

With the zeros having a multiplicity n, s^n, and the poles defined by Eq. (4.17) the expression for $p(j\omega)$ in Eq. (4.11) may now be written as:

$$p(j\omega) = \frac{s^n}{\prod_{k=1}^{n}(s - s_{pk})}. \tag{4.18}$$

By substituting Eq. (4.18) into Eq. (4.10), the driving-point impedance is obtained:

$$Z_{11} = \frac{\prod_{k=1}^{n}(s - s_{pk}) - s^n}{\prod_{k=1}^{n}(s - s_{pk}) + s^n} \tag{4.19}$$

The LC network indicated by Eq. (4.19) may now be synthesized by a continuous fraction expansion of Z_{11} in which a zero and pole are alternately removed until all zeros and poles have been removed.

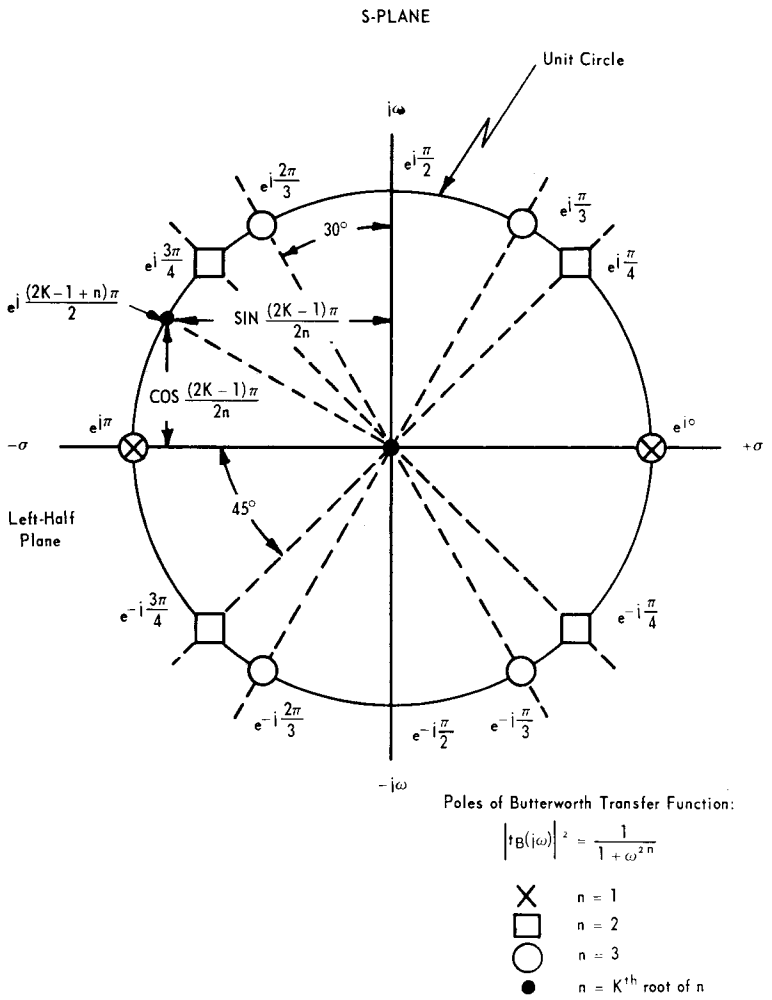

Figure 4.2. Pole Location on the Butterworth Circle

Illustrative Example 4.1

Assume a low-pass prototype filter having a Butterworth response of n = 3 is desired. By Eq. (4.17), the poles of $p(j\omega)$ are:

$$s_{p_1} = -0.5 + j\,0.866$$
$$s_{p_2} = -1.0 + j\,0 \qquad (4.20)$$
$$s_{p_3} = -0.5 - j\,0.866.$$

Then the product terms in Eq. (4.19) become:

$$\prod_{k=1}^{n} (s - s_{pk}) = s^3 + 2s^2 + 2s + 1. \qquad (4.21)$$

By substituting the value given in Eq. (4.21) into Eq. (4.19), the filter input impedance is obtained:

$$Z_{11} = \frac{2s^2 + 2s + 1}{2s^3 + 2s^2 + 2s + 1}. \qquad (4.22)$$

In synthesizing Z_{11} by a continuous fraction expansion, a choice must be made in the desired circuit configuration; that is, whether an input shunt capacitance or series inductance is wanted. Either is suitable since one can be directly obtained from the other by their dual relationship. For example, assume that the desired first element is a shunt capacitance, so that a pole at $s = \infty$ of Y_{11} must be removed. By inverting and proceeding with the continuous fraction expansion process, there results:

$$\begin{array}{r|l}
2s^2 + 2s + 1 & s \\
\hline
 & 2s^3 + 2s^2 + 2s + 1 \\
 & 2s^3 + 2s^2 + s \\
\hline
 & s + 1 \;\big|\; 2s \\
 & \quad 2s^2 + 2s + 1 \\
 & \quad 2s^2 + 2s \\
\hline
 & \quad 1 \;\big|\; s \\
 & \quad\quad s + 1 \\
 & \quad\quad s \\
\hline
 & \quad\quad 1 \;\big|\; 1 \\
 & \quad\quad\quad 1 \\
\hline
 & \quad\quad\quad 0.
\end{array} \qquad (4.23)$$

Therefore,

$$Z_{11} = \cfrac{1}{s + \cfrac{1}{2s + \cfrac{1}{s + 1}}}. \qquad (4.24)$$

Fig. 4.3 shows the resulting network. The dual of this network (input inductance) is shown in Fig. 4.4. This may be checked by

reversing the operation. If the admittance at the output terminals of Fig. 4.3, (s + 1), is formed, reciprocated so that the equivalent impedance [1/(s + 1)] can be added to that of the inductance (2s); the result reciprocated so that the equivalent admittance is added to that of the input capacitance; and again the result is reciprocated to yield an impedance, the expression given in Eq. (4.24), the input impedance Z_{11} is obtained.

The transfer function, $|t_B(j\omega)|^2$, yields a low-pass prototype network terminated at both ends with R = 1 and is symmetrical about the center. In fact, the coefficients of LC element values are identically equal to twice the decrement (Bennett's Formula; cf. Fig. 4.2):

$$\text{Coefficient of L's or C's} = 2 \sin \frac{(2k-1)\pi}{2n}, \quad k = 1,2, \ldots n. \quad (4.25)$$

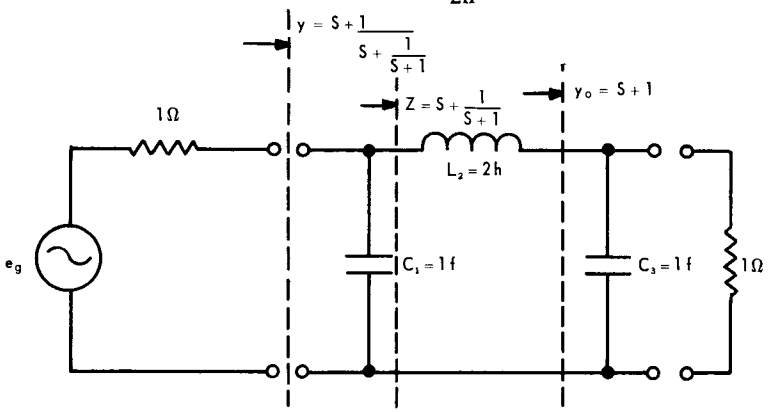

Figure 4.3. Synthesized Three-Stage, Butterworth, Low-Pass Prototype

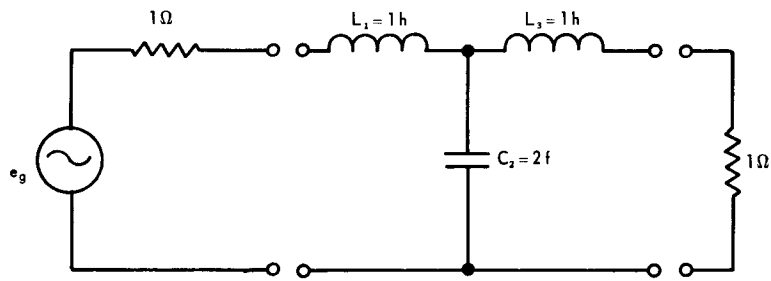

Figure 4.4. Dual of Network Shown in Figure 4.3

Table 4.1 lists the values of these coefficients for n = 1 to 20 for equal input-output resistance values of 1 ohm.

4.1.2[1] Low-Pass, Butterworth Prototype Design

The Butterworth transfer function given in Eq. (4.12) may be approximated in the stop band, when $\omega^{2n} \gg 1$, by the expression:

$$|t_B(j\omega)|^2 = \frac{1}{1+\omega^{2n}} \approx \omega^{2n} \text{ for } \omega^{2n} \gg 1, \tag{4.26}$$

or expressing Eq. (4.26) in decibels, the transmission loss, t_{db}, is:

$$t_{db} = -20n \log_{10}\omega. \tag{4.27}$$

Since the amplitude response is of special interest in the design of low-pass prototype filters, Eq. (4.26) is plotted in Fig. 4.5 between $\omega = 1$ radian/sec the normalized 3-db cut-off radial frequency and $\omega = 10$, for n = 1 to 10 and n = 12, 15, and 20. Eq. (4.26) is also plotted in Fig. 4.6 between $\omega = 10$ and 100 radians/sec and in Figs. 4.7 and 4.8 between 0 and 1 radian/sec.

Illustrative Example 4.2

Suppose it is desired to determine the transmission loss of a seven-stage (n = 7 LC elements) Butterworth, low-pass prototype filter ($\omega_c = 1$ rad/sec) at $\omega_1 = 2$ radians/sec. By reading down the n = 7 curve in Fig. 4.5 till the $\bar{\omega} = 2$ abscissa is intercepted, ($\bar{\omega} = \omega_1/\omega_c$), the ordinate or transmission loss is seen to be approximately 42 db. Alternatively, if Eq. (4.27) is used, the transmission loss is $-20 \times 7 \times \log_{10} 2$ or 42 db.

It was stated in Chap. 3 that the low-pass prototype response is used to design low-pass, high-pass, band-pass, and band-rejection filters. It was also remarked that to transform the low-pass prototype to any desired cut-off frequency and the impedance terminations to any other level, rules that follow apply.

Frequency Scaling—To change the cut-off frequency from one radian/sec to ω_c rad/sec ($\omega_c = 2\pi f_c$), divide all inductances and

[1]The filter design engineer should start reading this section. He may skip Chap. 2, and Sec. 4.1.1 if he is not interested in synthesis.

Table 4.1
ELEMENT VALUES OF BUTTERWORTH LOW-PASS FILTER PROTOTYPES
(Use this table when load and source resistance are within 30% of each other, viz when $0.7 < \overline{R} \leq 1.0$)*

n	C_1	L_2	C_3	L_4	C_5	L_6	C_7	L_8	C_9	L_{10}	n
1	2.000										1
2	1.414	1.414									2
3	1.000	2.000	1.000								3
4	0.765	1.848	1.848	0.765							4
5	0.618	1.618	2.000	1.618	0.618						5
6	0.518	1.414	1.932	1.932	1.414	0.518					6
7	0.445	1.247	1.802	2.000	1.802	1.247	0.445				7
8	0.390	1.111	1.663	1.962	1.962	1.663	1.111	0.390			8
9	0.347	1.000	1.532	1.879	2.000	1.879	1.532	1.000	0.347		9
10	0.313	0.908	1.414	1.782	1.975	1.975	1.782	1.414	0.908	0.313	10
11	0.285	0.832	1.319	1.683	1.920	2.000	1.920	1.683	1.319	0.832	11
12	0.261	0.765	1.220	1.591	1.849	1.983	1.983	1.849	1.591	1.220	12
13	0.240	0.707	1.133	1.493	1.768	1.943	2.000	1.943	1.768	1.493	13
14	0.223	0.661	1.066	1.414	1.694	1.889	1.988	1.988	1.889	1.694	14
15	0.209	0.618	1.000	1.338	1.618	1.827	1.956	2.000	1.956	1.827	15
16	0.199	0.581	0.942	1.269	1.545	1.764	1.913	1.990	1.990	1.913	16
17	0.185	0.548	0.892	1.206	1.479	1.699	1.866	1.966	2.000	1.966	17
18	0.174	0.518	0.845	1.147	1.414	1.638	1.813	1.932	1.992	1.992	18
19	0.164	0.491	0.804	1.095	1.354	1.578	1.759	1.891	1.973	2.000	19
20	0.157	0.467	0.765	1.045	1.299	1.521	1.705	1.848	1.945	1.994	20
n	L_1	C_2	L_3	C_4	L_5	C_6	L_7	C_8	L_9	C_{10}	n

n	C_{11}	L_{12}	C_{13}	L_{14}	C_{15}	L_{16}	C_{17}	L_{18}	C_{19}	L_{20}	n
1											1
2											2
3											3
4											4
5				ALL L's in henrys.							5
6				ALL C's in farads.							6
7											7
8											8
9											9
10											10
11	0.285										11
12	0.765	0.261									12
13	1.133	0.707	0.240								13
14	0.414	1.066	0.661	0.223							14
15	1.618	1.338	1.000	0.618	0.209						15
16	1.764	1.545	1.269	0.942	0.581	0.199					16
17	1.866	1.699	1.479	1.206	0.892	0.548	0.185				17
18	1.932	1.813	1.638	1.414	1.147	0.845	0.518	0.174			18
19	1.973	1.891	1.759	1.578	1.354	1.095	0.804	0.491	0.164		19
20	1.994	1.945	1.848	1.705	1.521	1.299	1.045	0.765	0.467	0.157	20
n	L_{11}	C_{12}	L_{13}	C_{14}	L_{15}	C_{16}	L_{17}	C_{18}	L_{19}	C_{20}	n

*Use Table 4.2 for $0.1 \leq \overline{R} \leq 0.7$ Use Table 4.3 for $\overline{R} < 0.1$

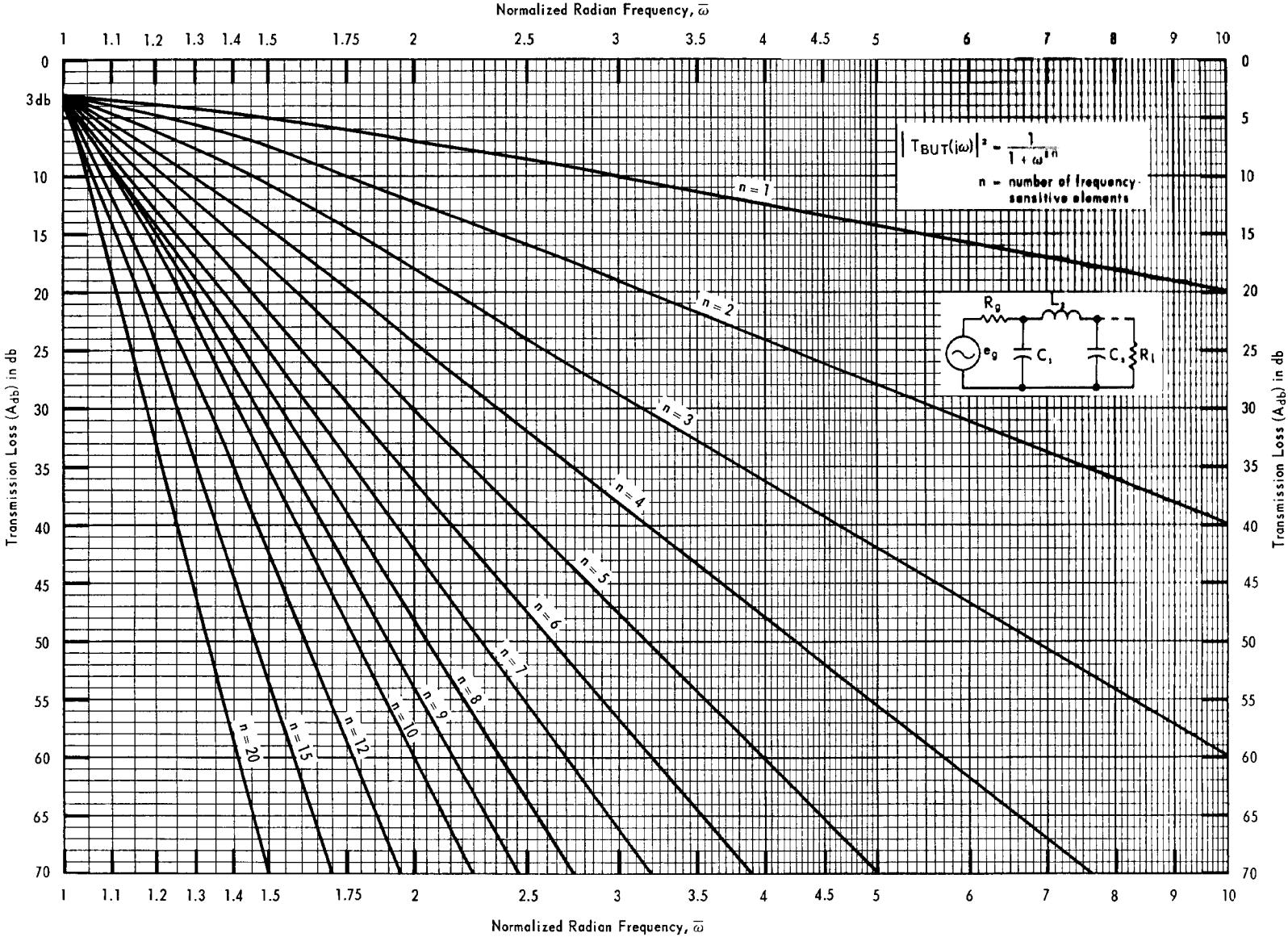

Figure 4.5. Transmission Loss of Butterworth Function vs. Frequency for $1.0 \leq \bar{\omega} \leq 10$

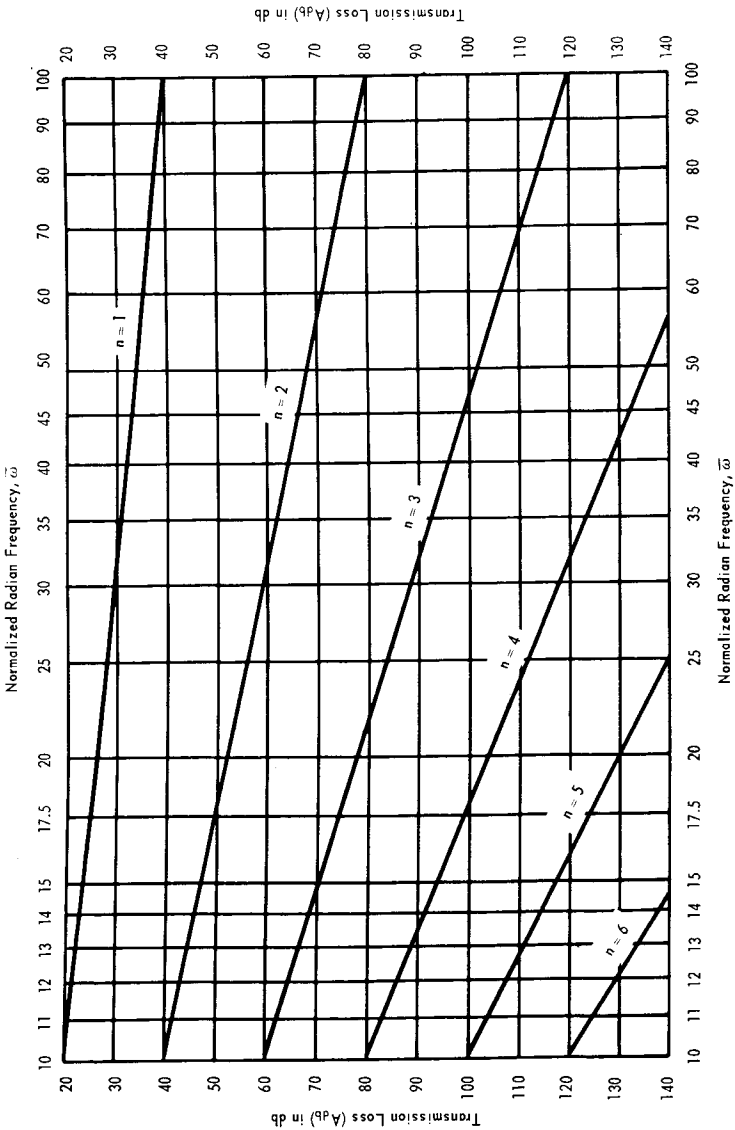

Figure 4.6. Transmission Loss of Butterworth Function vs. Frequency for $10 \leq \bar{\omega} \leq 100$

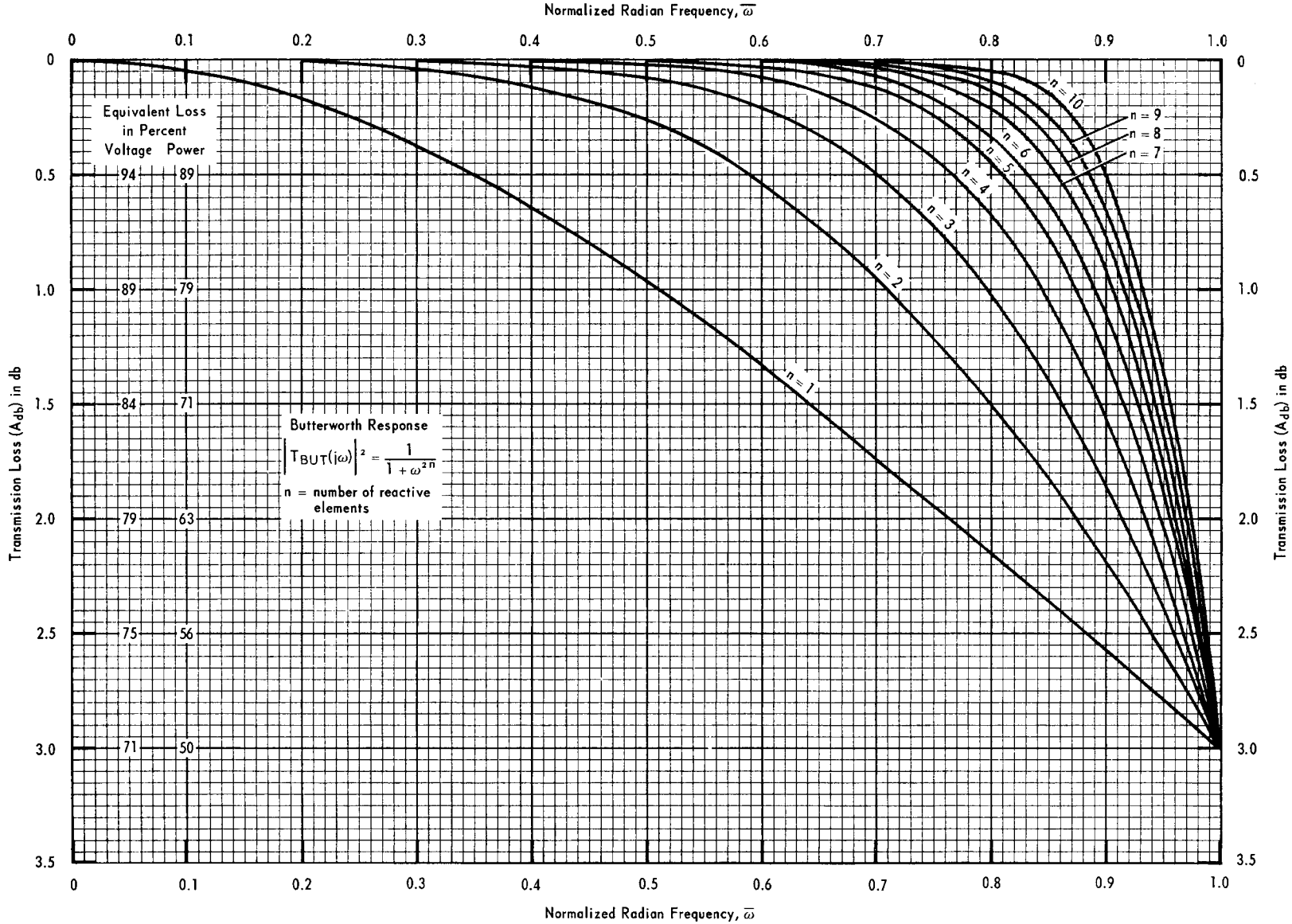

Figure 4.7. Transmission Loss of Butterworth Function vs. Frequency for $0 \leq \overline{\omega} \leq 1.0$ and $A_{db} \leq 3.5$ db

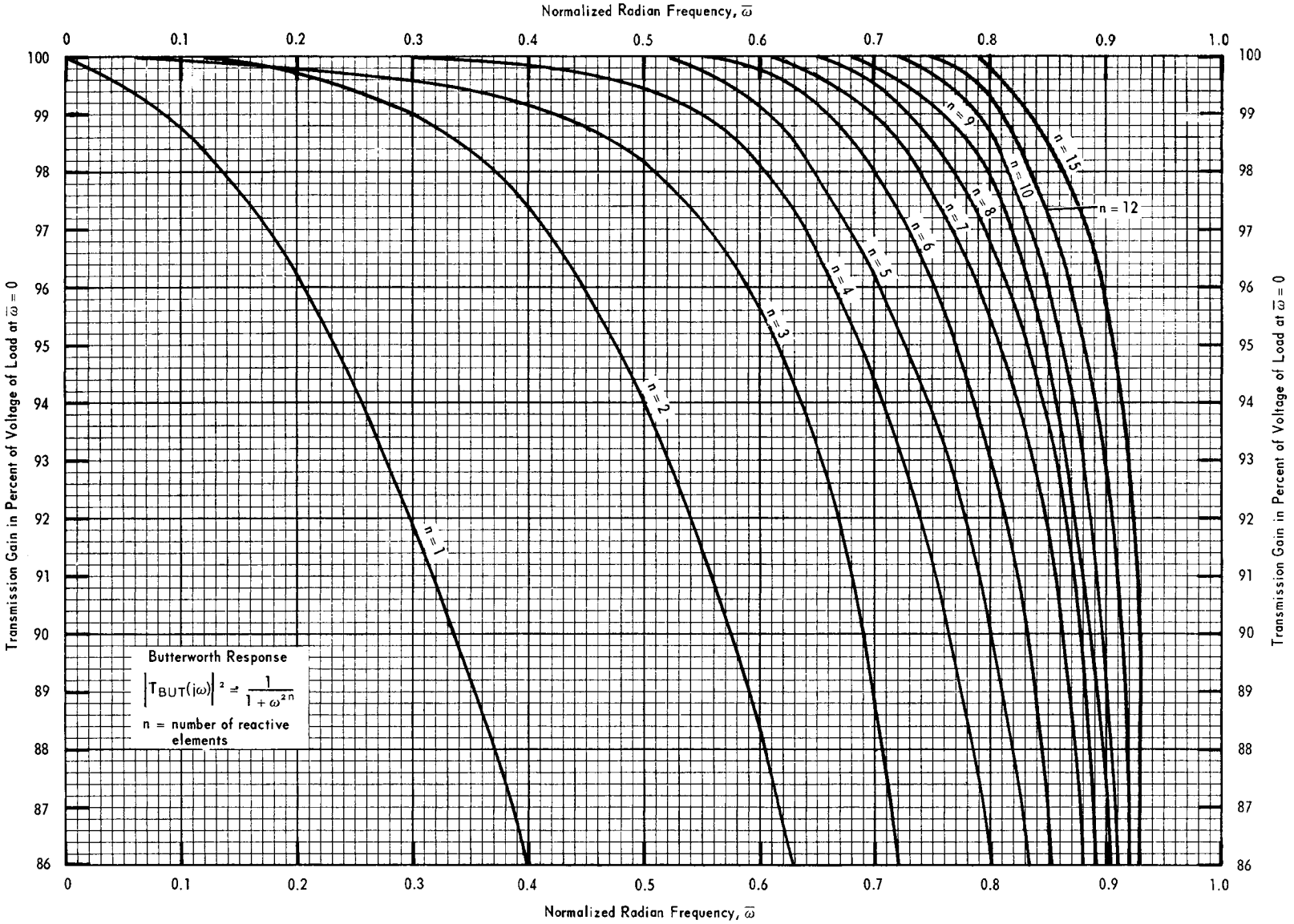

Figure 4.8. Transmission Loss of Butterworth Function vs. Frequency for $0 \leq \bar{\omega} \leq 1.0$ and $A_{db} \leq 1.0$ db

capacitances by ω_c. However, do not alter the values of the resistances.

Impedance Leveling—To change the source and terminating resistances from one ohm to R ohms, multiply all resistances and inductances by R and divide all capacitances by R.

Thus, the third rule follows when frequency scaling and impedance leveling are simultaneously applied.

Frequency and Impedance Scaling—To simultaneously change the cut-off frequency from one rad/sec to ω_c rad/sec and the source and terminating resistances from one ohm to R ohms, carry out the following operation:

$$L'_k = \frac{RL_k}{\omega_c} \tag{4.28}$$

$$C'_{k+1} = \frac{C_{k+1}}{R\omega_c} \tag{4.29}$$

The primed values of L's and C's pertain to the new low-pass network and the unprimed values correspond to the original prototype values given in Table 4.1.

Illustrative Example 4.3

Suppose it is desired to design a 300-ohm Butterworth, low-pass filter with a 3-db cut-off frequency, ω_c, of 10 kc and a skirt rejection of at least 40 db at 20 kc. Fig. 4.5 indicates that about 6-3/4 stages are required by the intersection of the 40-db transmission loss and $\bar{\omega} = 2$ (normalized $\bar{\omega} = 20/10$ kc $= 2$). Since only integer stages are possible, n = 7 is selected to yield a 42-db rejection at 20 kc. If a capacitor input is desired, Table 1 and Eqs. (4.28) and (4.29) yield:

$$C'_1 = C'_7 = \frac{C_1}{R\omega_c} = \frac{0.455}{300 \times 2\pi \times 10^4} = 0.0236\ \mu f$$

$$L'_2 = L'_6 = \frac{RL_2}{\omega_c} = \frac{300 \times 1.247}{2\pi \times 10^4} = 5.96\ mh$$

$$C'_3 = C'_5 = \frac{C_3}{R\omega_c} = \frac{1.802}{300 \times 2\pi \times 10^4} = 0.0955\ \mu f$$

$$L_4' = \frac{RL_4}{\omega_c} = \frac{300 \times 2.000}{2\pi \times 10^4} = 9.55 \text{ mh.}$$

The complete filter is shown in Fig. 4.9 and its response is depicted in Fig. 4.10.

In practical problems, it develops that the input-output or source and terminating resistances may not be equal as shown in all the preceding cases. Thus, either new tables of synthesized element values may be developed or some general rules must be set forth to operate on the symmetrically loaded networks in order to obtain the element values for the unequal source and load terminations. Both approaches are useful and will be discussed in connection with the corresponding tables.

If a symmetrical network having an odd number of stages, such as the 5-stage Butterworth prototype shown in Fig. 4.11, is bisected about its center into two networks, then mirror-image symmetry will exist as shown in Fig. 4.12. By multiplying the impedance of the right-hand side by R_r ohms and/or the impedance of the left-hand side by R_l ohms, the network may be scaled in impedance in either direction. Fig. 4.13 shows a scaling of the right-hand side to 10 ohms. Finally recombination of the two networks gives the unbalanced impedance prototype shown in Fig. 4.14. To accelerate filter design for unbalanced terminations, it is useful to develop tables for which[1] $0.1 \leq R_g \leq 10\,\Omega$ and $0.1 \leq R_L \leq 10\,\Omega$. To make the tables universal, a terminating impedance ratio, $\bar{R}$, is defined as:

$$\bar{R} = \frac{R_g}{R_L} = \frac{R_g}{1} = R_g, \text{ for } R_L = 1 \tag{4.30}$$

where R_g may take on convenient values between 0 and 1, such as 1/8, 1/4, 1/3, 1/2 and 1. For $\bar{R} = 1$, the network has balanced terminations and the previously presented Table 4.1 may be used. Thus, Table 4.2 gives the Butterworth prototype element values for $R_g = 1/8$, 1/4, 1/3, and 1/2 in which the values corresponding to an odd number of stages are obtained by the symmetrical bisection

[1] For situations in which $R_g \gg R_L$ or $R_g \ll R_L$, another set of tables can also be synthesized since the former approximates a current source and the latter a voltage source. This is discussed later.

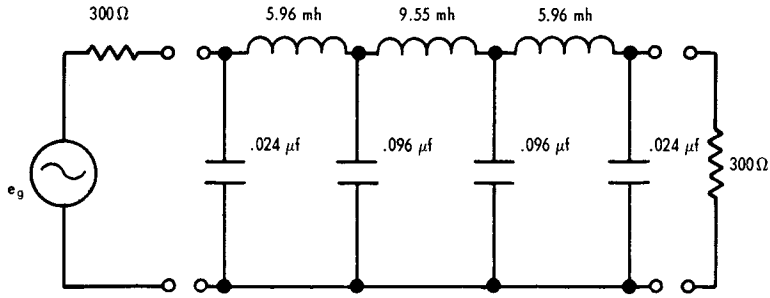

Figure 4.9. Seven-Stage Butterworth Low-Pass Filter with f_c = 10 kc

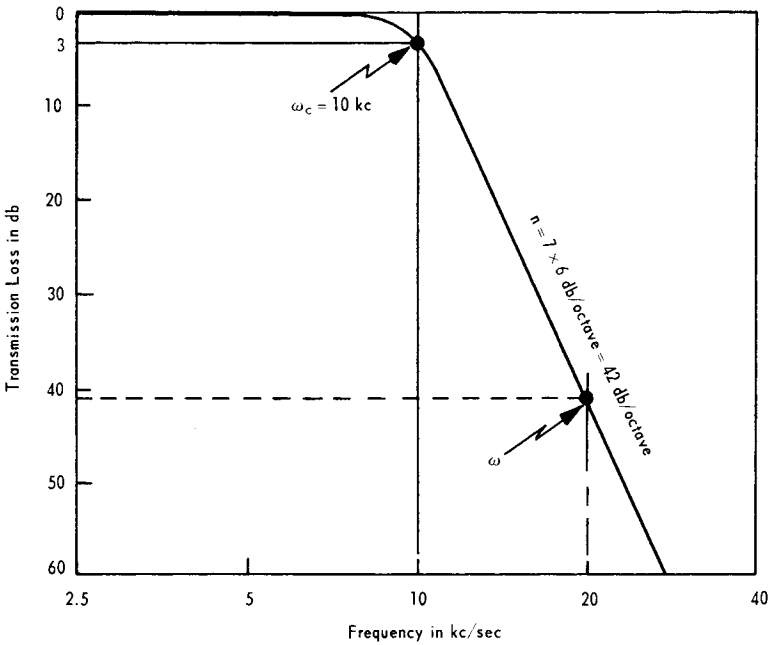

Figure 4.10. Frequency Response of Filter Depicted in Figure 4.9

process explained in connection with Fig. 4.14 and the values for the even number are obtained by resynthesizing the networks. The box shown at the bottom of Table 4.2 provides the interpretation of R_g; i.e., whether the values are in ohms or mhos.

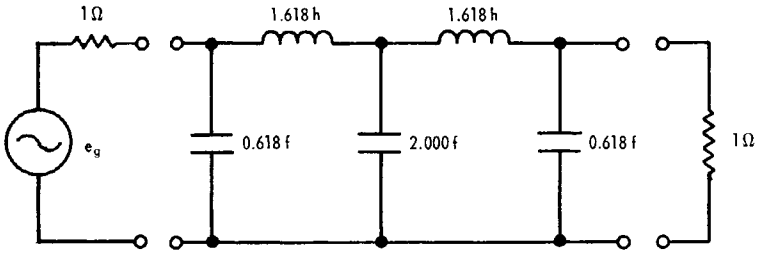

Figure 4.11. Five-Stage, Balanced Termination, Butterworth Prototype

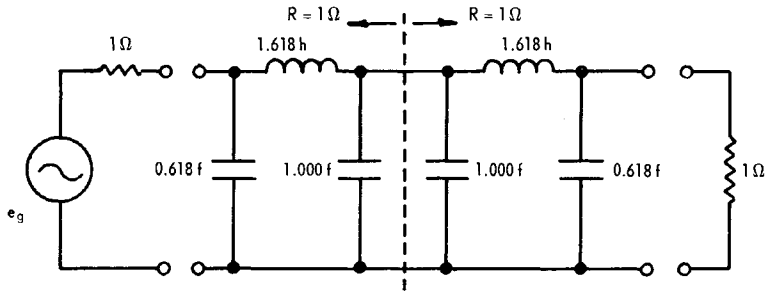

Figure 4.12. Bisection of Network Shown in Figure 4.11

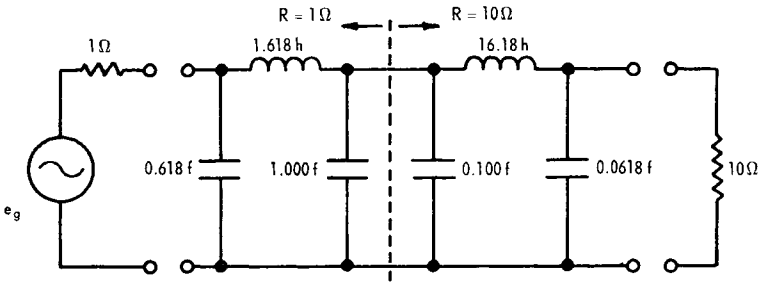

Figure 4.13. Impedance Leveling of Right-Hand Side to 10 Ω

Illustrative Example 4.4

Design a Butterworth, low-pass filter having a cut-off frequency of 10 mc, which provides a 50-db attenuation above 50 mc. The driving source impedance is 100 ohms and the output is terminated by an HF transistor which provides an equivalent 20-ohm

Table 4.2

ELEMENT VALUES FOR UNBALANCED SOURCE AND LOAD IMPEDANCES OF A NORMALIZED BUTTERWORTH LOW-PASS PROTOTYPE (Use for $0.1 \leq \bar{R} \leq 0.7$)*

n	C_1	L_2	C_3	L_4	C_5	L_6	C_7	L_8	C_9	L_{10}	R_g	R_L	n
					$\bar{R} = 1/8$ (Use for $0.1 \leq \bar{R} < 0.2$)								
1	9.000										0.125	1.000	1
2	0.094	11.976									0.125	1.000	2
3	8.000	1.125	1.000								0.125	1.000	3
4	0.069	14.541	0.897	1.253							0.125	1.000	4
5	4.944	0.202	9.000	1.618	0.618						0.125	1.000	5
6	0.052	9.826	0.208	10.642	1.441	0.697					0.125	1.000	6
7	3.560	0.156	14.416	1.125	1.802	1.247	0.445				0.125	1.000	7
8	0.041	7.755	0.189	16.520	0.947	1.990	1.246	0.483			0.125	1.000	8
9	2.778	0.125	12.257	0.235	9.000	1.879	1.532	1.000	0.347		0.125	1.000	9
10	0.034	6.430	0.161	13.541	0.223	10.492	1.697	1.567	1.026	0.370	0.125	1.000	10
					$\bar{R} = 1/4$ (Use for $0.2 \leq \bar{R} < 0.3$)								
1	5.000										0.250	1.000	1
2	0.199	6.274									0.250	1.000	2
3	4.000	1.250	1.000								0.250	1.000	3
4	0.140	7.173	1.032	1.205							0.250	1.000	4
5	2.472	0.405	5.000	1.618	0.618						0.250	1.000	5
6	0.104	4.929	0.423	5.735	1.465	0.687					0.250	1.000	6
7	1.780	0.312	7.208	1.250	1.802	1.247	0.445				0.250	1.000	7
8	0.082	3.890	0.380	8.127	1.087	1.948	1.247	0.480			0.250	1.000	8
9	1.389	0.250	6.128	0.470	5.000	1.879	1.532	1.000	0.347		0.250	1.000	9
10	0.068	3.223	0.323	6.771	0.453	5.657	1.727	1.561	1.024	0.368	0.250	1.000	10
					$\bar{R} = 1/3$ (Use for $0.3 \leq \bar{R} < 0.4$)								
1	4.000										0.333	1.000	1
2	0.276	4.828									0.333	1.000	2
3	3.000	1.333	1.000								0.333	1.000	3
4	0.189	5.339	1.124	1.174							0.333	1.000	4
5	1.854	0.539	4.000	1.618	0.618						0.333	1.000	5
6	0.139	3.705	0.570	4.505	1.479	0.680					0.333	1.000	6
7	1.335	0.416	5.406	1.333	1.802	1.247	0.445				0.333	1.000	7
8	0.110	2.924	0.507	6.038	1.183	1.924	1.247	0.477			0.333	1.000	8
9	1.042	0.333	4.596	0.627	4.000	1.879	1.532	1.000	0.347		0.333	1.000	9
10	0.091	2.422	0.431	5.078	0.610	4.446	1.745	1.557	1.023	0.367	0.333	1.000	10
					$\bar{R} = 1/2$ (Use for $0.4 \leq \bar{R} \leq 0.7$)								
1	3.000										0.500	1.000	1
2	0.448	3.346									0.500	1.000	2
3	2.000	1.500	1.000								0.500	1.000	3
4	0.291	3.515	1.313	1.117							0.500	1.000	4
5	1.236	0.809	3.000	1.618	0.618						0.500	1.000	5
6	0.212	2.483	0.872	3.268	1.503	0.666					0.500	1.000	6
7	0.890	0.624	3.604	1.500	1.802	1.247	0.445				0.500	1.000	7
8	0.166	1.959	0.764	3.962	1.376	1.881	1.246	0.472			0.500	1.000	8
9	0.695	0.500	3.064	0.940	3.000	1.879	1.532	1.000	0.347		0.500	1.000	9
10	0.137	1.621	0.649	3.387	0.930	3.233	1.777	1.548	1.020	0.365	0.500	1.000	10

n	L_1	C_2	L_3	C_4	L_5	C_6	L_7	C_8	L_9	C_{10}	R_g	R_L	n

Interpretation of R_g:

Input Element # 1	n = odd	n = even
Inductor	mhos	ohms
Capacitor	ohms	mhos

*Use Table 4.1 for $0.7 < \bar{R} \leq 1.0$
Use Table 4.3 for $\bar{R} < 0.1$

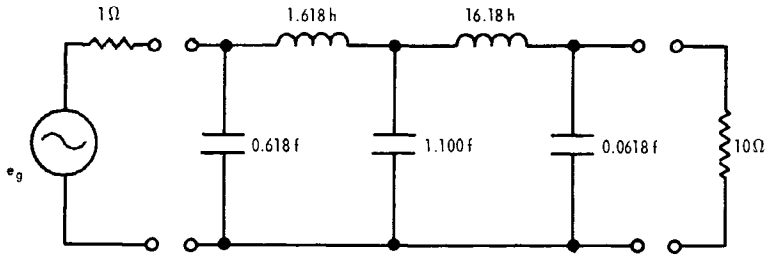

Figure 4.14. Recombination of Two Networks in Figure 4.13 to Yield Unbalanced, Five-Stage Butterworth Prototype

load. Thus, $\bar{R} = R_g/R_L = 100/20 = 5$. Since $\bar{R}$ is greater than unity, its reciprocal (0.2) is taken and the value interpretation will be in mhos. $\bar{R} = 1/4$ is chosen since 1/5 or 0.2 is closer to 1/4 than 1/8.

Fig. 4.5 indicates that for $\bar{\omega} = \omega_1/\omega_C = 50$ mc/10 mc = 5, and for a 50-db transmission loss, n = 3.7; 4 stages will be used. Returning to the bottom of Table 4.2 for n = 4 (even) and for an R_g interpretation of mhos, the input element must be a capacitor. Thus, Table 4.2 yields:

$C_1 = 0.140$ f

$L_2 = 7.173$ h

$C_3 = 1.032$ f

$L_4 = 1.205$ h

$R_g = 0.250$ mhos = 4 ohms (use 5 Ω as in example)

$R_L = 1.000$ ohms

Fig. 4.15 shows the prototype network. The dual of Fig. 4.15 may be formed by replacing all series inductances with shunt capacitances of the same values and vice versa. The resistances become conductances of the same value so that 5 ohms becomes 5 mhos or 0.2 ohms. Fig. 4.16 is the dual of Fig. 4.15 but cannot be used in the solution of the illustrative example since the source impedance must be five times the load impedance, not one-fifth. The application of network duality reverses the impedance ratio.

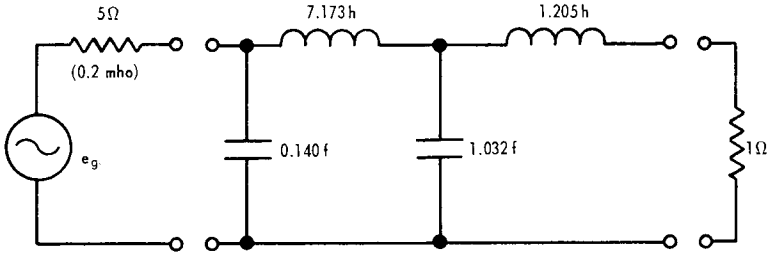

Figure 4.15. Unbalanced Butterworth Prototype (See Illustrative Example No. 4.4)

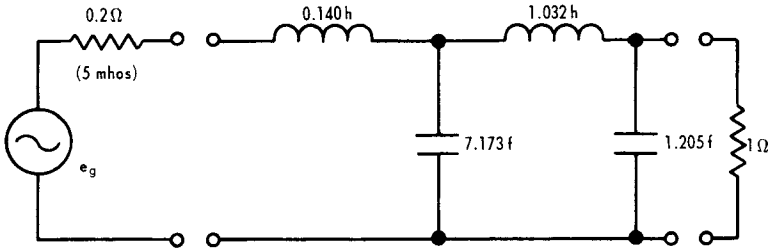

Figure 4.16. Dual of Figure 4.15

To demonstrate another variation of Fig. 4.15, the reciprocity theorem[1] may be employed in which the network is turned end-for-end and the sources and load are interchanged. If reciprocity is applied to Fig. 4.16, Fig. 4.17 results. Thus, reciprocity reinstates the desired source-to-load resistance ratio of five.

In the final solution of the illustrative example, either Fig. 4.15 or 4.17 may be used. Both will be used here so that element values may be compared.

From Fig. 4.15	From Fig. 4.17
$R'_g = R' R_g = 20 \times 5 = 100\,\Omega$	$100 \times 1 = 100\,\Omega$

[1]The reciprocity theorem states that for all linear bilateral networks, the ratio of excitation to response, with a single excitation applied at one point and the response observed at another, is invariant to an interchange of the points of excitation and observation.

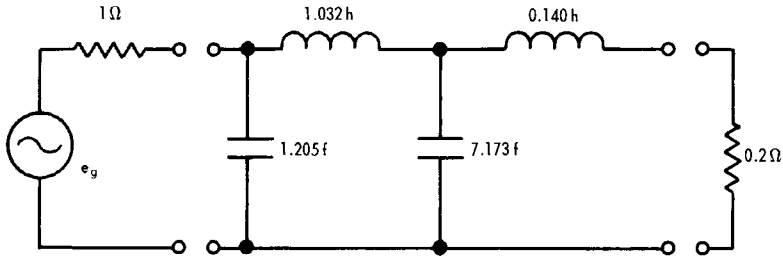

Figure 4.17. Application of Reciprocity to Figure 4.16

$$C_1' = \frac{C_1}{R\omega_c} = \frac{0.140\,\text{f}}{20 \times 2\pi \times 10^7} = 111\ \mu\mu\text{f} \qquad \frac{1.205\,\text{f}}{100 \times 2\pi \times 10^6} = 192\ \mu\mu\text{f}$$

$$L_2' = \frac{RL_2}{\omega_c} = \frac{20 \times 7.173\,\text{h}}{2\pi \times 10^7} = 2.28\ \mu\text{h} \qquad \frac{100 \times 1.032\,\text{h}}{2\pi \times 10^7} = 1.65\ \mu\text{h}$$

$$C_3' = \frac{C_3}{R\omega_c} = \frac{1.032\,\text{f}}{20 \times 2\pi \times 10^6} = 821\ \mu\mu\text{f} \qquad \frac{7.172\,\text{f}}{100 \times 2\pi \times 10^6} = 1142\ \mu\mu\text{f}$$

$$L_4' = \frac{RL_4}{\omega_c} = \frac{20 \times 1.205\,\text{h}}{2\pi \times 10^6} = 0.384\ \mu\text{h} \qquad \frac{100 \times 0.140\,\text{h}}{2\pi \times 10^6} = 0.223\ \mu\text{h}$$

The resulting low-pass filter networks are shown in Figs. 4.18 and 4.19. Either of these networks will give the desired response. The element values do not suggest any particular preference here.

When the ratio of source and load terminating resistance is less than 0.1, a voltage source is approximated. When this ratio is greater than 10, an equivalent current source exists. Thus, another set of tables can be prepared for these situations by executing the indicated synthesis procedure. It develops that it is also convenient to include in such tables of lossless single-end terminations, element values which correspond to associated finite loss (see Chap. 6, Sec. 6.1). Component loss serves to introduce insertion losses, to round off the sharp break of the response in the transition zone between pass and rejection bands, and to reduce the skirt slope or selectivity. While capacitors can be manufactured to have high Q_u-factors (e.g., Q_u's of 1,000–2,500), the Q_u-factor of inductors is considerably lower (cf.

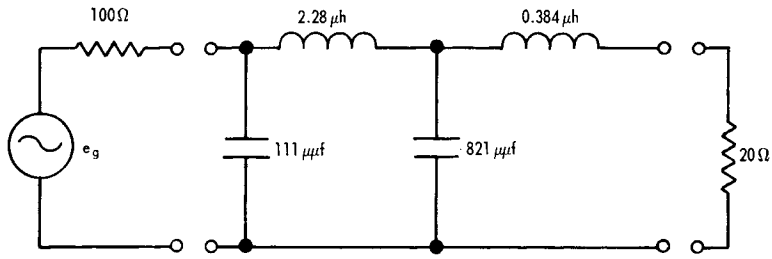

Figure 4.18. Four-Stage, Butterworth, Low-Pass Filter having a 10 mc Cut-Off Frequency (see Illustrative Example 4.4)

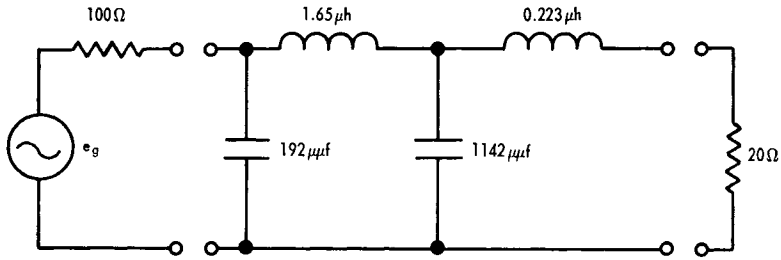

Figure 4.19. Variation of Four-Stage, Butterworth, Low-Pass Filter (cf. Fig. 4.18 and Illustrative Example 4.4)

Chap. 6). Thus, the technique of predistortion is used in the synthesis process in which s−d is substituted for s in the transfer function. After the element values are synthesized, s+d is substituted for s to remove the effect of the predistortion and a corresponding change is made in network element values. By carrying out the indicated predistortion synthesis process, Table 4.3 results.

Table 4.3 has been prepared for six values of $\overline{Q}$: ∞, 50, 30, 20, 10, and 5, where $\overline{Q}$ is the component Q_u-factor for low- and high-pass filters and $\overline{Q} = Q_u/Q_L$ for band-pass and band-rejection filters (Q_L is the loaded Q of the filter; viz, $Q_L = f_o/f_c$ − cf. Chaps. 5 and 6).

Illustrative Example 4.5

A cathode follower, providing a source resistance of about 100 ohms, is driving a 5K load termination. A 100-kc signal to be passed is rich in harmonics and the harmonic suppression requirements indicate that at least a 20-db attenuation is needed at

Table 4.3
ELEMENT VALUES FOR UNBALANCED TERMINATIONS ($\bar{R}$ < 0.1 ohms/mhos)* OF A NORMALIZED LOW-PASS BUTTERWORTH PROTOTYPE HAVING UNIFORM DISSIPATION

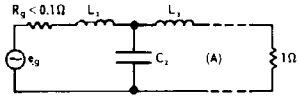

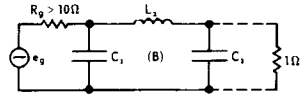

n	C_1	L_2	C_3	L_4	C_5	L_6	C_7	L_8	C_9	L_{10}	n
$\bar{Q} = \infty$ (Use for $\bar{Q} \geq 100$)											
1	1.000										1
2	1.414	0.707									2
3	1.500	1.333	0.500								3
4	1.531	1.577	1.082	0.383							4
5	1.545	1.694	1.382	0.894	0.309						5
6	1.553	1.759	1.553	1.202	0.758	0.259					6
7	1.558	1.799	1.659	1.397	1.055	0.656	0.223				7
8	1.561	1.825	1.729	1.528	1.259	0.937	0.578	0.195			8
9	1.563	1.842	1.777	1.620	1.404	1.141	0.841	0.516	0.174		9
10	1.564	1.855	1.812	1.687	1.510	1.292	1.041	0.763	0.465	0.156	10
$\bar{Q} = 50$ (Use for $40 \leq \bar{Q} < 100$)											
1	1.021										1
2	1.413	0.728									2
3	1.484	1.361	0.516								3
4	1.499	1.600	1.111	0.395							4
5	1.504	1.712	1.412	0.920	0.319						5
6	1.502	1.727	1.581	1.232	0.780	0.267					6
7	1.496	1.808	1.684	1.428	1.084	0.676	0.230				7
8	1.488	1.830	1.752	1.558	1.290	0.964	0.595	0.201			8
9	1.480	1.845	1.798	1.649	1.435	1.171	0.866	0.532	0.179		9
10	1.471	1.855	1.831	1.714	1.541	1.324	1.069	0.785	0.480	0.161	10
$\bar{Q} = 30$ (Use for $25 \leq \bar{Q} < 40$)											
1	1.035										1
2	1.413	0.742									2
3	1.473	1.379	0.526								3
4	1.482	1.616	1.130	0.403							4
5	1.476	1.724	1.433	0.938	0.326						5
6	1.465	1.781	1.601	1.253	0.796	0.273					6
7	1.451	1.815	1.703	1.450	1.104	0.690	0.235				7
8	1.436	1.835	1.769	1.580	1.311	0.982	0.608	0.206			8
9	1.420	1.849	1.813	1.669	1.457	1.192	0.883	0.543	0.183		9
10	1.403	1.858	1.845	1.733	1.563	1.346	1.089	0.801	0.490	0.165	10

n	L_1	C_2	L_3	C_4	L_5	C_6	L_7	C_8	L_9	C_{10}	n

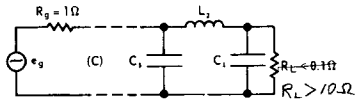

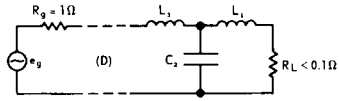

*Use Table 4.1 for $0.7 < \bar{R} \leq 1.0$
Use Table 4.2 for $0.1 \leq \bar{R} \leq 0.7$

Table 4.3 (Continued)
ELEMENT VALUES FOR UNBALANCED TERMINATIONS ($\bar{R}$ < 0.1 ohms/mhos)* OF A NORMALIZED LOW-PASS BUTTERWORTH PROTOTYPE HAVING UNIFORM DISSIPATION

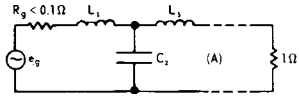

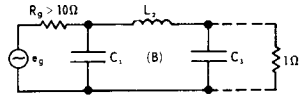

n	C_1	L_2	C_3	L_4	C_5	L_6	C_7	L_8	C_9	L_{10}	n
					$\bar{Q} = 20$ (Use for $15 \le \bar{Q} < 25$)						
1	1.053										1
2	1.410	0.761									2
3	1.457	1.403	0.541								3
4	1.455	1.636	1.156	0.414							4
5	1.439	1.740	1.460	0.961	0.335						5
6	1.417	1.794	1.627	1.280	0.817	0.281					6
7	1.392	1.825	1.727	1.478	1.130	0.708	0.241				7
8	1.366	1.844	1.791	1.607	1.340	1.007	0.624	0.212			8
9	1.339	1.857	1.835	1.696	1.486	1.219	0.906	0.558	0.188		9
10	1.310	1.866	1.867	1.760	1.592	1.374	1.115	0.822	0.504	0.170	10
					$\bar{Q} = 10$ (Use for $8 \le \bar{Q} < 15$)						
1	1.111										1
2	1.398	0.824									2
3	1.402	1.481	0.588								3
4	1.362	1.701	1.240	0.452							4
5	1.309	1.795	1.549	1.039	0.366						5
6	1.250	1.844	1.714	1.372	0.886	0.306					6
7	1.185	1.878	1.813	1.573	1.217	0.770	0.264				7
8	1.114	1.908	1.880	1.704	1.435	1.088	0.680	0.231			8
9	1.036	1.943	1.931	1.794	1.584	1.311	0.981	0.608	0.206		9
10	0.951	1.991	1.976	1.860	1.692	1.471	1.203	0.892	0.549	0.185	10
					$\bar{Q} = 5$ (Use for $3 \le \bar{Q} < 8$)						
1	1.330										1
2	1.340	0.986									2
3	1.250	1.667	0.714								3
4	1.113	1.879	1.459	0.552							4
5	0.945	2.018	1.796	1.243	0.447						5
6	0.731	2.258	2.008	1.621	1.070	0.375					6
7	0.422	3.177	2.233	1.862	1.453	0.924	0.323				7

n	L_1	C_2	L_3	C_4	L_5	C_6	L_7	C_8	L_9	C_{10}	n

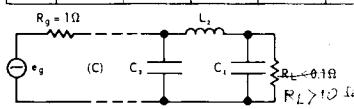

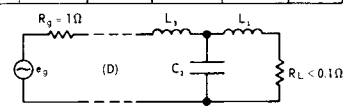

*Use Table 4.1 for $0.7 < \bar{R} \le 1.0$
Use Table 4.2 for $0.1 \le \bar{R} \le 0.7$

the second harmonic and a 50-db attenuation is required for harmonic suppression at and above 1 mc. No more than a 3-db attenuation to the 100-kc signal is permitted, i.e., $f_c \geq 100$ kc. The problem involves designing a suitable maximally-flat, low-pass filter to insert between the cathode follower output and the 5 K ohm load.

From the requirement that $f_c \geq 100$ kc, the pass-band attenuation may be kept less than 3 db to the 100-kc signal of interest, if f_c is chosen somewhat greater than 100 kc. At 100 kc:

$$\bar{\omega}\Big|_{20\,db} = \frac{\omega_1}{\omega_c} = \frac{2\pi \times 200\text{ kc}}{2\pi \times 100\text{ kc}} = 2.0.$$

From Fig. 4.5, for 20 db and $\bar{\omega} = 2.0$, $n = 3.3$. Thus, $n = 4$ is a minimum. Also from Fig. 4.5, the 20-db transmission loss for $n = 4$ corresponds to $\bar{\omega}' = 1.75$. Thus:

$$\bar{\omega}'\Big|_{20\,db} = \frac{\omega_1}{\omega_c'} = 1.75 \text{ or } f_c' = \frac{200\text{ kc}}{1.75} = 114\text{ kc}.$$

It is concluded that 100 kc $\leq f_c \leq$ 114 kc will simultaneously give no more than a 3-db attenuation at 100 kc, and at least 20 db at 200 kc. The cut-off frequency is chosen at $f_c = 110$ kc. For $n = 4$, this has an attenuation at $\bar{\omega}_2|_{50db} = \omega_2/\omega_c = 2\pi \times 1000$ kc/ $2\pi \times 110$ kc $= 9.1$ or more than 70 db according to Fig. 4.5, which readily satisfies the other rejection requirement. Thus, for $n = 4$ (use $\bar{Q} \geq 100$), Table 4.3 indicates that:

$$L_1 = 1.531\,h$$
$$C_2 = 1.577\,f$$
$$L_3 = 1.082\,h$$
$$C_4 = 0.383\,f$$

Network (A) or (C) may be chosen in Table 4.3 since the load resistance is much greater than the source resistance. Network (A) is used in this example. Scaling the load from 1 ohm to 5 KΩ and the cut-off frequency from 1 radian to $\omega_c = 2\pi \times 110 \times 10^3$ radians, yields:

$$L_1' = \frac{R_L L_1}{\omega_c} = \frac{5 \times 10^3 \times 1.531}{2\pi \times 110 \times 10^3} = 11.1\text{ mh}$$

$$C_2' = \frac{C_2}{R_L \omega_c} = \frac{1.577}{5 \times 10^3 \times 2\pi \times 110 \times 10^3} = 456\,\mu\mu f$$

$$L_3' = \frac{R_L L_3}{\omega_c} = \frac{5 \times 10^3 \times 1.082}{2\pi \times 110 \times 10^3} = 7.84\,\text{mh}$$

$$C_4' = \frac{C_4}{R_L \omega_c} = \frac{0.383}{5 \times 10^3 \times 2\pi \times 110 \times 10^3} = 111\,\mu\mu f.$$

The complete filter is shown in Fig. 4.20 and its response is depicted in Fig. 4.21.

In addition to illustrating the application of unbalanced source and terminations in filter design, the previous example showed the flexibility required in choosing the cut-off frequency, ω_c in order to assure that the pass-band transmission loss and band rejection are simultaneously satisfied. In order to remove the trial tests on ω_c as indicated above, a more formal approach is possible in which ω_c can be determined explicitly to satisfy the requirements of both transmission losses.

The pass-band transmission gain, G_i, of a Butterworth response is:

$$G_i = \frac{1}{1 + \left(\frac{f_s}{f_c}\right)^{2n}} = \text{a numeric} \leq 1 \qquad (4.31)$$

where, f_s = signal frequency of interest

f_c = cut-off frequency.

The desired band-rejection transmission loss, G_r, at frequency f_1, is:

$$G_r = \frac{1}{1 + \left(\frac{f_1}{f_c}\right)^{2n}} \approx \left(\frac{f_c}{f_1}\right)^{2n} \text{ for } \left(\frac{f_1}{f_c}\right)^{2n} \gg 1. \qquad (4.32)$$

The transmission gain in db is:

$$G_r = 10 \log_{10}\left(\frac{f_c}{f_1}\right)^{2n} = -10 \log_{10}\left(\frac{f_1}{f_c}\right)^{2n}. \qquad (4.33)$$

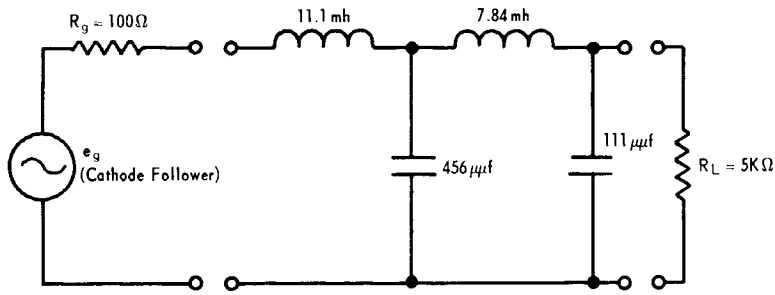

Figure 4.20. Four-Stage Butterworth, Low-Pass Filter Driven by Voltage Source

The transmission loss in db, $L_r = -G_r$, is:

$$L_r = 10 \log_{10}\left(\frac{f_1}{f_c}\right)^{2n}. \tag{4.34}$$

Since G_p, L_r, f_s, and f_1 are known for nearly all applications and since f_c and n are to be determined, Eqs. (4.31) and (4.34) may be solved simultaneously to yield:

$$n = \frac{L_r + 10 \log_{10}\left(\frac{G_i}{1 - G_i}\right)}{20 \log_{10}\left(\frac{f_1}{f_s}\right)} \tag{4.35}$$

$$f_1 = f_c \times 10 \exp\left[\frac{L_r \log_{10}\left(\frac{f_1}{f_s}\right)}{L_r + 10 \log_{10}\left(\frac{G_i}{1 - G_i}\right)}\right]. \tag{4.36}$$

It is remembered that there exists an infinite number of solutions to the choice of n and f_c, but Eqs. (4.35) and (4.36) yield the lowest n, and Eq. (4.36) is the corresponding f_c. To facilitate computation and selection of n and f_c, Figs. 4.22 through 4.26 depict the plots of Eqs. (4.35) and (4.36) for L_r = 20, 30, 40, 50, and 60 db.

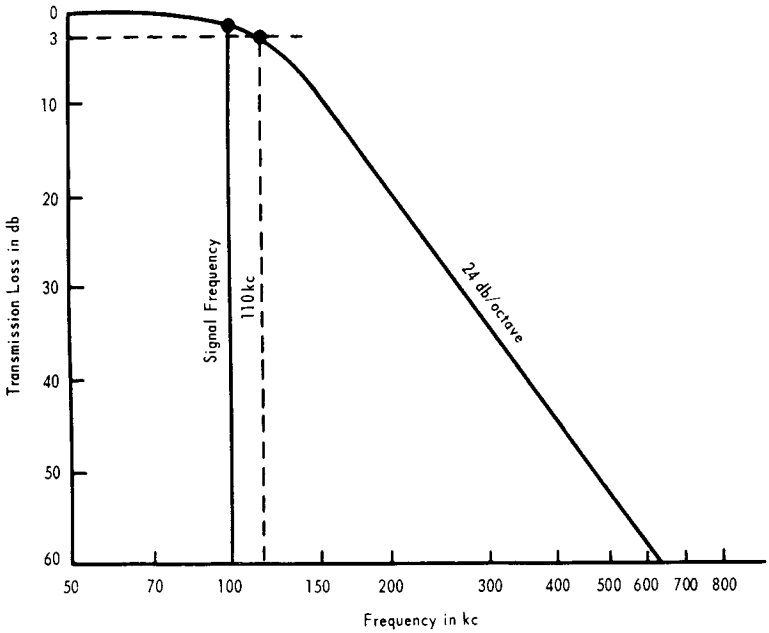

Figure 4.21. Transmission Response of Four-Stage Filter Depicted in Figure 4.20

Illustrative Example 4.6

Let it be required to filter harmonics emanating from a 400-cps, 120-volt, 5-kva generator in such a way that frequency components at and above 5 kc are reduced by 40 db. The voltage regulation of the 400-cps generator corresponds to a 10% drop from no load to full load. Expected load variation is from 20% to 80%. The transmission loss of the required low-pass filter at full load shall correspond to a voltage drop not to exceed 1.5 volts.

A 20% to 80% load variation corresponds to an arithmetic mean of 50%. Since a 10% voltage drop at the load corresponds to the variation from no load to full load, a 50% load variation corresponds to about 50% × 10% or a 5% voltage drop change. Consequently, the load resistance, corresponding to a 50% load, is 100% − 5% or 95% of the combined generator and load resistance; viz, $R_L = 0.95(R_L + R_g)$ or $R_L = 19\ R_g$.

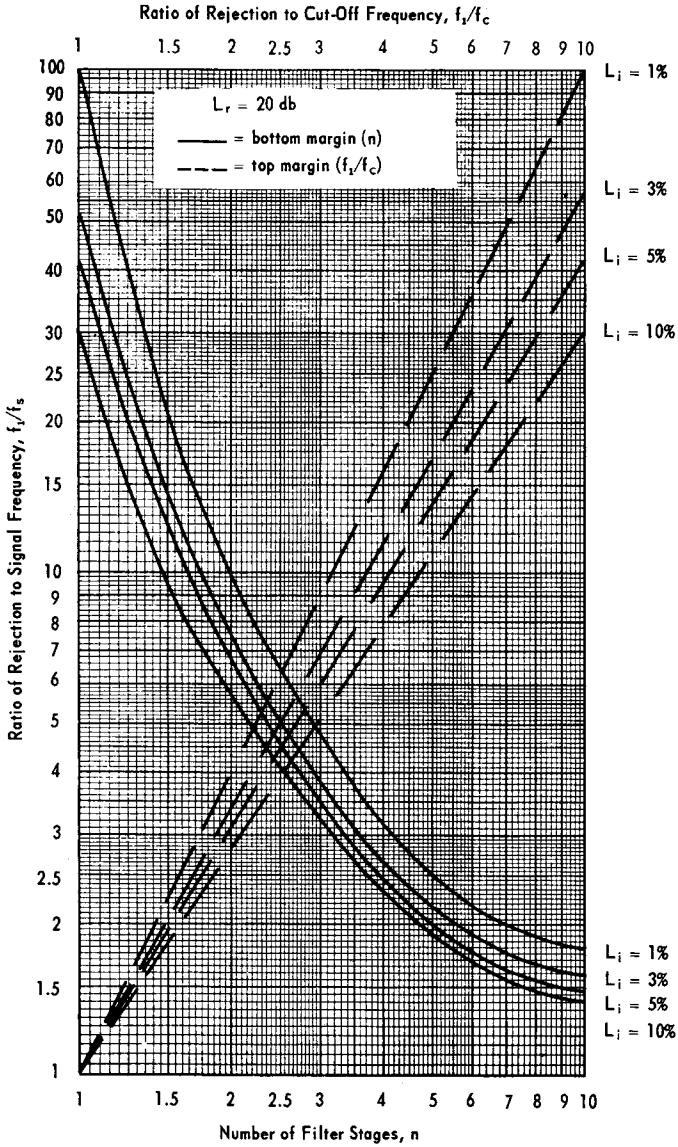

Figure 4.22. Number of Stages and Cut-Off Frequency for L_r = 20 db

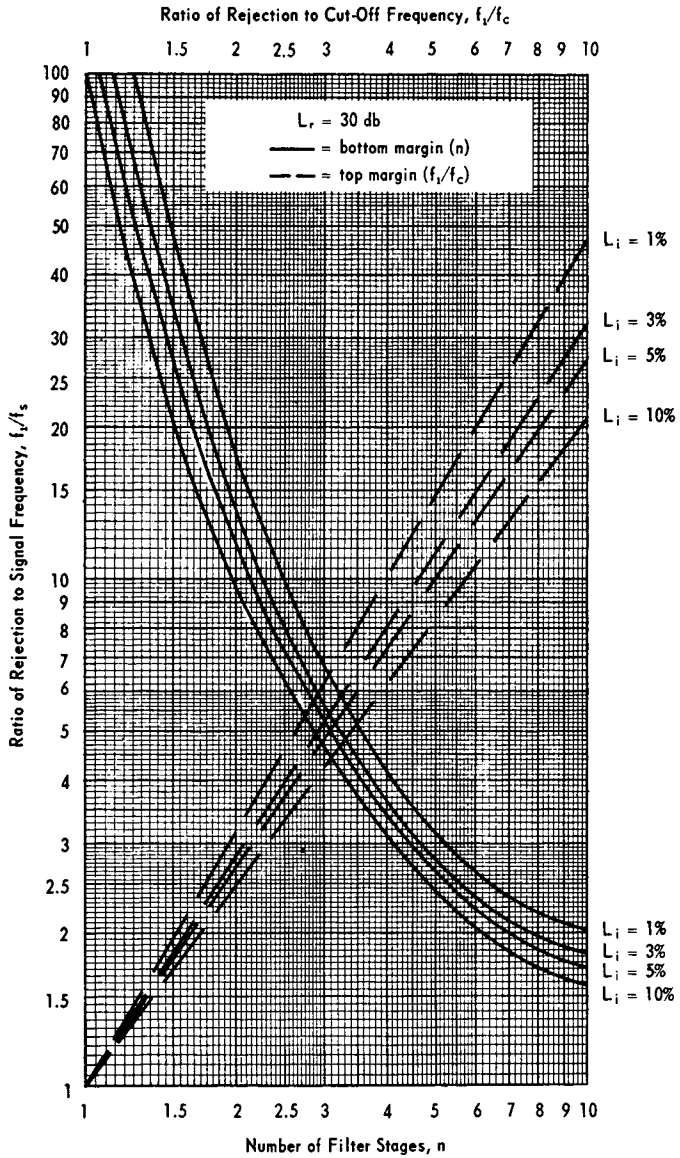

Figure 4.23. Number of Stages and Cut-Off Frequency for L_r = 30 db

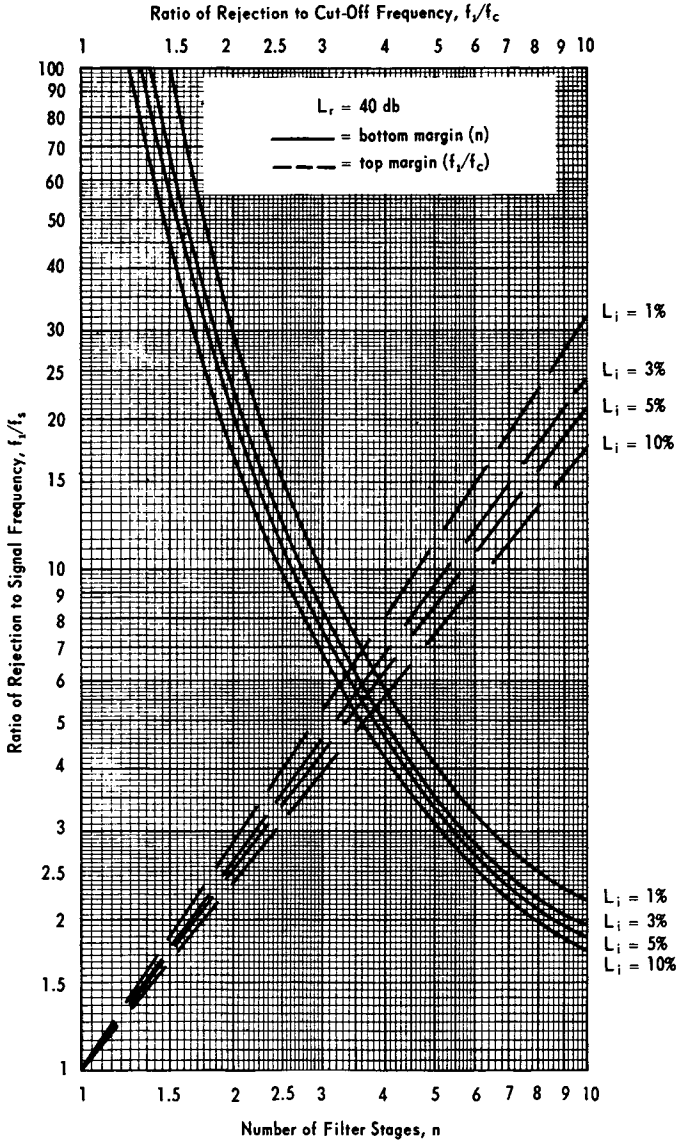

Figure 4.24. Number of Stages and Cut-Off Frequency for L_r = 40 db

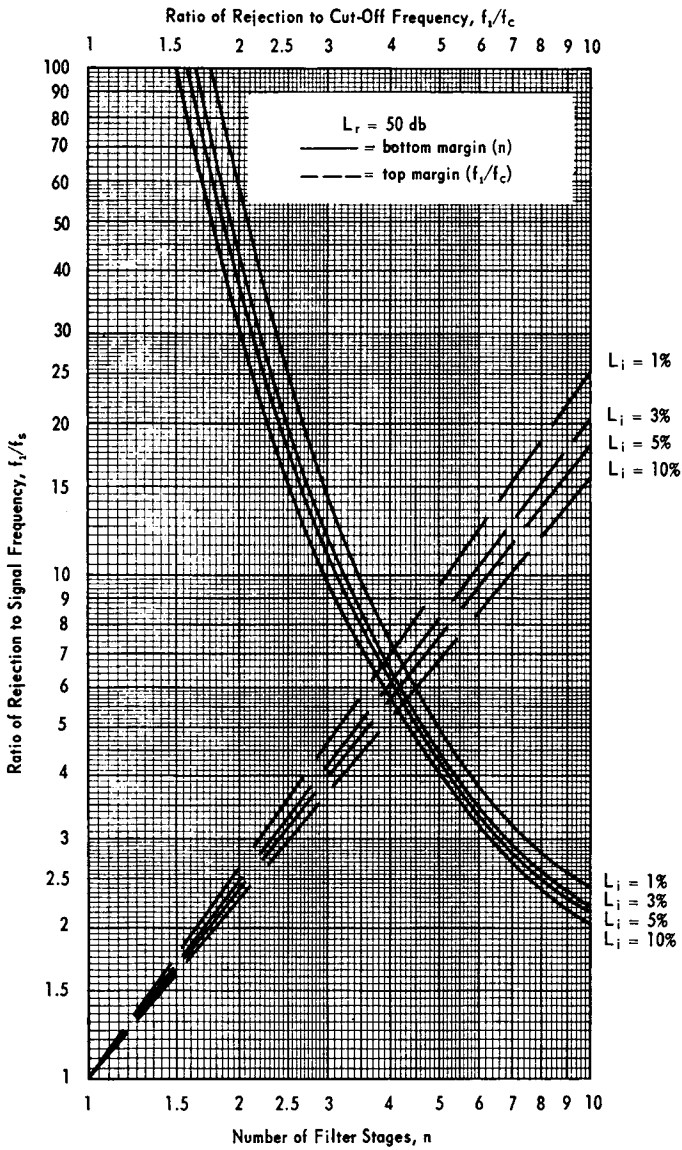

Figure 4.25. Number of Stages and Cut-Off Frequency for L_r = 50 db

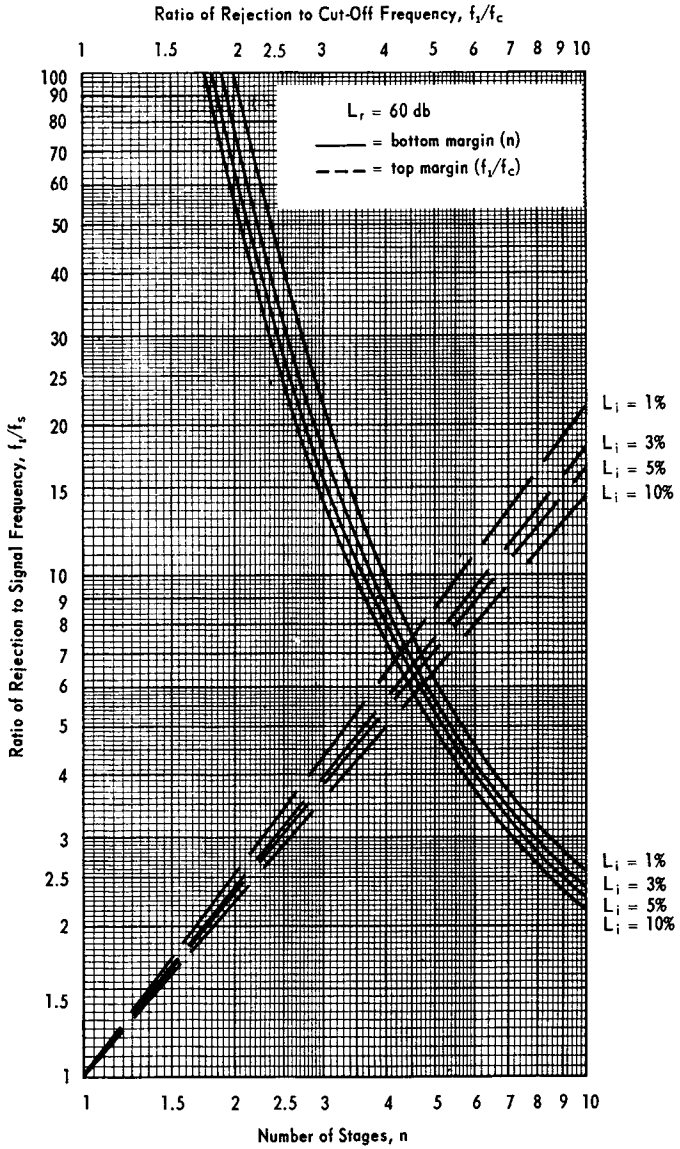

Figure 4.26. Number of Stages and Cut-Off Frequency for L_r = 60 db

At 50% load, the current, I_{50}, is:

$$I_{50} = \frac{0.5P}{E} \approx \frac{0.5 \times 5{,}000}{120} = 20.8 \text{ amperes}$$

and $$R_L = \frac{0.95 \times E}{I_{50}} = \frac{114}{20.8} \approx 5.5\,\Omega \text{ (mean load).}$$

Since L_r = 40 db at 5 kc, L_i = 1.5-volt drop/120 volts = 1-1/4% at 400 cps, and f_1/f_S = 5000/400 or 12.5, Fig. 4.24 shows that n = 2.7 stages and $f_1/f_C \approx 5.5$. Since only a discrete number of stages can be used, n = 3 is chosen; this also yields better performance of both pass- and rejection-band losses. Thus for n = 3, Fig. 4.24 now indicates f_1/f_S = 9.9 and f_1/f_C = 4.6 for L_i = 1%. Thus:

$$f_C = f_1/4.6 = 9.9\, f_S/4.6 = 2.15\, f_S = 2.15 \times 400 = 860 \text{ cps.}$$

To confirm the adequacy of attenuation for n = 3 at f_1 = 5 kc, $f = f_1/f_C$ = 5000/860 = 5.8, the transmission loss shown in Fig. 4.5 indicates L_r = 45 db or 5 db more than enough.

As in the preceding example of a voltage source, network (A) or (C) of Table 4.3 may be used. To minimize insertion loss, network (C) is chosen since only one inductor is required for n = 3. Here let it be supposed that the average Q_u of the components is 80, so that $\bar{Q}$ = 50 is used; in Table 4.3 viz,

$$C_1 = 1.484\,\text{f}$$
$$L_2 = 1.361\,\text{h}$$
$$C_3 = 0.516\,\text{f.}$$

Finally, for f_C = 860 cps and R_L = 5.5 Ω (see above):

$$C_1' = \frac{C_1}{R_L \omega_C} = \frac{1.484}{5.5 \times 2\pi \times 860} = 50\,\mu\text{h}$$

$$L_2' = \frac{R_L L_2}{\omega_C} = \frac{5.5 \times 1.361}{2\pi \times 860} = 1.39\,\text{mh}$$

$$C_3' = \frac{C_3}{R_L \omega_C} = \frac{0.516}{5.5 \times 2\pi \times 860} = 17.5\,\mu\text{f.}$$

4.1.3 Transient Response and Time Delay

Any transmission line or network, lumped or distributed, will have an associated time delay. Insofar as LC filters are concerned, this delay may be a few orders of magnitude greater than an equal length of physical transmission line and is dependent upon the bandwidth and number of stages. The delay time is part of the more general overall transient properties. Thus far in this handbook, nearly all filter performance considerations have been in terms of the steady-state properties, which are generally treated in the frequency domain. Since the amplitude and phase vs. frequency characteristics could be satisfactory and the transient response unacceptable, it is necessary to give some brief considerations regarding the latter now.

The time delay, τ_d, of a network, is:

$$\tau_d = \frac{d\phi}{d\omega} \tag{4.37}$$

where, ϕ is the phase angle (see Fig. 4.27).

Fig. 4.27 shows that the phase angle of a single stage, low-pass filter at any frequency, ω, is:

$$\phi = \tan^{-1} \omega/B. \tag{4.38}$$

Thus, applying Eq. (4.38) to (4.37) yields:

$$\tau_d = -\frac{d}{d\omega}(\tan^{-1} \omega/B)$$

$$= -\frac{1/B}{1 + (\omega/B)^2}. \tag{4.39}$$

From Eq. (4.39) the time delay at $\omega = 0$ and $\omega = B$ are:

$$\tau_d\Big|_{\omega = 0} = \frac{1/B}{1 + 0} = \frac{1}{B} \tag{4.40}$$

$$\tau_d\Big|_{\omega = B} = \frac{1/B}{1 + 1} = \frac{1}{2B}. \tag{4.41}$$

It can be shown that the time delay of an n-stage, Butterworth low-pass filter is:

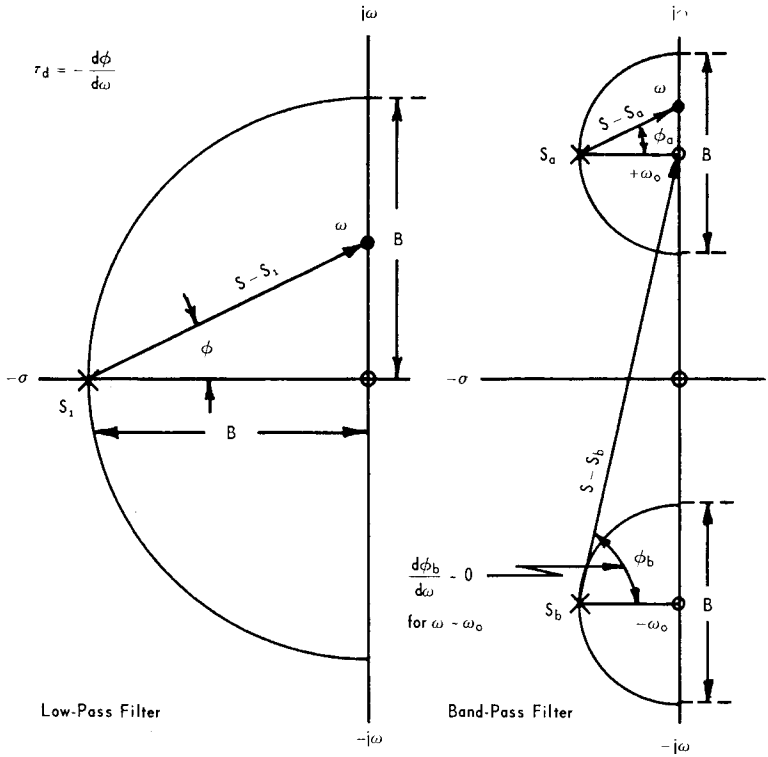

Figure 4.27. Phase Angle, ϕ, Used in Computing Time Delay

$$\tau_d = \frac{\frac{1}{B}\sum_{k=1}^{n} \frac{\left(\frac{\omega}{B}\right)^{2k-2}}{\sin\,(2k-1)\frac{\pi}{2n}}}{1+\left(\frac{\omega}{B}\right)^{2n}} \quad \text{for any } \omega. \tag{4.42}$$

The center frequency delay of the n-stage, low-pass filter is obtained by setting $\omega = 0$ after the indicated operation in Eq. (4.42) is carried out; viz,

$$\tau_d = \frac{1}{B \sin \pi/2n} \text{ seconds} \tag{4.43}$$

$$\approx \frac{2n}{\pi B} = 0.636n/B \text{ for } n > 3. \tag{4.44}$$

Eq. (4.44) is plotted in Fig. 4.28 for an n-stage, Butterworth low-pass filter. Fig. 4.28 also shows the band-edge ($\omega = B$) time delay for n stages. Note the substantial delay distortion from center to edge which corresponds to a slope ratio of about 4.5. The delay time for a band-pass filter of bandwidth B is exactly twice as great for a low-pass filter of bandwidth B.

Fig. 4.29 shows the transient response of a Butterworth low-pass filter to both an impulse and step driving function for n equals one through ten stages. Since the impulse response is the time derivative of the step response, the impulse response curves provide a means of estimating the rate of rise of the step response curves.

Fig. 4.29 indicates that the impulse response of a ten-stage Butterworth filter corresponds to a time delay of about 7 seconds for a 1-rad/sec bandwidth. Fig. 4.28 shows that the midband delay was about 6.4 seconds and that at band-edge it was about 24 seconds. The integrated or average delay over the band is the seven-second value shown in Fig. 4.29. While these transient distortions may seem high, it will be shown later that they are considerably less than those of the Tchebycheff response.

4.2 TCHEBYCHEFF PROTOTYPE

4.2.1[1] Synthesis of Tchebycheff Function

A second transfer function, based on the Tchebycheff polynomial, $T_n(\omega)$, which causes an equal-ripple, oscillatory behavior in the pass-band in the complex-frequency plane, is the following Tchebycheff low-pass prototype function:

$$|t_T(j\omega)|^2 = \frac{1}{1 + \epsilon^2 T_n^2(\omega)} \tag{4.45}$$

[1]This section may be omitted by the technologist who is only interested in design and realization of filters. Start reading Sec. 4.2.2.

where, ϵ^2 is the ripple tolerance in the pass-band and expressed in db,

$$\epsilon_{db} = -10 \log (1 + \epsilon^2) \tag{4.46}$$

$T_n(\omega)$ is chosen as the Tchebycheff polynomial of the first kind.

By substituting Eq. (4.45) into Eq. (4.2), the power reflection coefficient of the Tchebycheff function becomes:

$$|p(j\omega)|^2 = 1 - \frac{1}{1 + \epsilon^2 T_n^2(\omega)} = \frac{\epsilon^2 T_n^2(\omega)}{1 + \epsilon^2 T_n^2(\omega)}. \tag{4.47}$$

Following a derivation similar to the Butterworth, the left-half plane zeros of Eq. (4.47) are:

$$s_{zm} = -j\cos \frac{(2m-1)\pi}{2n}, \quad m = 1,2 \ldots n. \tag{4.48}$$

The poles of Eq. (4.47) are all the complex roots of $1 + \epsilon^2 T_n^2(\omega) = 0$ and lie on the periphery of an ellipse having a semi-major axis of $\omega_n(\epsilon)$ and a semi-minor axis of $\sigma_n(\epsilon)$, as shown in Fig. 4.30. The same method for finding the zeros and poles of the Butterworth function (cf. Eqs. (4.14)–(4.16)) is followed for the Tchebycheff function. The details are somewhat more extensive, however, and the results only are presented. The left-half, s-plane poles of Eq. (4.47) or $|p(j\omega)|$ are:

$$s_{pk} = -\sin \frac{(2k-1)\pi}{2n} \sinh \phi + j\cos \frac{(2k-1)\pi}{2n} \cosh \phi \tag{4.49}$$

where, k is the kth pole in an integer number, n, of stages

$$\sinh \phi \, \frac{(\alpha + \beta)^{1/n} - (\alpha - \beta)^{1/n}}{2} \approx \frac{\beta}{n\alpha^{1-1/n}} \text{ for large n} \tag{4.50}$$

$$\cosh \phi = \frac{(\alpha + \beta)^{1/n} + (\alpha - \beta)^{1/n}}{2} \approx \alpha^{1/n} \text{ for large n} \tag{4.51}$$

$$\alpha = \sqrt{1 + 1/\epsilon^2} \text{ and } \beta = 1/\epsilon. \tag{4.52}$$

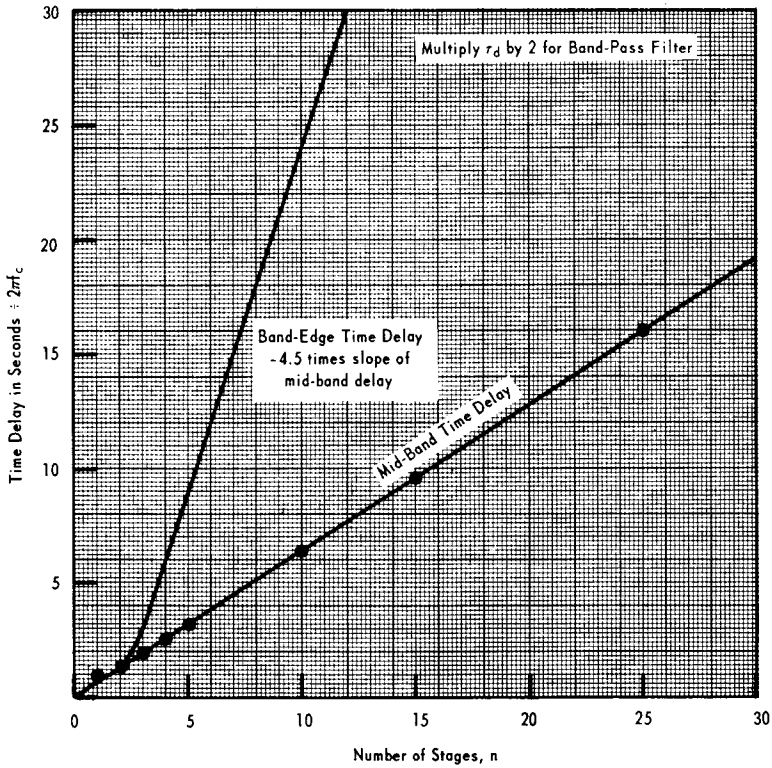

Figure 4.28. Mid-Band and Band-Edge Time Delay of Butterworth, Low-Pass Filter

Finally, the voltage reflection coefficient, $p(j\omega)$, and driving-point impedance, Z_{11}, are calculated as before in Eqs. (4.10) and (4.11) respectively.

Illustrative Example 4.7

Assume a low-pass prototype having a Tchebycheff response is desired for n = 3 and a 3-db pass-band, ripple tolerance. The synthesis technique is identical to the Butterworth; using Eqs. (4.50) to (4.52) the results are:

$\epsilon = 3$ db; $\alpha = \sqrt{2}$, $\beta = 1$; $\sinh \phi = 0.298$ and $\cosh \phi = 1.043$.

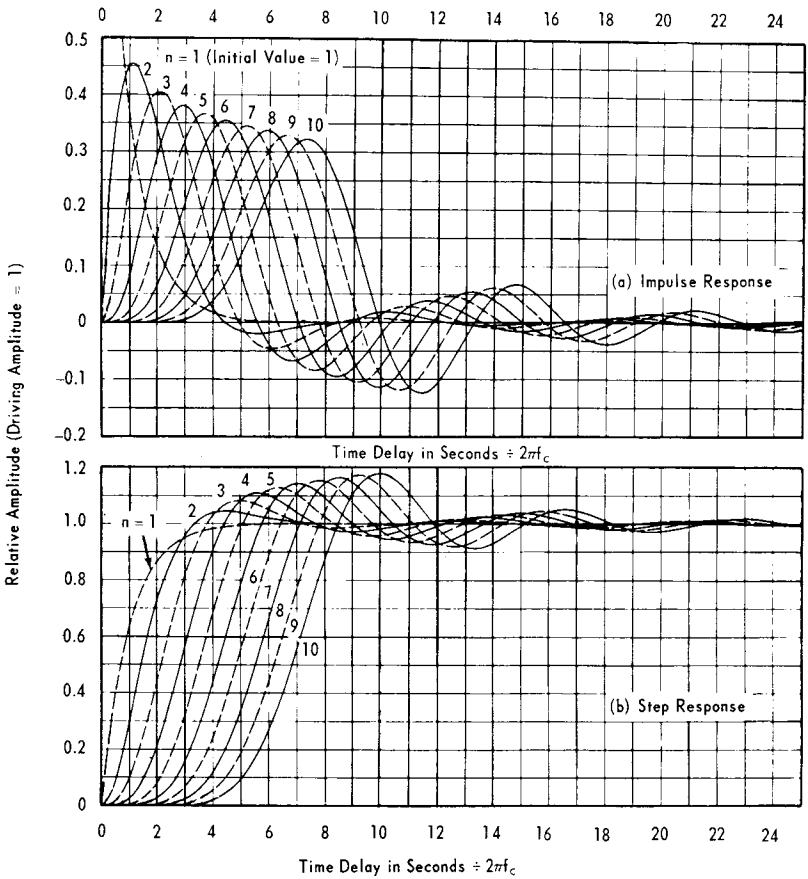

Reprinted from: "Transient Responses of Conventional Filters" by K.W. Henderson & W.H. Kautz, pp. 334, 335, & 337. IRE Transactions on Circuit Theory, Vol. CT-5, Mo. 4, December, 1958. Copyright 1959– The Institute of Radio Engineers, Inc.

Figure 4.29. Transient Response of Low-Pass Butterworth Filter having a Bandwidth of f_c cps

From Eqs. (4.48) and (4.49):

$$s_{z_1} = -j0.866 \qquad s_{p_1} = -0.149 + j0.903$$
$$s_{z_2} = -j0 \qquad s_{p_2} = -0.298$$
$$s_{z_3} = j0.866 \qquad s_{p_3} = -0.149 - j0.903.$$

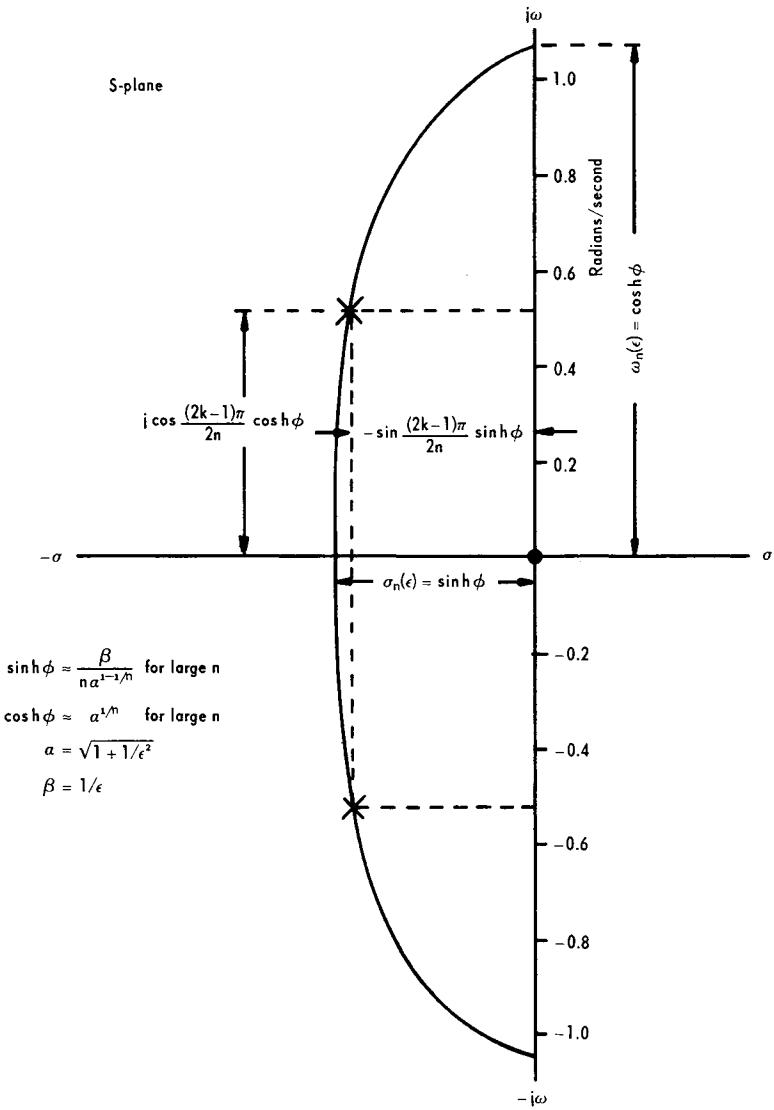

Figure 4.30. Pole Location on the Tchebycheff Semi-Ellipse

From Eqs. (4.10) and (4.11):

$$Z_{11} = \frac{0.596s^2 + 0.177s + 0.250}{2s^2 + 0.596s^2 + 1.667s + 0.250}.$$

By continuous fraction expansion (cf. Eq. 4.23):

$$Z_{11} = \cfrac{1}{3.36s + \cfrac{1}{0.71s + \cfrac{1}{3.36s + 1.}}}$$

The synthesized network, therefore, consists of an input and output shunt capacitance of 3.36 farads, a center series inductance of 0.71 henrys, and a terminating resistance of 1 ohm, as shown in Fig. 4.31. The associated steady-state frequency response is shown in Fig. 4.32.

As in the case of Butterworth prototype, the coefficients of the L's and C's in the Tchebycheff prototype network terminated at both ends are symmetrical from both ends to the middle. It develops, however, that both the source and terminating impedance are not equal to one ohm when the number of stages is even; equality exists when the number is odd. While either inter-stage impedance scaling or a terminating impedance transformer can be used for an even number of stages, it develops that an odd number is generally chosen to avoid this.

The coefficients of the L's and C's of the Tchebycheff low-pass prototype may be computed more directly than the preceding synthesis method from the following relations:

$$g_1 = \frac{2a_1}{\gamma} \tag{4.53}$$

$$g_k = \frac{4a_{k-1}a_k}{b_{k-1}g_{k-1}}, \quad (k = 2,3,4 \ldots n) \tag{4.54}$$

where,

$$\gamma = \sinh \beta/2n \tag{4.55}$$

$$\beta = \ln (\coth \epsilon_{db}/17.37) \tag{4.56}$$

$$a_k = \sin \frac{(2k-1)\pi}{2n}, \quad (k = 1,2,3 \ldots n) \tag{4.57}$$

$$b_k = \gamma^2 + \sin^2 (k\pi/n), \quad (k = 1,2,3 \ldots n) \tag{4.58}$$

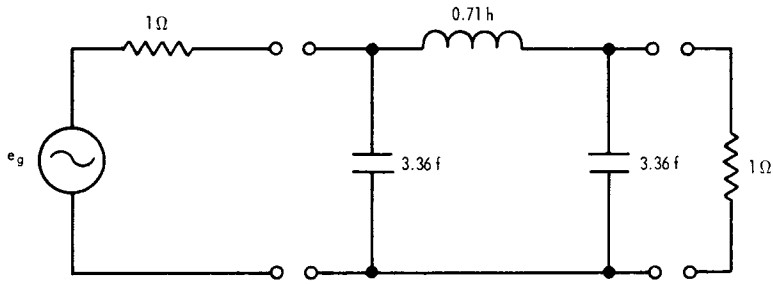

Figure 4.31. Three-Stage, 3-db Ripple, Tchebycheff Low-Pass Filter Prototype

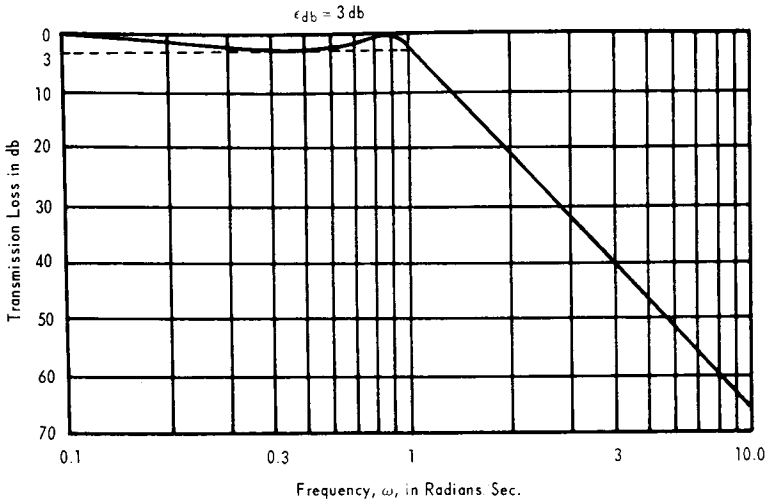

Figure 4.32. Frequency Response of Network Shown in Figure 4.31

ϵ_{db} = ripple amplitude in db

n = number of stages.

Table 4.4 lists the values of these coefficients for 1 through 10 stages and for ϵ_{db} = 0.1, 0.25, 0.5, 1.0, 2.0, and 3.0 db.

Table 4.4
ELEMENT VALUES OF TCHEBYCHEFF LOW-PASS FILTER PROTOTYPES
(Use this table when source and load resistances are within 30% of each other, viz when $0.7 < \bar{R} \leq 1.0$ for n = odd)*

n	db Ripple	C_1	L_2	C_3	L_4	C_5	L_6	C_7	L_8	C_9	L_{10}	R_g	R_L	n
1	1/10	0.305										1.000	1.000	1
	1/4	0.487										1.000	1.000	
	1/2	0.699										1.000	1.000	
	1	1.018										1.000	1.000	
	2	1.530										1.000	1.000	
	3	1.995										1.000	1.000	
2	1/2	0.707	1.403									0.504	1.000	2
	1	0.685	1.822									0.376	1.000	
	2	0.608	2.489									0.244	1.000	
	3	0.534	3.101									0.172	1.000	
3	1/10	1.032	1.147	1.032								1.000	1.000	3
	1/4	1.303	1.146	1.303								1.000	1.000	
	1/2	1.596	1.097	1.596								1.000	1.000	
	1	2.024	0.994	2.024								1.000	1.000	
	2	2.711	0.833	2.711								1.000	1.000	
	3	3.349	0.712	3.349								1.000	1.000	
4	1/2	0.842	2.366	1.193	1.670							0.504	1.000	4
	1	0.789	2.831	1.064	2.099							0.376	1.000	
	2	0.682	3.606	0.881	2.793							0.244	1.000	
	3	0.592	4.347	0.748	3.439							0.172	1.000	
5	1/10	1.147	1.371	1.975	1.371	1.147						1.000	1.000	5
	1/4	1.382	1.326	2.209	1.326	1.382						1.000	1.000	
	1/2	1.706	1.230	2.541	1.230	1.706						1.000	1.000	
	1	2.135	1.091	3.001	1.091	2.135						1.000	1.000	
	2	2.831	0.899	3.783	0.899	2.831						1.000	1.000	
	3	3.481	0.762	4.538	0.762	3.481						1.000	1.000	
6	1/2	0.870	2.476	1.314	2.606	1.248	1.725					0.504	1.000	6
	1	0.810	2.937	1.152	3.063	1.104	2.155					0.376	1.000	
	2	0.696	3.716	0.939	3.847	0.907	2.852					0.244	1.000	
	3	0.603	4.464	0.793	4.606	0.769	3.505					0.172	1.000	
7	1/10	1.181	1.423	2.097	1.573	2.097	1.423	1.181				1.000	1.000	7
	1/4	1.447	1.356	2.348	1.469	2.348	1.356	1.447				1.000	1.000	
	1/2	1.737	1.258	2.638	1.344	2.638	1.258	1.737				1.000	1.000	
	1	2.167	1.112	3.094	1.174	3.094	1.112	2.167				1.000	1.000	
	2	2.865	0.912	3.877	0.954	3.877	0.912	2.865				1.000	1.000	
	3	3.519	0.772	4.639	0.804	4.639	0.772	3.519				1.000	1.000	
8	1/2	0.880	2.509	1.339	2.696	1.359	2.656	1.265	1.745			0.504	1.000	8
	1	0.818	2.969	1.170	3.149	1.184	3.111	1.116	2.174			0.376	1.000	
	2	0.702	3.748	0.951	3.934	0.961	3.895	0.915	2.873			0.244	1.000	
	3	0.607	4.499	0.802	4.699	0.809	4.658	0.775	3.528			0.172	1.000	
9	1/10	1.196	1.443	2.135	1.167	2.205	1.617	2.135	1.443	1.196		1.000	1.000	9
	1/4	1.460	1.370	2.380	1.500	2.441	1.500	2.380	1.370	1.460		1.000	1.000	
	1/2	1.750	1.269	2.668	1.367	2.724	1.367	2.668	1.269	1.750		1.000	1.000	
	1	2.180	1.119	3.121	1.190	3.175	1.190	3.121	1.119	2.180		1.000	1.000	
	2	2.879	0.917	3.906	0.964	3.960	0.964	3.906	0.917	2.879		1.000	1.000	
	3	3.534	0.776	4.669	0.812	4.727	0.812	4.669	0.776	3.534		1.000	1.000	
10	1/2	0.884	2.524	1.349	2.723	1.381	2.739	1.373	2.675	1.272	1.754	0.504	1.000	10
	1	0.821	2.982	1.176	3.174	1.199	3.189	1.193	3.129	1.121	2.184	0.376	1.000	
	2	0.704	3.762	0.955	3.959	0.970	3.974	0.967	3.913	0.919	2.883	0.244	1.000	
	3	0.609	4.514	0.805	4.726	0.816	4.743	0.814	4.677	0.777	3.538	0.172	1.000	
n	db Ripple	L_1	C_2	L_3	C_4	L_5	C_6	L_7	C_8	L_9	C_{10}	R_g	R_L	n

C in farads
L in henrys
R in ohms
n = number of frequency sensitive elements
= 1 radian/sec = $2\pi f_c$
f_c = cutoff frequency

*Use Tables 4.5–4.10 for $0.1 \leq \bar{R} \leq 0.7$
Use Tables 4.11–4.16 for $\bar{R} < 0.1$

4.2.2 Low-Pass, Tchebycheff Prototype Design

The Tchebycheff transfer function given in Eq. (4.45) may be approximated in the stop or rejection band, when $\omega \gg 1$, by the expression:

$$|t_T(j\omega)|^2 = \frac{1}{1 + \epsilon^2 T_n^2(\omega)} \approx [\epsilon T_n(\omega)]^{-2} \tag{4.59}$$

where, $T_n(\omega)$, the Tchebycheff polynominal of the first kind is:

$$\begin{aligned} T_1(\omega) &= \omega & T_4(\omega) &= 8\omega^4 - 8\omega^2 + 1 \\ T_2(\omega) &= 2\omega^2 - 1 & T_5(\omega) &= 16\omega^5 - 20\omega^3 + 5\omega \\ T_3(\omega) &= 4\omega^3 - 3\omega & T_6(\omega) &= 32\omega^6 - 48\omega^4 + 18\omega^2 - 1 \end{aligned} \tag{4.60}$$

$$T_n(\omega) = 2^{n-1}\omega^n - \ldots\ldots$$

$$T_{n+1}(\omega) = 2\omega T_n(\omega) - T_{n-1}(\omega).$$

Substituting the $T_n(\omega)$ term in Eq. (4.60) into (4.59) yields:

$$|t_T(j\omega)|^2 \approx [(2\omega)^n \cdot \epsilon/2]^{-2} \text{ for } \omega \gg 1 \tag{4.61}$$

or expressing Eq. (4.61) in db, the transmission loss t_{db}, is:

$$\begin{aligned} t_{db} &= -20n \log_{10}(2\omega) - 20 \log_{10}(\epsilon/2) \\ &= -20n \log_{10} \omega - 20 \log_{10} \epsilon - 6(n-1). \end{aligned} \tag{4.62}$$

Since the amplitude response is of special interest in the design of low-pass prototype filters, Eq. (4.59) is plotted in Figs. 4.33 to 4.38 between $\omega = 1$ radian/sec and $\omega = 10$ radians/sec for $n = 1$ to 10 and $n = 15$ and 20 and $\epsilon_{db} = 0.1$, 0.25, 0.5, 1.0, 2.0, and 3.0 db. Note that the cut-off frequency for the Tchebycheff response corresponds to the ϵ_{db} bandwidth and not the 3-db bandwidth except when $\epsilon_{db} = 3$ db.

Illustrative Example 4.8

Compute the transmission loss at $\omega = 2$ rad/sec for $n = 7$ LC elements and an allowable 1-db ripple variation in the pass band. Using Fig. 4.36 for $\epsilon_{db} = 1$ db, the transmission loss is 68 db.

This 68-db figure may be compared with the 42-db attenuation (cf. Fig. 4.5) provided by a competitive seven-stage, Butterworth low-pass filter. Alternatively, n = 10 stages are required to give comparable attenuation by the Butterworth response at $\omega = 2$ (cf. Fig. 4.5). This demonstrates that the Tchebycheff response yields better attenuation in the stop band at the price of ripple or greater attenuation in the pass band.

Illustrative Example 4.9

Suppose for the front-end protection of a receiver, it is desired to design a 50-ohm low-pass, Tchebycheff filter having a maximum pass-band ripple tolerance of 1/2 db and cut-off frequency of about 100 mc. It is desired to provide about a 25-db rejection to interference at 150 mc. Fig. 4.35 indicates that five stages are required from the intersection of 25 db and $\bar{\omega} = 1.5$ ($\bar{\omega} = \omega_1/\omega_c = 150$ mc/100 mc). If a capacitor input is desired, Table 4.4 (n = 5; $\epsilon_{db} = 1/2$ db) and Eqs. (4.28) and (4.29) yield:

$$C_1' = C_5' = \frac{C_1}{R\omega_c} = \frac{1.706}{50 \times 2\pi \times 10^8} = 5.450\,\mu\mu f$$

$$L_2' = L_4' = \frac{RL_2}{\omega_c} = \frac{50 \times 1.230}{2\pi \times 10^8} = 0.098\,\mu h$$

$$C_3' = \frac{C_3}{R\omega_c} = \frac{2.541}{50 \times 2\pi \times 10^8} = 8{,}100\,\mu\mu f.$$

The complete filter is shown in Fig. 4.39.

The dual of this filter (inductor input) may be obtained by computing the element values directly (cf. Fig. 4.40); viz,

$$L_1' = L_5' = \frac{RL_1}{\omega_c} = \frac{50 \times 1.706}{2\pi \times 10^8} = 0.136\,\mu h$$

$$C_2' = C_4' = \frac{C_2}{R\omega_c} = \frac{1.230}{50 \times 2\pi \times 10^8} = 3{,}920\,\mu\mu f$$

$$L_3' = \frac{RL_3}{\omega_c} = \frac{50 \times 2.541}{2\pi \times 10^8} = 0.202\,\mu h.$$

Alternatively, the L's and C's of a dual network may be computed directly by:

(1) Replacing all series inductances with shunt capacitances whose values are $C = L/R^2$, and by

(2) Replacing all shunt capacitances with series inductances whose values are $L = CR^2$.

Applying the above relations to the network depicted in Fig. 4.39 yields its dual shown in Fig. 4.40.

As previously discussed in regard to the Butterworth response, it develops that the input-output or source and terminating resistances may not be equal as was the situation for the odd number of stages in the Tchebycheff function element values presented in Table 4.4. Tables of synthesized element values are developed for situations corresponding to input-output resistances or conductance ratios between about 0.1 and 1. Tables 4.5 through 4.10 correspond to these resistance termination ratios of 1/8, 1/4, 1/3, and 1/2. The box shown at the bottom of each table provides the interpretation of R_g, the source resistance or conductance.

Illustrative Example 4.10

Design a 1/2-db ripple, Tchebycheff, low-pass filter having a cut-off frequency of 10 mc, which provides a 50-db attenuation above 50 mc (cf. Illustrative Example 4.4). The driving source impedance is 100 ohms and the output is terminated by an HF transistor having an equivalent 20-ohm load. Thus, $\overline{R} = R_g/R_L = 100\,\Omega/20\,\Omega = 5$. Since $\overline{R}$ is greater than unity, but the tables are based on values less than 1, its reciprocal (0.2) is taken and the value interpretation is now in mhos. R = 1/4 is chosen in Table 4.7 since 1/5 is closer to 1/4 than 1/8.

Fig. 4.35 indicates that for $\overline{\omega} = \omega_1/\omega_c = 50$ mc/10 mc = 5 and for a 50-db transmission loss, n = 3.8 or 4 stages will be used. Returning to the bottom of Table 4.7, for n = 4(even) and for an R_g interpretation of mhos, the input element must be a capacitor; viz,

$C_1 = 0.327$ f

$L_2 = 7.616$ h

$C_3 = 0.573$ f

$L_4 = 2.309$ h

$R_g = 0.25$ mhos = 4 ohms (use 5 Ω as in example)

$R_L = 1.00$ ohms.

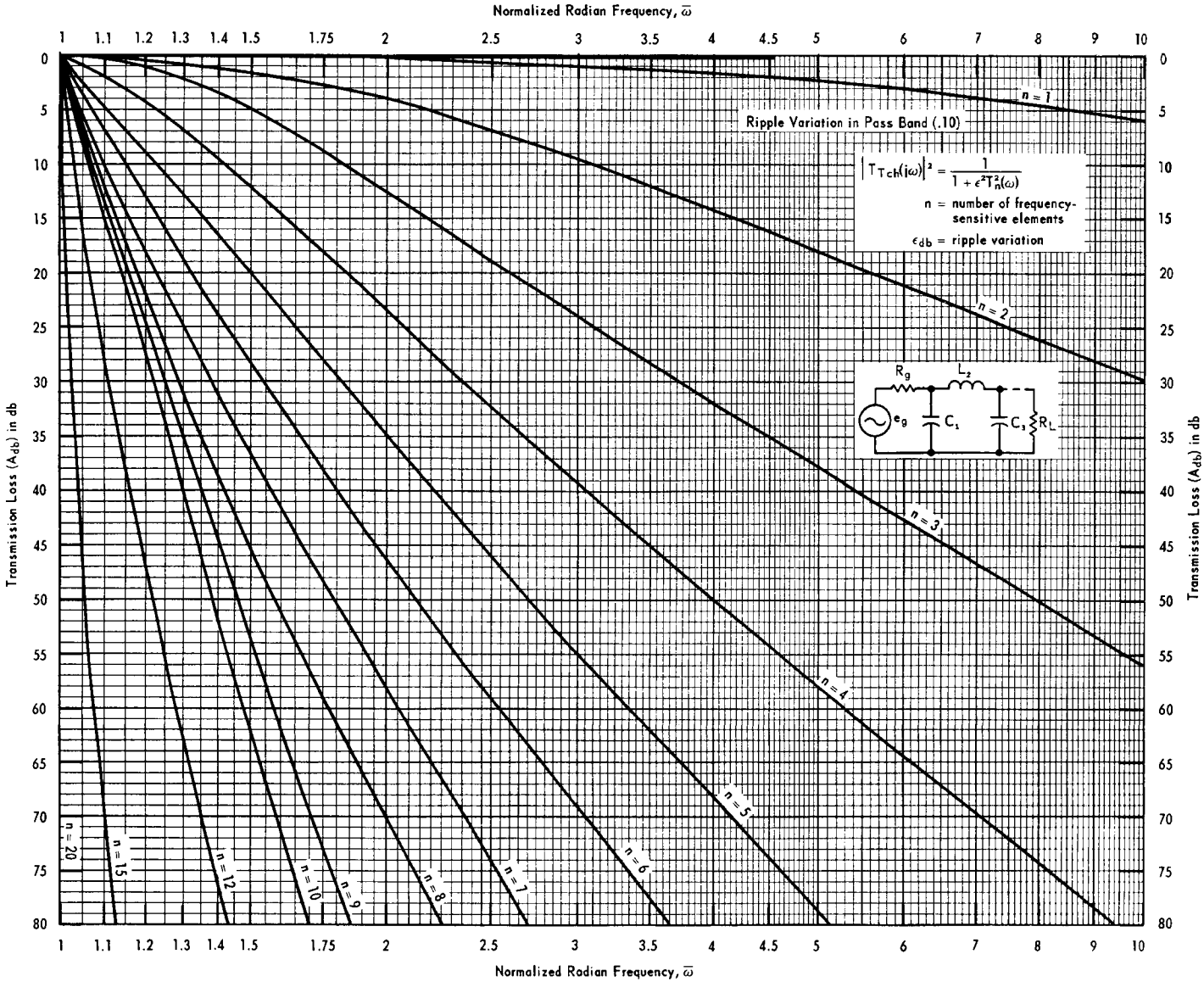

Figure 4.33. Transmission Loss of Tchebycheff Function vs. Frequency (ϵ_{db} = 0.1-db Ripple)

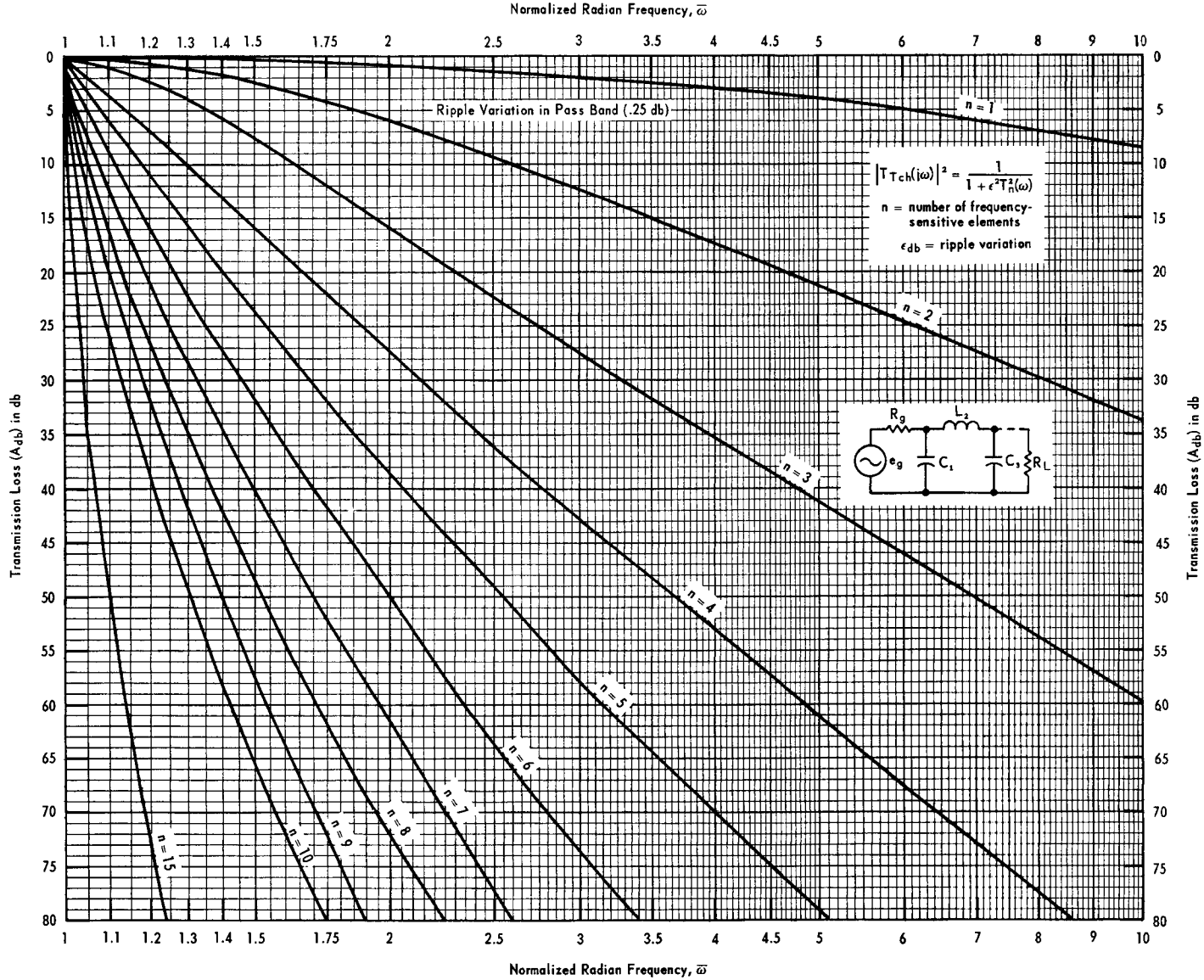

Figure 4.34. Transmission Loss of Tchebycheff Function vs. Frequency (ϵ_{db} = 0.25-db Ripple)

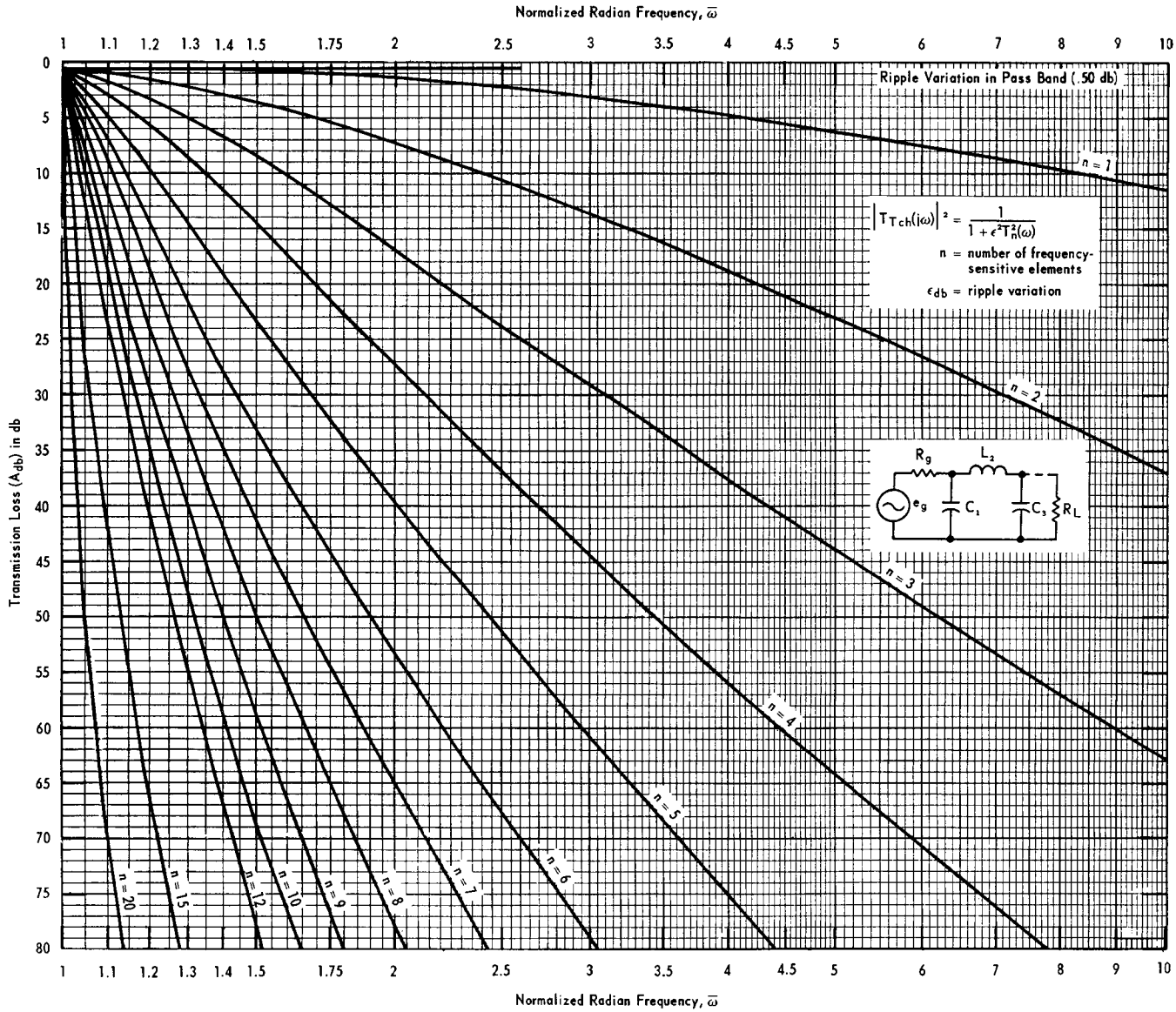

Figure 4.35. Transmission Loss of Tchebycheff Function vs. Frequency (ϵ_{db} = 0.5-db Ripple)

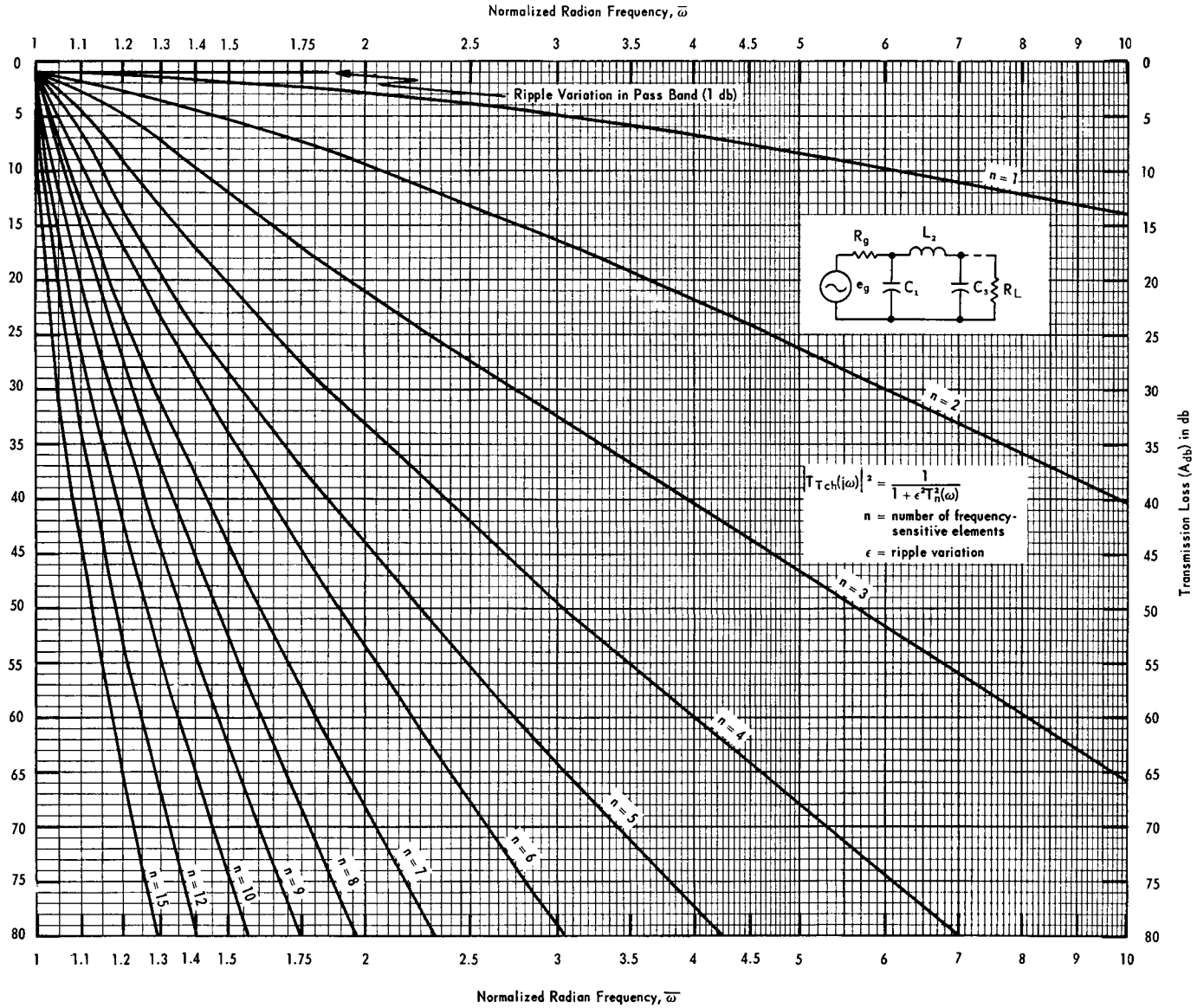

Figure 4.36. Transmission Loss of Tchebycheff Function vs. Frequency (ϵ_{db} = 1.0-db Ripple)

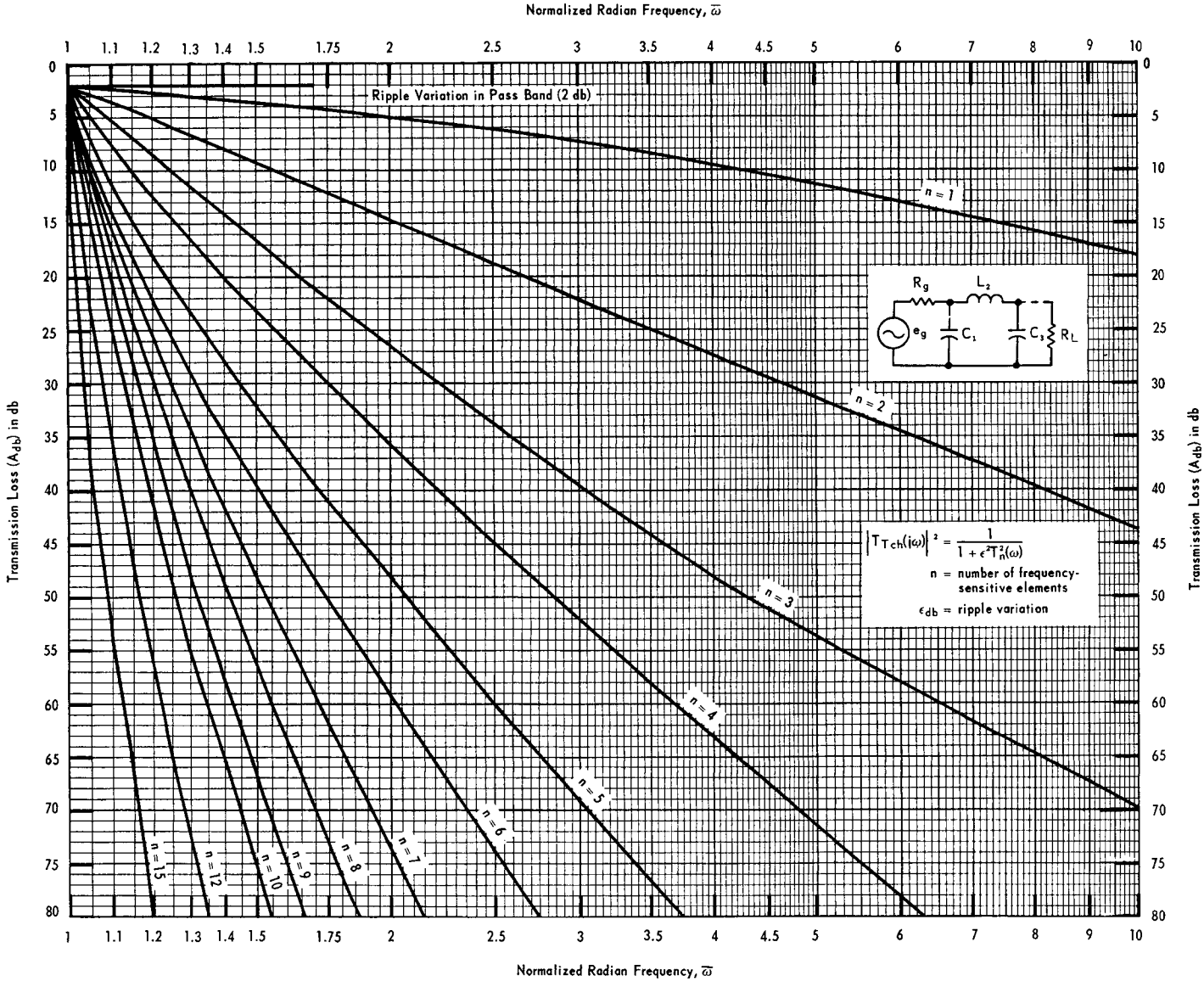

Figure 4.37. Transmission Loss of Tchebycheff Function vs. Frequency (ϵ_{db} = 2-db Ripple)

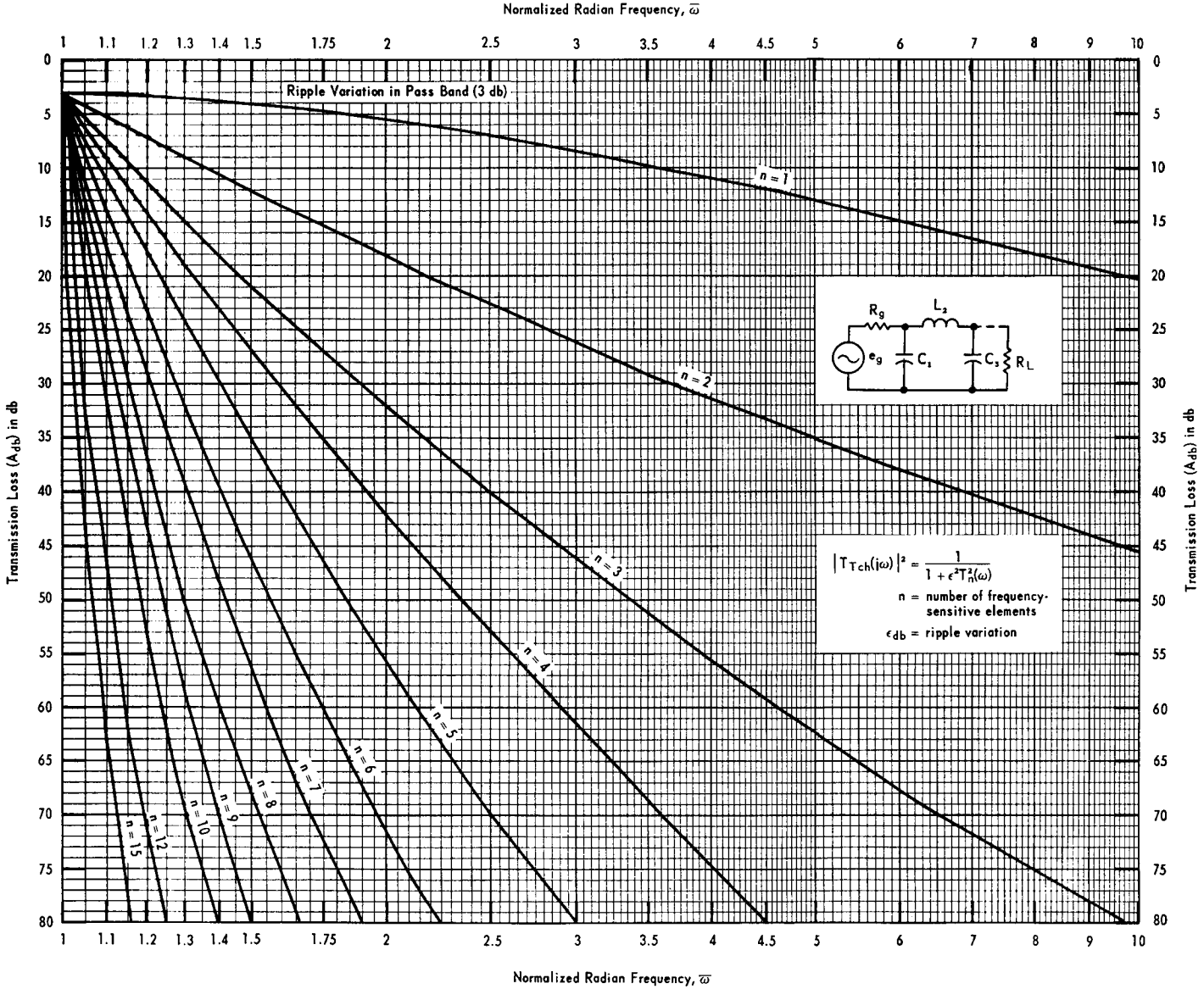

Figure 4.38. Transmission Loss of Tchebycheff Function vs. Frequency (ϵ_{db} = 3-db Ripple)

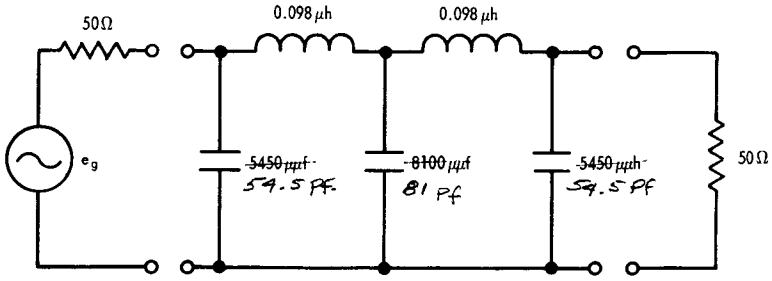

Figure 4.39. Five-Stage, 1/2-db Ripple, Tchebycheff Low-Pass Filter with f_c = 100 mc

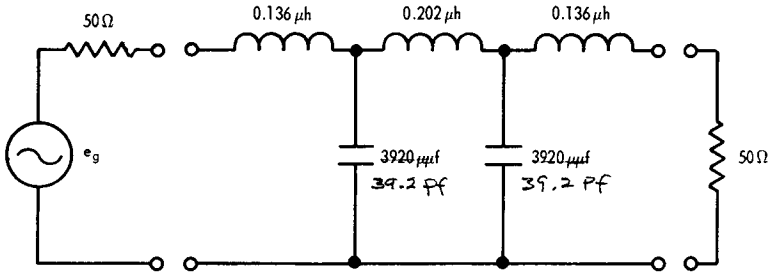

Figure 4.40. Dual of Filter Shown in Figure 4.39

The remainder of the problem follows that of illustrative example 4.4 (cf. Fig. 4.15–4.19).

When the ratio $\overline{R}$ of source to load terminating resistance is less than 0.1, a voltage source is approximated since $R_g \leq 0.1$. When the ratio is greater than 10, an equivalent current source exists since $R_g \geq 10$. Thus, another set of tables can be prepared for these situations by executing the indicated synthesis procedures.

It develops that it is also convenient to include in such tables of lossless single-end terminations, element values which correspond to associated finite losses (see Chap. 6, Sec. 6.1). Component loss serves to introduce insertion loss, to round off the sharp break of the response in the transition zone between pass and rejection bands, and to reduce the skirt slope or selectivity. While capacitors can be manufactured to have high Q_u-factors (e.g., Q_u's of 1,000–2,500) the Q_u factor of inductors is

Table 4.5
ELEMENT VALUES FOR A NORMALIZED TCHEBYCHEFF FILTER
WITH 1/10-db RIPPLE (Use for $0.1 \leq \bar{R} \leq 0.7$)*

n	C_1	L_2	C_3	L_4	C_5	L_6	C_7	L_8	C_9	L_{10}	R_g	R_L	n
$\bar{R} = 1/8$ (Use for $0.1 \leq \bar{R} < 0.2$)													
1	1.374										0.125	1.000	1
2	0.057	5.989									0.125	1.000	2
3	8.253	0.645	1.032								0.125	1.000	3
4	0.101	15.494	0.493	1.756							0.125	1.000	4
5	9.175	0.171	8.888	1.371	1.147						0.125	1.000	5
6	0.118	13.296	0.163	14.382	0.966	1.537					0.125	1.000	6
7	9.449	0.178	16.773	0.885	2.097	1.423	1.181				0.125	1.000	7
8	0.126	12.941	0.209	23.234	0.446	3.699	1.146	1.449			0.125	1.000	8
9	9.565	0.180	17.076	0.202	9.924	1.617	2.135	1.443	1.196		0.125	1.000	9
10	0.131	12.752	0.225	17.097	0.154	19.203	0.873	3.022	1.234	1.399	0.125	1.000	10
$\bar{R} = 1/4$ (Use for $0.2 \leq \bar{R} < 0.3$)													
1	0.763										0.250	1.000	1
2	0.122	3.091									0.250	1.000	2
3	4.126	0.717	1.032								0.250	1.000	3
4	0.210	7.358	0.598	1.637							0.250	1.000	4
5	4.587	0.343	4.938	1.371	1.147						0.250	1.000	5
6	0.241	6.538	0.344	7.284	1.031	1.481					0.250	1.000	6
7	4.725	0.356	8.387	0.983	2.097	1.423	1.181				0.250	1.000	7
8	0.257	6.396	0.429	10.574	0.582	3.317	1.187	1.413			0.250	1.000	8
9	4.783	0.361	8.538	0.404	5.513	1.617	2.135	1.443	1.196		0.250	1.000	9
10	0.266	6.317	0.458	8.292	0.335	9.289	0.982	2.852	1.264	1.373	0.250	1.000	10
$\bar{R} = 1/3$ (Use for $0.3 \leq \bar{R} < 0.4$)													
1	0.611										0.333	1.000	1
2	0.171	2.350									0.333	1.000	2
3	3.095	0.765	1.032								0.333	1.000	3
4	0.286	5.335	0.674	1.563							0.333	1.000	4
5	3.440	0.457	3.950	1.371	1.147						0.333	1.000	5
6	0.327	4.845	0.477	5.489	1.075	1.444					0.333	1.000	6
7	3.544	0.474	6.290	1.049	2.097	1.423	1.181				0.333	1.000	7
8	0.347	4.757	0.582	7.482	0.684	3.105	1.215	1.388			0.333	1.000	8
9	3.587	0.481	6.404	0.539	4.411	1.617	2.135	1.443	1.196		0.333	1.000	9
10	0.359	4.705	0.618	6.090	0.471	6.810	1.056	2.747	1.284	1.355	0.333	1.000	10
$\bar{R} = 1/2$ (Use for $0.4 \leq \bar{R} \leq 0.7$)													
1	0.458										0.500	1.000	1
2	0.288	1.572									0.500	1.000	2
3	2.063	0.861	1.032								0.500	1.000	3
4	0.455	3.311	0.847	1.420							0.500	1.000	4
5	2.294	0.686	2.963	1.371	1.147						0.500	1.000	5
6	0.510	3.140	0.778	3.643	1.168	1.367					0.500	1.000	6
7	2.362	0.711	4.193	1.180	2.097	1.423	1.181				0.500	1.000	7
8	0.536	3.108	0.910	4.445	0.922	2.738	1.275	1.335			0.500	1.000	8
9	2.391	0.721	4.269	0.808	3.308	1.617	2.135	1.443	1.196		0.500	1.000	9
10	0.552	3.086	0.956	3.871	0.791	4.300	1.216	2.549	1.328	1.315	0.500	1.000	10

n	L_1	C_2	L_3	C_4	L_5	C_6	L_7	C_8	L_9	C_{10}	R_g	R_L	n

Interpretation of R_g:

Input Element # 1	n = odd	n = even
Inductor	mhos	ohms
Capacitor	ohms	mhos

*Use Table 4.4 for $0.7 < \bar{R} \leq 1.0$
Use Table 4.11 for $\bar{R} < 0.1$

Table 4.6
ELEMENT VALUES FOR A NORMALIZED TCHEBYCHEFF FILTER WITH 1/4-db RIPPLE (Use for $0.1 \leq \bar{R} \leq 0.7$)*

n	C_1	L_2	C_3	L_4	C_5	L_6	C_7	L_8	C_9	L_{10}	R_g	R_L	n
						$\bar{R} = 1/8$ (Use for $0.1 \leq \bar{R} < 0.2$)							
1	2.191										0.125	1.000	1
2	0.076	7.045									0.125	1.000	2
3	10.427	0.645	1.303								0.125	1.000	3
4	0.127	16.688	0.468	2.151							0.125	1.000	4
5	11.059	0.166	9.941	1.326	1.382						0.125	1.000	5
6	0.145	13.483	0.166	15.753	0.885	1.872					0.125	1.000	6
7	11.575	0.170	18.781	0.826	2.348	1.356	1.447				0.125	1.000	7
8	0.155	12.857	0.220	24.491	0.394	4.355	1.050	1.761			0.125	1.000	8
9	11.683	0.171	19.040	0.188	10.987	1.500	2.380	1.370	1.460		0.125	1.000	9
10	0.161	12.529	0.239	17.116	0.152	20.975	0.762	3.525	1.135	1.700	0.125	1.000	10
						$\bar{R} = 1/4$ (Use for $0.2 \leq \bar{R} < 0.3$)							
1	1.217										0.250	1.000	1
2	0.165	3.591									0.250	1.000	2
3	5.214	0.716	1.303								0.250	1.000	3
4	0.265	7.735	0.585	1.977							0.250	1.000	4
5	5.529	0.332	5.523	1.326	1.382						0.250	1.000	5
6	0.299	6.547	0.360	7.776	0.963	1.789					0.250	1.000	6
7	5.787	0.339	9.390	0.918	2.348	1.356	1.447				0.250	1.000	7
8	0.317	6.295	0.457	10.771	0.539	3.795	1.103	1.707			0.250	1.000	8
9	5.842	0.343	9.520	0.375	6.104	1.500	2.380	1.370	1.460		0.250	1.000	9
10	0.328	6.159	0.492	8.156	0.340	9.805	0.883	3.259	1.175	1.660	0.250	1.000	10
						$\bar{R} = 1/3$ (Use for $0.3 \leq \bar{R} < 0.4$)							
1	0.974										0.333	1.000	1
2	0.234	2.698									0.333	1.000	2
3	3.910	0.764	1.303								0.333	1.000	3
4	0.364	5.505	0.674	1.869							0.333	1.000	4
5	4.147	0.442	4.418	1.326	1.382						0.333	1.000	5
6	0.408	4.803	0.508	5.744	1.018	1.733					0.333	1.000	6
7	4.341	0.452	7.043	0.979	2.348	1.356	1.447				0.333	1.000	7
8	0.430	4.646	0.627	7.433	0.654	3.484	1.140	1.670			0.333	1.000	8
9	4.381	0.457	7.140	0.500	4.883	1.500	2.380	1.370	1.460		0.333	1.000	9
10	0.443	4.560	0.670	5.907	0.489	7.006	0.971	3.096	1.203	1.632	0.333	1.000	10
						$\bar{R} = 1/2$ (Use for $0.4 \leq \bar{R} \leq 0.7$)							
1	0.730										0.500	1.000	1
2	0.410	1.729									0.500	1.000	2
3	2.607	0.860	1.303								0.500	1.000	3
4	0.592	3.234	0.899	1.650							0.500	1.000	4
5	2.765	0.663	3.314	1.326	1.382						0.500	1.000	5
6	0.647	3.022	0.877	3.590	1.146	1.610					0.500	1.000	6
7	2.894	0.678	4.695	1.102	2.348	1.356	1.447				0.500	1.000	7
8	0.673	2.970	1.015	4.114	0.956	2.931	1.228	1.584			0.500	1.000	8
9	2.921	0.685	4.760	0.750	3.662	1.500	2.380	1.370	1.460		0.500	1.000	9
10	0.688	2.939	1.064	3.602	0.878	4.108	1.180	2.773	1.269	1.566	0.500	1.000	10

n	L_1	C_2	L_3	C_4	L_5	C_6	L_7	C_8	L_9	C_{10}	R_g	R_L	n

Interpretation of R_g:

Input Element # 1	n = odd	n = even
Inductor	mhos	ohms
Capacitor	ohms	mhos

*Use Table 4.4 for $0.7 < \bar{R} \leq 1.0$
Use Table 4.12 for $\bar{R} < 0.1$

Table 4.7
ELEMENT VALUES FOR A NORMALIZED TCHEBYCHEFF FILTER WITH 1/2-db RIPPLE (Use for $0.1 \leq \bar{R} \leq 0.7$)*

n	C_1	L_2	C_3	L_4	C_5	L_6	C_7	L_8	C_9	L_{10}	R_g	R_L	n
$\bar{R} = 1/8$ (Use for $0.1 \leq \bar{R} < 0.2$)													
1	3.144										0.125	1.000	1
2	0.097	7.691									0.125	1.000	2
3	12.770	0.617	1.596								0.125	1.000	3
4	0.155	17.034	0.439	2.561							0.125	1.000	4
5	13.646	0.154	11.434	1.230	1.706						0.125	1.000	5
6	0.176	13.112	0.174	16.489	0.804	2.229					0.125	1.000	6
7	13.898	0.157	21.106	0.756	2.638	1.258	1.737				0.125	1.000	7
8	0.187	12.309	0.235	24.690	0.356	5.024	0.952	2.098			0.125	1.000	8
9	14.004	0.159	21.342	0.171	12.258	1.367	2.668	1.269	1.750		0.125	1.000	9
10	0.193	11.895	0.258	16.582	0.155	21.864	0.672	4.060	1.030	2.026	0.125	1.000	10
$\bar{R} = 1/4$ (Use for $0.2 \leq \bar{R} < 0.3$)													
1	1.747										0.250	1.000	1
2	0.215	3.843									0.250	1.000	2
3	6.385	0.685	1.596								0.250	1.000	3
4	0.327	7.616	0.573	2.309							0.250	1.000	4
5	6.823	0.307	6.352	1.230	1.706						0.250	1.000	5
6	0.365	6.253	0.390	7.849	0.897	2.106					0.250	1.000	6
7	6.949	0.315	10.553	0.840	2.638	1.258	1.737				0.250	1.000	7
8	0.385	5.946	0.498	10.342	0.517	4.222	1.017	2.017			0.250	1.000	8
9	7.002	0.317	10.671	0.342	6.810	1.367	2.668	1.269	1.750		0.250	1.000	9
10	0.396	5.784	0.539	7.701	0.362	9.747	0.811	3.658	1.081	1.965	0.250	1.000	10
$\bar{R} = 1/3$ (Use for $0.3 \leq \bar{R} < 0.4$)													
1	1.397										0.333	1.000	1
2	0.311	2.828									0.333	1.000	2
3	4.789	0.731	1.596								0.333	1.000	3
4	0.455	5.253	0.684	2.150							0.333	1.000	4
5	5.117	0.410	5.082	1.230	1.706						0.333	1.000	5
6	0.502	4.514	0.567	5.610	0.966	2.020					0.333	1.000	6
7	5.212	0.419	7.915	0.896	2.638	1.258	1.737				0.333	1.000	7
8	0.525	4.337	0.697	6.851	0.657	3.772	1.067	1.958			0.333	1.000	8
9	5.251	0.423	8.003	0.456	5.448	1.367	2.668	1.269	1.750		0.333	1.000	9
10	0.538	4.242	0.746	5.451	0.540	6.683	0.919	3.407	1.119	1.921			10
$\bar{R} = 1/2$ (Use for $0.4 \leq \bar{R} \leq 0.7$)													
1	1.048										0.500	1.000	1
2	0.654	1.513									0.500	1.000	2
3	3.193	0.823	1.596								0.500	1.000	3
4	0.808	2.543	1.114	1.728							0.500	1.000	4
5	3.412	0.615	3.811	1.230	1.706						0.500	1.000	5
6	0.844	2.576	1.209	2.827	1.207	1.764					0.500	1.000	6
7	3.475	0.629	5.277	1.008	2.638	1.258	1.737				0.500	1.000	7
8	0.858	2.586	1.275	2.956	1.244	2.774	1.236	1.774			0.500	1.000	8
9	3.501	0.635	5.336	0.684	4.086	1.367	2.668	1.269	1.750		0.500	1.000	9
10	0.858	2.670	1.248	2.879	1.321	2.874	1.292	2.889	1.210	1.795	0.500	1.000	10

n	L_1	C_2	L_3	C_4	L_5	C_6	L_7	C_8	L_9	C_{10}	R_g	R_L	n

Interpretation of R_g:

Input Element # 1	n = odd	n = even
Inductor	mhos	ohms
Capacitor	ohms	mhos

*Use Table 4.4 for $0.7 < \bar{R} \leq 1.0$
Use Table 4.13 for $\bar{R} < 0.1$

Table 4.8
ELEMENT VALUES FOR A NORMALIZED TCHEBYCHEFF FILTER
WITH 1-db RIPPLE (Use for $0.1 \leq \bar{R} \leq 0.7$)*

n	C_1	L_2	C_3	L_4	C_5	L_6	C_7	L_8	C_9	L_{10}	R_g	R_L	n
					$\bar{R} = 1/8$ (Use for $0.1 \leq \bar{R} < 0.2$)								
1	4.580										0.125	1.000	1
2	0.129	7.932									0.125	1.000	2
3	16.189	0.559	2.024								0.125	1.000	3
4	0.198	16.300	0.406	3.116							0.125	1.000	4
5	17.079	0.136	13.504	1.091	2.135						0.125	1.000	5
6	0.222	12.028	0.193	16.357	0.709	2.735					0.125	1.000	6
7	17.333	0.139	24.749	0.660	3.094	1.112	2.167				0.125	1.000	7
8	0.235	11.140	0.264	23.257	0.322	5.877	0.832	2.581			0.125	1.000	8
9	17.438	0.140	24.972	0.149	14.286	1.190	3.121	1.119	2.180		0.125	1.000	9
10	0.243	10.691	0.292	15.174	0.169	21.447	0.583	4.792	0.900	2.497	0.125	1.000	10
					$\bar{R} = 1/4$ (Use for $0.2 \leq \bar{R} < 0.3$)								
1	2.544										0.250	1.000	1
2	0.300	3.778									0.250	1.000	2
3	8.094	0.621	2.024								0.250	1.000	3
4	0.429	6.726	0.581	2.705							0.250	1.000	4
5	8.540	0.273	7.502	1.091	2.135						0.250	1.000	5
6	0.470	5.515	0.465	7.183	0.830	2.523					0.250	1.000	6
7	8.666	0.278	12.375	0.734	3.094	1.112	2.167				0.250	1.000	7
8	0.490	5.231	0.587	8.762	0.532	4.605	0.921	2.440			0.250	1.000	8
9	8.719	0.280	12.486	0.297	7.937	1.190	3.121	1.119	2.180		0.250	1.000	9
10	0.502	5.082	0.634	6.658	0.431	8.620	0.762	4.108	0.969	2.391	0.250	1.000	10
					$\bar{R} = 1/3$ (Use for $0.3 \leq \bar{R} < 0.4$)								
1	2.035										0.333	1.000	1
2	0.470	2.572									0.333	1.000	2
3	6.071	0.663	2.024								0.333	1.000	3
4	0.620	4.189	0.773	2.407							0.333	1.000	4
5	6.405	0.364	6.002	1.091	2.135						0.333	1.000	5
6	0.663	3.784	0.753	4.603	0.947	2.351					0.333	1.000	6
7	6.500	0.371	9.281	0.782	3.094	1.112	2.167				0.333	1.000	7
8	0.682	3.679	0.875	5.087	0.779	3.819	1.005	2.319			0.333	1.000	8
9	6.539	0.373	9.364	0.397	6.349	1.190	3.121	1.119	2.180		0.333	1.000	9
10	0.693	3.622	0.919	4.372	0.734	5.163	0.941	3.620	1.034	2.298	0.333	1.000	10
					$\bar{R} = 1/2$ (Use for $0.4 \leq \bar{R} < 0.7$)								
1	1.527										0.500	1.000	1
2	–	–									0.500	1.000	2
3	4.047	0.746	2.024								0.500	1.000	3
4	–	–	–	–							0.500	1.000	4
5	4.270	0.546	4.501	1.091	2.135						0.500	1.000	5
6	–	–	–	–	–	–					0.500	1.000	6
7	4.333	0.556	6.187	0.880	3.094	1.112	2.167				0.500	1.000	7
8	–	–	–	–	–	–	–	–			0.500	1.000	8
9	4.359	0.560	6.243	0.595	4.762	1.190	3.121	1.119	2.180		0.500	1.000	9
10	–	–	–	–	–	–	–	–	–	–	0.500	1.000	10

n	L_1	C_2	L_3	C_4	L_5	C_6	L_7	C_8	L_9	C_{10}	R_g	R_L	n

Interpretation of R_g:

Input Element # 1	n = odd	n = even
Inductor	mhos	ohms
Capacitor	ohms	mhos

*Use Table 4.4 for $0.7 < \bar{R} \leq 1.0$
Use Table 4.14 for $\bar{R} < 0.1$

Table 4.9
ELEMENT VALUES FOR A NORMALIZED TCHEBYCHEFF FILTER
WITH 2-db RIPPLE (Use for $0.1 \leq \bar{R} \leq 0.7$)*

n	C_1	L_2	C_3	L_4	C_5	L_6	C_7	L_8	C_9	L_{10}	R_g	R_L	n
$\bar{R} = 1/8$ (Use for $0.1 \leq \bar{R} < 0.2$)													
1	6.883										0.125	1.000	1
2	0.188	7.290									0.125	1.000	2
3	21.686	0.468	2.711								0.125	1.000	3
4	0.273	13.480	0.384	3.869							0.125	1.000	4
5	22.648	0.112	17.022	0.899	2.831						0.125	1.000	5
6	0.302	9.893	0.243	14.172	0.610	3.481					0.125	1.000	6
7	22.920	0.114	31.019	0.536	3.877	0.912	2.865				0.125	1.000	7
8	0.317	9.129	0.330	18.508	0.313	6.809	0.700	3.319			0.125	1.000	8
9	23.032	0.115	31.245	0.121	17.819	0.964	3.906	0.917	2.879		0.125	1.000	9
10	0.326	8.746	0.366	12.314	0.213	17.953	0.513	5.746	0.749	3.229	0.125	1.000	10
$\bar{R} = 1/4$ (Use for $0.2 \leq \bar{R} < 0.3$)													
1	3.824										0.250	1.000	1
2	–	–									0.250	1.000	2
3	10.843	0.520	2.711								0.250	1.000	3
4	–	–	–	–							0.250	1.000	4
5	11.324	0.225	9.457	0.899	2.831						0.250	1.000	5
6	–	–	–	–	–	–					0.250	1.000	6
7	11.460	0.228	15.510	0.596	3.877	0.912	2.865				0.250	1.000	7
8	–	–	–	–	–	–	–	–			0.250	1.000	8
9	11.516	0.229	15.622	0.241	9.899	0.964	3.906	0.917	2.879		0.250	1.000	9
10	–	–	–	–	–	–	–	–	–	–	0.250	1.000	10
$\bar{R} = 1/3$ (Use for $0.3 \leq \bar{R} < 0.4$)													
1	3.059										0.333	1.000	1
2	–	–									0.333	1.000	2
3	8.132	0.555	2.711								0.333	1.000	3
4	–	–	–	–							0.333	1.000	4
5	8.493	0.300	7.566	0.899	2.831						0.333	1.000	5
6	–	–	–	–	–	–					0.333	1.000	6
7	8.595	0.304	11.632	0.636	3.877	0.912	2.865				0.333	1.000	7
8	–	–	–	–	–	–	–	–			0.333	1.000	8
9	8.637	0.306	11.717	0.321	7.920	0.964	3.906	0.917	2.879		0.333	1.000	9
10	–	–	–	–	–	–	–	–	–	–	0.333	1.000	10
$\bar{R} = 1/2$ (Use for $0.4 \leq \bar{R} \leq 0.7$)													
1	2.294										0.500	1.000	1
2	–	–									0.500	1.000	2
3	5.421	0.625	2.711								0.500	1.000	3
4	–	–	–	–							0.500	1.000	4
5	5.662	0.449	5.674	0.899	2.831						0.500	1.000	5
6	–	–	–	–	–	–					0.500	1.000	6
7	5.730	0.456	7.755	0.715	3.877	0.912	2.865				0.500	1.000	7
8	–	–	–	–	–	–	–	–			0.500	1.000	8
9	5.758	0.459	7.811	0.482	5.940	0.964	3.906	0.917	2.879		0.500	1.000	9
10	–	–	–	–	–	–	–	–	–	–	0.500	1.000	10

n	L_1	C_2	L_3	C_4	L_5	C_6	L_7	C_8	L_9	C_{10}	R_g	R_L	n

Interpretation of R_g:

Input Element # 1	n = odd	n = even
Inductor	mhos	ohms
Capacitor	ohms	mhos

*Use Table 4.4 for $0.7 < \bar{R} \leq 1.0$
Use Table 4.15 for $\bar{R} < 0.1$

Table 4.10
ELEMENT VALUES FOR A NORMALIZED TCHEBYCHEFF FILTER
WITH 3-db RIPPLE (Use for $0.1 \leq \bar{R} \leq 0.7$)*

n	C_1	L_2	C_3	L_4	C_5	L_6	C_7	L_8	C_9	L_{10}	R_g	R_L	n
					$\bar{R} = 1/8$ (Use for $0.1 \leq \bar{R} < 0.2$)								
1	8.979										0.125	1.000	1
2	0.260	6.122									0.125	1.000	2
3	26.790	0.400	3.349								0.125	1.000	3
4	0.356	10.152	0.405	4.343							0.125	1.000	4
5	27.850	0.095	20.419	0.762	3.481						0.125	1.000	5
6	0.386	7.924	0.327	11.001	0.570	4.052					0.125	1.000	6
7	28.148	0.097	37.112	0.452	4.639	0.772	3.519				0.125	1.000	7
8	0.401	7.416	0.423	13.116	0.355	7.022	0.631	3.921			0.125	1.000	8
9	28.272	0.097	37.353	0.102	21.272	0.812	4.669	0.776	3.534		0.125	1.000	9
10	0.410	7.159	0.461	9.544	0.295	13.189	0.508	6.241	0.665	3.846	0.125	1.000	10
					$\bar{R} = 1/4$ (Use for $0.2 \leq \bar{R} < 0.3$)								
1	4.988										0.250	1.000	1
2	–	–									0.250	1.000	2
3	13.395	0.445	3.349								0.250	1.000	3
4	–	–	–	–							0.250	1.000	4
5	13.925	0.191	11.344	0.762	3.481						0.250	1.000	5
6	–	–	–	–	–	–					0.250	1.000	6
7	14.074	0.193	18.556	0.502	4.639	0.772	3.519				0.250	1.000	7
8	–	–	–	–	–	–	–	–			0.250	1.000	8
9	14.136	0.194	18.676	0.203	11.818	0.812	4.669	0.776	3.534		0.250	1.000	9
10	–	–	–	–	–	–	–	–	–	–	0.250	1.000	10
					$\bar{R} = 1/3$ (Use for $0.3 \leq \bar{R} < 0.4$)								
1	3.991										0.333	1.000	1
2	–	–									0.333	1.000	2
3	10.046	0.475	3.349								0.333	1.000	3
4	–	–	–	–							0.333	1.000	4
5	10.444	0.254	9.075	0.762	3.481						0.333	1.000	5
6	–	–	–	–	–	–					0.333	1.000	6
7	10.556	0.257	13.917	0.536	4.639	0.772	3.519				0.333	1.000	7
8	–	–	–	–	–	–	–	–			0.333	1.000	8
9	10.602	0.259	14.007	0.271	9.454	0.812	4.669	0.776	3.534		0.333	1.000	9
10	–	–	–	–	–	–	–	–	–	–	0.333	1.000	10
					$\bar{R} = 1/2$ (Use for $0.4 \leq \bar{R} \leq 0.7$)								
1	2.993										0.500	1.000	1
2	–	–									0.500	1.000	2
3	6.698	0.534	3.349								0.500	1.000	3
4	–	–	–	–							0.500	1.000	4
5	6.963	0.381	6.806	0.762	3.481						0.500	1.000	5
6	–	–	–	–	–	–					0.500	1.000	6
7	7.037	0.386	9.278	0.603	4.639	0.772	3.519				0.500	1.000	7
8	–	–	–	–	–	–	–	–			0.500	1.000	8
9	7.068	0.388	9.338	0.406	7.091	0.812	4.669	0.776	3.534		0.500	1.000	9
10	–	–	–	–	–	–	–	–	–	–	0.500	1.000	10
n	L_1	C_2	L_3	C_4	L_5	C_6	L_7	C_8	L_9	C_{10}	R_g	R_L	n

Interpretation of R_g:

Input Element #1	n = odd	n = even
Inductor	mhos	ohms
Capacitor	ohms	mhos

*Use Table 4.4 for $0.7 < \bar{R} \leq 1.0$
Use Table 4.16 for $\bar{R} < 0.1$

considerably lower (cf. Chap. 6). Thus, the technique of predistortion is used in the synthesis process in which s−d is substituted for s in the transfer function. After the element values are synthesized, s+d is substituted for s to remove the effect of the predistortion and a corresponding change is made in network element values by carrying out the indicated predistortion synthesis process. The result is Tables 4.11–4.16.

These predistortion tables have been prepared for five values of $\overline{Q}$: ∞, 30, 20, 10, and 5, where $\overline{Q}$ is the component Q_u factor for low- and high-pass filters and $\overline{Q} = Q_u/Q_L$ for band-pass and band-rejection filters (Q_L is the loaded Q of the filter, viz, $Q_L = f_o/f_c$ − cf. Chap. 5 and 6).

Illustrative Example 4.11

An emitter follower, having an internal resistance of about 10 ohms, is driving a 1000-ohm load. A 2-mc signal to be passed is rich in harmonics, and at least a 50-db attenuation is required at its second harmonic. The maximum allowable insertion loss is 1 db and the Q_u of the inductors is about 80. The problem involves designing a suitable low-pass filter to insert between the emitter follower output and the 1 K ohm load.

A Tchebycheff response is chosen since fewer stages are generally required than with a Butterworth response. A 1/2-db ripple is chosen to ensure that the attenuation is well within the 1-db insertion loss limitations which must also accommodate element losses. Due to the variation in components, let $f_c = 1.05 \times 1$ mc or 2.1 mc to ensure that $f_c > 2$ mc in the selection of components and fabrication (see Chap. 6). The normalized frequency of the second harmonic is: $\overline{\omega} = \omega_1/\omega_c = 4.0/2.1 \approx 1.9$. Fig. 4.35 shows that for $\epsilon_{db} = 1/2$ db and for a transmission loss of at least 40 db, n = 6.0.

Table 4.13 is used to determine the element values of a 1/2-db ripple, unbalanced termination, Tchebycheff filter. The $\overline{Q} = \infty$ sub-table is used since $Q_u \geq 50$. Finally, either network (A) or (C) can be used since a voltage source is approximated. For this example, network (A) will be chosen since the load is likely to be better controlled (defined) than the emitter-follower source resistance. Thus, from Table 4.13:

$$L_1 = 1.404\,\text{h}$$
$$C_2 = 1.902\,\text{f}$$

Table 4.11
ELEMENT VALUES FOR UNBALANCED TERMINATIONS ($\bar{R}<0.1$ ohms/mhos)* OF A NORMALIZED LOW-PASS, TCHEBYCHEFF FILTER (1/10-db Ripple) HAVING UNIFORM DISSIPATION

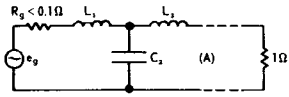

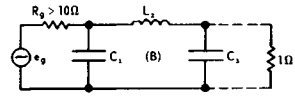

n	C_1	L_2	C_3	L_4	C_5	L_6	C_7	L_8	C_9	L_{10}	n
					$\bar{Q}=\infty$ (Use for $\bar{Q}\geq 50$)						
1	0.153										1
2	0.716	0.422									2
3	1.090	1.086	0.516								3
4	1.245	1.458	1.199	0.554							4
5	1.376	1.592	1.556	1.249	0.573						5
6	1.404	1.724	1.675	1.600	1.275	0.584					6
7	1.475	1.740	1.799	1.711	1.624	1.291	0.591				7
8	1.466	1.816	1.807	1.830	1.730	1.638	1.301	0.595			8
9	1.518	1.799	1.881	1.834	1.847	1.742	1.648	1.308	0.598		9
10	1.496	1.859	1.860	1.907	1.849	1.858	1.750	1.654	1.312	0.600	10
					$\bar{Q}=30$ (Use for $25\leq\bar{Q}<50$)						
1	0.153										1
2	0.713	0.434									2
3	1.069	1.108	0.544								3
4	1.185	1.482	1.245	0.599							4
5	1.283	1.592	1.611	1.316	0.634						5
6	1.251	1.727	1.703	1.680	1.364	0.661					6
7	1.276	1.709	1.844	1.760	1.728	1.401	0.685				7
8	1.184	1.798	1.823	1.906	1.799	1.767	1.432	0.707			8
9	1.152	1.742	1.941	1.883	1.952	1.830	1.802	1.461	0.729		9
10	0.945	1.863	1.934	2.035	1.932	1.994	1.859	1.836	1.488	0.750	10
					$\bar{Q}=20$ (Use for $15\leq\bar{Q}<25$)						
1	0.382										1
2	0.711	0.440									2
3	1.058	1.119	0.559								3
4	1.152	1.496	1.269	0.624							4
5	1.229	1.593	1.643	1.353	0.669						5
6	1.157	1.736	1.724	1.730	1.414	0.708					6
7	1.131	1.706	1.892	1.799	1.797	1.465	0.745				7
8	0.913	1.863	1.902	2.000	1.861	1.859	1.511	0.781			8
9	0.122	8.281	2.657	2.130	2.122	1.924	1.921	1.557	0.818		9
					$\bar{Q}=10$ (Use for $5\leq\bar{Q}<15$)						
1	0.812										1
2	0.704	0.460									2
3	1.020	1.153	0.610								3
4	1.035	1.547	1.348	0.712							4
5	1.009	1.623	1.781	1.484	0.804						5
6	0.602	2.163	1.974	1.995	1.608	0.899					6

n	L_1	C_2	L_3	C_4	L_5	C_6	L_7	C_8	L_9	C_{10}	n

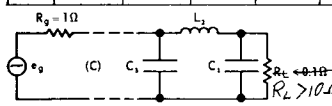

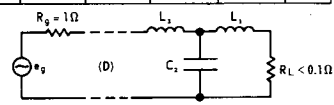

*Use Table 4.4 for $0.7<\bar{R}\leq 1.0$
Use Table 4.5 for $0.1\leq\bar{R}\leq 0.7$

Table 4.12
ELEMENT VALUES FOR UNBALANCED TERMINATIONS ($\bar{R} < 0.1$ ohms/mhos)* OF A NORMALIZED LOW-PASS, TCHEBYCHEFF FILTER (1/4-db Ripple) HAVING UNIFORM DISSIPATION

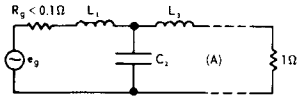

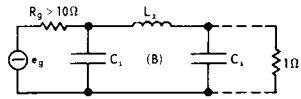

n	C_1	L_2	C_3	L_4	C_5	L_6	C_7	L_8	C_9	L_{10}	n
					$\bar{Q} = \infty$ (Use for $\bar{Q} \geq 50$)						
1	0.243										1
2	0.850	0.557									2
3	1.225	1.220	0.652								3
4	1.300	1.598	1.322	0.689							4
5	1.448	1.637	1.674	1.354	0.691						5
6	1.419	1.811	1.714	1.727	1.387	0.717					6
7	1.532	1.750	1.882	1.745	1.748	1.400	0.723				7
8	1.465	1.881	1.812	1.910	1.761	1.760	1.408	0.727			8
9	1.565	1.793	1.944	1.837	1.925	1.771	1.768	1.414	0.730		9
10	1.486	1.912	1.851	1.968	1.849	1.934	1.778	1.773	1.418	0.732	10
					$\bar{Q} = 30$ (Use for $25 \leq \bar{Q} < 50$)						
1	0.244										1
2	0.845	0.573									2
3	1.199	1.241	0.697								3
4	1.219	1.631	1.368	0.759							4
5	1.341	1.623	1.743	1.424	0.781						5
6	1.230	1.823	1.728	1.832	1.479	0.837					6
7	1.300	1.692	1.950	1.781	1.886	1.514	0.870				7
8	1.108	1.874	1.815	2.026	1.819	1.933	1.545	0.903			8
9	1.056	1.724	2.088	1.898	2.093	1.853	1.978	1.574	0.935		9
10	0.050	2.028	2.569	2.389	2.005	2.172	1.890	2.025	1.603	0.969	10
					$\bar{Q} = 20$ (Use for $15 \leq \bar{Q} < 25$)						
1	0.246										1
2	0.837	0.589									2
3	1.184	1.251	0.722								3
4	1.173	1.651	1.392	0.799							4
5	1.275	1.617	1.787	1.462	0.836						5
6	1.102	1.843	1.747	1.905	1.532	0.914					6
7	1.078	1.696	2.053	1.831	1.992	1.583	0.969				7
8	0.417	2.945	2.197	2.290	1.923	2.084	1.634	1.026			8
					$\bar{Q} = 10$ (Use for $5 \leq \bar{Q} < 15$)						
1	0.250										1
2	0.821	0.626									2
3	1.135	1.282	0.810								3
4	1.004	1.734	1.476	0.951							4
5	0.955	1.670	2.024	1.610	1.056						5

n	L_1	C_2	L_3	C_4	L_5	C_6	L_7	C_8	L_9	C_{10}	n

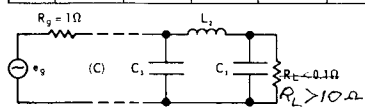

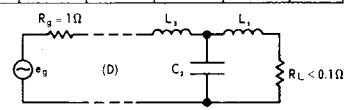

*Use Table 4.4 for $0.7 < \bar{R} \leq 1.0$
Use Table 4.6 for $0.1 \leq \bar{R} \leq 0.7$

Table 4.13
ELEMENT VALUES FOR UNBALANCED TERMINATIONS ($\bar{R}<0.1$ ohms/mhos)* OF A NORMALIZED LOW-PASS, TCHEBYCHEFF FILTER (1/2-db Ripple) HAVING UNIFORM DISSIPATION

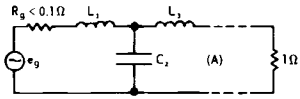

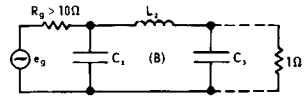

n	C_1	L_2	C_3	L_4	C_5	L_6	C_7	L_8	C_9	L_{10}	n
					$\bar{Q}=\infty$ (Use for $\bar{Q}\geq 50$)						
1	0.349										1
2	0.940	0.701									2
3	1.347	1.300	0.798								3
4	1.314	1.728	1.392	0.835							4
5	1.539	1.643	1.814	1.429	0.853						5
6	1.404	1.902	1.710	1.850	1.448	0.863					6
7	1.598	1.725	1.971	1.737	1.868	1.460	0.869				7
8	1.438	1.957	1.784	1.998	1.751	1.875	1.467	0.873			8
9	1.624	1.757	2.020	1.806	2.012	1.759	1.886	1.471	0.875		9
10	1.454	1.982	1.812	2.043	1.817	2.020	1.765	1.891	1.475	0.877	10
					$\bar{Q}=30$ (Use for $25\leq\bar{Q}<50$)						
1	0.353										1
2	0.925	0.736									2
3	1.317	1.314	0.867								3
4	1.208	1.776	1.430	0.940							4
5	1.419	1.603	1.913	1.489	0.994						5
6	1.172	1.933	1.701	1.994	1.530	1.043					6
7	1.326	1.631	2.086	1.752	2.061	1.562	1.090				7
8	0.969	1.990	1.782	2.198	1.794	2.124	1.591	1.137			8
9	0.590	2.544	2.669	1.977	2.337	1.841	2.192	1.620	1.187		9
					$\bar{Q}=20$ (Use for $15\leq\bar{Q}<25$)						
1	0.356										1
2	0.916	0.754									2
3	1.301	1.321	0.907								3
4	1.148	1.806	1.450	1.003							4
5	1.337	1.583	1.982	1.523	1.084						5
6	0.998	1.980	1.719	2.111	1.580	1.164					6
7	0.876	1.764	2.376	1.843	2.245	1.632	1.248				7
					$\bar{Q}=10$ (Use for $5\leq\bar{Q}<15$)						
1	0.362										1
2	0.886	0.816									2
3	1.241	1.338	1.049								3
4	0.914	1.954	1.527	1.254							4
5	0.674	1.982	2.577	1.700	1.487						5

n	L_1	C_2	L_3	C_4	L_5	C_6	L_7	C_8	L_9	C_{10}	n

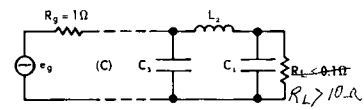

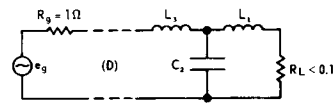

*Use Table 4.4 for $0.7<\bar{R}\leq 1.0$
Use Table 4.7 for $0.1\leq\bar{R}\leq 0.7$

Table 4.14
ELEMENT VALUES FOR UNBALANCED TERMINATIONS ($\bar{R}$ < 0.1 ohms/mhos)* OF A NORMALIZED LOW-PASS, TCHEBYCHEFF FILTER (1 db Ripple) HAVING UNIFORM DISSIPATION

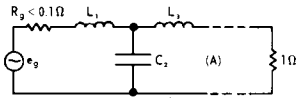

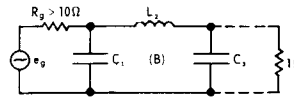

n	C_1	L_2	C_3	L_4	C_5	L_6	C_7	L_8	C_9	L_{10}	n
					$\bar{Q} = \infty$ (Use for $\bar{Q} \geq 50$)						
1	0.509										1
2	0.996	0.911									2
3	1.509	1.333	1.012								3
4	1.282	1.909	1.413	1.050							4
5	1.665	1.591	1.994	1.444	1.067						5
6	1.346	2.049	1.651	2.027	1.460	1.077					6
7	1.712	1.649	2.119	1.674	2.044	1.469	1.083				7
8	1.369	2.092	1.702	2.145	1.685	2.054	1.475	1.087			8
9	1.732	1.671	2.157	1.721	2.158	1.692	2.060	1.479	1.090		9
10	1.380	2.111	1.722	2.180	1.731	2.166	1.696	2.065	1.482	1.092	10
					$\bar{Q} = 30$ (Use for $25 \leq \bar{Q} < 50$)						
1	0.518										1
2	0.966	0.970									2
3	1.481	1.330	1.126								3
4	1.141	1.991	1.428	1.220							4
5	1.535	1.510	2.153	1.477	1.298						5
6	1.049	2.129	1.601	2.262	1.510	1.373					6
7	1.338	1.500	2.361	1.658	2.366	1.537	1.450				7
8	0.455	2.959	1.921	2.665	1.731	2.482	1.564	1.531			8
					$\bar{Q} = 20$ (Use for $15 \leq \bar{Q} < 25$)						
1	0.522										1
2	0.905	1.002									2
3	1.464	1.326	1.193								3
4	1.058	2.046	1.437	1.328							4
5	1.420	1.472	2.282	1.500	1.456						5
6	0.757	2.307	1.657	2.507	1.553	1.592					6
					$\bar{Q} = 10$ (Use for $5 \leq \bar{Q} < 15$)						
1	0.536										1
2	0.895	1.114									2
3	1.392	1.314	1.453								3
4	0.706	2.412	1.509	1.809							4

n	L_1	C_2	L_3	C_4	L_5	C_6	L_7	C_8	L_9	C_{10}	n

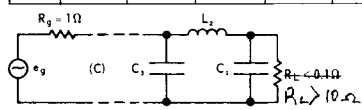

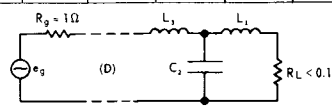

*Use Table 4.4 for $0.7 < \bar{R} \leq 1.0$
Use Table 4.8 for $0.1 \leq \bar{R} \leq 0.7$

Table 4.15
ELEMENT VALUES FOR UNBALANCED TERMINATIONS ($\bar{R}<0.1$ ohms/mhos)* OF A NORMALIZED LOW-PASS, TCHEBYCHEFF FILTER (2 db Ripple) HAVING UNIFORM DISSIPATION

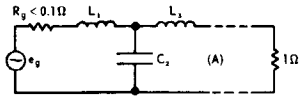

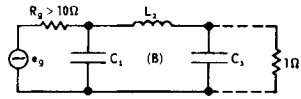

n	C_1	L_2	C_3	L_4	C_5	L_6	C_7	L_8	C_9	L_{10}	n
					$\bar{Q}=\infty$ (Use for $\bar{Q}\geq 50$)						
1	0.765										1
2	0.977	1.244									2
3	1.772	1.274	1.355								3
4	1.173	2.217	1.339	1.396							4
5	1.900	1.447	2.305	1.364	1.416						5
6	1.214	2.330	1.497	2.338	1.377	1.426					6
7	1.938	1.484	2.406	1.516	2.355	1.384	1.433				7
8	1.228	2.365	1.530	2.433	1.525	2.365	1.388	1.437			8
9	1.955	1.496	2.439	1.550	2.446	1.530	2.371	1.391	1.440		9
10	1.235	2.379	1.542	2.461	1.554	2.454	1.534	2.375	1.393	1.442	10
					$\bar{Q}=30$ (Use for $25\leq\bar{Q}<50$)						
1	0.785										1
2	0.925	1.357									2
3	1.758	1.236	1.568								3
4	0.982	2.386	1.311	1.716							4
5	1.752	1.302	2.623	1.344	1.853						5
6	0.798	2.558	1.401	2.830	1.369	1.995					6
7	0.624	2.040	3.581	1.551	3.089	1.394	2.152				7
					$\bar{Q}=20$ (Use for $15\leq\bar{Q}<25$)						
1	0.795										1
2	0.896	1.421									2
3	1.744	1.215	1.701								3
4	0.864	2.512	1.301	1.937							4
5	1.482	1.265	2.975	1.357	2.191						5
					$\bar{Q}=10$ (Use for $5\leq\bar{Q}<15$)						
1	0.828										1
2	0.802	1.656									2
3	1.631	1.162	2.284								3
4	0.175	7.133	1.530	3.162							4

n	L_1	C_2	L_3	C_4	L_5	C_6	L_7	C_8	L_9	C_{10}	n

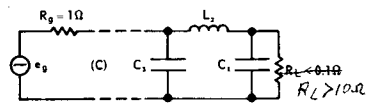

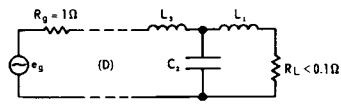

*Use Table 4.4 for $0.7<\bar{R}\leq 1.0$
Use Table 4.9 for $0.1\leq\bar{R}<0.7$

Table 4.16
ELEMENT VALUES FOR UNBALANCED TERMINATIONS ($\bar{R} < 0.1$ ohms/mhos)* OF A NORMALIZED LOW-PASS, TCHEBYCHEFF FILTER (3 db Ripple) HAVING UNIFORM DISSIPATION

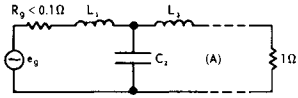

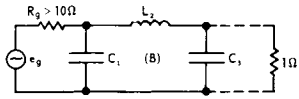

n	C_1	L_2	C_3	L_4	C_5	L_6	C_7	L_8	C_9	L_{10}	n
					$\bar{Q} = \infty$ (Use for $\bar{Q} \geq 50$)						
1	0.998										1
2	0.911	1.551									2
3	2.030	1.174	1.674								3
4	1.058	2.527	1.229	1.720							4
5	2.149	1.302	2.623	1.250	1.741						5
6	1.088	2.631	1.346	2.658	1.261	1.752					6
7	2.183	1.328	2.714	1.361	2.675	1.267	1.759				7
8	1.098	2.662	1.369	2.744	1.369	2.685	1.270	1.764			8
9	2.197	1.338	2.741	1.383	2.758	1.373	2.692	1.273	1.767		9
10	1.103	2.675	1.377	2.768	1.389	2.766	1.376	2.696	1.274	1.769	10
					$\bar{Q} = 30$ (Use for $25 \leq \bar{Q} < 50$)						
1	1.032										1
2	0.841	1.729									2
3	2.038	1.108	2.011								3
4	0.829	2.816	1.166	2.231							4
5	1.949	1.113	3.179	1.192	2.452						5
6	0.498	3.326	1.290	3.602	1.218	2.698					6
					$\bar{Q} = 20$ (Use for $15 \leq \bar{Q} < 25$)						
1	1.050										1
2	0.803	1.835									2
3	2.027	1.074	2.236								3
4	0.680	3.064	1.148	2.621							4
5	1.068	1.354	4.215	1.225	3.082						5
					$\bar{Q} = 10$ (Use for $5 \leq \bar{Q} < 15$)						
1	1.108										1
2	0.681	2.248									2
3	1.791	1.020	3.364								3
n	L_1	C_2	L_3	C_4	L_5	C_6	L_7	C_8	L_9	C_{10}	n

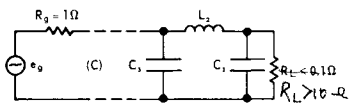

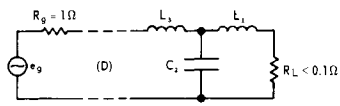

*Use Table 4.4 for $0.7 < \bar{R} \leq 1.0$
Use Table 4.10 for $0.1 \leq \bar{R} \leq 0.7$

$$L_3 = 1.710\,\text{h}$$
$$C_4 = 1.849\,\text{f}$$
$$L_5 = 1.448\,\text{h}$$
$$C_6 = 0.863\,\text{f}$$
$$R_g < 0.1\,\Omega$$
$$R_L = 1\ \text{ohm}.$$

The corresponding 2-mc, low-pass filter elements are:

$$L_1' = \frac{RL_1}{\omega_c} = \frac{10^3 \times 1.404}{2\pi \times 2.1 \times 10^6} = 107\,\mu\text{h}$$

$$C_2' = \frac{C_2}{R\omega_c} = \frac{1.902}{10^3 \times 2\pi \times 2.1 \times 10^6} = 144\,\mu\mu\text{f}$$

$$L_3' = \frac{RL_3}{\omega_c} = \frac{10^3 \times 1.710}{2\pi \times 2.1 \times 10^6} = 130\,\mu\text{h}$$

$$C_4' = \frac{C_4}{R\omega_c} = \frac{1.849}{10^3 \times 2\pi \times 2.1 \times 10^6} = 140\,\mu\mu\text{f}$$

$$L_5' = \frac{RL_5}{\omega_c} = \frac{10^3 \times 1.448}{2\pi \times 2.1 \times 10^6} = 110\,\mu\text{h}$$

$$C_6' = \frac{C_6}{R\omega_c} = \frac{0.863}{10^3 \times 2\pi \times 2.1 \times 10^6} = 66\,\mu\mu\text{f}.$$

4.2.3 Transient Response and Time Delay

Section 4.1.3 presented some derivations of the time delay characteristics of filters in general and the Butterworth response in particular. It can be shown that the time delay, τ_d, of a Tchebycheff, low-pass filter of n stages is

$$\tau_d = \frac{\dfrac{1}{B}\displaystyle\sum_{k=1}^{n} \frac{U_{2k-2}\left(\dfrac{\omega}{B}\right) \sinh\,(2n - 2k - 1)\,\phi_2}{\epsilon^2 \sin\,(2k-1)\dfrac{\pi}{2n}}}{1 + \epsilon^2 T_n^2\left(\dfrac{\omega}{B}\right)} \tag{4.63}$$

where,
$$U_{2k-2}\left(\frac{\omega}{B}\right) = \frac{\sin (n+1)\cos^{-1}\left(\frac{\omega}{B}\right)}{\sqrt{1-\left(\frac{\omega}{B}\right)^2}} \tag{4.64}$$

$$\phi_2 = \frac{1}{n}\sinh^{-1}(1/\epsilon). \tag{4.65}$$

The center frequency time delay is obtained by setting $\omega = 0$ in Eq. (4.63). This results in:

$$\tau_d = \frac{1}{B\epsilon^2}\sum_{k=1}^{n}\frac{\sin (n+1)\frac{\pi}{2}\sinh (2n-2k+1)\frac{1}{n}\sinh^{-1} 1/\epsilon}{\sin (2k-1)\frac{\pi}{2n}} \tag{4.66}$$

Eq. (4.66) was computed for several values of n corresponding to $\epsilon_{db} = 1/2$, 1, and 2 db. The results are plotted in Figs. 4.41, 4.42, and 4.43 respectively. It is noted that the slope of the time delay vs. n results in two values: for n = odd, the slope is greater than for n = even. Additionally, these slopes merge into a single slope as ϵ_{db} because smaller (cf. Fig. 4.41–4.43).

For ϵ_{db} = 1-db Tchebycheff ripple, the slope is approximately unity. This may be compared with a slope of 0.64 for the Butterworth. Thus, the time delay per stage for a 1-db ripple Tchebycheff is 1.0/0.64 or 57% greater than that for the Butterworth response. On the other hand, the delay distortion of the Tchebycheff is more severe than the Butterworth over the pass band, especially at the band edge. For both responses, time delay of the low-pass filter is exactly equal to twice that for a band-pass filter of the same bandwidth.

Figs. 4.44, 4.45, and 4.46 show the transient response of an ϵ_{db} = 1/2-db, 1-db, and 2-db ripple Tchebycheff, low-pass filter to both an impulse and step driving function for the number of stages n equals one through ten. Since the impulse response is the time derivative of the step response, the impulse response curves provide a means of estimating the rate of rise of the step response curves.

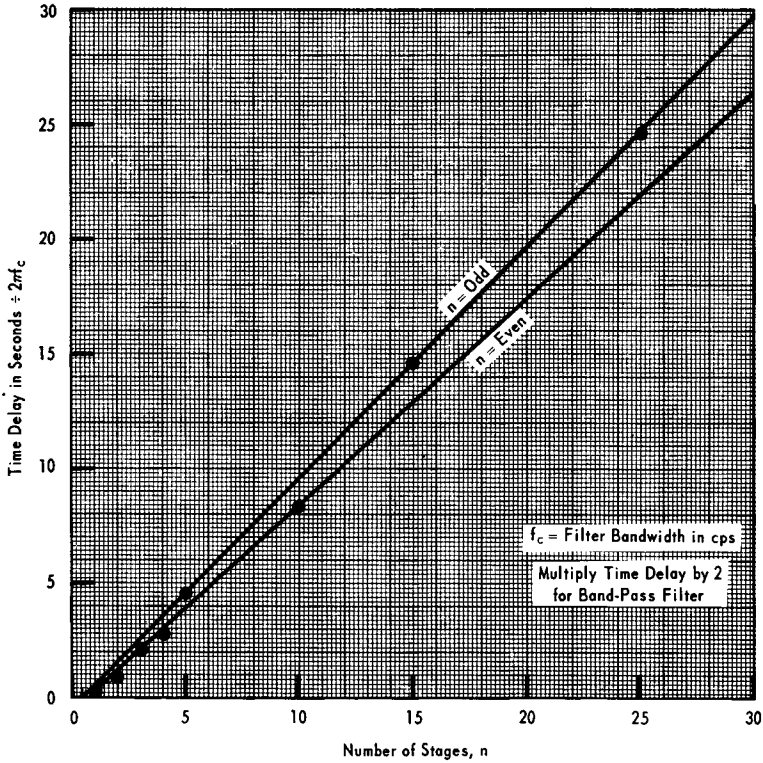

Figure 4.41. Mid-Band Time Delay of Tchebycheff (ϵ_{db} = 1/2-db Ripple), Low-Pass Filter

4.3 BUTTERWORTH-THOMPSON PROTOTYPE

4.3.1 Comparison of Transient Responses

The Butterworth function permits a maximally-flat amplitude response to be obtained over its pass band. It suffers from phase and time delay distortion over its pass band especially out near the cut-off frequency region (cf. Sec. 4.1.3). As a consequence, its transient response to a unit step function exhibits considerable overshoot. The time delay distortion of the Tchebycheff response (cf. Sec. 4.2.3) is even worse, although the overshoot of

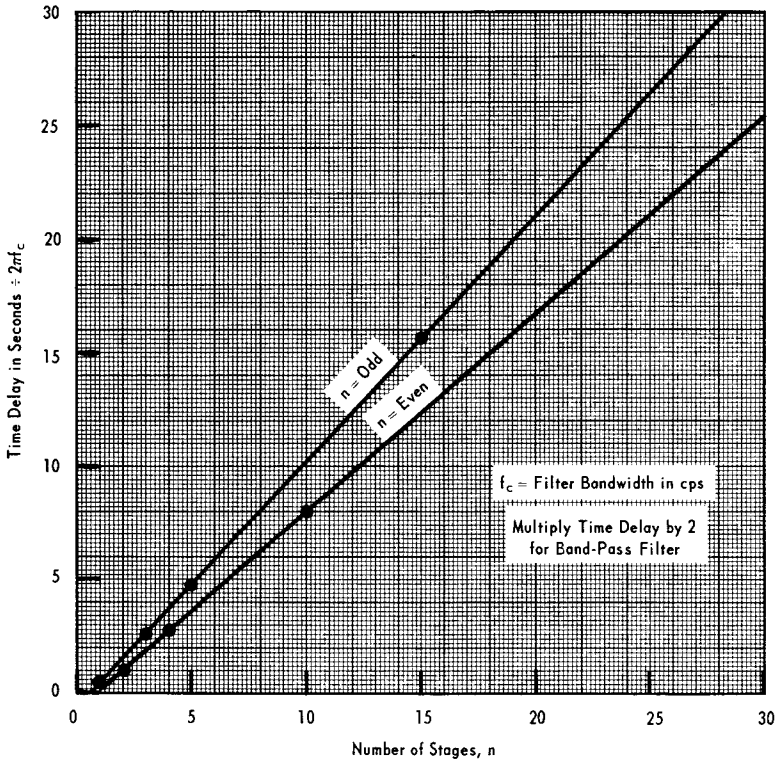

Figure 4.42. Mid-Band Time Delay of Tchebycheff (ϵ_{db} = 1-db Ripple), Low-Pass Filter

the Tchebycheff response is somewhat less than that of the Butterworth. The rise time and the overshoot of both responses are summarized in Table 4.17.

The maximally-flat time delay function, derived from the Bessel polynominals, exhibits extremely small overshoot. Its rise time, however, is longer than either the Butterworth or Tchebycheff function. These properties of the Bessel function are also shown in Table 4.17.

4.3.2 Desirable Properties of Butterworth-Thompson Responses

It is often desirable in practice to obtain a better transient response with respect to overshoot and rise time than any of the

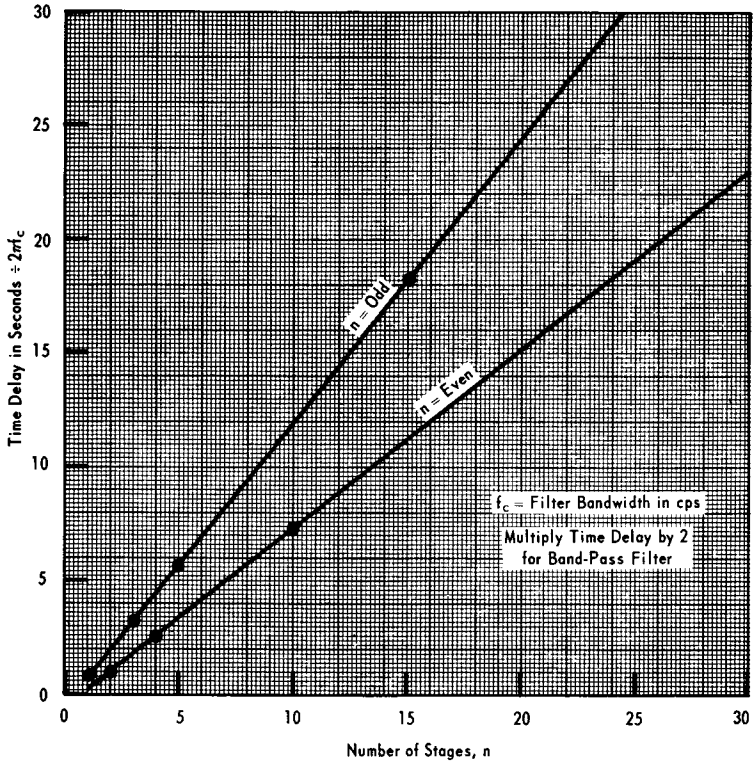

Figure 4.43. Mid-Band Time Delay of Tchebycheff (ϵ_{db} = 2-db Ripple), Low-Pass Filter

three functions summarized in Table 4.17. The Tchebycheff response can be eliminated since it does not perform well in either rise time or overshoot. Thus, what is needed is a new function which exhibits some of the fast rise time and flat amplitude properties of the Butterworth and the low overshoot properties of the Bessel function. Such a combination function has been developed and is called a transitional Butterworth-Thompson prototype; viz,

$$r = r_T^n \text{ and } \phi = \phi_B - n(\phi_B - \phi_T) \qquad (4.67)$$

where, r = radius vector of poles

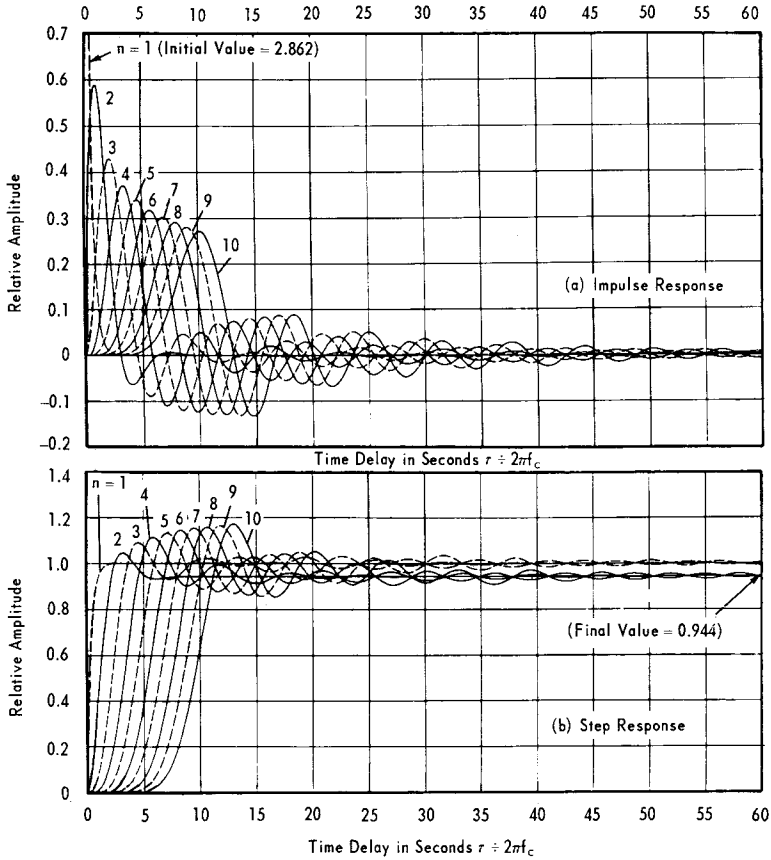

Reprinted from: "Transient Responses of Conventional Filters" by K.W. Henderson & W.H. Kautz, pp. 334, 335, & 337. IRE Transactions on Circuit Theory, Vol. CT-5, Mo. 4, December, 1958. Copyright 1959– The Institute of Radio Engineers, Inc.

Figure 4.44. Transient Response of Low-Pass, Tchebycheff Filter ($\bar{\epsilon} = 0.5$ db) having a Bandwidth of f_c cps

ϕ = phase angle of poles

B = subscript which refers to Butterworth or maximally-flat amplitude properties

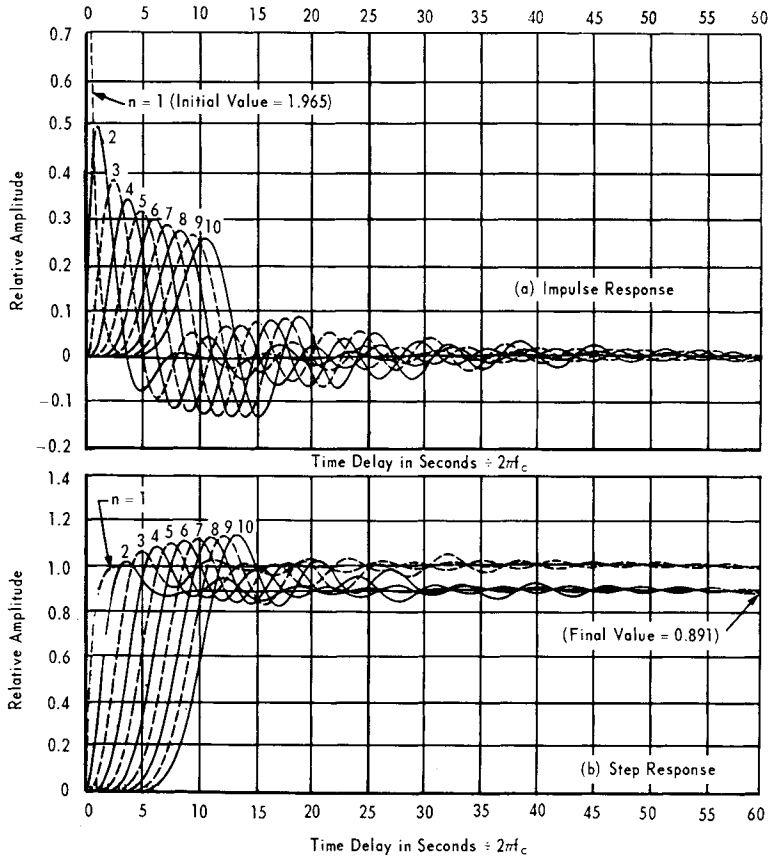

Figure 4.45. Transient Response of Low-Pass Tchebycheff Filter ($\overline{\epsilon} = 1$ db) having a Bandwidth of f_c cps

T = subscript which refers to Thompson or maximally-flat time delay properties

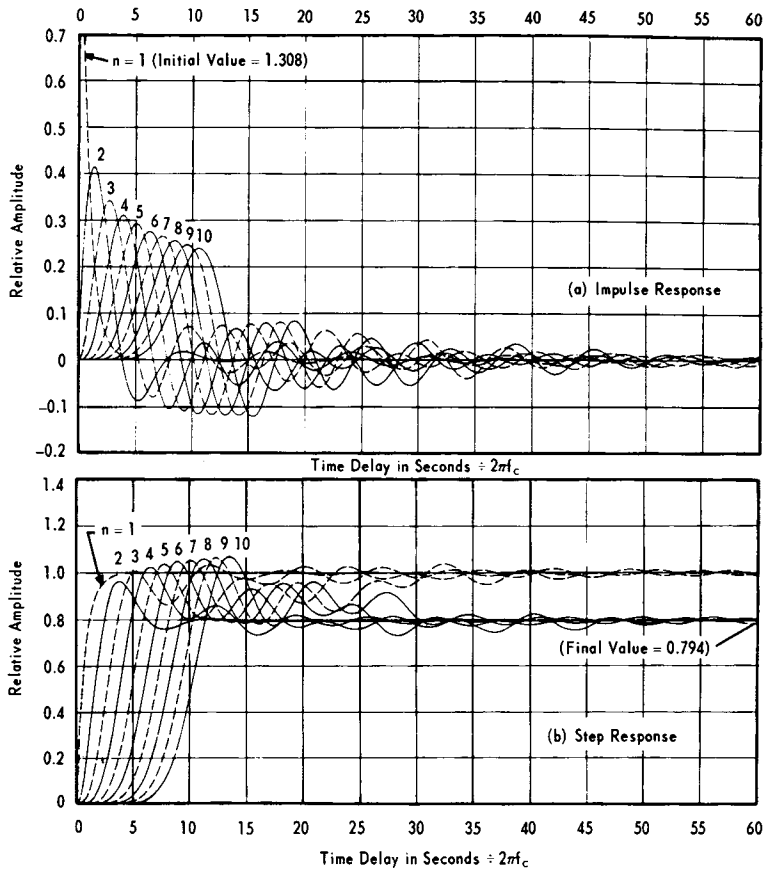

Reprinted from: "Transient Responses of Conventional Filters" by K. W. Henderson & W. H. Kautz, pp. 334, 335, & 337. IRE Transactions on Circuit Theory, Vol. CT-5, Mo. 4, December, 1958. Copyright 1959— The Institute of Radio Engineers, Inc.

Figure 4.46. Transient Response of Low-Pass Tchebycheff Filter ($\bar{\epsilon}$ = 2 db) having a Bandwidth of f_c cps

n = a number between 0 and 1.

When n = 0 in Eq. (4.67), the response is that of a Butterworth function, whereas when n = 1, the Thompson (Bessel) response is

obtained. Thus, the bandwidth of the amplitude characteristic increases when n is decreased from unity (emphasizing more the Butterworth response). The phase linearity increases, the rise time becomes longer, and the overshoot decreases when n is increased from zero (emphasizing more the Thompson response).

At the time of the preparation of this handbook, sufficient Butterworth-Thompson prototype design data were not yet developed to include in this volume. Thus, the reader interested in more information is referred to the work of Peless and Murakami cited in reference 42 of this Chapter.

Table 4.17
RISE TIME AND OVERSHOOT OF BUTTERWORTH, BESSEL, AND TCHEBYCHEFF RESPONSES TO A UNIT STEP FUNCTION

Number of stages, n	Rise Time			Overshoot in Percent		
	Buttw*	Bessel	Tcheby	Buttw	Bessel**	Tcheby
1	2.2	2.2	1.1	0	0	0
2	2.2	2.7	1.6	4	0.4	2
3	2.3	3.1	2.4	8	0.8	6
4	2.4	3.4	2.7	11	0.8	9
5	2.6	3.6	3.1	13	0.8	11
6	2.7	3.8	3.2	14	0.7	12
7	2.9	3.9	3.3	15	0.7	12
8	3.0	3.9	3.5	16	0.6	13
9	3.0	4.0	3.7	17	0.5	14
10	3.1	4.0	3.8	18	0.4	15

*Butterworth, Maximally-flat amplitude has fastest rise time but greatest overshoot.
**Bessel, Maximally-flat time delay has least overshoot but slowest rise time.

4.4 REFERENCES

1. Aseltine, John A., "Transform Method in Linear System Analysis," McGraw-Hill Book Co., New York, 1958.

2. Balabanion, Norman and Lepage, Wilbur R., "What is a Minimum-Phase Network?" *Communications and Electronics,* January 1956.

3. Belevitch, V., "Fundamental Results and Outstanding Problems of Network Synthesis," *Tijdschmed Radiogenot,* Vol. I, 1952.

4. Bennett, B. J., "Linear Phase Electric Filters," *Stanford Electronics Research Lab.,* Report 43, February 14, 1952.

5. Berekowitz, R. S., "Optimum Linear Shaping and Filtering Networks," *Proceedings of the IRE,* Vol. 41, pp. 532–537, April 1953.

6. Bode, H. W., "Network Analysis and Feedback Amplifier Design," D. Van Nostrand Company, Inc., New York, 1945.

7. Bower, J. L. and Ardung, P. F., "The Synthesis of Resistor-Capacitor Networks," *Proceedings of the IRE,* Vol. 38, pp. 263–269, March 1960.

8. Brune, O., "Synthesis of a Finite Two-Terminal Network Whose Driving-Point Impedance is a Prescribed Function of Frequency," *Journal of Mathematics and Physics,* Vol. 10, pp. 191–236, 1931.

9. Butterworth, S., "On the Theory of Filter Amplifiers," *Experimental Wireless,* Vol. 7, pp. 536–541, October 1930.

10. Campbell, G. A., "Physical-Theory on the Electric Wave-Filter," *Bell System Technical Journal,* Vol. 1, p. 2, November 1922.

11. Cauer, W., "Die Verwirklichung von Wechslestromwiderstanden Vorgeschriebener Frequenzabhangigkeit," *Archiv f. Elektrotechnik,* Vol. 17, p. 355, 1927.

12. Cauer, W., "Theorie der Linearen Wechselstromschaltungen," Becker and Erler, Leipzig, Germany, Vol. 1, 1941.

13. Cauer, Wilhelm, "Synthesis of Linear Communication Networks," McGraw-Hill Book Co., New York, 1958. (Translated from the German second edition by G. E. Knausenberger and J. N. Warfield.)

14. Darlington, S., "Synthesis of Reactance 4-Poles Which Produce Prescribed Insertion Loss Characteristics Including Special Applications to Filter Design," *Journal of Mathematics and Physics,* Vol. 18, pp. 257–353, 1939.

15. Darlington, S., "Network Synthesis Using Tchebycheff Polynomial Series," *Bell Systems Technical Journal,* Vol. 31, p. 613.

16. DeClaris, N., "A Method of Rational Function Approximation for Network Synthesis," (MIT, Cambridge, Mass.), *IRE Session XXXIX, No. 39.1,* IRE Convention Program, p. 368, March 1955.

17. Destebelle, Savant, and Savant, C. J., Jr., "A Less-than-Minimum Phase Shift Network," *Tele-Tech and Electronic Industries,* August 1956.

18. Epstein, H., "Synthesis of Passive RC Networks with Gains Greater than Unity," *Proceedings of the IRE,* Vol. 39, pp. 833–835, July 1951.

19. Fano, R. M., "A Note on the Solution of Certain Approximation Problems in Network Synthesis," *Journal of the Franklin Institute,* Vol. 249, pp. 189–205, March 1950.

20. Fano, R. M. and A. W. Lawson, "The Theory of Microwave Filters," *Radiation Laboratory Series,* Chapter 9, Vol. 9, Microwave Transmission Circuits, McGraw-Hill Book Company, Inc., 1948.

21. Falkow, A. D. and Gerst, I., "RLC Lattice Transfer Functions," *Proceedings of the IRE,* pp. 462–469, April 1955.

22. Gardner, M. F. and J. L. Barnes, "Transients In Linear Systems," Vol. I, John Wiley & Sons, New York, 1942.

23. Guillemin, E. A., "Communication Networks," Vol. 1 and 2, John Wiley & Sons, Inc., New York, 1935.

24. Guillemin, E. A., "A Summary of Modern Methods of Network Synthesis," *Advances in Electronics,* Vol. 2, pp. 261–303, Academic Press, Inc., New York, 1951.

25. Guillemin, E. A., "Introductory Circuit Theory," John Wiley & Sons, Inc., New York, 1953.

26. Kahal, R., "Synthesis of the Transfer Function of Two-Terminal Pair Networks," *Transactions of the IRE*, Part I, pp. 127–134, 1952.

27. Kautz, W. H., "Network Synthesis for Specified Transient Response," Tech. Report No. 209, Research Lab. for Electronics, MIT, also paper No. 134, *IRE National Convention*, N.Y., March 1952.

28. Kuh, E. S. and Pederson, D. O., "Principles of Circuit Synthesis," McGraw-Hill Book Co., New York, 1959.

29. LePage, W. R. and Seely, S., "General Network Analysis," McGraw-Hill Book Co., Inc., 1952.

30. Levy, M., "The Impulse Response of Electrical Networks with Special Reference to Use of Artificial Lines in Network Design," *Journal of the IEE*, Vol. 90, Part III, pp. 153–164.

31. Linden, D. A. and Steinberg, B. D., "Synthesis of Delay Line Networks," *Philco Report No. 248.*

32. Longmire, C. L., "An RC Circuit Giving Over Unity-Gain," *Tele-Tech*, Vol. 6, pp. 40–41, April 1947.

33. Longo, C. V. and Wolf, E., "R-F Filter Design," *Electronics*, p. 176, February 1955.

34. Malligan, J. H., "The Effect of Pole and Zero Locations on the Transient Response of Linear Dynamic Systems," *Proceedings of the IRE*, Vol. 37, No. 5, pp. 516–529, May 1949.

35. Matthaei, G. L., "Synthesis of Tchebycheff Impedance Matching Networks, Filters, and Interstages," Report No. 43, ONR Contract Nb our 29429.

36. Matthaei, G. L., "Some Techniques for Network Synthesis," *Proc. of the IRE*, pp. 1126–1137, July 1954.

37. Matthaei, G. L., "Conformal Mappings for Filter Transfer Function Synthesis," *Proceedings of the IRE*, Vol. 41, pp. 1658–1664, November 1953.

38. Matthaei, G. L., "Filter Transfer Function Synthesis," *Proceedings of the IRE*, Vol. 41, pp. 377–382, March 1953. Also, Paper No. 72, IRE National Convention, New York, N.Y., March 1952.

39. Orchard, H. J., "Phase and Envelope Delay of Butterworth and Tchebycheff Filters," *IRE PGCT*, p. 180, June 1960.

40. Pantell, R. H., "New Methods of Driving-Point and Transfer Function Synthesis," *Technical Report No. 76, Stanford University*, July 1954.

41. Pantell, R. H., "Synthesis Techniques," (Elec. Eng. Dept., Stanford University), *Proceedings of the IRE*, p. 625, May 1955.

42. Peless, Y. and T. Murakami, "Analysis and Synthesis of Transitional Butterworth-Thompson Filters and Bandpass Amplifiers," *RCA Review*, Vol. 18, No. 1, pp. 60–94, March 1957.

43. Reza, F. M. and Lewis, P. M., III, "A Note on the Transfer Voltage Ratio of Passive RLC Networks," *Elect. Engr. Abstracts*, Vol. 58, No. 687, p. 163, March 1955, No. 1143.

44. Rosenbrock, H. H., "An Approximate Method for Obtaining Transient Response from Frequency Response," *Proc. Inst. Elect. Engrs.*, Part B, Vol. 102, No. 6, pp. 744–752, November 1955.

45. Seshu, Sundaram and N. Balabanian, "Linear Network Analysis," John Wiley & Sons, New York, 1959.

46. Skilling, H. H., "Electrical Engineering Circuits," John Wiley & Sons, New York, 1957.

47. Scott, R. E., "Network Synthesis by the Use of Potential Analogs," *Proceedings of the IRE*, Vol. 40, p. 970, 1952.

48. Scott, R. E., "Potential Analog Methods of Solving the Approximation Problem of Network Synthesis," *Proc. NEC*, Vol. 9, pp. 543–553, 1953.

49. Sharpe, C. B., "A General Tchebycheff Rational Function," *Proc. of the IRE*, pp. 454–457, February 1954.

50. Staffin, R. E. (2), "Network Synthesis Procedures with a Potential Analog Computer," Report R-391-54, pp. 13–324, Microwave Research Institute of Brooklyn.

51. Stewart, J. L., "Circuit Theory and Design," John Wiley & Sons, New York, 1956.

52. Storer, J. E., "Passive Network Synthesis, McGraw-Hill Book Co., New York, 1957.

53. Tellegen, B. D. H., "Synthesis of Passive Resistanceless 4-Poles that May Violate the Reciprocity Relation," *Philips Res. Report,* Vol. 3, pp. 321–337, October 1948.

54. Tellegen, B. D. H., "Complementary Note on the Synthesis of Passive Resistanceless 4-Poles," *Philips Res. Report,* Vol. 4, pp. 336–369, October 1949.

55. Truxal, J. G., "Automatic Feedback Control System Synthesis," McGraw-Hill Book Co., New York, 1955.

56. Tuttle, D. F., "A Problem in Synthesis," *IRE Transaction on Circuit Theory,* Vol. CT-2, pp. 6–18, 1953.

57. Tuttle, D. F., Jr., "Network Synthesis," Vol. I, John Wiley & Sons, New York, 1958.

58. Ulinkhamer, J. F., (1), "Empirical Determination of Wave-Filter Transfer Functions with Specified Properties," *Philips Research Reports,* No. 3 and No. 5(1948).

59. Van Valkenburg, M. E., "An Introduction to Modern Network Synthesis," John Wiley & Sons, Inc., 1960, New York.

60. Van Valkenburg, M. E., "Network Analysis," Prentice-Hall, 1955, Englewood Cliffs, N. J.

61. Ware, L. A. and Reed, H. R., "Communication Circuits," John Wiley & Sons, Inc., 1944, New York.

62. Weber, Ernst, "Linear Transient Analysis," Vols. I and II, John Wiley & Sons, New York, 1954 and 1956.

63. Weinberg, L., "Network Design by Use of Modern Synthesis Techniques and Tables," Hughes Research Labs., Technical Memo Number 427.

64. Weinberg, L., "Modern Synthesis Network Design from Tables–1," *Electronic Design,* September 15, 1956.

65. Weinberg, L., "Networks Terminated in Resistance at Both Input and Output," *Proceedings of the IRE,* p. 625, March 1954.

66. Weinberg, L., "New Synthesis Procedure for Realizing Transfer Functions of RLC and RC Networks," *Technical Report No. 201, MIT,* 1951.

67. Weinberg, L., "Network Analysis and Synthesis," McGraw-Hill Book Co., Inc., 1962, New York.

68. White, D. R. J., "Band-Pass Filter Design Techniques," *Electronics, 31, 1,* January 3, 1958.

69. White, D. R. J., "Charts Simplify Passive LC Filter Design," *Electronics,* pp. 160–163, December 1, 1957.

70. White Electromagnetics, Inc., "RF Delay Line Filters," Final Report under NOLC Contract No. N123(62738)-29779A, 30 June 1962.

71. Zobel, O. J., "Theory and Design of Uniform and Composite Electric Wave-Filters," *Bell System Technical Journal,* Vol. 2, p. 1, January 1923.

CHAPTER 5

FILTER CIRCUIT DESIGN

The previous chapter discussed the development of the low-pass prototype responses with special emphasis on the maximally-flat Butterworth and equal-ripple Tchebycheff responses. It was mentioned that the universal low-pass prototype approach, used in modern network synthesis, affords the ability to directly design high-pass, band-pass, and band-rejection filters as well as low-pass filters by parameter scaling. This chapter emphasizes the development of the four filter types from the low-pass prototype with special consideration of the development and use of a new family of band-pass filter prototypes so that the most physically realizable configuration can be selected.

5.1 LOW-PASS FILTERS

Summarizing the preceding chapter, the design of a low-pass filter proceeds along the following lines:

(1) Select either a Butterworth or Tchebycheff response. If a flat pass-band response and/or a high-power handling capability is required (e.g., variation of attenuation not to exceed, say, 0.1 db up to some frequency $< \omega_c$), choose the Butterworth response. If a ripple variation for a low-power filter is permissible, choose the Tchebycheff response. Generally, the Tchebycheff response will require a fewer number of filter stages at a price of pass-band ripple variation and greater insertion loss.

(2) Determine the transmission loss or attenuation, A_{db}, which is required at some frequency, ω_1, beyond the cut-off frequency, ω_c. Form the normalized frequency ratio, $\overline{\omega} = \omega_1/\omega_c$, at which the attenuation must be equal to or greater than A_{db}.

(3) Determine the required number of stages from the Butterworth response plot depicted in Fig. 4.5 or the Tchebycheff response plots depicted in Figs. 4.33 to 4.38 (whichever applies from the determination in (1)). Enter the abscissa at $\overline{\omega}$ rad/sec and the ordinate at A_{db}. Interpolate the number of stages, n,

required to give the desired response. Choose the next highest integer number of stages. For Tchebycheff responses, increase this integer by one if it is an even number and if the source and terminating resistances must be equal; otherwise use an even number of Tchebycheff stages.

(4) Choose the prototype element values. First determine if the source and load impedances are equal or substantially equal (within 30% of each other; viz, $R \geq 0.7$). If they are substantially equal, use Table 4.1 for a Butterworth response or Table 4.4 for a Tchebycheff response. If the resistance ratio is between $0.1 \leq \overline{R} < 0.7$, use Table 4.2 for a Butterworth response or Tables 4.5 through 4.10 (ϵ_{db} from 0.1 to 3 db) for a Tchebycheff response. Finally, if the resistance ratio is $\overline{R} < 0.1$, use Table 4.3 for a Butterworth response or Tables 4.11 through 4.16 (ϵ_{db} from 0.1 to 3 db) for a Tchebycheff response.

(5) Impedance leveling. To change the source and terminating resistances from one to R ohms, multiply all resistances and inductances by R and divide all capacitances by R.

(6) Bandwidth Scaling. To change the cut-off frequency from one rad/sec to ω_c, divide all L's and C's by ω_c. Do not alter the resistances.

Steps (5) and (6) may be combined in the following manner:

$$C_k' \text{ (new)} = \frac{C_k \text{ (prototype)}}{R\omega_c} = \frac{C_k}{2\pi f_c R} \tag{5.1}$$

$$L_{k-1}' \text{ (new)} = \frac{RL_{k-1} \text{ (prototype)}}{\omega_c} = \frac{RL_{k-1}}{2\pi f_c}. \tag{5.2}$$

Matters regarding physical realizability of the C's and L's, including insertion loss and Q-factors, are discussed in the next chapter.

5.2 HIGH-PASS FILTERS

The design of high-pass filters (ω_{hp}) may be directly obtained from the low-pass prototype (ω_{lp}) by a change in the frequency variable of the transfer function:

$$\omega_{hp} = 1/\omega_{lp}. \tag{5.3}$$

By use of this transformation, the impedance of an inductance, $L\omega_{1p}$, becomes the impedance L/ω_{hp}; the impedance of a capacitance, $1/C\omega_{1p}$, becomes ω_{hp}/C; and the value of the resistance(s) remains unchanged.

This transformation is equivalent to replacing all capacitances and inductances with inductances and capacitances respectively, with each taking on the value of the reciprocal of the replaced component. Impedance leveling and bandwidth scaling of the new high-pass prototype, which also has an impedance level of one ohm and a cut-off frequency of 1 rad/sec respectively, are accomplished in the same manner as in Eqs. (5.1) and (5.2).

Illustrative Example 5.1

Assume a ~~band-pass~~ HIGH PASS filter having a 600-ohm input-output resistance, a cut-off frequency of 1 mc (ω_c), an attenuation of 70 db at 250 kc (ω_1), and no ripple (maximally-flat) in the pass band above 1 mc is desired.

Since the desired attenuation or band-rejection of a high-pass filter lies below the cut-off frequency in contrast to the low-pass filter, form the normalized frequency:

$$\overline{\omega}_{hp} = \omega_c/\omega_1 = 2\pi \times 10^6/2\pi \times 250 \times 10^3 = 4.0.$$

From Fig. 4.5, the required number of stages for the Butterworth low-pass prototype ($\overline{\omega} = 4$ rad/sec and $A_{db} = 70$ db) is about 5.9. Therefore, n = 6 will yield the required response.

Table 4.1 indicates that the high-pass prototype element values should be (arbitrarily selecting a capacitor input; primes pertain to high pass and unprimes to low pass):

$$C_1' = L_6' = 1/L_1 = 1/C_6 = 1/0.518 = 1.932 \text{ farads/henrys}$$

$$L_2' = C_5' = 1/C_2 = 1/L_5 = 1/1.414 = 0.707 \text{ henrys/farads}$$

$$C_3' = L_4' = 1/L_3 = 1/C_4 = 1/1.932 = 0.518 \text{ farads/henrys.}$$

Employing Eqs. (5.1) and (5.2), the final element values are obtained:

$$C_1'' = \frac{C_1'}{2\pi R f_c} = \frac{1.932}{2\pi \times 600 \times 10^6} = 512\ \mu\mu f$$

$$L_2'' = \frac{RL_2}{2\pi f_c} = \frac{600 \times 0.707}{2\pi \times 10^6} = 6.75\ \mu h$$

$$C_3'' = \frac{C_3}{2\pi R f_c} = \frac{0.518}{2\pi \times 600 \times 10^6} = 137\ \mu\mu f$$

$$L_4'' = \frac{RL_4}{2\pi f_c} = \frac{600 \times 0.518}{2\pi \times 10^6} = 4.94\ \mu h$$

$$C_5'' = \frac{C_5}{2\pi R f_c} = \frac{0.707}{2\pi \times 600 \times 10^6} = 188\ \mu\mu f$$

$$L_6'' = \frac{RL_6}{2\pi f_c} = \frac{600 \times 1.932}{2\pi \times 10^6} = 18.4\ \mu h.$$

The fact that all final filter element values are not symmetrical from the ends to the center has nothing to do with the fact that this is a high-pass filter rather than a low-pass filter. It is only because the design has an even number of stages rather than an odd number and the impedance level is other than one ohm. The desired high-pass filter is shown in Fig. 5.1, its dual in Fig. 5.2, and the frequency response of both is depicted in Fig. 5.3. It should be observed that the dual network of the filter in Fig. 5.1, having an even number of elements, is exactly equal to interchanging the source and termination or turning the filter end for end. This illustrates the principle of reciprocity previously discussed in connection with Fig. 4.17. This equivalence of duality and reciprocity does not apply to a filter having an odd number of elements.

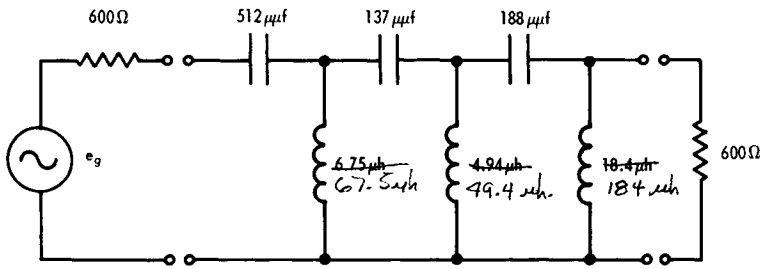

Figure 5.1. Six-Stage, Butterworth High-Pass Filter with 1 mc Cut-Off Frequency

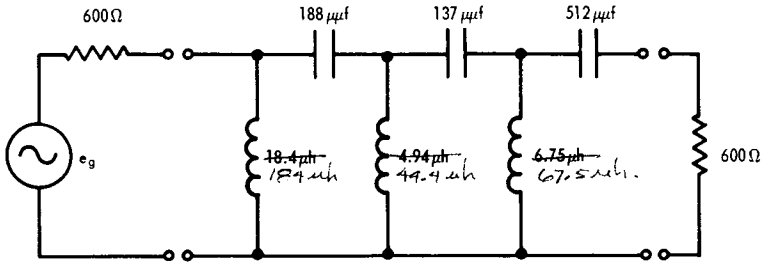

Figure 5.2. Dual of Network Shown in Figure 5.1

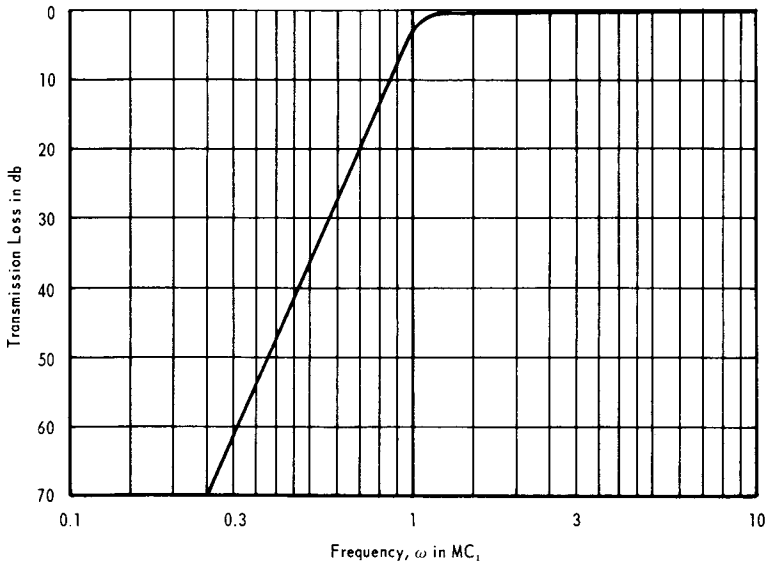

Figure 5.3. Frequency Response of High-Pass Filters Shown in Figures 5.1 and 5.2

5.3 BAND-PASS FILTERS

Like the high-pass filter, the design of band-pass filters may also be directly obtained from the low-pass prototype by a change in the frequency variable of the transfer function. The low-pass prototype has a "center-frequency" (in the parlance of band-pass filters) of 0 rad/sec. In order to make a low-pass to band-pass

filter transformation, therefore, the frequency variable, ω, must be replaced by a variable displaying a resonance (pole of the transfer function) at $\omega = \omega_o$ rad/sec instead of at 0 rad/sec. Since LC networks can display this resonant effect, the transformed variable will be of the form:

$$\omega_{bp} = \omega - 1/\omega. \tag{5.4}$$

This is equivalent to replacing in the low-pass prototype all shunt capacitances (impedance varies with frequency as $1/\omega$) with parallel-tuned circuits and all series inductances (impedance varies as ω) with series-tuned circuits.

The frequency at which Eq. (5.5) is resonant is:

$$\omega - 1/\omega = 0$$

or, $$\omega^2 = 1; \ \omega = \pm 1 \text{ rad/sec}. \tag{5.5}$$

In order for either the impedance of a series-tuned or the admittance of a parallel-tuned network to be reduced to zero (to give band-pass filter action) at $\omega = \omega_o$ rather than at ± 1 rad/sec, the frequency variable in Eq. (5.4) must be normalized to the resonant frequency, ω_o:

$$\omega'_{bp} = \omega_o \left(\frac{\omega}{\omega_o} - \frac{\omega_o}{\omega} \right) \tag{5.6}$$

where the order of the terms is chosen, as in Eq. (5.4), to correspond to a negative reactance or susceptances for $\omega < \omega_o$, which is the case for tuned circuits.

The change in variable of the low-pass prototype to yield a band-pass network having a center frequency of ω_o, a bandwidth of ω_c, and hence a loaded Q-factor of $Q_L = \omega_o/\omega_c$, requires bandwidth scaling by dividing the 1-rad/sec cut-off frequency by ω_c; viz,

$$\frac{\omega'_{bp}}{\omega_c} = \frac{\omega_o}{\omega_c} \left(\frac{\omega}{\omega_o} - \frac{\omega_o}{\omega} \right) = Q_L \left(\frac{\omega}{\omega_o} - \frac{\omega_o}{\omega} \right) \tag{5.7}$$

$$= \frac{\omega^2 - \omega_o^2}{\omega \omega_c} = \frac{\omega}{\omega_c} - \frac{\omega_o^2}{\omega \omega_c}. \tag{5.8}$$

The right-hand expression of Eq. (5.8) is equivalent to saying that each series inductance in the low-pass prototype (which varies with frequency as ω) can be replaced by:

$$L_s = \frac{L_k}{\omega_c} \tag{5.9}$$

in series with a capacitance (which varies with frequency as $-1/\omega$). This is expressed in the second term of Eq. (5.8) as:

$$\begin{aligned} C_s &= 1/L_k(\omega_o^2/\omega_c) = \omega_c/\omega_o^2 L_k \\ &= \frac{1}{\omega_o Q_L L_k}. \end{aligned} \tag{5.10}$$

Similarly, each shunt capacitance is replaced by a capacitance,

$$C_p = \frac{C_k}{\omega_c}, \tag{5.11}$$

in parallel with an inductance, L_p,

$$L_p = \frac{1}{\omega_o Q_L C_k}. \tag{5.12}$$

As a check, the resonant frequency of the above elements is:

$$\omega_o^2 = \frac{1}{L_s C_s} = \frac{1}{L_k/\omega_c} \times \frac{\omega_o Q_L L_k}{1} = \omega_c \omega_o Q_L = \omega_c \omega_o \frac{\omega_o}{\omega_c} = \omega_o^2$$

and, $$\omega_o^2 = \frac{1}{C_k/\omega_c} \times \frac{\omega_o Q_L C_k}{1} = \omega_c \omega_o Q_L = \omega_o^2.$$

Finally, as in the cases of the low- and high-pass filters, the impedance level may be changed from one ohm to R ohms by multiplying all resistances and inductances by R ohms and dividing all capacitances by R ohms.

In summary, the design of a band-pass filter from a low-pass prototype proceeds along the following lines:

(1) Select either a Butterworth or Tchebycheff response. If a flat pass-band response and/or a high-power handling

capability is required (e.g., variation of attenuation not to exceed, say, 0.1 db up to some frequency $< \omega_c$), choose the Butterworth response. If a ripple variation for a low power filter is permissible, choose the Tchebycheff response. Generally, the Tchebycheff response will require a fewer number of filter stages at a price of pass-band ripple variation and greater insertion loss.

(2) Determine the transmission loss or attenuation, A_{db}, which is required at some frequency, ω_1, beyond the cut-off frequency, $\omega_o \pm \omega_c/2$. Form the normalized frequency ratio, $\overline{\omega}_{bp} = 2|\omega_o - \omega_1|/\omega_c$, at which the attenuation must be equal to or greater than the specified A_{db}. This normalized ratio is sometimes expressed in fractions of half bandwidths or units of $\omega_c/2$.

(3) Determine the required number of stages from the Butterworth response plot depicted in Fig. 4.5 or the Tchebycheff response plots depicted in Figs. 4.33 through 4.38 (whichever applies from the determination in (1). Enter the abscissa at $\overline{\omega}_{bp}$ rad/sec and the ordinate at A_{db}. Determine by interpolation the number of stages, n, required to give the desired response. Choose the next highest integer. For Tchebycheff responses, increase this integer by one if it is an even number and if the source and terminating resistances must be equal; otherwise use an even number of Tchebycheff stages.

(4) Choose the prototype element values. First determine if the source and load impedances are equal or substantially equal (within 30% of each other; viz, $\overline{R} \geq 0.7$). If they are substantially equal, use Table 4.1 for a Butterworth response or Table 4.4 for a Tchebycheff response. If the resistance ratio is between $0.1 \leq \overline{R} < 0.7$, use Table 4.2 for a Butterworth or Tables 4.5 through 4.10 (ϵ_{db} from 0.1 to 3 db) for a Tchebycheff response. Finally, if the resistance ratio is $\overline{R} < 0.1$, use Table 4.3 for a Butterworth or Tables 4.11 through 4.16 (ϵ_{db} from 0.1 to 3 db) for a Tchebycheff response.

(5) Impedance leveling. To change the source and terminating resistances from one to R ohms, multiply all resistances and inductances by R and divide all capacitances by R.

Thus far, this is exactly the same procedure as for low-pass filters.

(6) Bandwidth scaling. To change the cut-off frequency from 1 rad/sec to ω_c rad/sec (the bandwidth of the band-pass filter), divide all L's and C's by ω_c. Do not alter the resistances.

(7) To change the low-pass filter to the desired band-pass filter, add a capacitance in series with each inductance so that the combination will resonate at ω_o. Similarly, to each capacitance, add an inductance in parallel so that the combination will resonate at ω_o.

Steps (5) through (7) may be summarized in the following manner:

$$L'_{sk}\ (\text{new}) = \frac{RL_{sk}\ (\text{prototype})}{\omega_c} \tag{5.13}$$

$$C'_{sk}\ (\text{new}):\ \omega_o^2 = \frac{1}{L'_{sk}C'_{sk}};\ C'_{sk} = \frac{1}{\omega_o^2 L'_{sk}} = \frac{\omega_c}{\omega_o^2 RL_{sk}} = \frac{1}{\omega_o Q_L RL_{sk}} \tag{5.14}$$

$$C'_{pk}\ (\text{new}) = \frac{C_{pk}\ (\text{prototype})}{R\omega_c} \tag{5.15}$$

$$L'_{pk}\ (\text{new}):\ \omega_o^2 = \frac{1}{L'_{pk}C'_{pk}};\ L'_{pk} = \frac{1}{\omega_o^2 C'_{pk}} = \frac{R\omega_c}{\omega_o^2 C_{pk}} = \frac{R}{\omega_o Q_L C_{pk}}. \tag{5.16}$$

Illustrative Example 5.2

Assume it is desired to design a 300-ohm, band-pass filter, centered at 15 mc, which will have a 3-db bandwidth of 3 mc ($Q_L = f_o/f_c = 15\ \text{mc}/3\ \text{mc} = 5$) and a skirt rejection of at least 40 db at 3 mc on either side of the 15-mc center frequency. Assume that a 1-db, pass-band ripple variation is permissible.

The number of half bandwidths off the center frequency is 3 divided by 3/2, or 2, to yield the normalized frequency, $\overline{\omega}_{bp} = 2$. Fig. 4.36 shows that a 5-stage Tchebycheff (cf., 7-stage Butterworth from Fig. 4.5) filter will have the required results.

From Table 4.4 (same source and load resistance), the 5-element prototype values for a 5-stage Tchebycheff filter may be obtained directly. These values together with the above ω_o,

ω_c, and R values are substituted into Eqs. (5.13) through (5.16) as follows:

$$C_1' = C_5' = \frac{C_1}{2\pi R f_c} = \frac{2.135}{2\pi \times 300 \times 3 \times 10^6} = 378\ \mu\mu f$$

$$L_1' = L_5' = \frac{R}{2\pi f_o Q_L C_1} = \frac{300}{2\pi \times 15 \times 10^6 \times 5 \times 2.135} = 0.298\ \mu h$$

$$L_2' = L_4' = \frac{RL_2}{2\pi f_c} = \frac{300 \times 1.091}{2\pi \times 3 \times 10^6} = 17.39\ \mu h$$

$$C_2' = C_4' = \frac{1}{2\pi f_o Q_L R L_2} = \frac{1}{2\pi \times 15 \times 10^6 \times 5 \times 300 \times 1.091} = 6.49\ \mu\mu f$$

$$C_3' = \frac{C_3}{2\pi R f_c} = \frac{3.001}{2\pi \times 300 \times 3 \times 10^6} = 531\ \mu\mu f$$

$$L_3' = \frac{R}{2\pi f_o Q_L C_3} = \frac{300}{2\pi \times 15 \times 10^6 \times 5 \times 3.001} = 0.212\ \mu h.$$

The resulting network and its response are shown in Figs. 5.4 and 5.5.

One interesting fact in the previous example which should be noted is that while the value of the shunt capacitors, such as C_1' and C_5' (378 $\mu\mu$f), are readily realized, the values of the shunt inductance, such as L_1' and L_5' (0.298 μh), are becoming hard to control due to their small values and associated parasitics (see

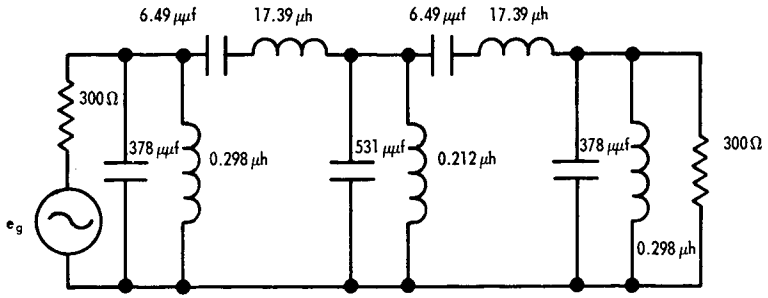

Figure 5.4. Five-Stage, 15 mc, Tchebycheff Band-Pass Filter

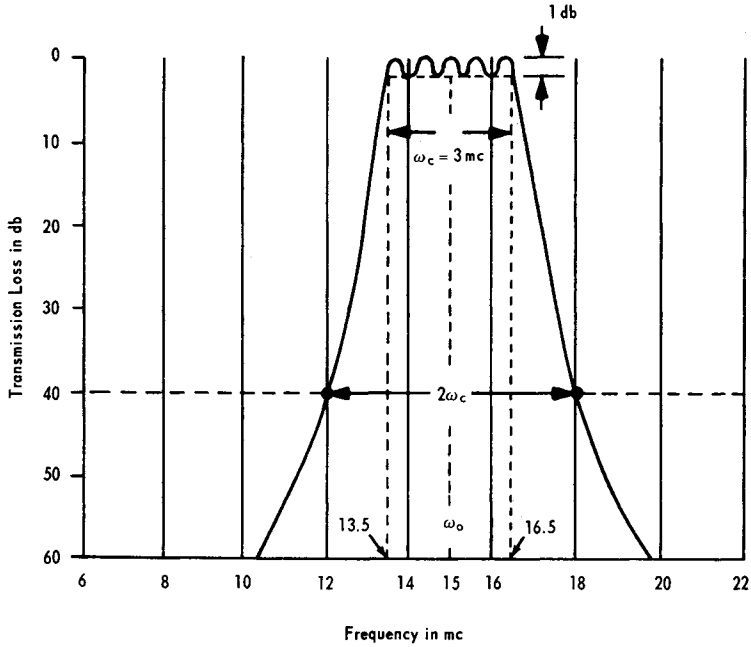

Figure 5.5. Transmission Response of Five-Stage Filter Depicted in Figure 5.4

Chap. 6). The same situation applies to the series elements, with the capacitances now becoming the hard-to-control element. The ratio of similar series to shunt elements is of the order of magnitude of Q_L^2 for inductances and $1/Q_L^2$ for capacitances. In fact, if the frequency had been much higher than 15 mc, or the Q_L factor much higher than about 5, or the resistance of a different order of magnitude than 300 ohms, it is questionable that the L's or C's could be realistically obtained. Thus, what is needed is a list of physically realizable components and other band-pass filter configurations which make the theoretical design more implementable from a practical point of view. This is discussed in Chap. 7.

Eqs. (5.13) through (5.16) are summarized in Fig. 5.6 which will be referred to hereafter as the first type of band-pass prototype. The dual of this network is obtained by replacing each

series (or shunt) inductance with a shunt (or series) capacitance whose value is divided by R^2, and by replacing each series (or shunt) capacitance with a shunt (or series) inductance whose value is multiplied by R^2. The dual of Fig. 5.6 is shown in Fig. 5.7 which provides the second type of band-pass prototype.

5.4[1] BAND-PASS PROTOTYPE BALANCED FILTERS

Other classes of band-pass filter prototypes may be obtained from the networks shown in Figs. 5.6 and 5.7 with the use of the configuration shown in Fig. 5.8. The inductor L-configurations will presently be substituted for an equivalent network.

Fig. 5.9 can be put in the same format as Fig. 5.8 if:

$$L_b - L_m = 0 \text{ or } L_b = L_m \tag{5.17}$$

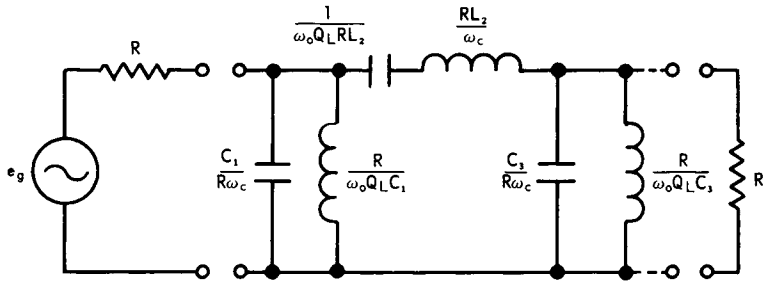

Figure 5.6. First Type of Band-Pass Filter Prototype

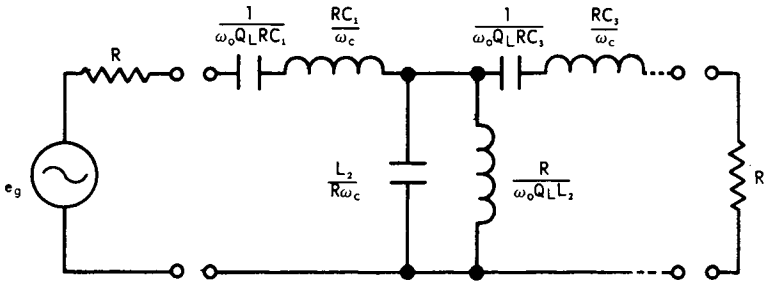

Figure 5.7. Second Type of Band-Pass Filter Prototype (Dual of Filter shown in Figure 5.6)

[1]This section may be omitted by the technologist who is only interested in design and realization of filters.

and the coupling coefficient, k, becomes:

$$k = \frac{L_m}{\sqrt{L_a L_b}} = \frac{L_b}{\sqrt{L_a L_b}} = \sqrt{\frac{L_b}{L_a}}. \tag{5.18}$$

For this situation, then, the equivalent network of Fig. 5.9 becomes that depicted in Fig. 5.10. If Eqs. (5.17) and (5.18) are applied to Fig. 5.8, the third type of band-pass filter prototype depicted in Fig. 5.11 results. In terms of the low-pass prototype terminology, Fig. 5.12 is obtained from Fig. 5.11 and from Eqs. (5.13) through (5.16).

If the same transformation as developed above is applied to the band-pass filter prototype depicted in Fig. 5.6, a fourth class of band-pass network prototype is obtained as shown in Fig. 5.13.

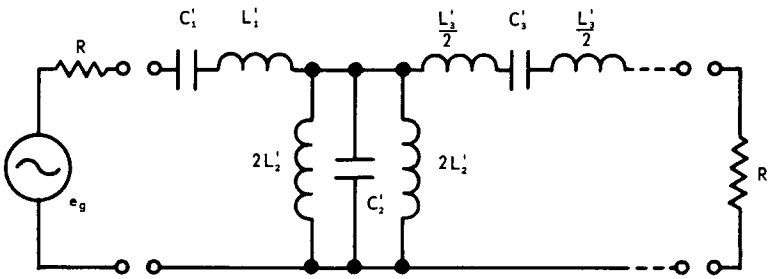

Figure 5.8. Modification of Filter Shown in Figure 5.7

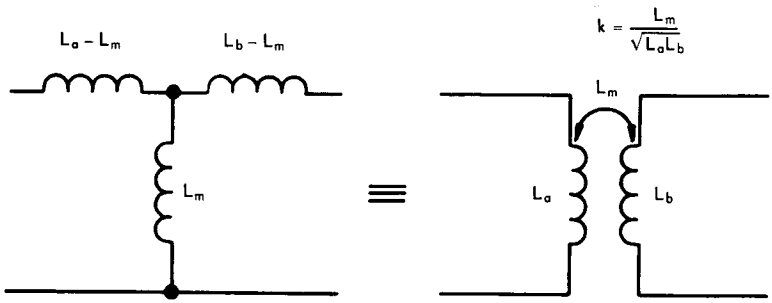

Figure 5.9. Equivalent Circuit of Transformer

Illustrative Example 5.3

Let the same example of the 15-mc, band-pass, 1-db Tchebycheff filter, as previously discussed (Illustrative Example 5.2, pp. 137–140), be applied, but to the filter network depicted in Fig. 5.13, rather than to its predecessor shown in Fig. 5.6; therefore:

$$\omega_o = 2\pi \times 15 \times 10^6$$

$$\omega_c = 2\pi \times 3 \times 10^6$$

$$Q_L = \omega_o/\omega_c = 5$$

$$n = 5 \text{ stages}$$

$$C_1 = C_5 = 2.135 \text{ farads}$$

$$L_2 = L_4 = 1.091 \text{ henrys}$$

$$C_3 = 3.001 \text{ farads}$$

$$R = 300 \text{ ohms}$$

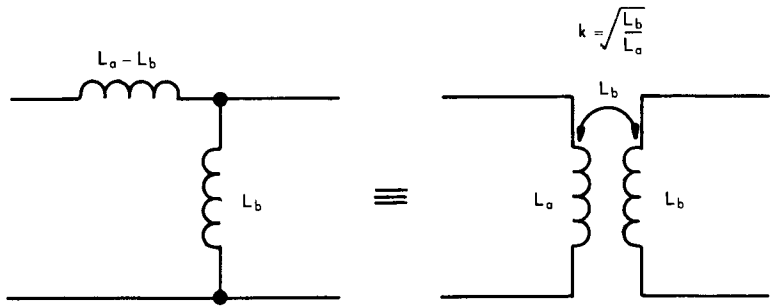

Figure 5.10. Equivalent Circuit of Figure 5.9 for $L_b = L_a$

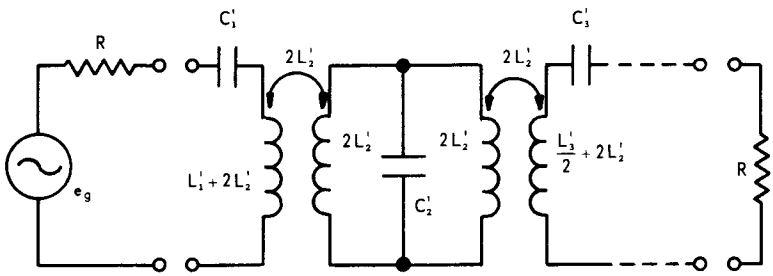

Figure 5.11. Application of Figure 5.10 to Figure 5.8

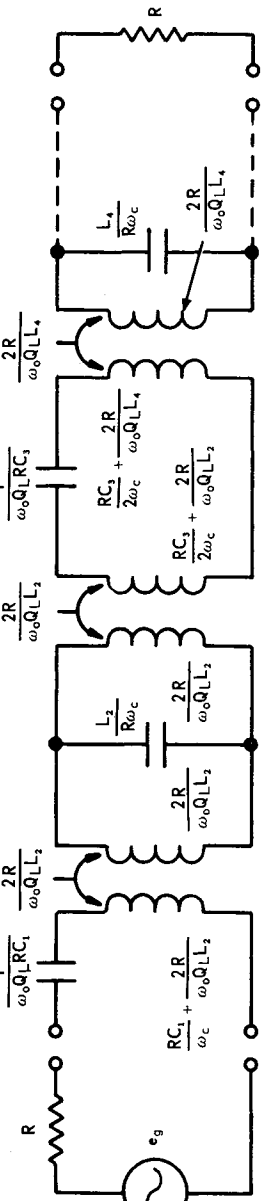

Figure 5.12. Third Type of Band-Pass Filter Prototype

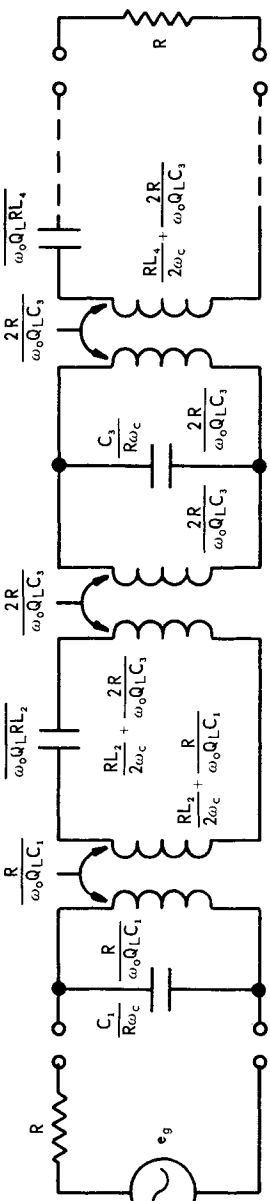

Figure 5.13. Fourth Type of Band-Pass Filter Prototype

$$\frac{C_1}{R\omega_c} = \frac{C_5}{R\omega_c} = \frac{2.135}{300 \times 2\pi \times 3 \times 10^6} = 378\ \mu\mu f$$

$$\frac{R}{\omega_o Q_L C_1} = \frac{R}{\omega_o Q_L C_5} = \frac{300}{2\pi \times 15 \times 10^6 \times 5 \times 2.135} = 0.298\ \mu h$$

$$\frac{RL_2}{2\omega_c} = \frac{RL_4}{2\omega_c} = \frac{300 \times 1.091}{4\pi \times 3 \times 10^6} = 8.70\ \mu h$$

$$\frac{2R}{\omega_o Q_L C_3} = \frac{2 \times 300}{2\pi \times 15 \times 10^6 \times 5 \times 3.001} = 0.424\ \mu h$$

$$\frac{C_3}{R\omega_c} = \frac{3.001}{300 \times 2\pi \times 3 \times 10^6} = 531\ \mu\mu f$$

$$\frac{1}{\omega_o Q_L R L_2} = \frac{1}{\omega_o Q_L R L_4} = \frac{1}{2\pi \times 15 \times 10^6 \times 5 \times 300 \times 1.091} = 6.49\ \mu\mu f$$

Thus;

$$\frac{RL_2}{2\omega_c} + \frac{R}{\omega_o Q_L C_1} = \frac{RL_4}{2\omega_c} + \frac{R}{\omega_o Q_L C_5} = 8.70 + 0.298 = 9.00\ \mu h$$

$$\frac{RL_2}{2\omega_c} + \frac{2R}{\omega_o Q_L C_3} = \frac{RL_4}{2\omega_c} + \frac{2R}{\omega_o Q_L C_3} = 8.70 + 0.424 = 9.12\ \mu h$$

$$k_{12} = k_{45} = \sqrt{\frac{L_a}{L_b}} = \sqrt{\frac{0.298}{9.00}} = 0.182$$

$$k_{23} = k_{34} = \sqrt{\frac{L_c}{L_d}} = \sqrt{\frac{0.424}{9.12}} = 0.216.$$

The resulting Tchebycheff, band-pass filter is shown in Fig. 5.14. It has identically the same response (see Fig. 5.5) as the filter shown in Fig. 5.4.

It will be shown presently that for certain applications (e.g., high Q_L factors, such as $Q_L > 25$) difficulties may arise in trying to physically realize the above four band-pass prototypes because of some unrealistic element values. It develops that other band-pass prototypes exist which have certain very positive

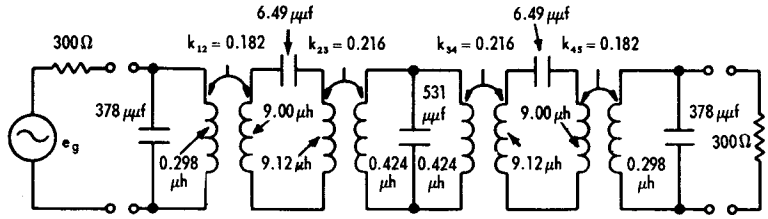

Figure 5.14. Five-Stage, 15 mc, Inductively-Coupled, Band-Pass Tchebycheff Filter (cf., Figure 5.4 and Response in Figure 5.5)

features, especially pertaining to physical realizability of the elements. A single prototype, from which a family of band-pass filters can be readily developed, will be chosen for synthesis. This prototype band-pass filter is depicted in Fig. 5.15 together with the corresponding low-pass prototype shown in Fig. 5.16.

Let Z be the impedance of any one of the series resonant loops, resonating at ω_o, depicted in Fig. 5.15. The value of Z at any frequency is:

$$Z = j\omega L - j/\omega C. \tag{5.19}$$

Since $\omega_o^2 = 1/LC$:

$$Z = j\omega L - \frac{j\omega_o^2 L}{\omega} = j\omega_o L\left(\frac{\omega}{\omega_o} - \frac{\omega_o}{\omega}\right) \text{ (cf. Eq. 5.6).} \tag{5.20}$$

The input impedance, Z_{11}, of the band-pass network depicted in Fig. 5.15 can be written in the form of a continuous-fraction expansion as follows:

$$Z_{11}(j\omega) = Z + \cfrac{X_{12}^2}{Z + \cfrac{X_{23}^2}{Z + \cfrac{X_{34}^2}{Z + \ddots + \cfrac{X_{n-1,\,n}^2}{Z + \cfrac{X_{n,\,n+1}^2}{1 + jX_o}}}}} \tag{5.21}$$

where X_{mn} = mutual inductive reactance.

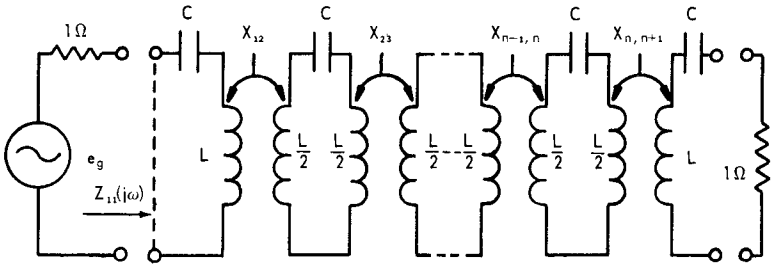

Figure 5.15. Inductively-Coupled, Series Resonant, Band-Pass Filter Prototype

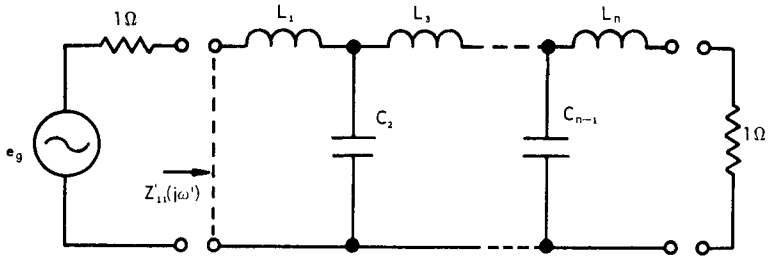

Figure 5.16. Low-Pass Filter Prototype Used in Synthesis of the Network Shown in Figure 5.15

The input impedance, Z'_{11}, of the low-pass prototype filter depicted in Fig. 5.16 is:

$$Z'_{11}(j\omega') = j\omega' L_1 + \cfrac{1}{j\omega' C_2 + \cfrac{1}{j\omega' L_3 + \cfrac{1}{j\omega' C_4 + \ddots \cfrac{1}{j\omega' C_{n-1} + \cfrac{1}{j\omega' L_n + 1}}}}} \qquad (5.22)$$

Eq. (5.22) corresponds to an odd number of elements (input and output inductance). If an even number of LC elements were indicated (output shunt capacitance), the last terms of Eq. (5.22) would become:

$$\text{-------} + \cfrac{1}{j\omega' L_{n-1} + \cfrac{1}{j\omega' C_n + 1}}. \tag{5.23}$$

In order to synthesize Eq. (5.21), which represents the desired band-pass prototype network, from Eqs. (5.22 or 5.23), which represents the known low-pass prototype network, the change of variable previously presented in Eq. (5.7) is made:

$$\omega' = \frac{\omega_o}{\omega_c}\left(\frac{\omega}{\omega_o} - \frac{\omega_o}{\omega}\right) = Q_L\left(\frac{\omega}{\omega_o} - \frac{\omega_o}{\omega}\right). \tag{5.7}$$

This variable transformation is necessary for both equations to correspond to band-pass networks. This transformation, however, will be performed after a term-by-term equivalence of Eqs. (5.21) and (5.22) is made. The forms of both equations may be made identical if Eq. (5.21) is rewritten in the following manner:

$$Z_{11}(j\omega) = jX_L + \cfrac{1}{\cfrac{Z}{X_{12}^2} + \cfrac{1}{\cfrac{ZX_{12}^2}{X_{23}^2} + \ddots + \cfrac{1}{\cfrac{X_{12}^2 X_{34}^2 \text{ ------- } X_{n-2,\,n-1}^2}{X_{23}^2 X_{45}^2 \text{ ------- } X_{n-1,\,n}^2}(1 + jX_o)}}}}. \tag{5.24}$$

The last term of Eq. (5.24) corresponds to n equals an odd number of terms. For an even number, the X^2 multiplying terms are reciprocated.

If the substitution indicated in Eq. (5.20) is made in Eq. (5.24) and if Eq. (5.7) is substituted in Eq. (5.22) and if the later equation is compared term-by-term with Eq. (5.24), the following relations result:

$$\frac{L_1}{\omega_c} = L = \frac{1}{\omega_o^2 C} \tag{5.25}$$

$$\frac{C_2}{\omega_c} = \frac{L}{X_{12}^2}$$

$$\frac{L_3}{\omega_c} = \frac{LX_{12}^2}{X_{23}^2} \qquad \frac{L_n}{\omega_c} = \frac{LX_{12}^2 X_{34}^2 \text{ ------- } X_{n-2,\,n-1}^2}{X_{23}^2 X_{45}^2 \text{ ------- } X_{n-1,\,n}^2}, \text{ for n = odd}$$

(Continued)

$$\frac{C_4}{\omega_c} = \frac{LX_{23}^2}{X_{12}^2 X_{34}^2} \qquad \frac{C_n}{\omega_c} = \frac{LX_{23}^2 X_{45}^2 \text{ ------- } X_{n-2,\,n-1}^2}{X_{12}^2 X_{34}^2 \text{ ------- } X_{n-1,\,n}^2}, \text{ for n = even.}$$

The mutual inductance, M_{nm}, is equal to:

$$\omega M_{mn} = X_{mn} \tag{5.26}$$

$$\text{or } M_{mn} = \frac{X_{mn}}{\omega} \approx \frac{X_{mn}}{\omega_o} \text{ near resonance.} \tag{5.27}$$

Solving successively for the X_{mn} terms in Eq. (5.25) and substituting the approximation near resonance indicated in Eq. (5.27), yields:

$$L = \frac{L_1}{\omega_c}; \qquad C = \frac{1}{\omega_o Q_L L}; \qquad Q_L = \omega_o/\omega_c \tag{5.28}$$

$$M_{12} = \frac{1}{\omega_o}\sqrt{\frac{L_1}{C_2}} \qquad M_{34} = \frac{L_1}{\omega_o}\sqrt{\frac{1}{L_3 C_4}}$$

$$M_{23} = \frac{L_1}{\omega_o}\sqrt{\frac{1}{C_2 L_3}} \qquad M_{n-1,\,n} = \frac{L_1}{\omega_o}\sqrt{\frac{1}{C_{n-1} L_n}}. \tag{5.29}$$

The new (fifth) band-pass prototype filter depicted in Fig. 5.15 and the relations of Eqs. (5.28) and (5.29) are summarized in Fig. 5.17.

From Fig. 5.17, several additional band-pass filter prototypes can now be developed. This is achieved by redrawing Fig. 5.17 in the form of an equivalent T-circuit of its transformers. If this is carried out and the series arm inductances are recombined, Fig. 5.18 results. This is known as an inductively coupled, n-stage filter. Another manifestation of this network, which is a popular form finding frequent use, is its dual shown in Fig. 5.19. This is called a capacitively-coupled, n-stage, band-pass filter.

The resonant frequency of either all the elements connected to a node or all the elements in a series loop of the above filter prototypes is equal to the center frequency, ω_o, of the band-pass filter. This provides a good final check on the computation of all element values. For example, the two inductors in the left-hand loop in Fig. 5.18 combine in series to yield:

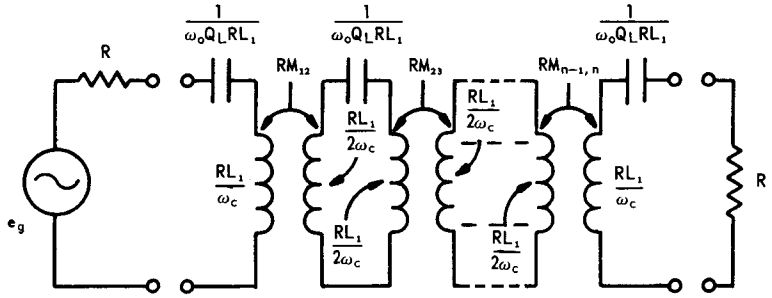

DEFINITIONS:

$$Q_L = \omega_o/\omega_c;\ M_{12} = \frac{L_1}{\omega_o}\sqrt{\frac{1}{L_1C_2}} = \frac{1}{\omega_o}\sqrt{\frac{L_1}{C_2}};\ M_{23} = \frac{L_1}{\omega_o}\sqrt{\frac{1}{C_2L_3}}$$

$$M_{34} = \frac{L_1}{\omega_o}\sqrt{\frac{1}{L_3C_4}};\ M_{n-1,\,n} = \frac{L_1}{\omega_o}\sqrt{\frac{1}{C_{n-1}L_n}} \text{ for n odd}$$

$$M_{n-1,\,n} = \frac{L_1}{\omega_o}\sqrt{\frac{1}{L_{n-1}C_n}} \text{ for n even}$$

NOTE:

If first element of the low-pass prototype filter is a capacitor (C_1) rather than an indicator (L_1), the element types would be interchanged. However, no difference in element values exist since $L_1 = C_1$, $C_2 = L_2$, ------, and $L_n = C_n$.

Figure 5.17. Fifth Type of Band-Pass Filter Prototype

$$\left(\frac{RL_1}{\omega_c} - RM_{12}\right) + RM_{12} = \frac{RL_1}{\omega_c}. \tag{5.30}$$

This equivalent inductance resonates with the loop series capacity at a frequency:

$$\omega_o = \sqrt{\frac{1}{LC}} = \sqrt{\frac{1}{\frac{RL_1}{\omega_c} \times \frac{1}{\omega_o Q_L R L_1}}} = \sqrt{\omega_c \omega_o Q_L} = \omega_o. \tag{5.31}$$

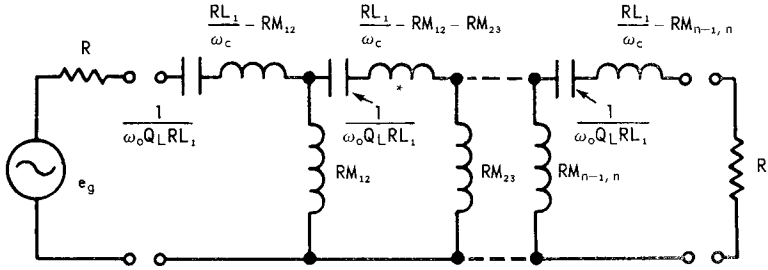

*All series inductors other than the first and last have three terms. Definitions and Note of Figure 5.17 apply.

Figure 5.18. Sixth Type of Band-Pass Filter Prototype

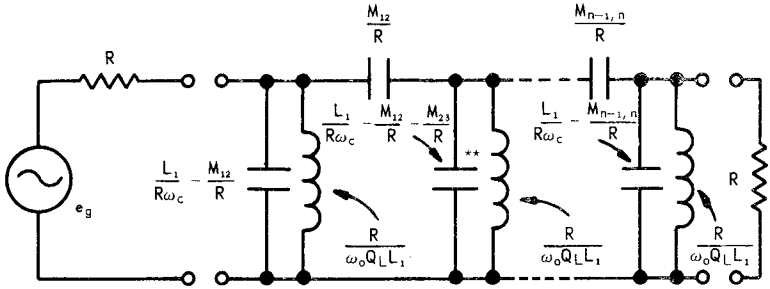

**All shunt capacitors other than the first and last have three terms. Definitions and Note of Figure 5.17 apply.

Figure 5.19. Seventh Type of Band-Pass Filter Prototype (Dual of Network Shown in Figure 5.18)

Loop resonance at ω_0 can also be shown for all other loops depicted in Fig. 5.18.

As a second example, the two capacitances connected to the left node of Fig. 5.19 combine in parallel to yield:

$$\left(\frac{L_1}{R\omega_c} - \frac{M_{12}}{R}\right) + \frac{M_{12}}{R} = \frac{L_1}{R\omega_c}. \tag{5.32}$$

This equivalent capacitance resonates with the shunt inductance connected to the same node at a frequency:

$$\omega_o = \sqrt{\frac{1}{LC}} = \sqrt{\frac{1}{\frac{R}{\omega_o Q_L L_1} \times \frac{L_1}{R\omega_c}}} = \sqrt{\omega_c \omega_o Q_L} = \omega_o. \quad (5.33)$$

Again, the purpose for considering different manifestations of band-pass filters is that some prototypes will be more physically realizable (element values more easily obtained) than others as will be discussed in Chap. 7.

Figs. 5.18 and 5.19 may be modified by changing the shunt inductance into a capacitance and the series capacitance into an inductance, respectively. It is the coupling coefficients, which are critical, that determine the location of the poles of the transfer function in the complex-frequency plane. The only remaining requirement is that resonance at ω_o be preserved at each node or in each loop as illustrated above. This is achieved in practice by tuning the filter (cf. Chap. 8).

If the coupling inductances, RM_{mn}, in Fig. 5.18 are to be replaced with an equivalent capacitance, then their reactances must be equal at $\omega = \omega_o$:

$$|jR\omega_o M_{mn}| = |-j/\omega_o C_{mn}|$$

or,

$$C_{mn} = \frac{1}{R\omega_o^2 M_{mn}}. \quad (5.34)$$

By changing the shunt inductance to an equivalent capacitance in Fig. 5.18, series-loop resonance at $\omega = \omega_o$ has temporarily been destroyed. To reinstate this resonance, therefore, either the series inductance or capacitance must be changed. Since all series capacitances were previously equal, this convenient relation will be maintained, and the series inductance will be modified to give resonance at $\omega = \omega_o$. The total series capacitance, C_T, of the two capacitances (including the new one, C_{mn}) in the first loop of Fig. 5.18 is:

$$C_T = \frac{\frac{1}{\omega_o Q_L R L_1} \times \frac{1}{R\omega_o^2 M_{mn}}}{\frac{1}{\omega_o Q_L R L_1} + \frac{1}{R\omega_o^2 M_{mn}}}$$

$$= \frac{1}{R\omega_o^2 (M_{mn} + L_1/\omega_c)}. \quad (5.35)$$

In order that resonance will exist at $\omega = \omega_o$:

$$\omega_o^2 = \frac{1}{L_T C_T} = \frac{R\omega_o^2(M_{mn} + L_1/\omega_c)}{L_T}. \tag{5.36}$$

Therefore:
$$L_T = R(M_{mn} + L_1/\omega_c). \tag{5.37}$$

It is observed that this series inductance is the same as before (cf., Fig. 5.18) with the negative sign changed to a positive value. This outcome is not surprising since a change of coupling inductance to equivalent capacitance merely changes the sign of the reactance near resonance from RM_{mn} to $-RM_{mn}$. The new (eighth) band-pass filter prototype is shown in Fig. 5.20.

By applying the same technique as used above, the series coupling capacitance shown in Fig. 5.19 may be changed to an inductance as shown in Fig. 5.21.

Another interesting phenomenon of principal concern when Q_L is low, say less than 10, has to do with the effects brought about by the approximation indicated in Eqs. (5.27) and (5.34) in which the coupling reactance is considered to be constant over the pass band. This leads to an amplitude skewing of the band-pass response in such a manner as to result in greater transmission loss at the band edge favoring the plurality of zeros[1] of the transfer function. In other words, a larger number of zeros forces the attenuation function to decrease more rapidly. This is illustrated in Fig. 5.22.

To determine the number of zeros of the transfer function at zero and infinite frequency, redraw the equivalent network as it exists at both frequencies and count the zeros for each. This is illustrated in Figs. 5.23 and 5.24 which are the equivalents for Fig. 5.21 at zero and infinite frequency respectively. The total number of zeros at both frequencies must equal two times the number of tuned circuits or 2n; where n is the number of elements in the low-pass prototype. Fig. 5.24 shows that (2n – 1) zeros exist at infinite frequency and that only one zero exists (Fig. 5.23) at zero frequency. Consequently, the filter will skew with more attenuation in the upper skirt, as suggested in Fig. 5.22, due to the plurality of zeros at infinite frequency.

[1] cf., Chap. 2 – re poles and zeros.

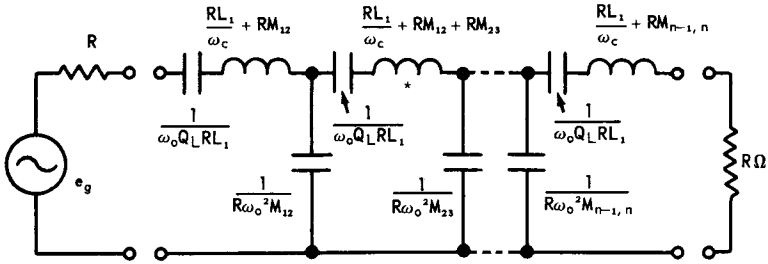

*All series inductors other than the first and last have three terms. Definitions and Note of Figure 5.17 apply.

Figure 5.20. Eighth Type of Band-Pass Filter Prototype Derived from Figure 5.18

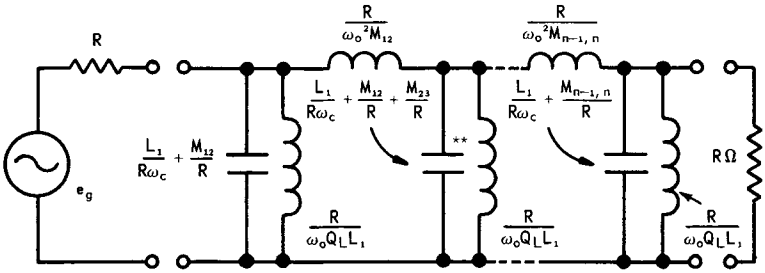

**All shunt capacitors other than the first and last have three terms. Definitions and Note of Figure 5.17 apply.

Figure 5.21. Ninth Type of Band-Pass Filter Prototype Derived from Figure 5.19

One technique, which involves reapportioning the zeros at zero and infinite frequency, to eliminate the skewing effect, is to replace every other coupling inductor or capacitor with a capacitor or inductor respectively. If this is done, the equivalent network of Fig. 5.18, for example, is shown in Fig. 5.25 and the zero and infinite frequency equivalent circuits are shown in Figs 5.26 and 5.27. This balances the zero displacement so that a symmetrical frequency response should once again be obtained for low Q_L networks as shown in Fig. 5.22.

Eq. (5.34) indicated the value of the capacitor that would be required to replace a shunt inductor. Since the loop resonant

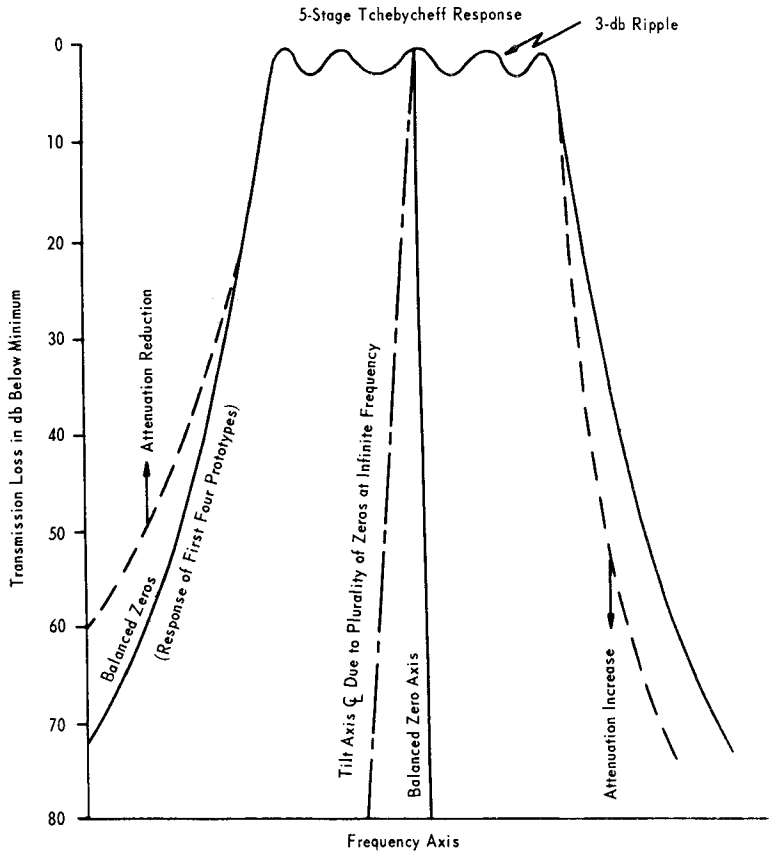

Figure 5.22. Skewing of Band-Pass Filter Response Due to Plurality of Zeros of Transfer Function at Infinite Frequency

frequency was thereby changed, it was necessary to change the remaining inductor in the loop as developed in Eqs. (5.35), (5.36), and (5.37). If this same approach is used in developing alternating capacitive and inductive coupling reactances to the sixth through ninth (Figs. 5.18 through 5.21) band-pass filter prototypes, two new balanced-zero filter prototypes result as depicted in Figs. 5.28 and 5.29.

Chap. 7 summarizes all the foregoing eleven band-pass filter prototypes in terms of the techniques for choosing which one(s)

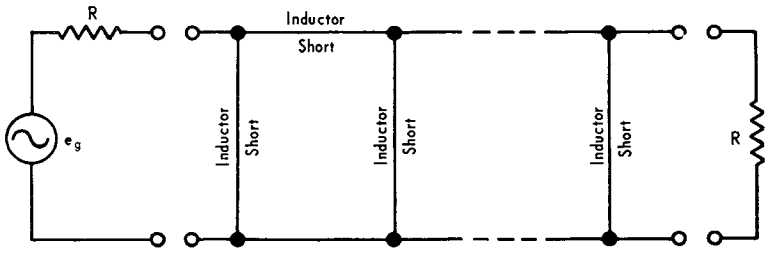

(a) Equivalent Circuit of Figure 5.21 at Zero Frequency

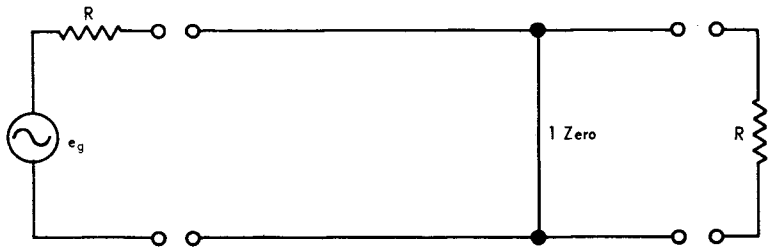

(b) Equivalence of (a): Combine Shunt Shorts (One Zero Only)

Figure 5.23. Determining Number of Network Zeros at Zero Frequency

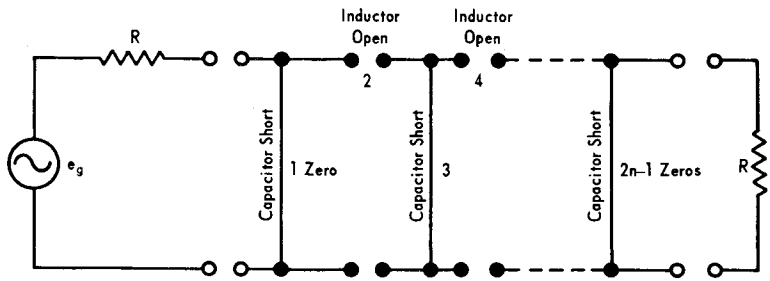

Figure 5.24. Determining Number of Network Zeros at Infinite Frequency (2n–1 Zeros)

to use for a given design problem. The emphasis in Chap. 7 is on physical realizability or the ability to obtain the computed component values in terms of the filter R, Q_L, and ω_o.

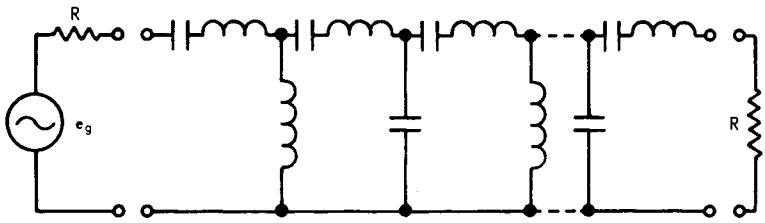

Figure 5.25. Band-Pass Filter Composed of Alternating Inductor and Capacitor Coupling Elements

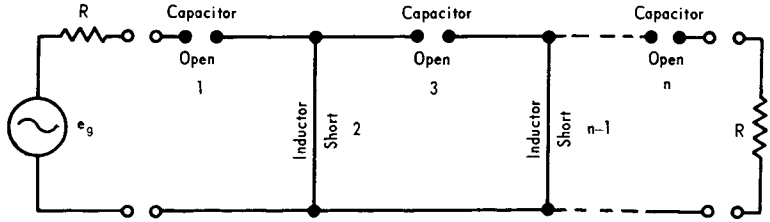

Figure 5.26. Determining Number of Zeros (n Zeros) at Zero Frequency

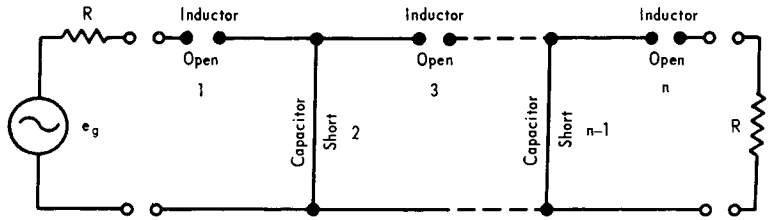

Figure 5.27. Determining Number of Zeros (n Zeros) of Figure 5.25 at Infinite Frequency

Illustrative Example 5.4

Design a 60-mc, IF band-pass filter having a 6-mc bandwidth and providing an 80-db rejection to interfering signals at 50 and 70 mc. The filter is driven by an equivalent 20-ohm grounded-base source and is terminated in a 300-ohm, twin-lead transmission line load. Assume that a 1/2-db ripple variation is allowable in the pass band and that a capacitively-coupled, band-pass filter is to be used (see Fig. 5.19, seventh prototype).

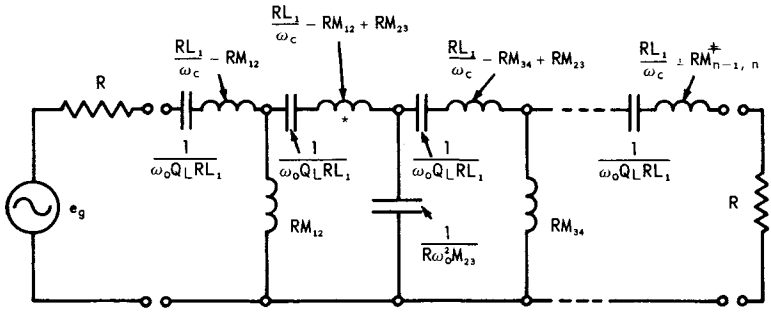

*All series inductors other than the first and last have three terms. Definitions and Note of Figure 5.17 apply.

Figure 5.28. Tenth Type of Band-Pass Filter Prototype (+ choose a + for n = odd and a − for n = even)

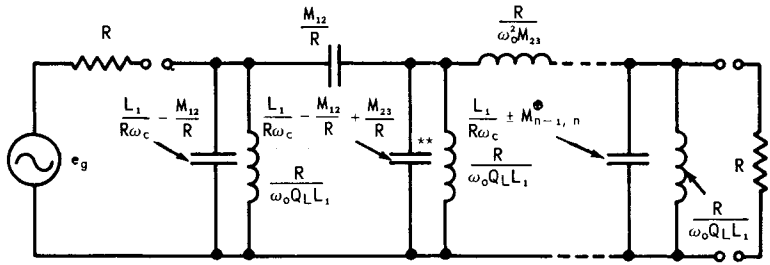

**All shunt capacitors other than the first and last have three terms. Definitions and Note of Figure 5.17 apply.

Figure 5.29. Eleventh Type of Band-Pass Filter Prototype (⊛ choose a + for n = odd and a − for n = even)

The prototype band-pass filters are designed to be driven by and terminated in equal resistances. Thus, the unbalanced load, low-pass prototypes and n = even stage Tchebycheff filters cannot be used. Consequently, only balanced n = odd Tchebycheff, equal-ripple prototypes listed in Table 4.3 can be used.

The load, Q_L, of the filter is: $Q_L = \omega_o/\omega_c = 2\pi \times 60 \times 10^6/2\pi \times 6 \times 10^6 = 10$. The normalized rejection frequency, $\overline{\omega}$, is:

$\overline{\omega} = 2\pi(\omega_o - \omega_1)/\omega_c = 2\pi(60 - 50) \times 10^6/2\pi \times 6 \times 10^6 = 3.33$. Fig. 4.35, the 1/2-db ripple Tchebycheff response curves, indicates that n = 5.8 for $\overline{\omega} = 3.33$ and $A_{db} = 80$ db. Thus, n is chosen equal to 7, rather than the usual next highest integer, 6, for the reason explained above.

Table 4.4 indicates that for $\epsilon_{db} = 1/2$ db and n = 7, the element values are:

$$L_1 = L_7 = 1.737 \text{ henrys}$$

$$C_2 = C_6 = 1.258 \text{ farads}$$

$$L_3 = L_5 = 2.638 \text{ henrys}$$

$$C_4 = 1.344 \text{ farads.}$$

The final band-pass filter element values are shown in Fig. 5.19. The load may be taken as any value since input and output impedance matching transformers are to be used. The latter is for the purpose of connecting an unbalanced filter to a balanced line. Since it is shown in Chaps. 6 and 7 that inductors less than 0.05 μh are hard to control, the inductor in Fig. 5.19 will be used as the requirement to determine R; viz,

$$\frac{R}{\omega_o Q_L L_1} \geq 0.05 \ \mu\text{h or } R \geq 5 \times 10^{-8} \omega_o Q_L L_1.$$

Thus, $R \geq 5 \times 10^{-8} \times 2\pi \times 60 \times 10^6 \times 10 \times 1.737 = 327\,\Omega$.

For convenience, a value of R = 500 will be picked. Fig. 5.19 indicates the element values are:

$$\frac{L_1}{R\omega_c} = \frac{1.737}{500 \times 2\pi \times 6 \times 10^6} = 92 \ \mu\mu\text{f}$$

$$\frac{M_{12}}{R} = \frac{M_{67}}{R} = \frac{L_1}{R\omega_o}\sqrt{\frac{1}{L_1 C_2}} = \frac{1}{Q_L}\left(\frac{L_1}{R\omega_c}\right)\sqrt{\frac{1}{L_1 C_2}} = 9.2\sqrt{\frac{1}{1.737 \times 1.258}}$$

$$= 6.2 \ \mu\mu\text{f}$$

$$\frac{M_{23}}{R} = \frac{M_{56}}{R} = \frac{L_1}{R\omega_o}\sqrt{\frac{1}{C_2 L_3}} = 9.2\sqrt{\frac{1}{1.258 \times 2.638}} = 5.1 \ \mu\mu\text{f}$$

$$\frac{M_{34}}{R} = \frac{M_{45}}{R} = \frac{L_1}{R\omega_o}\sqrt{\frac{1}{L_3 C_4}} = 9.2\sqrt{\frac{1}{2.638 \times 1.344}} = 4.9 \ \mu\mu\text{f}$$

$$\frac{L_1}{R\omega_c} - \frac{M_{12}}{R} = \frac{L_1}{R\omega_c} - \frac{M_{67}}{R} = 92 - 6.2 \approx 86\ \mu\mu f$$

$$\frac{L_1}{R\omega_c} - \frac{M_{12}}{R} - \frac{M_{23}}{R} = \frac{L_1}{R\omega_c} - \frac{M_{56}}{R} - \frac{M_{67}}{R} = 92 - 6.2 - 5.1 \approx 81\ \mu\mu f$$

$$\frac{L_1}{R\omega_c} - \frac{M_{23}}{R} - \frac{M_{34}}{R} = \frac{L_1}{R\omega_c} - \frac{M_{45}}{R} - \frac{M_{56}}{R} = 92 - 5.1 - 4.9 = 82\ \mu\mu f$$

$$\frac{L}{R\omega_c} - \frac{M_{34}}{R} - \frac{M_{45}}{R} = 92 - 4.9 - 4.9 \approx 82\ \mu\mu f$$

$$\frac{R}{\omega_o Q_L L_1} = \frac{500}{2\pi \times 60 \times 10^6 \times 10 \times 1.737} = 0.076\ \mu h$$

$R_g = R_L = 500$ ohms.

Regarding the design of the input and output transformers, the inductors of each transformer loads the input and output tank circuits respectively and becomes a part of these overall inductances. The turns ratio, n_r, of the input transformers is (see Fig. 5.30):

$$\sqrt{n_r} = \frac{L_{fi}}{L_i} = \sqrt{\frac{R_f}{R_g}} = \sqrt{\frac{500\Omega}{20\Omega}} = 5 \qquad (5.38)$$

where, L_{fi} is the filter input

L_i is the source primary inductance

R_f is the filter impedance level

R_g is the source (generator) resistance.

Since the input (primary) inductance must be one-fifth of the filter inductance, and since the inductance of the first stages of the filter is 0.076 μh, the source primary inductance, L_i, would be 0.076/5 or about 0.015 μh too small to be practical (see practical limit above of 0.05 μh). Therefore, $L_i \geq 0.05\ \mu h$. L_i is somewhat arbitrarily chosen at 0.1 μh, thus $L_{fi} = 5\ L_i = 0.5\ \mu h$. Because L_{fi} is part of the first tank circuit the remaining tank inductance, L_{t_1}, becomes:

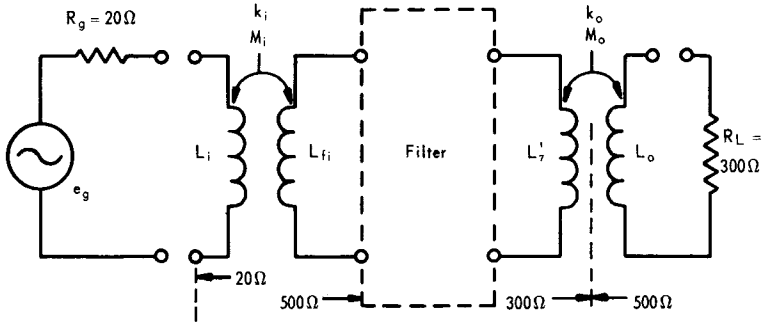

Figure 5.30. Input-Output Transformers of Seven-Stage, Band-Pass Filter (see Illustrative Example 5.4)

$$L_i' = 0.076\ \mu h = \frac{L_{fi}L_{t_1}}{L_{fi} + L_{t_1}} = \frac{0.5L_{t_1}}{0.5 + L_{t_1}} \tag{5.39}$$

or, $$L_{t_1} = 0.09\ \mu h.$$

Fig. 5.31 shows the equivalent circuits of the input and output transformers. The source inductance arm must equal zero so that the input transformer on the input side presents a pure resistance input load to the filter; viz,

$$L_i - M_i = 0.$$

Also, $$k_i = \frac{M_i}{\sqrt{L_i L_{fi}}} = \frac{L_i}{\sqrt{5L_i^2}} \text{ for } L_{fi} = 5L_i.$$

Thus, $$k_i = 1/\sqrt{5} \approx 0.45.$$

In a like manner, the coupling coefficient, k_o, of the output transformer is:

$$k_o = \frac{1}{\sqrt[4]{n_r}} = \sqrt[4]{\frac{R_L}{R_f}} = \sqrt[4]{\frac{300\Omega}{500\Omega}} = 0.88. \tag{5.40}$$

Since the turns ratio in the output transformer is small ($\sqrt{n_r} = \sqrt{R_f/R_L} = \sqrt{500/300} = 1.29$), both the primary and secondary inductances are comparable. Thus, the inductance of the last tank circuit, L_7', will also be used as the primary inductance of the

output transformer. The secondary inductance is $L_o = L_7'/\sqrt{n_r} = 0.076\ \mu h/1.29 = 0.059\ \mu h$, which is within the suggested $0.05\ \mu h$ lower limit discussed above.

The final design of the filter is shown in Fig. 5.32. This example shows some of the flexibility the circuit designer enjoys in trying to physically realize practical element values when a first approach may indicate that element values are unrealistic.

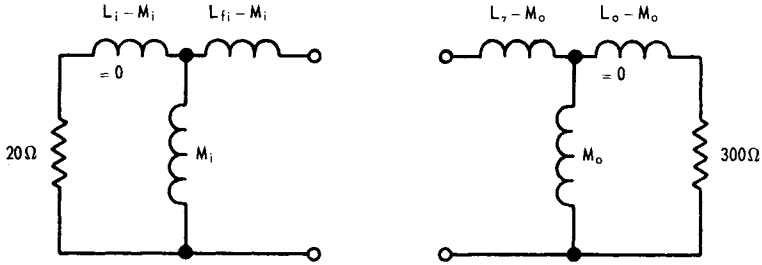

Figure 5.31. Equivalent Circuits of Transformers in Figure 5.30

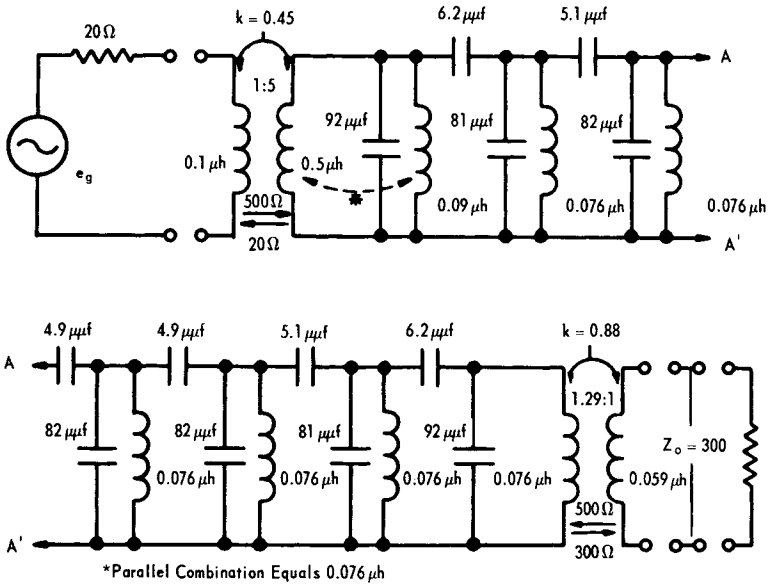

Figure 5.32. Seven-Stage, Capacitively-Coupled, Band-Pass Filter

5.5 BAND-REJECTION FILTERS

Like band-pass filters, band-rejection filters may also be derived from the low-pass prototype by a change in the frequency variable of the transfer function. In order to make a low-pass to band-pass transformation, therefore, the frequency variable, ω, must be replaced by a variable having a resonance at $\omega = \omega_o$ rad/sec instead of at 0 rad/sec [cf., Eq. (5.4)]:

$$\omega_{br} = \omega - 1/\omega.$$

This is equivalent to replacing in the low-pass prototype all shunt capacitances (impedance varies with frequency as $1/\omega$) with series-tuned circuits and all series inductances (impedance varies as ω) with parallel-tuned circuits. This development follows along the same general lines of the band-pass filter derivation where both bandwidth scaling and impedance leveling were employed; viz,

$$L'_{pk}\ (\text{new}) = \frac{RL_{pk}}{\omega_c} \tag{5.41}$$

is connected in parallel with $C'_{pk} = \dfrac{1}{\omega_o^2 L'_{pk}}$

$$= \frac{\omega_c}{\omega_o^2 RL_{pk}} = \frac{1}{\omega_o Q_L RL_{pk}} \tag{5.42}$$

and

$$C'_{sk}\ (\text{new}) = \frac{C_{sk}}{R\omega_c} \tag{5.43}$$

is connected in series with $L'_{sk} = \dfrac{1}{\omega_o^2 C'_{sk}}$

$$= \frac{R\omega_c}{\omega_o^2 C_{sk}} = \frac{R}{\omega_o Q_L C_{sk}}. \tag{5.44}$$

The resulting network and its dual are shown in Figs. 5.33 and 5.34.

In summary, the design of a band-rejection filter from a low-pass prototype proceeds along the following lines:

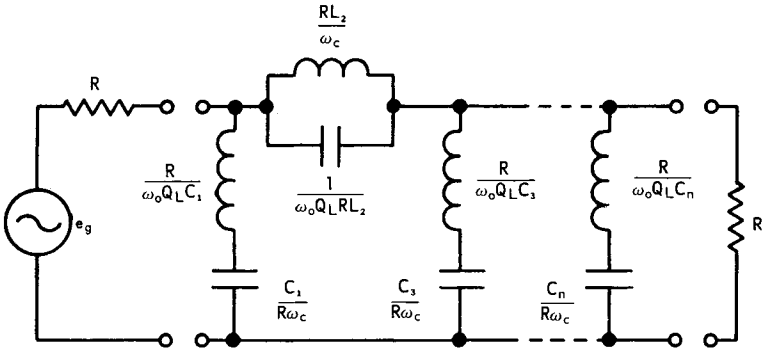

Figure 5.33. Band-Rejection Filter (cf., Band-Pass Filter in Figure 5.6)

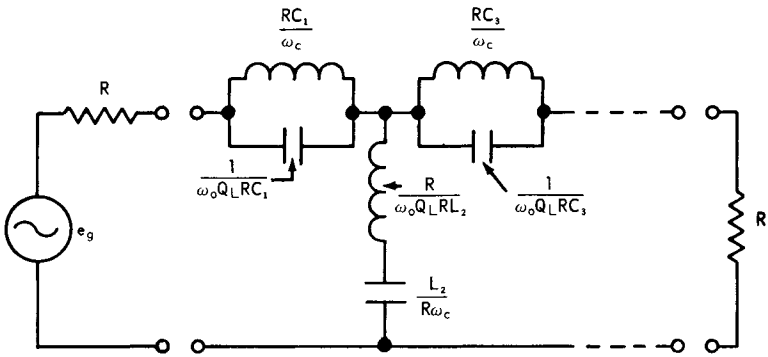

Figure 5.34. Band-Rejection Filter–Dual of Figure 5.33

(1) Select either a Butterworth or Tchebycheff response. If a flat band-response and/or a higher power handling capability is required (e.g., variation of attenuation in the pass band not to exceed say, about 0.1 db), choose a Butterworth response. If a ripple variation in the pass band is permissible, choose the Tchebycheff response. The Tchebycheff filter will generally require a fewer number of filter stages at a price of pass-band ripple variation and greater insertion loss.

(2) Determine the transmission loss or attenuation, A_{db}, which is required at some frequency, ω_1, within the cut-off frequency band, $\omega_o \pm \omega_c/2$. Form the normalized frequency ratio,

$\overline{\omega}_{br} = \omega_c/2|\omega_o - \omega_1|$, at which the attenuation must be equal to or greater than the specified A_{db}.

(3) Determine the required number of stages from the Butterworth response plot depicted in Fig. 4.5 or the Tchebycheff response plots depicted in Figs. 4.33 through 4.38 (whichever applies from the determination in (1)). Enter the abscissa at $\overline{\omega}_{br}$ rad/sec and the ordinate at A_{db}. Determine by interpolation the number of stages, n, required to give the desired response. Choose the next highest integer. For Tchebycheff responses, increase this integer by one if it is an even number and if the source and terminating resistances must be equal; otherwise, use an even number of Tchebycheff stages.

(4) Choose the prototype element values. First determine if the source and load impedances are equal or substantially equal (within 30% of each other; viz, $\overline{R} \geq 0.7$). If they are substantially equal, use Table 4.1 for a Butterworth response or Table 4.4 for a Tchebycheff response. If the resistance ratio is between $0.1 \leq \overline{R} < 0.7$, use Table 4.2 for a Butterworth or Tables 4.5 through 4.10 (ϵ_{db} from 0.1 to 3 db) for a Tchebycheff response. Finally, if the resistance ratio is $\overline{R} < 0.1$, use Table 4.3 for a Butterworth or Tables 4.11 through 4.16 (ϵ_{db} from 0.1 to 3 db) for a Tchebycheff response.

(5) Impedance Leveling. To change the source and terminating resistance from one to R ohms, multiply all resistances and inductances by R and divide all capacitances by R.

Thus far, this is exactly the same procedure for a low-pass filter.

(6) Bandwidth scaling. To change the cut-off frequency from 1 rad/sec to ω_c rad/sec (the bandwidth of the band-rejection filter), divide all L's and C's by ω_c. Do not alter the resistances.

(7) To change the low-pass filter to the desired band-rejection filter, add a capacitance in parallel with each inductance so that the combination will resonate at ω_o. Similarly, to each capacitance add in series an inductance so that the combination will resonate at ω_o.

Steps (5) through (7) are summarized in Eqs. (5.41) through (5.44).

Illustrative Example 5.5

A strong, saturating R-F signal exists at 100 kc and is in the middle of the LF band being monitored. It is desired to reject this signal in the front end of an intercept monitor receiver, but to put as small a "hole" in the receivable spectrum as possible. From a consideration of the modulation bandwidth, the transmitter and receiver LO frequency drift, and the like, it is determined that a 500-cps rejection window is to be centered at about 100 kc. Specifically, the attenuation should be 50 db between 100 kc ± 250 cps (ω_1 points), but should not exceed 3 db outside of the band 100 kc ± 1 kc (f_c points). The band-rejection filter is to be inserted between 72-ohm coaxial lines which connect a loop antenna to the receiver input terminals.

The loaded Q_L factor is $f_o/f_c = 100 \times 10^3/2 \times 10^3 = 50$. Since this is high in terms of component Q_u-factors (see Chaps. 6 and 7), it is desired to use as few components as possible. Therefore, a 2-db ripple Tchebycheff response will be used. The normalized $\overline{\omega_{br}}$ frequency is $\overline{\omega_{br}} = \omega_c/2|\omega_o - \omega_1| = 2\pi \times 2 \times 10^3/2 \times 2\pi(100 - 100.25) \times 10^3| = 4.0$.

From Fig. 4.37, the intersection of $\overline{\omega_{br}} = 4.0$ and $A_{db} = 50$ db yields n = ~~2.9~~ 5.1. Since the source and terminating resistances are equal, Table 4.4 is used and gives the following low-pass prototype values for n = 3 and $\bar{\epsilon} = 2_{db}$:

$$C_1 = C_3 = 2.711 \text{ farads}$$
$$L_2 = 0.833 \text{ henrys}$$
$$R_g = R_L = 1 \text{ ohm.}$$

Eqs. (5.41) through (5.44) yield the following values:

$$C_1' = C_3' = \frac{C_1}{R\omega_c} = \frac{2.711}{72 \times 2\pi \times 2 \times 10^3} = 3.0\ \mu\text{f}$$

$$L_1' = L_3' = \frac{R}{\omega_o Q_L C_1} = \frac{72}{2\pi \times 10^5 \times 50 \times 2.711} = 0.85\ \mu\text{h}$$

$$L_2' = \frac{RL_2}{\omega_c} = \frac{72 \times 0.833}{2\pi \times 2 \times 10^3} = 4.77 \text{ mh}$$

$$C_2' = \frac{1}{\omega_o Q_L R L_2} = \frac{1}{2\pi \times 10^5 \times 50 \times 72 \times 0.833} = 532\ \mu\mu\text{f.}$$

It is noticed that similar elements differ by a factor of the order of Q_L^2 (2500), which makes physical realizability difficult for either higher frequencies, high Q_L, or low values of R. This is readily apparent, for example, by noting that the $L_1' = L_3'$ inductors are very small; viz, 0.85 μh. If the center frequency had been, say 10 mc, these inductors would have been 8.5×10^{-9} henrys, which is not physically realizable.

This physical realizability problem is the same as that which existed for types 1 and 2 of the band-pass filter. The solution here is the same as before and suggests developing a series of band-rejection filter prototypes having the same frequency response, but whose configuration corresponds to element values within one or two orders of magnitude, rather than three or four as in the above case. The authors are presently developing these prototypes along the same lines used for the band-pass filters.

5.6 REFERENCES

1. Bower, J. L., "R-C Band-Pass Filter Design," *Electronics 20,* pp. 131–133, April 1947.
2. Brown, J. S. and Theyer, W., Jr., "High-Q Low-Frequency Resonant Filters," *Proc. Nat'l Electronics Conf.,* Vol. 7, 1951.
3. Burns, L. L., Jr., "A Band-Pass Mechanical Filter for 100 kc," *RCA Review,* No. 1, pp. 31–46, March 1952.
4. Cohn, S. B., "Direct-Coupled-Resonator Filters," *Proc. IRE,* Vol. 45, 2, pp. 187–196, February 1957.
5. Cowles, L. G., "The Parallel-T, R-C Networks," *Proc. IRE,* Vol. 40, pp. 1712–1717, December 1952.
6. Cuccia, C. L., "Resonant Frequencies and Characteristics of a Resonant Coupled Circuit," *RCA Review,* p. 121, March 1950.
7. Davidson, R., "No. 27-Band-Pass Filter Nomograph," *Tele-Tech,* pp. 113–114, June 1954.
8. DeWitz, G. H., "Consideration of Mechanical and LC Type Filters," *Trans. IRE,* Vol. CS-4, No. 2, Comms. System, May 1956.
9. Dishal, M., "Modern-Network-Theory Design of Crystal Filter for Communications & Navigation," (Federal Telecommunication Labs., Inc.), *Aeronautical Electronics Digest,* pp. 381–382, 1955.
10. Dishal, M., "Design of Dissipative Band-Pass Filters Producing Desired Exact Amplitude Frequency Characteristics," *Proc. IRE,* Vol. 37, pp. 1015–1069, September 1949.
11. Farkas, F. F., Hollenbeck, F. J., and Stenhlik, F. E., "Band-Pass Filters, Band Elimination Filter and Phase Simulating Network for Carrier Program," *The Bell Systems Technical Journal,* p. 176, April 1949.
12. Fialkow, A. D. and Gerst, I., "RLC Lattice Transfer Functions," *Proc. IRE,* pp. 462–469, April 1955.
13. Geipel, D. H. and Bright, R. L., "Maximizing the Band-Pass Ratio in Impedance Transforming Filters (493)," *IRE Conv. Record,* Vol. III, p. 71, 1955.

14. Geza, Z., "Tunable Audio Filters," *Electronics*, pp. 173–175, November 1954.

15. Gitzendanner, L. G., "Resistance and Capacitance Twin-T Filter Analysis," *Tele-Tech.*, pp. 46–48, February and April 1951.

16. Hastings, A. E., "Analysis of an R-C Parallel-T Network and Application," *Proc. IRE*, Vol. 34, pp. 126–129, March 1946.

17. Jensen, G. K. and McGeogh, "An Active Filter," *NRL Report 4630*, Library of Congress PB 111787, November 10, 1955.

18. Johnson, W., "Designing Wide-Range Tuning Circuits," *Electronics*, pp. 176–179, August 1954.

19. Karakash, J. J., *Transmission Lines and Filter Networks*, The MacMillan Co., N. Y., 1950.

20. Levy, M., "The Impulse Response of Electrical Networks with Special Reference to Use of Artificial Lines in Network Design," *Jour. IEEE*, Vol. 90, Part III, pp. 153–164, December 1943.

21. Lawson, A. W. and Fano, R. M., "The Design of Microwave Filters," Chap. 10, Vol. 9, *Radiation Laboratory Series*, McGraw Hill Book Co., New York, 1948.

22. Longo, C. V. and Wolf, E., "R-F Filter Design," *Electronics*, p. 176, February 1955.

23. Mason, W. P., "Resistance Compensated Band-Pass Filters for Use in Unbalanced Circuits," *Bell Systems Technical Journal*, 16.4, 423, October 1937.

24. McCaughan, H. S., "Variation of an R-C Parallel-T Null Network," *Tele-Tech*, pp. 48–51 and 95, August 1947.

25. Mingens, C. R., Frost, A. D., Howard, L. A., and Perry, R. W., "An Investigation of the Characteristics of Electromechanical Filters," Contr. No. DA36-039-sc-5402, February 1, 1951 through February 10, 1954.

26. Narda, L., "Modern Methods of Filter Design," *Jour. Audio Eng. Soc.*, Vol. 1, pp. 186–198, April 1953.

27. O'Meara, "The Synthesis of Band-Pass, All-Pass Time Delay Networks with Graphical Approximation Tech.," Hughes Aircraft Research Labs., Research Report No. 114, June 1959.

28. Oono, Y., "Design of Parallel-T Resistance-Capacitance Networks," *Proc. IRE*, pp. 617–619, May 1955.

29. Peterson, A., "Continuously Adjustable Low and High-Pass Filters for Audio Frequencies," *Proc. Nat'l Electronics Conf.*, Vol. 5, p. 550, 1949.

30. Roberts, W. V. B. and Burns, L. L., Jr., "Mechanical Filters for Radio Frequency," *RCA Review*, No. 3, pp. 348–365, September 1949.

31. Savant, C. J., Jr., "Designing Notch Networks," *Electronics Buyers' Guide*, Twin T. Networks, Mid-Month, p. R-14, June 1955.

32. Sherman, J. B., "Some Aspects of Coupled and Resonant Circuits," *Proc. IRE*, p. 505, November 1942.

33. Shumard, C. C., "Design of High-Pass, Low-Pass and Band-Pass Filters using R-C Networks and Direct-Current Amplifiers with Feedback," *RCA Review*, Vol. XI, No. 4, p. 534, December 1950.

34. Spangenberg, K. R., "The Universal Characteristics of Triple-Resonate Band-Pass Filters," *Proc. IRE*, Vol. 34, pp. 624–629, September 1946.

35. Stanton, L., "Theory and Application of Parallel-T, T-C Frequency-Selective Networks," *Proc. IRE*, Vol. 34, pp. 447–457, July 1946.

36. Tuttle, W. N., "Bridged-T & Parallel-T Null Circuits for Measurements at Radio Frequencies," *Proc. IRE*, Vol. 28, pp. 23–29, 1940.

37. Vergara, Wm. C., "Design Procedure for Crystal Lattice Filters," *Tele-Tech*, pp. 86–87, September 1953.

38. Wagner, T. C. G., "The General Design of Triple and Quadruple-Tuned Circuits," *Proc. IRE*, Vol. 39, pp. 279–285, March 1951.

39. Weinberg, L., "Modern Synthesis Network Design From Tables – 1," *Electronics Design*, September 15, 1956.

40. White, C. F., "Synthesis of RC Shunted High-Pass Networks," *Proc. Nat'l Electronics Conf.*, Vol. IX, p. 711, 1953.

41. White, D. R. J., "Band-Pass Filter Design Techniques," *Electronics*, 31, 1, January 3, 1958.

42. White, D. R. J., "Charts Simplify Passive LC Filter Design," *Electronics*, pp. 160–163, December 1, 1957.

43. White Electromagnetics, Inc., "RF Delay-Line Filters," Final Report, under NOLC Contract No. N123(62738)-29779A, June 30, 1962.

CHAPTER 6

INSERTION LOSS AND COMPONENT CHARACTERISTICS

The previous chapters developed the basis for the theoretical design of practical LC filters. There was little discussion, however, about the reasonableness of the computed component values in terms of their physical realizability. The most significant physical realizability characteristics involve component Q_u-factors[1] vs. frequency, upper and lower element values for different power handling capabilities, size and form factors, and other considerations such as environmental effects. Most of these constraints and the method of designing around them are covered in this chapter. The overall physical realizability of filters is discussed in the next chapter.

6.1[2] INSERTION LOSS AND Q_u-FACTORS

A filter is an imperfect device with finite resistive losses associated with each component. As such, it is important to design filters with this loss in mind; otherwise the stop-band rejection slope[1] or frequency-rate-of-attenuation will suffer and the pass-band attenuation (insertion loss)[1] may become too high, especially for either multi-stage or power filters. Ordinarily the insertion loss of a filter can be identified with its inductors since their Q_u-factor is considerably less than the Q_u-factors of most capacitors. Due to the individual Q's of both elements, the total Q-factor, Q_T, of a resonant circuit is:

$$Q_T = \frac{Q_l Q_c}{Q_l + Q_c} = \frac{Q_l}{1 + m_c} \tag{6.1}$$

where, $m_c = Q_l/Q_c$, and

$Q_l = Q_u$ of the inductor

$Q_c = Q_u$ of the capacitor.

---

[1]See Chap. 1 for definitions and see Glossary of Symbols.

[2]This section may be omitted by the technologist who is only interested in design and realization of filters.

Empirically, most Q_l-factors of inductors generally range between 50 and 300 while the Q_C-factors of capacitors generally range between 500 and 2500. As a first order estimate, therefore, $m_C \approx 0.1$ and the total Q_T-factor of a lumped-element series or parallel resonant circuit without intentional dissipation is (cf., Eq. (6.1):

$$Q_T \approx Q_l/(1 + 0.1) \approx 0.9Q_l \text{ for } m_C \approx 0.1. \tag{6.2}$$

Consider the band-pass filter depicted in Fig. 5.6 (first fundamental filter type). At resonance, replace all the LC elements with their associated losses as shown in Fig. 6.1. The series inductor losses (the even resistances, R_e) are:

$$Q_e = \frac{\omega_o L_e}{R_e}; \quad R_e = \frac{\omega_o L_e}{Q_e}. \tag{6.3}$$

Since $L_e = RL_k/\omega_c$ (see Fig. 5.6):

$$R_e = \frac{\omega_o R L_k}{\omega_c Q_e} = \frac{Q_L R L_k}{Q_e} \tag{6.4}$$

where, Q_L = loaded Q-factor of filter ($Q_L = \omega_o/\omega_c$). The associated shunt inductor losses (odd resistance, R_o) are:

$$Q_o = \frac{R_o}{\omega_o L_o}; \quad R_o = \omega_o L_o Q_o. \tag{6.5}$$

Since $L_o = R/C_k\omega_o Q_L$ (see Fig. 5.6):

$$R_o = \frac{\omega_o Q_o R}{C_k \omega_o Q_L} = \frac{Q_o R}{Q_L C_k}. \tag{6.6}$$

The determination of the exact insertion loss of the equivalent resistance network depicted in Fig. 6.1 is a complicated process since it is dependent upon n, the number of stages, and the specific transfer function which effects the L_k and C_k prototype terms. However, when Q_e or $Q_o \gg Q_L$[1], as must be the case to control the response, the total series resistances, ΣR_e, are

[1] Q_L/Q_e and Q_L/Q_o are the element-filter dissipation factors and are generally $\ll 1$.

much less than R and the total equivalent shunt resistances, $(\Sigma G_o)^{-1}$, are much greater than R, as evident from Eqs. (6.4) and (6.6). For these situations the voltage, e_o, appearing across the load R, may be approximated by (cf., Fig. 6.2):

$$e_o \approx \frac{\dfrac{R(\Sigma G_o)^{-1}}{R + (\Sigma G_o)^{-1}}}{R + \Sigma R_e + \dfrac{R(\Sigma G_o)^{-1}}{R + (\Sigma G_o)^{-1}}} e_g \tag{6.7}$$

$$e_o = \frac{R(\Sigma G_o)^{-1}}{R^2 + 2R(\Sigma G_o)^{-1} + R\Sigma R_e + \Sigma R_e(\Sigma G_o)^{-1}} e_g$$

$$\approx \frac{R(\Sigma G_o)^{-1}}{R^2 + 2R(\Sigma G_o)^{-1} + \Sigma R_e(\Sigma G_o)^{-1}} \text{ for } \Sigma R_e \ll R \ll (\Sigma G_o)^{-1} \tag{6.8}$$

where, $G_o = 1/R_o$.

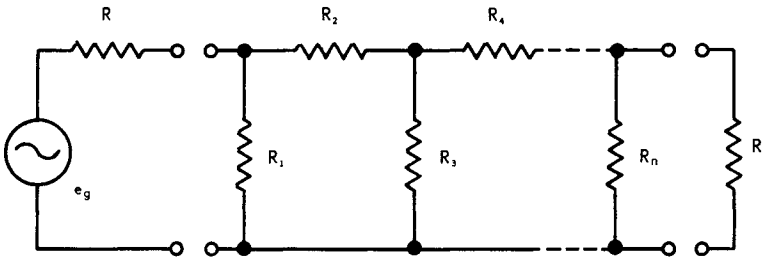

Figure 6.1. Equivalent Circuit of Band-Pass Filter at Resonance Depicted in Figure 3.6

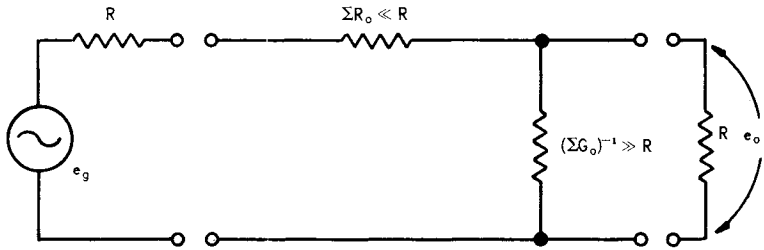

Figure 6.2. Equivalent Loss Network of Figure 6.1

If the number of elements in the filter is even, the series and shunt loss resistances associated with the inductors are equal in number:

$$\Sigma R_e = \sum_{k=1}^{n/2} \frac{Q_L R L_{2k-1}}{Q_e} \approx \frac{nQ_L R L_g}{2Q_o} \tag{6.9}$$

where, L_g is the average value of L in the prototype filter,

and $$(\Sigma G_o)^{-1} = \frac{1}{n/2} \cdot \frac{Q_o R}{Q_L C_g} = \frac{2Q_o R}{nQ_L C_g} \tag{6.10}$$

where, C_g is the average value of C in the prototype filter.

Substituting Eqs. (6.9) and (6.10) into Eq. (6.8) yields:

$$e_o = \frac{\frac{2Q_o R^2}{nQ_L C_g}}{R^2 + \frac{4Q_o R^2}{nQ_L C_g} + R^2 \frac{L_g}{C_g}} e_g$$

$$e_o = \frac{2Q_o}{4Q_o + nQ_L(C_g + L_g)} e_g. \tag{6.11}$$

Now the insertion loss in db, L_{db}, is defined as the ratio of e_o before the insertion of the filter to that after insertion. Therefore:

$$L_{db} = 20 \log_{10} \frac{e_o \text{ (before)}}{e_o \text{ (after)}} \tag{6.12}$$

where, e_o (before) $= e_g/2$.

Substituting Eq. (6.11) into Eq. (6.12), yields:

$$L_{db} = 20 \log_{10} \left(\frac{4Q_o + 2nQ_L \bar{C}}{4Q_o} \right) \tag{6.13}$$

$$L_{db} = 20 \log_{10}\left(1 + \frac{nQ_L\bar{C}}{2Q_o}\right)^1 \text{ for } \frac{nQ_L}{Q_o} < 1 \qquad (6.14)$$

where, $\bar{C}$ is a function of n and is the average prototype element values of the filter type (C is plotted in Fig. 6.3).

Eq. (6.14) is plotted in Fig. 6.4 for the Butterworth prototype and in Figs. 6.5 through 6.7 for the $\epsilon_{db} = 1/4$, 1/2, and 1 db, equal-ripple, Tchebycheff, both for n = 1 to 10 stages. These insertion loss plots apply to the first four filter types depicted in Figs. 5.6, 5.7, 5.12, and 5.13 for $nQ_L/Q < 1$.

The remaining filter types will exhibit different insertion loss characteristics due to the different total number of inductances and circuit configurations. Figs. 5.19 and 5.20 have the least number of inductors. It can be shown that the total equivalent parallel resistance of the former is:

$$\bar{R}_p = \frac{L_1}{RQ_{pc}}\left[\sum_{k=1}^{n} Q_L - 2\sum_{k=1}^{n-1}\frac{1}{\sqrt{L_k'C_{k+1}}}\right] + \sum_{k=1}^{n}\frac{Q_L L_1}{RQ_{p1}}. \qquad (6.15)$$

It can also be shown that the total equivalent series resistance is:

$$\bar{R}_S = \frac{R}{Q_{sc}L_1}\sum_{k=1}^{n-1}\sqrt{L_k'C_{k1}}. \qquad (6.16)$$

The expression for the ratio of the output voltages before and after the filter has been inserted is:

---

[1] cf., with well-known equation, $L_{db} = 20n \log_{10}(1 + Q_L/Q_o)$; $20 \log_{10}\left(1 + \frac{nQ_L\bar{C}}{2Q_o}\right) \approx 20 \log_{10}\left(1 + \frac{Q_L\bar{C}}{2Q_o}\right)^n$. Now, from Fig. 6.3, $1.1 \leq \bar{C} \leq 2.1$ for $n \geq 3$ (average $\bar{C} \approx 1.4$ for $3 \leq n \leq 7$), so that $L_{db} \approx 20n \log_{10}\left(1 + \frac{.7Q_L}{Q_o}\right)$. Thus, the common insertion loss equation usually yields too high an insertion loss calculation, although it is difficult to generalize due to dependency on n and the type of response.

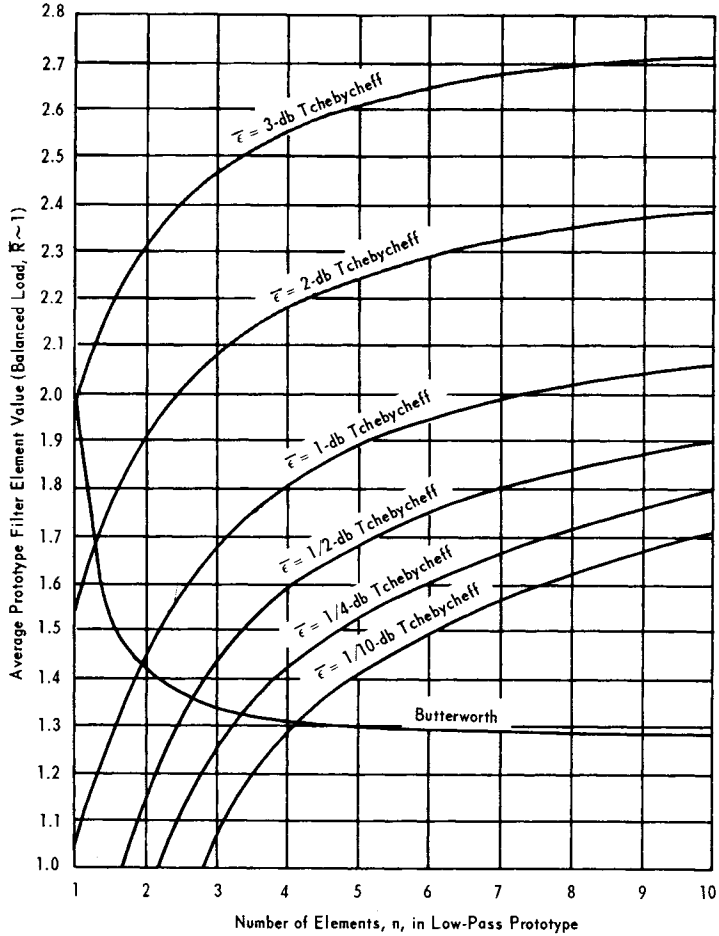

Figure 6.3. Average Low-Pass Filter Prototype Element Values

$$\frac{E_o \text{ (before)}}{E_o \text{ (after)}} = \frac{\dfrac{R\bar{R}_p}{R + \bar{R}_p}}{R + \bar{R}_S + \dfrac{R\bar{R}_p}{R + \bar{R}_p}}. \tag{6.17}$$

Finally, the insertion loss is given by:

$$L_{db} = 20 \log_{10}\left[1 + \frac{L_{1n}Q_L}{Q_o} + \left(\frac{nQ_L}{Q_{pL}Q_{So}} + \frac{1}{2Q_{Sc}L_1}\right)\sum_{k=1}^{n-1}\sqrt{L_k{}'C_{k+1}}\right]. \tag{6.18}$$

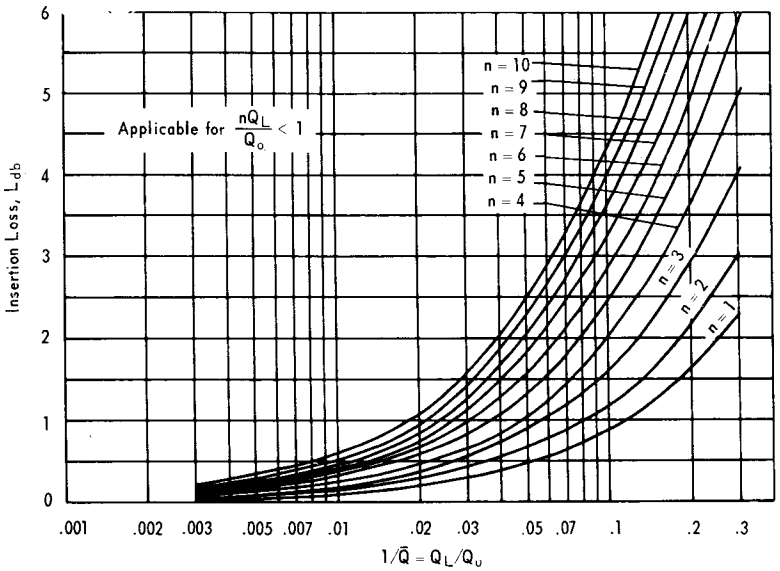

Figure 6.4. Insertion Loss of Butterworth, Band-Pass Filter Prototype (Types 1 through 4)

Eq. (6.18) is plotted in Figs. 6.8 and 6.9 for the Butterworth case, for n = 1 to 10 stages, and in Figs. 6.10 to 6.12 for the Tchebycheff response for odd n = 1 to 19 stages, and for values of db ripple equal to 0.25, 0.50, and 1 db, respectively.

Illustrative Example 6.1

Assume it is desired to design a 60-mc I-F, capacitively-coupled, band-pass filter, which is to be driven by and coupled into 50-ohm coaxial lines. The filter must pass 1/2 μsec pulses having a rise time τ_r of about 0.14 μsec so that the bandwidth will be about 5 mc ($f_c \approx 5$ mc). The filter must also provide about 60 db of attenuation to expected sources of interfering signals located 10 mc on either side of the center frequency, i.e., at 50 mc and 70 mc. The maximum allowable insertion loss is 2 db and the inductors to be used have a Q_u-factor of 200 and the capacitors have a Q_u-factor of 1500.

Fig. 4.5 indicates that a five-stage Butterworth filter ($\bar{\omega}_{bp} = 2|\omega_o - \omega_1| \div \omega_c = 2 \times 10/5 = 4$ and $A_{db} = 60$) and Fig. 4.36 indicates that a 4-stage, 1-db Tchebycheff filter will yield the desired

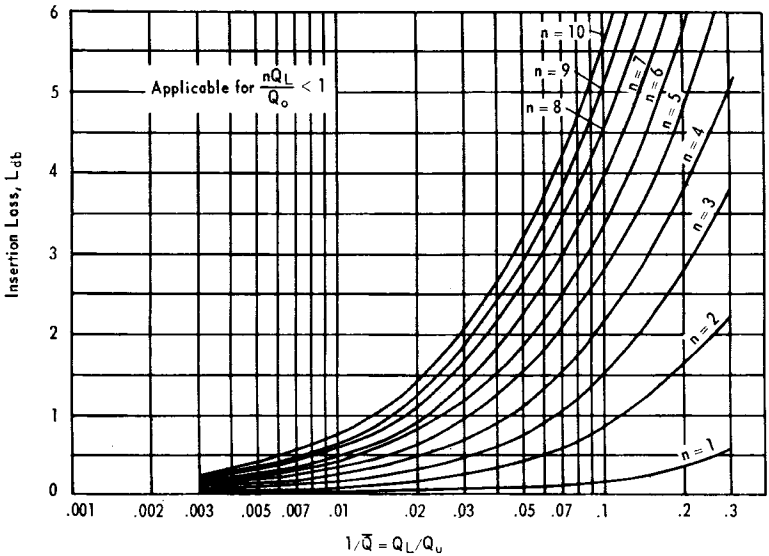

Figure 6.5. Insertion Loss of Tchebycheff, Band-Pass Filter Prototype (ϵ_{db} = 0.25-db Ripple)

response. Since $Q_L = f_o/f_c = 60/5 = 12$ and $Q_T = 180$ ($Q_T = Q_L Q_c/(Q_L + Q_c) = 200 \times 1500/200 + 1500 \approx 180$), $Q_L/Q_o = 12/180 = 0.067$. Fig. 6.9 indicates that the insertion loss of an n = 5, Butterworth, band-pass filter will be about 1.5 db and Fig. 6.12 indicates that the loss of the n = 4, 1-db ripple, Tchebycheff filter will be about 3.7 db. Since the Tchebycheff filter exceeds the allowable 2-db insertion loss, the five-stage Butterworth filter is chosen to give the desired results.

6.2 INDUCTOR CHARACTERISTICS

Lumped-element inductors and capacitors are reviewed in this and the next section. The emphasis here is on the physical realizability of filter components, not on the overall filter realizability, per se, which is discussed in Chap. 7.

The physical realizability of component parts of the filters involves such characteristics as:

Q_u-factors

Obtainable range of element values

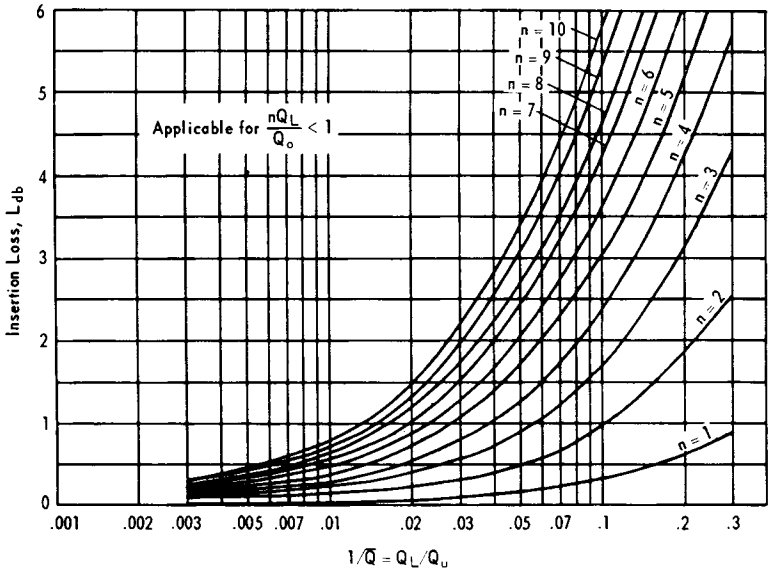

Figure 6.6. Insertion Loss of Tchebycheff, Band-Pass Filter Prototype (ϵ_{db} = 0.5-db Ripple)

Design data for fabrication

Parasitics and useful frequency range

Size and shape factors

Current, voltage, or power ratings

Stability and environmental effects.

Fig. 6.13 shows a typical inductor having distributed capacitance. The approximate equivalent circuit of this inductor is shown in Fig. 6.14 in which the associated R-F resistance exists in series with the inductance. The equivalent impedance, Z, of the inductor at any frequency, ω, is:

$$Z = \frac{1}{Cs + \frac{1}{R + Ls}} = \frac{R + Ls}{s^2LC + sRC + 1} \tag{6.19}$$

$$= \frac{s/C + R/LC}{(s - s_{p_1})(s - s_{p_2})} \tag{6.20}$$

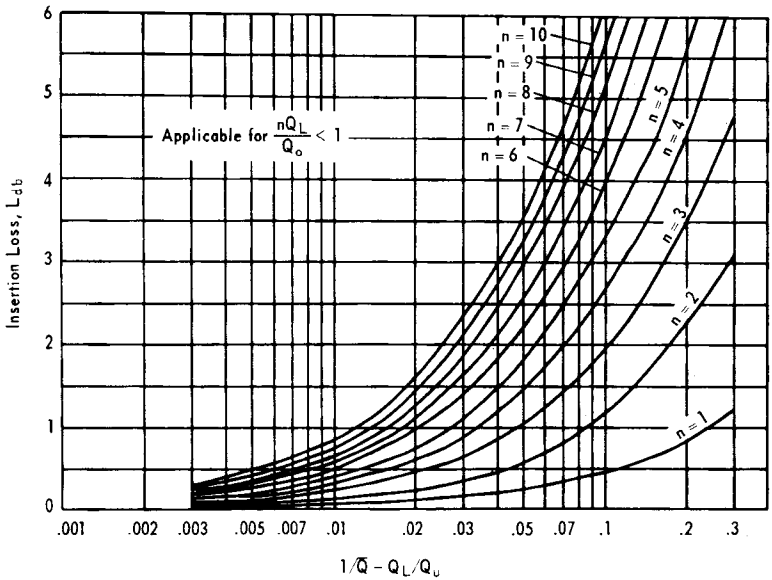

Figure 6.7. Insertion Loss of Tchebycheff, Band-Pass Filter Prototype (ϵ_{db} = 1-db Ripple)

where,
$$s_{p_1} \text{ and } s_{p_2} = -\frac{R}{2L} \pm \sqrt{\left(\frac{R}{2L}\right)^2 - \frac{1}{LC}} \qquad (6.21)$$

$$= -\frac{R}{2L} \pm \omega_o \sqrt{\frac{1}{4Q_\mu^2} - 1} \qquad (6.22)$$

and
$$\omega_o^2 = 1/LC \text{ and } Q_\mu = \omega L/R.$$

Since $Q_\mu \gg 1$, Eq. (6.21) becomes:

$$s_{p_1} \text{ and } s_{p_2} \approx -\frac{R}{2L} \pm j\omega_o \text{ (cf., Eq. (2.17))}. \qquad (6.23)$$

At low frequencies, $s \to 0$, Eq. (6.19) becomes $Z \approx R$ (R now approaches the dc resistance). At somewhat higher frequencies (s^2LC and $sRC \ll 1$), so that $Z \approx R + j\omega L$. At resonance ($s^2LC + 1 = 0$ or $\omega = \omega_o = 1/\sqrt{LC}$); thus Eq. (6.19) becomes:

$$Z \approx \frac{Ls}{sRC} = \frac{L}{RC} = \frac{Q_u}{\omega_o C} = Q_u \omega_o L = RQ_u^2 \text{ at resonance.} \qquad (6.24)$$

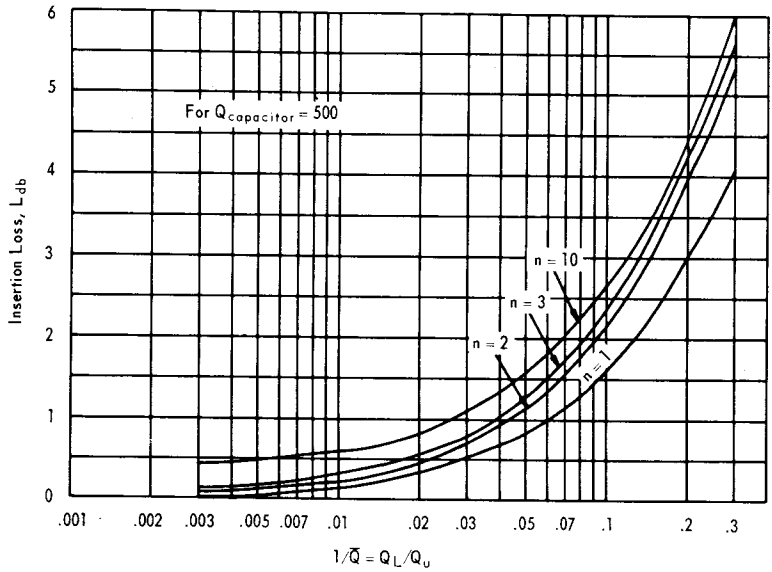

Figure 6.8. Insertion Loss of Butterworth, Band-Pass Filter Prototype (Types 5 through 11) for $Q_{capacitor} = 500$

Finally, at high frequencies beyond resonance, $Z = j\omega L/(-\omega^2 LC) = -j/\omega C$ (behaves as parasitic capacitance).

The above behavior of the inductor is depicted in Fig. 6.15 along with an identification of the practical frequency range over which it nominally may be used. This range is predicted on an allowable 10% departure from the prime inductance value.

Regarding physical realizability, toroidal inductors may be wound on toroids of molybdenum permalloy dust, carbonyl, or ferrites. The practical range of lumped inductance is nearly 10 decades; viz, from about 0.05 μh to 150 henrys. Some typical characteristics corresponding to peak-rated Q_u-factors are shown in Fig. 6.16.

Unless the Q_u-factor is unimportant or unless the magnetic field of the inductor need not be tightly confined to maintain a small size, there seems little reason for not using toroids today. They are available from several suppliers in sizes ranging from about 30 cu. in. for applications below about 2 kc, where higher Q_u is relatively more important than size, to less than 10^{-3} cu.

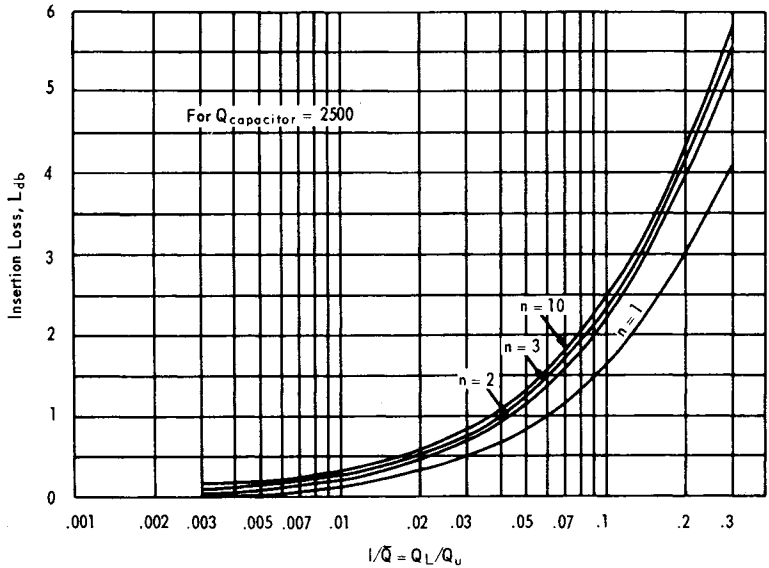

Figure 6.9. Insertion Loss of Butterworth, Band-Pass Filter Prototype (Types 5 through 11) for $Q_{capacitor}$ = 2,500

in. for applications in the 100-mc region where a Q_u of the order to 100 is adequate.

In the design of low-pass filters, where a direct current passes through the toroids, such as the filtering of audio-frequency or R-F on dc lines, inductance derating with current increase should be considered. Most suppliers of the larger toroidal inductors provide this information as a parameter in specifying performance characteristics.

The effect of a decrease in inductance (due to direct current) in a low-pass filter is an increase in the cut-off frequency. For a single-stage series inductance filter, the transfer function Z_{12} is:

$$Z_{12} = \frac{2R}{2R + Ls}. \tag{6.25}$$

The cut-off frequency, ω_o, corresponds to:

$$2R = Ls \text{ or } s = j\omega_c = \frac{2R}{L}. \tag{6.26}$$

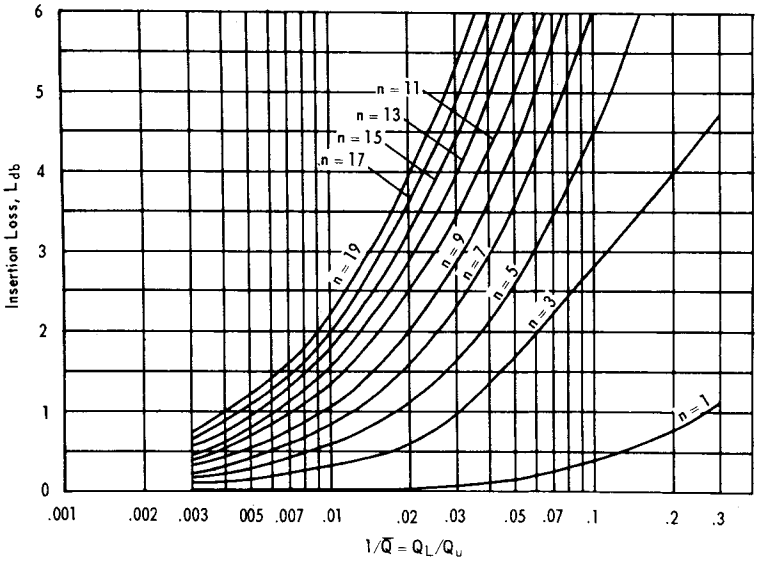

Figure 6.10. Insertion Loss of Tchebycheff Band-Pass Filter Prototype (ϵ_{db} = 0.25-db Ripple) (Types 5 through 11)

Therefore, ω_c is inversely proportional to L; based on the derating properties of L, ω_c increases with direct current.

Regarding the subject of nontoroidal inductors, Fig. 6.17 is a nomograph for designing a single-layer coil. Again the matter of parasitic capacitance previously discussed, must be considered in determining the upper useful frequency range. Fig. 6.18 presents a design nomograph for determining the distributed capacitance of single-layer coils.

The self-inductance of a round, straight nonmagnetic wire is:

$$L_S = 0.0051r(2.3 \log_{10}\frac{4r}{d} - 1 + \delta) \ \mu\text{henrys} \qquad (6.27)$$

where, δ is a skin-effect factor

d = diameter of inductor in inches

r = length of inductor in inches.

Fig. 6.19 is a plot of Eq. (6.27) for $\delta = +1/4$ which corresponds to frequencies below HF where skin depth is generally

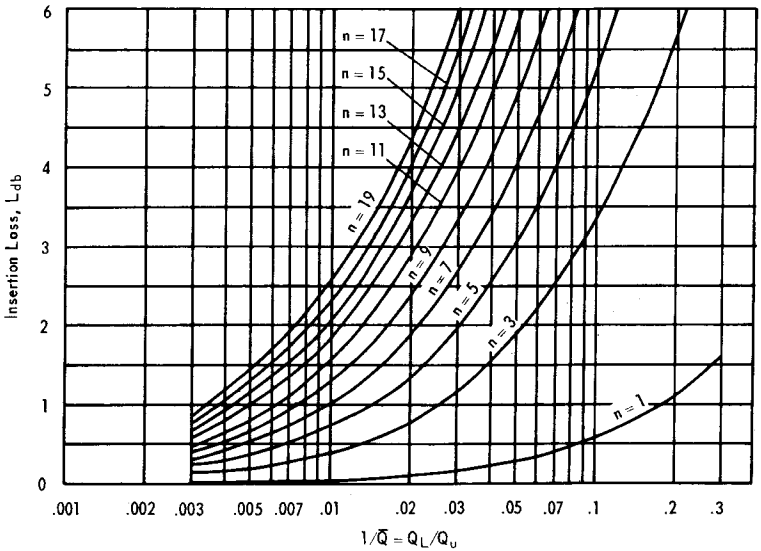

Figure 6.11. Insertion Loss of Tchebycheff, Band-Pass Filter Prototype (ϵ_{db} = 0.50-db Ripple) (Types 5 through 11)

unimportant. The skin depth correction factor may be determined from Fig. 6.20 for any frequency and diameter of wire.

6.3 CAPACITOR CHARACTERISTICS

This discussion of capacitors includes those parameters that affect the capacitance magnitude used in the design of filter networks. Parameters such as ideal capacitance variations, natural resonant frequencies resulting from parasitics, and leakage resistance, shall be emphasized.

The capacitance of two conducting parallel plates situated close together (fringing field is small when $\sqrt{A}/t$ is large; i.e., when $\sqrt{A}/t$ is > 10) is:

$$C = 0.0885\frac{KS}{t}\mu\mu f \qquad (6.28)$$

where, C = capacitance in $\mu\mu$f
K = dielectric constant (1 for air)
S = area of one plate in sq. cm.
t = distance between plates in cm.

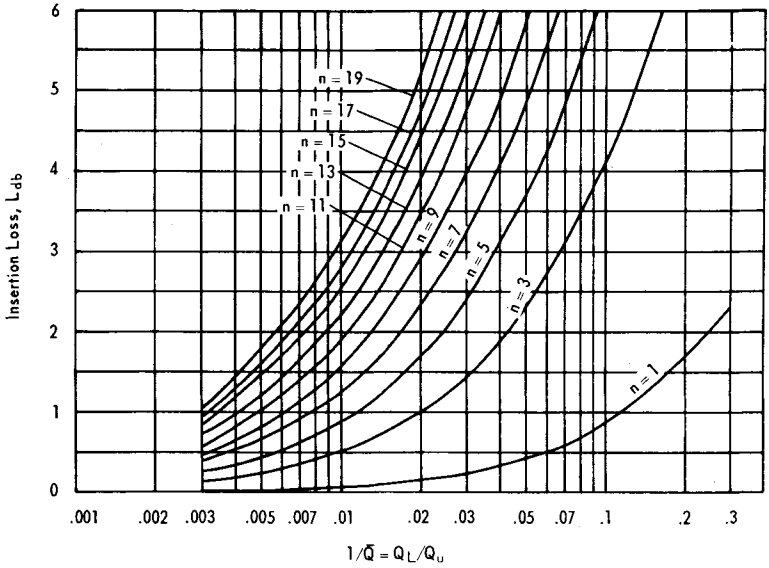

Figure 6.12. Insertion Loss of Tchebycheff Band-Pass Filter Prototype (ϵ_{db} = 1-db Ripple) (Types 5 through 11)

Fig. 6.21 is a plot of Eq. (6.28) for various values of K from 1 to 1,000.

There exist many factors which may result in variations of apparent values of capacitance which should be noted in order that adequate tolerances may be realized and compatible capacitor types selected. The following factors influence the magnitude of the dielectric constant K, and consequently effect nonlinearities in the apparent values of capacitance:

(1) Leakage resistance and lead impedance
(2) Frequency of applied voltage
(3) Parasitic resonance
(4) Temperature characteristics
(5) Aging.

The degree to which such factors effect changes in apparent capacitance, is a function of the type of capacitor utilized; viz,

(1) Mica (molded or potted)
(2) Paper (hermetically sealed in metallic case)

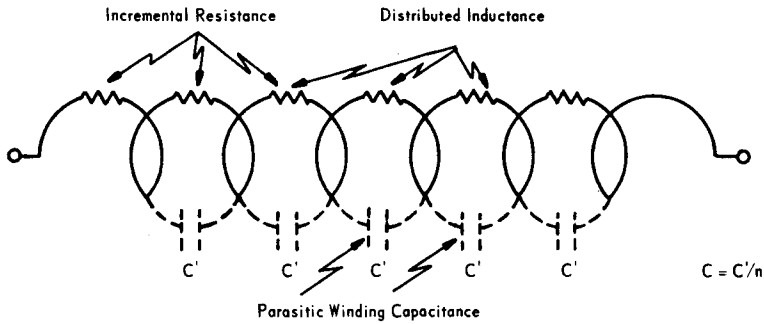

Figure 6.13. Typical Inductor with Distributed Capacitance

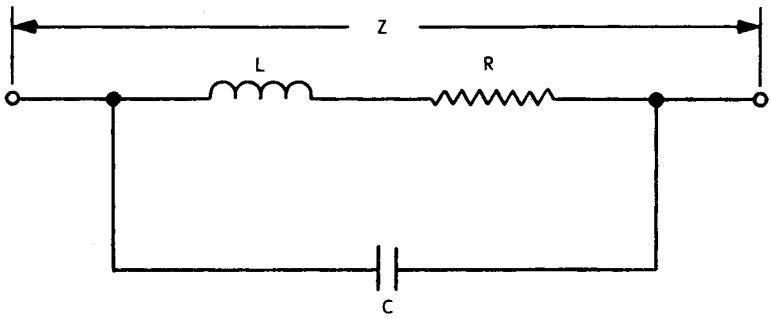

Figure 6.14. Simplified Equivalent Circuit of Inductor

(3) Paper (nonmetallic case)
(4) Ceramic (general purpose)
(5) Electrolytic (tantalum)
(6) Electrolytic (dc).

6.3.1 Leakage Resistance and Lead Impedance

Like the inductor, the capacitor has various parasitic reactive elements; viz, (1) the insulation or leakage resistance, R_p, which governs the leakage of current through the capacitor and is of concern only at dc and low frequencies, (2) the lead inductances and resistances, and (3) the ideal capacitance.

Fig. 6.22 shows the typical capacitor and Fig. 6.23 is the approximate equivalent circuit.

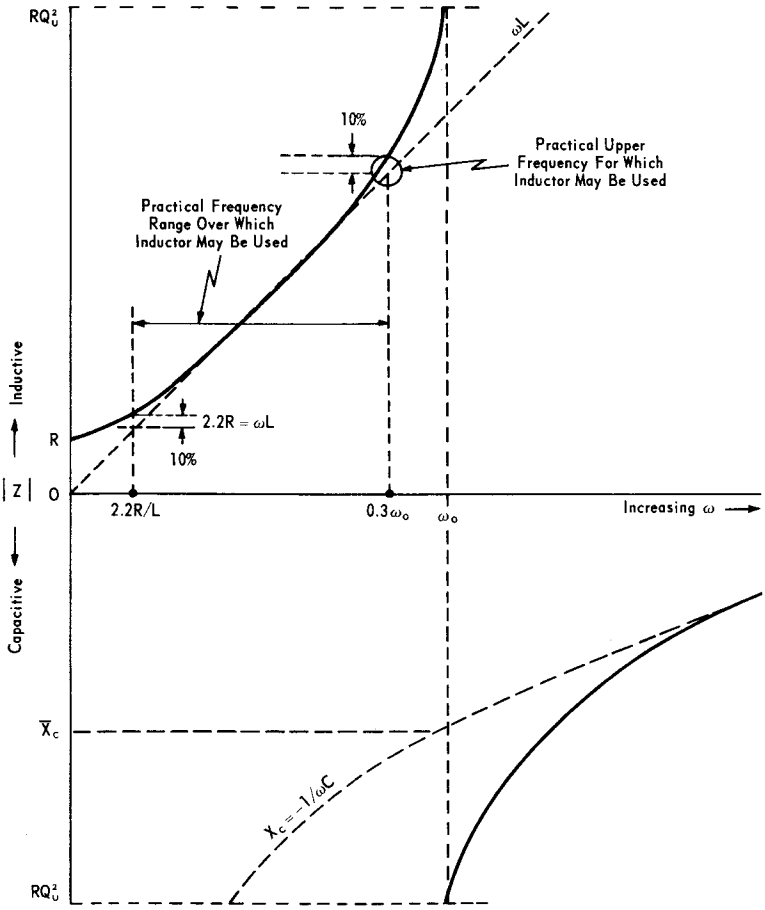

Figure 6.15. Equivalent Impedance of Inductor

6.3.2 Frequency Behavior

The equivalent impedance, Z, of the capacitor at any frequency, ω, is (cf., Fig. 6.22):

$$Z = R_S + LS + \frac{1}{\frac{1}{R_P} + CS}$$

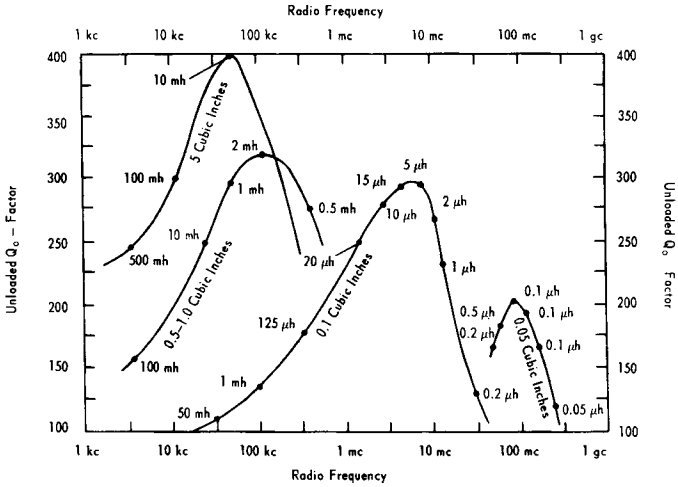

Figure 6.16. Typical Characteristics of Toroidal Inductors (obtained by combining three leading suppliers)

$$\approx \frac{s^2LC + s(L/R_p + CR_S) + (1 + R_S/R_p)}{CS + 1/R_p} \qquad (6.29)$$

where, $s = j\omega$.

At dc and low frequencies, $s \to 0$, Eq. (6.29) becomes $Z \approx R_p$, the leakage resistance. At higher frequencies for which $CS \gg 1/R_p$ (shunt capacitive reactance much less than the leakage resistance), Eq. (6.29) becomes $Z = R_S + LS + 1/CS$. Finally, a resonant frequency, ω_o, is reached for which $LS = 1/CS$ in the above relation ($\omega_o^2 = 1/LC$) and $Z = R_S$. Beyond resonance, again $Z = R_S + LS + 1/CS$ and may be approximated by $Z = LS$ when $\omega \gg \omega_o$. Fig. 6.24 shows these relations including the recommended operating frequency range.

Table 6.1 shows measured resonant frequencies for various types of high-voltage capacitors to illustrate the importance of considering the natural resonant frequencies of capacitors in filter design. The capacitors in Table 6.1 were not chosen to exemplify normal capacitor characteristics, but rather to illustrate possible excursions in resonant frequencies due to extremities in types of construction and rated voltages.

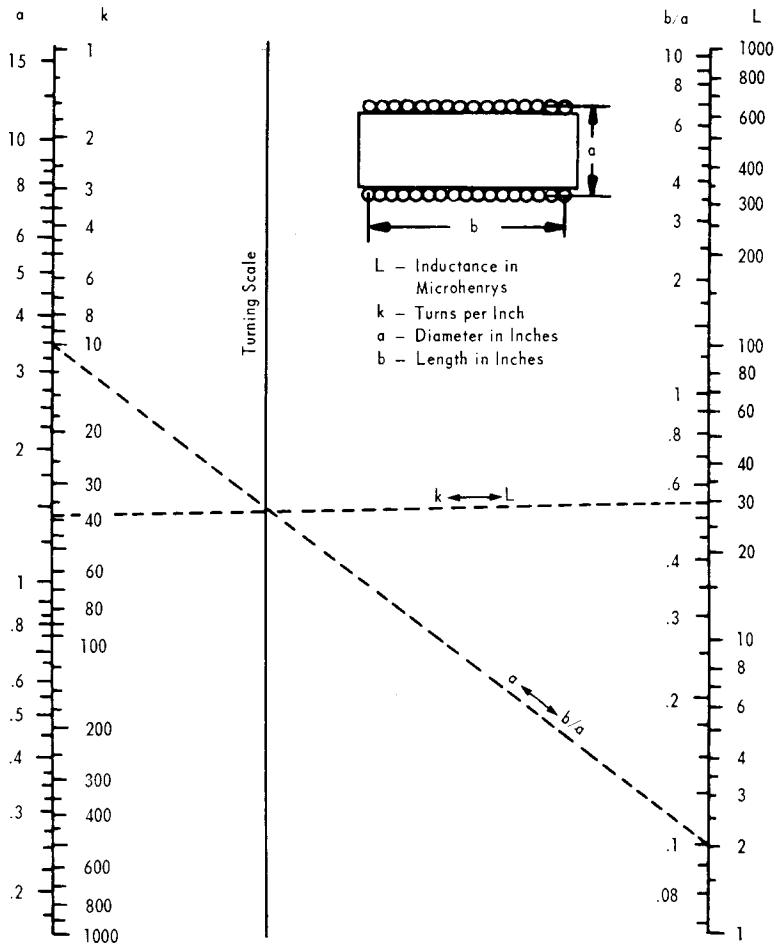

Figure 6.17. Nomograph for Designing a Single-Layer Coil

The frequency of the applied voltage is also responsible for fluctuations in capacitance as a result of other phenomena. As the frequency of the applied voltage is increased, the value of the dielectric constant, K, may decrease as shown in the qualitative curve in Fig. 6.25. Fluctuations will also occur in the equivalent series resistances of capacitors as a function of the frequency of the applied voltage, as illustrated in Fig. 6.26. In general, such variations cannot be calculated but must be measured or obtained from capacitor manufacturers.

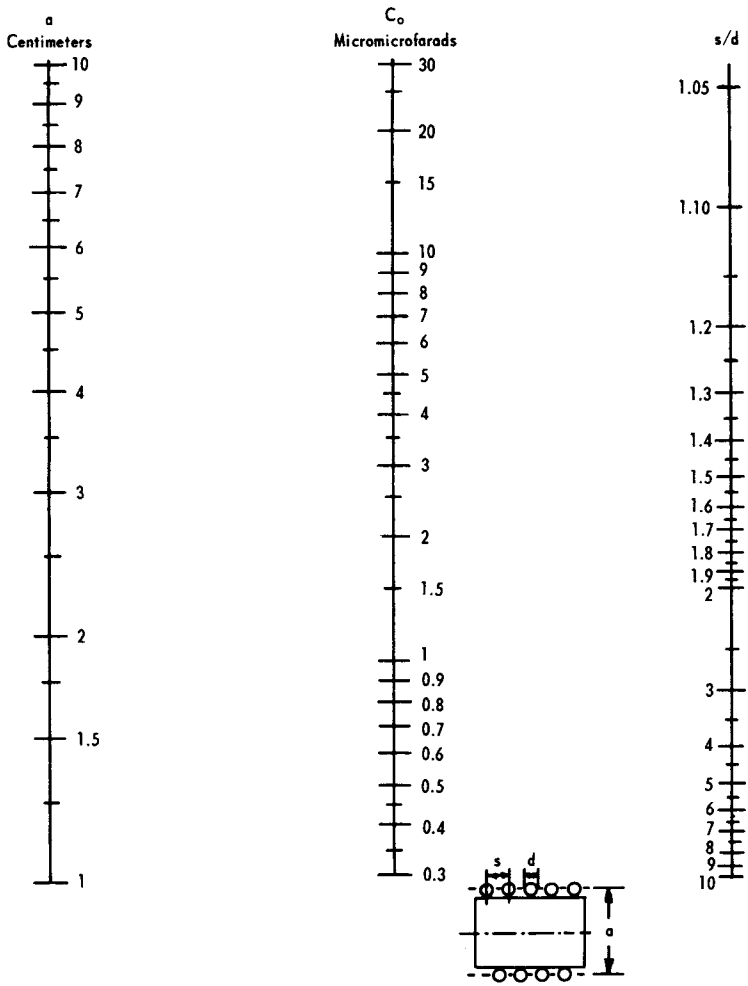

Figure 6.18. Nomograph for Determining Distributed Capacitance of Single-Layer Coils

Leads are a major contributor to the inductance which determines the natural resonant frequency, and their lengths should be kept to an absolute minimum for radio frequency applications. Fig. 6.27 illustrates variations in natural resonant

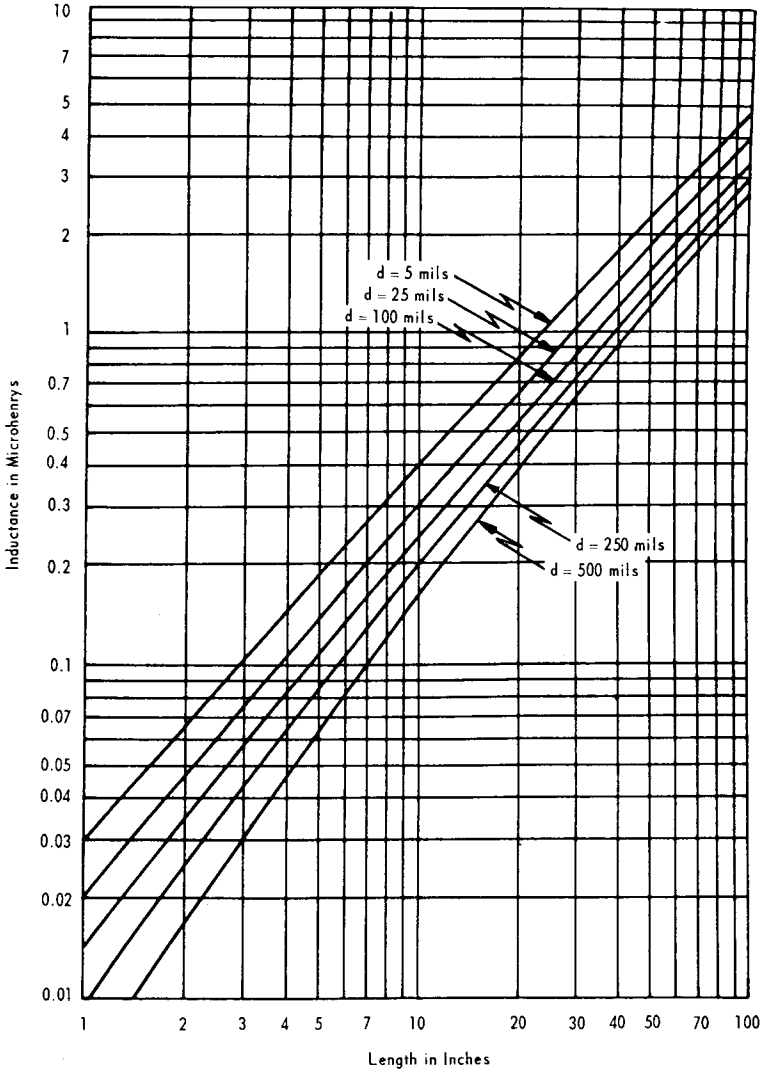

Figure 6.19. Self-Inductance of a Straight Round Wire at High Frequencies

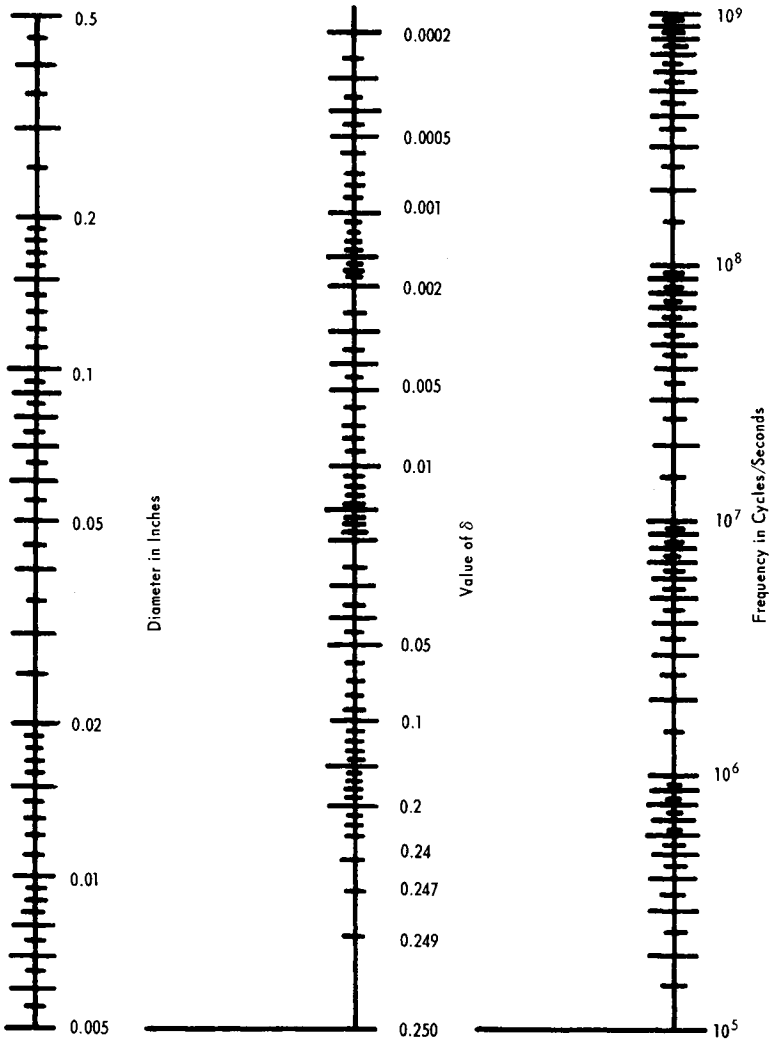

Figure 6.20. Skin-Effect Correction Factor δ as a Function of Wire Diameter and Frequency

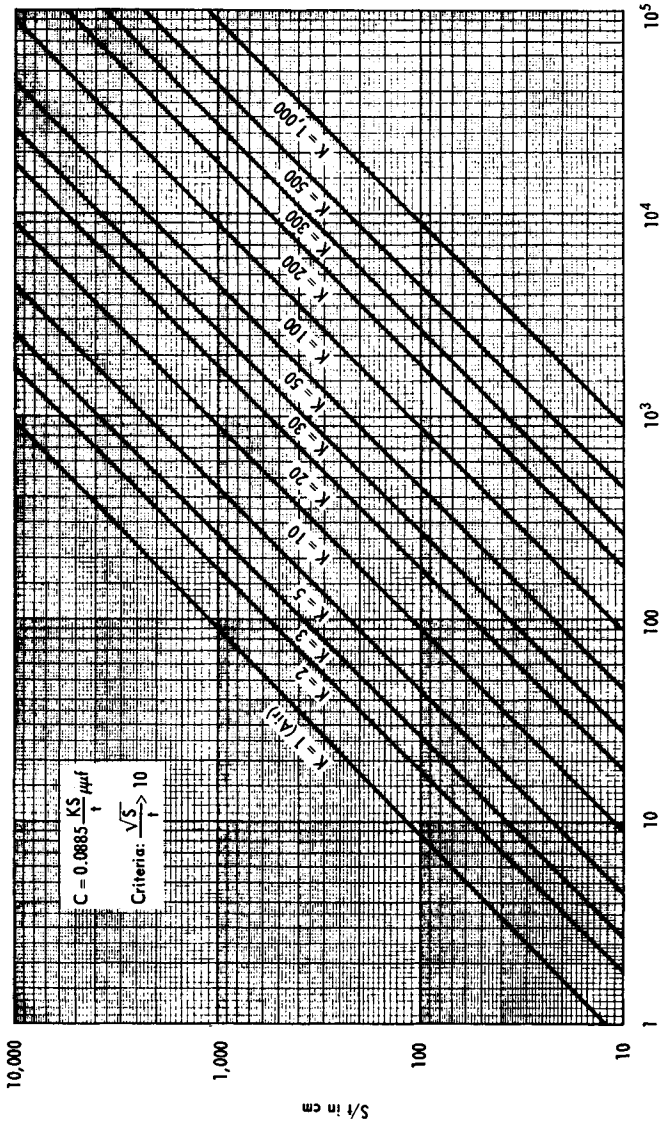

Figure 6.21. Capacitance of Parallel Plate Condenser

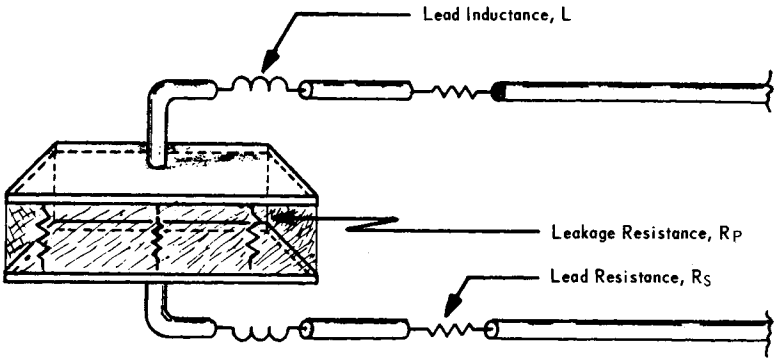

Figure 6.22. Typical Capacitor with Leakage Resistance and Lead Impedance

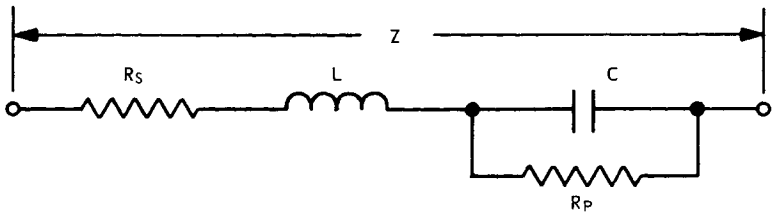

Figure 6.23. Simplified Equivalent Circuit of Capacitance

Table 6.1
RESONANT FREQUENCIES OF TYPICAL HIGH VOLTAGE CAPACITORS

Capacitance (μf)	Voltage rating	Watt-seconds	Resonant frequency (kc)
0.1	600	0.018	3,500
0.1	1,000	0.05	3,400
0.1	1,500	0.113	2,750
0.1	3,000	0.45	2,000
0.12	20,000	24	1,120
0.5	600	0.09	1,450
0.5	2,000	1	1,380
0.5	4,000	4	1,150
0.5	5,000	6.25	950
1.0	600	0.18	1,000
1.0	2,000	2.0	750
2.0	2,500	6.25	500
2.0	3,000	9	510
2.0	4,000	16	800
4.0	2,500	12.5	480
4.0	3,000	18	500
75.0	1,120	47	5

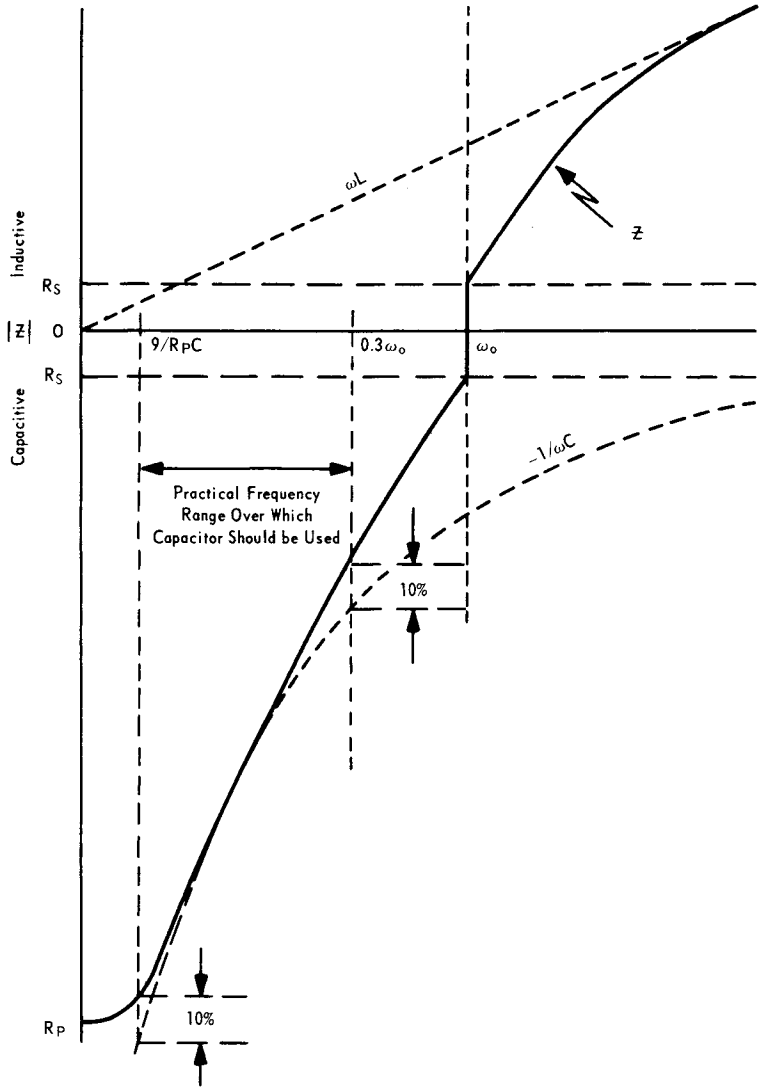

Figure 6.24. Equivalent Impedance of Capacitor

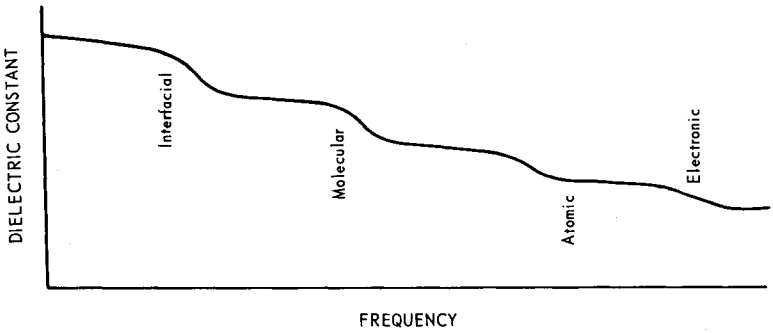

Figure 6.25. Effect of Frequency on Dielectric

frequencies of some typical capacitors as a function of lead length.

The leakage resistance is generally so high that it need not be considered from a leakage current or an internal heating viewpoint. Leakage is of concern, however at direct current and low frequencies, where the capacitive reactance is very high.

6.3.3 UHF Resonance

The capacitor may act as a long-line oscillator or a cavity resonator and introduce spurious resonant frequencies other than the natural frequencies. The frequencies at which such resonances will occur can only be determined accurately in the laboratory; generally, such resonances will occur above the natural resonant frequency of the capacitor and should cause no problems if adequate considerations are given to the natural resonant frequency points (see Fig. 6.23).

6.3.4 Temperature Characteristics

The effects of temperature variation on capacitor performance is important when the filter is required to operate over a broad temperature range or at a temperature different than 25°C (77°F), which is the temperature at which most commercial capacitors are rated. Capacitor temperature is a function of I^2R losses, ambient temperatures, physical construction of the capacitor, internal heat transfer by conduction and convections, and heat losses by the container.

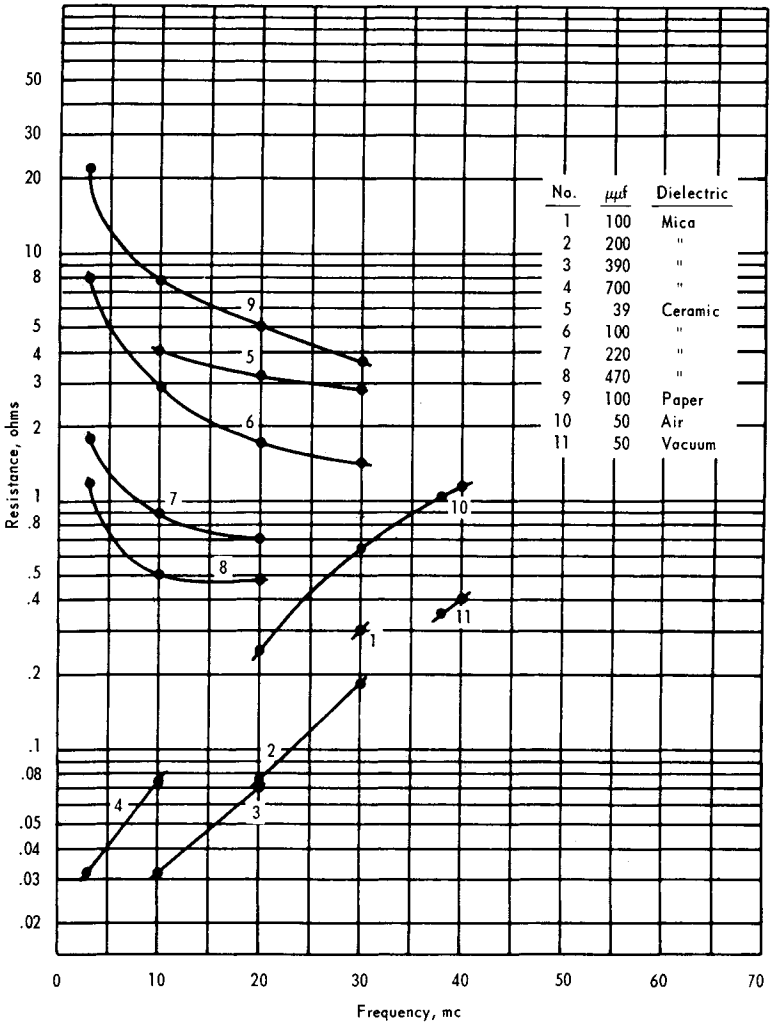

Figure 6.26. Equivalent Series Resistance vs. Frequency for Several Typical Capacitors

Temperature coefficients are generally supplied with commercially available capacitors. Temperature coefficients are obtained from Fig. 6.28. Line F is the actual capacitance over the frequency range of −55 to +85°C. Lines A and B are drawn from

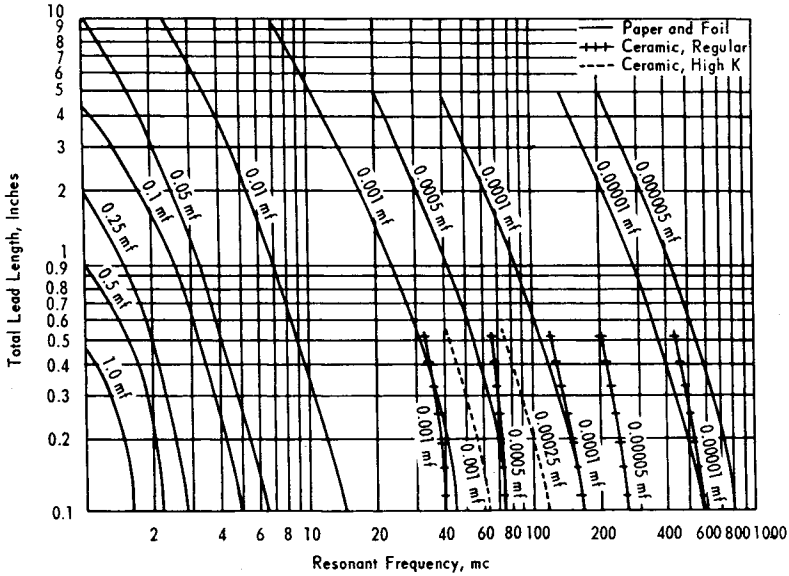

Figure 6.27. Resonant Frequency of Noninductive Capacitors as a Function of Lead Length

each end of the actual capacitance curve, F, through the coordinate intercept at 25°C, to the opposite temperature extremity. The slope of line A is considered as the nominal temperature coefficient. Therefore:

$$TC = \frac{\Delta C \times 10^6}{C_{25} \times \Delta T}$$

where, TC = temperature coefficient (ppm/°C)

ΔC = change in capacitance ($\mu\mu$f)

ΔT = absolute difference between 25°C and the test temperature

C_{25} = actual capacitance at 25°C.

Since the temperature coefficient is based upon a straight line approximation, which is a departure from the true capacitance curve, commercially available capacitors will have stipulated tolerances usually designated as ± ppm. Fig. 6.29

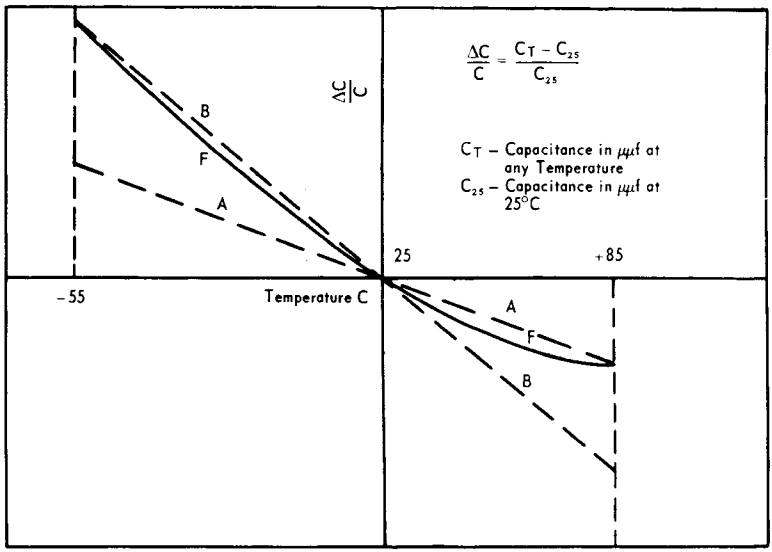

Figure 6.28. Method of Obtaining the Temperature Coefficient

illustrates the typical temperature characteristics of commercially available ceramic capacitors.

6.4 RESISTORS

Resistors are not an integral part of LC filter design, but variations in such, should be considered from a driving source or terminating load point of view. Transmission loss characteristics of filters are dependent upon the impedance characteristics of both the source and load terminations as discussed in Chap. 4.

Resistors decrease in value at high frequencies and may behave more like capacitors or inductors than a pure resistance. For example, Fig. 6.30 illustrates the inductive reactance as a function of frequency of applied voltage for various noninductive, wire-wound resistors. Such reactive components are further evidenced in Table 6.2 which shows some high frequency characteristics of typical bobbin-type resistors.

Carbon resistors also decrease in value at radio frequencies, although the reactive component is not nearly as high as for

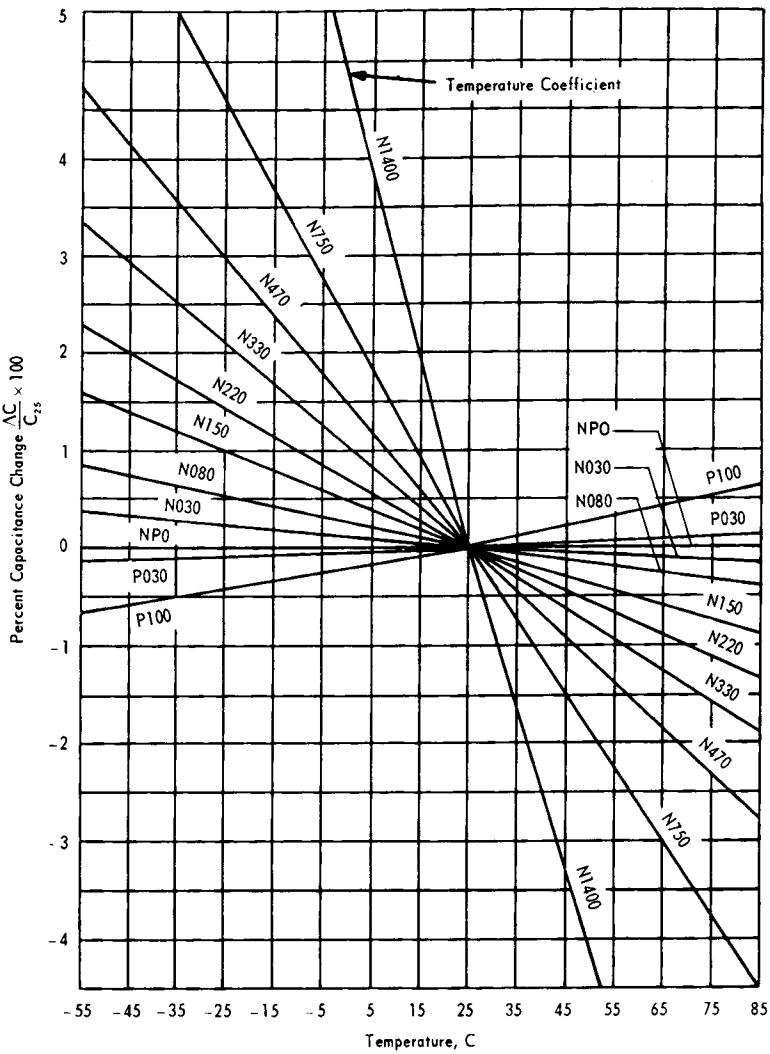

Figure 6.29. Typical Temperature Characteristics of Commercially Available Ceramic Capacitors

wire-wound resistors. Fig. 6.31 shows the frequency characteristics of special "high-frequency" resistors which are actually little better than a normal carbon resistor.

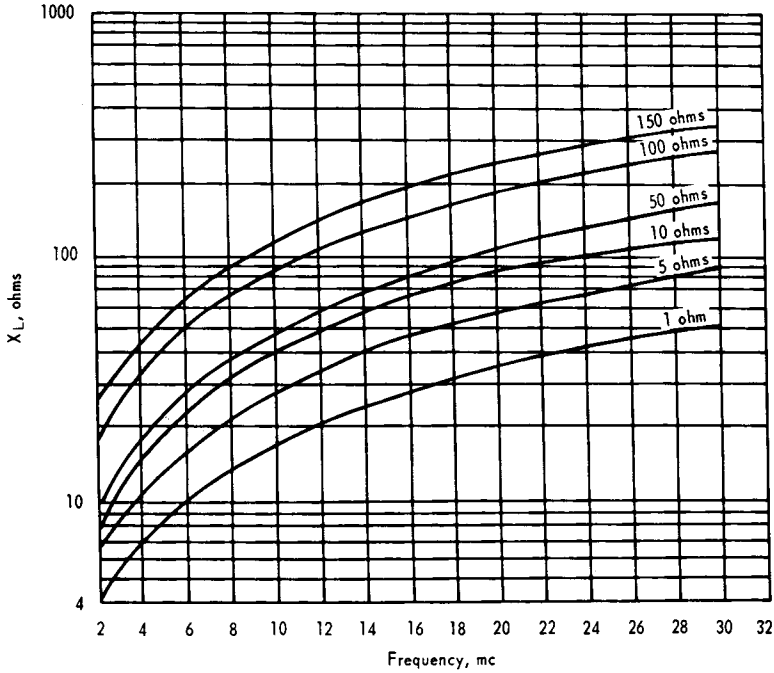

Figure 6.30. Net Inductive Reactance of "Noninductive" Wire-Wound Resistors

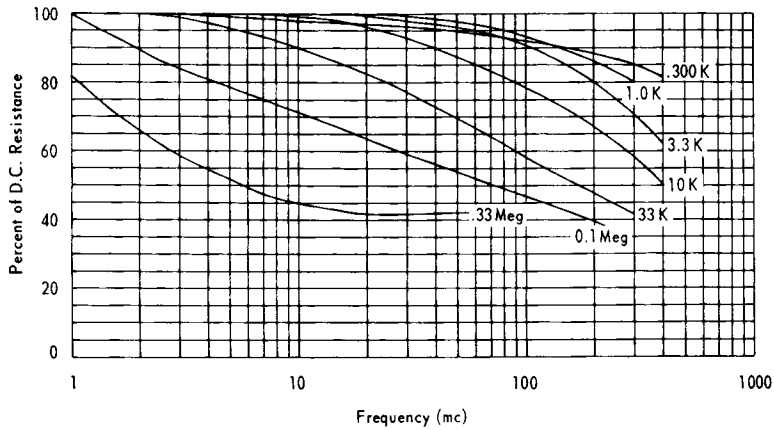

Figure 6.31. Frequency Characteristics of "High-Frequency" Resistor

Table 6.2
HIGH-FREQUENCY CHARACTERISTICS OF TYPICAL BOBBIN-TYPE RESISTORS

Manufacturer	Frequency (mc)	1,000-ohm resistors		100,000-ohm resistors	
		R_{eff} (ohms)*	X_{eff} (ohms)*	R (ohms)	Shunt capacitance ($\mu\mu$f)
A	1	4,700	−278	85,000	14
A	10	93	−390	5,000	12
B	1	914	+2,550	132,000	3
B	10	161,000	resonates at 6.5 mc	14,200	2.8
C	1	990	− 44	73,000	2
C	10	830	−341.5	25,500	1.4
D	1	1,090	+2,960	14,800	2
D	10	92,000	resonates at 4 mc	24,000	2.3
E	1	1,120	+1,600	97,000	3.2
E	10	44,000	resonates at 6 mc	14,200	3.2

*R_{eff} and X_{eff} are the effective series resistances and reactances at the frequency of measurement.

6.5 REFERENCES

1. Blackburn, J. F., "Components Handbook," *Radiation Laboratory Series*, McGraw-Hill Book Co., Inc., M.I.T., 1949.
2. Brown, J. S. and Theyer, W., Jr., "High-Q Low-Frequency Resonant Filters," *Proc. Nat'l Electronics Conf.*, Vol. 7, 1951.
3. Bryan, H. E., "Printed Inductors and Capacitors," *Tele-Tech & Electronic Industries*, pp. 68–694, 120–124, December 1955.
4. Carlin, H. J., "On the Physical Realizability of Linear Nonreciprocal Networks," *Proc. IRE*, pp. 608–616, May 1955.
5. Chi Lung Kang, "Circuit Effects on Q," *The Boonton Radio Corp., Notebook*, No. 8, Winter 1956.
6. Cohn, S. B., "Direct-Coupled-Resonator Filters," *Proc. IRE*, 45, 2, pp. 187–196, February 1957.
7. Cohn, S. B., "Microwave Filter Design for Interference Suppression," *Proceedings of the Symposium Electromagnetic Interference*, Asbury Park, N. J., June 1958.
8. Duncan, R. S., "A Survey of the Application of Ferrites to Inductor Design," *Proc. IRE*, pp. 3–13, January 1956.
9. Edson, W. A., "The Single Layer Solenoid as an RF Transformer," *Proc. IRE*, pp. 932–936, August 1955.
10. Ergul, "Miniaturized High-Efficiency R-F Filters," AD-43261, ASTIA Tab. U-79, p. 29.
11. Judge, W. L., "Spurious Emission Filter Design," *Tele-Tech*, p. 86, April 1956.
12. Karakash, J. J., "Transmission Lines and Filter Networks," The MacMillan Co., N. Y., 1950.
13. Medhurst, R. G., "H. F. Resistance and Self-Capacitance of Single-Layer Solenoids," *Wireless Engineer*, Vol. 24, No. 281, pp. 35–43, February 1947, and pp. 80–92, March 1947.
14. Slake, M. W., "Resonate Effects in Tubular Feedthrough Capacitors," *Tele-Tech*, pp. 98–101 and 180, June 1954.
15. Terman, F. E., *Radio Engineers' Handbook*, McGraw-Hill Book Company, Inc., 1943.

16. Wheeler, H., "The Design of Radio-Frequency Choke Coils," *Proc. IRE*, Vol. 24, No. 6, pp. 850–858, June 1936.

17. Wheeler, H., "Inductance Chart for Solenoid Coil," *Proc. IRE*, pp. 1398–1400, December 1950.

18. White, D. R. J., "Charts Simplify Passive LC Filter Design," *Electronics*, pp. 160–163, December 1, 1957.

19. White Electromagnetics, Inc., "RF Delay-Line Filters," Final Report, under NOLC Contract No. N123(62738)-29779A, June 30, 1962.

20. MIL-STD-220A, pp. 3–5, December 15, 1954.

21. *Filtron RF Interference Filter (SP-120) Specifications*, FIL-1001-59, Issue A.

22. Electronic Components Laboratory, *Electronic Components Handbook*, McGraw Hill Book Company, Inc., pp. 21–153, 1957.

CHAPTER 7

PHYSICAL REALIZABILITY OF FILTERS

Chap. 4 developed the lumped-element, low-pass filter prototypes for Butterworth and Tchebycheff responses. Chap. 5 developed the high-pass, band-pass, and band-rejection filters from these low-pass prototypes. Special attention was given to eleven different manifestations of band-pass filters which all yield essentially the same responses. Problems, such as Q_u-factors and element values, pertaining to the physical realizability of lumped-elements were reviewed in Chap. 6. This chapter summarizes the physical realizability of the entire lumped-element filter in terms of their element realizability.

The following four definitions of element physical realizability are established:

(1) Readily realizable (R),

$$\begin{aligned} 1\ \mu\text{h} \leq L \leq 1\ \text{h} \\ 5\ \mu\mu\text{f} \leq C \leq 1\ \mu\text{f}; \end{aligned} \tag{7.1}$$

(2) Practical (P),

$$\begin{aligned} 0.2\ \mu\text{h} \leq L \leq 10\ \text{h} \\ 2\ \mu\mu\text{f} \leq C \leq 10\ \mu\text{f}; \end{aligned} \tag{7.2}$$

(3) Marginally practical (M),

$$\begin{aligned} 0.05\ \mu\text{h} \leq L \leq 100\ \text{h} \\ 0.5\ \mu\mu\text{f} \leq C \leq 500\ \mu\text{f}; \end{aligned} \tag{7.3}$$

(4) Impractical (I),

All element values exceeding the bounds of Marginal; viz,

$$\begin{aligned} L &< 0.05\ \mu\text{h} \\ L &> 100\ \text{h} \\ C &< 0.5\ \mu\mu\text{f} \\ C &> 500\ \mu\text{f}. \end{aligned} \tag{7.4}$$

Some degree of caution obviously must be exercised in employing the above definitions since certain exceptions may exist and since no mention is made of the current handling capacity of the inductors or voltage rating of the capacitors, all of which are most important in the selection of components.

The following tables of physical realizability in the next four sections are based on the radio frequency, the loaded Q_L-factor, and the impedance level. First, the following table heading terms are explained:

(1) Frequency,[1]

$$\begin{aligned}
&f_o = 10 \text{ cps means: } 3 \text{ cps} \le f_o < 30 \text{ cps}\\
&f_o = 100 \text{ cps means: } 30 \text{ cps} \le f_o < 300 \text{ cps}\\
&f_o = 1 \text{ kc means: } 300 \text{ cps} \le f_o < 3 \text{ kc}\\
&f_o = 10 \text{ kc means: } 3 \text{ kc} \le f_o < 30 \text{ kc}\\
&f_o = 100 \text{ kc means: } 30 \text{ kc} \le f_o < 300 \text{ kc}\\
&f_o = 1 \text{ mc means: } 300 \text{ kc} \le f_o < 3 \text{ mc}\\
&f_o = 10 \text{ mc means: } 3 \text{ mc} \le f_o < 30 \text{ mc}\\
&f_o = 100 \text{ mc means: } 30 \text{ mc} \le f_o < 300 \text{ mc};
\end{aligned} \tag{7.5}$$

(2) Loaded Q_L-factors (for band-pass filters),

$$\begin{aligned}
&Q_L = 5 \text{ means: } 3 \le Q_L < 10\\
&Q_L = 15 \text{ means: } 10 \le Q_L < 30\\
&Q_L = 50 \text{ means: } 30 \le Q_L \le 100;
\end{aligned} \tag{7.6}$$

(3) Impedance Level (Equal source and load resistances assumed; i.e., $\overline{R} \approx 1$),

$$\begin{aligned}
&R = 3\Omega \text{ means: } 1 \le R < 10 \text{ (usually implies power filters)}\\
&R = 50\Omega \text{ means: } 10 \le R < 150\\
&R = 500\Omega \text{ means: } 150 \le R < 2.5\,\text{k}\\
&R = 10\text{k}\Omega \text{ means: } 2.5\,\text{k} \le R \le 50\,\text{k}.
\end{aligned} \tag{7.7}$$

7.1 LOW- AND HIGH-PASS FILTERS

Table 7.1 lists the physical realizability scores of R, P, M, and I (see Eqs. (7.1) through (7.4)) for four different driving and

[1] For low-pass filters, replace f_o with f_c.

terminating impedance loads covering eight decades in the frequency spectrum. Note that physical realizability of low- and high-pass filters are impractical at the four extreme points.

Table 7.1
PHYSICAL REALIZABILITY OF LOW- AND HIGH-PASS FILTERS*

R in ohms	Cut-Off Frequency, f_c							
	10 cps	100 cps	1 kc	10 kc	100 kc	1 mc	10 mc	100 mc
3	I	M	M	P	R	P	M	I
50	M	M	M	R	R	R	R	M
500	M	P	R	R	R	R	R	R
10k	I	M	P	R	R	R	P	I

*See Eqs. (7.1) through (7.4) for definitions of Scores.

7.2 BAND-PASS FILTERS

Each of the eleven band-pass filter prototypes discussed in Chap. 5 is tabulated in Table 7.2, according to its physical realizability score of R, P, M, or I. The frequencies are stepped by an order of magnitude and the Q_L-factors by about 3. The "50-, 500- and 10-K" terms pertain to the impedance level. All terms are defined in Eqs. (7.5) through (7.7).

Illustrative Example 7.1

Let it be desired to design a maximum-flat, band-pass filter which will exactly bracket the 88–108-mc FM band. This filter is to be installed at the input terminals of an FM receiver so that nearby high-power radiations existing both below 88 mc and above 108 mc will not cause radio-frequency interference by heterodyning or intermodulation action. It is determined that 40 db of attenuation is desired at and below about 50 mc and at and above 150 mc. The filter is to be a balanced type since it is fed by and terminated in a 300-ohm twin-lead transmission line.

The center frequency, f_o, of the filter is:

$$f_o = \sqrt{f_L \times f_h} = \sqrt{88 \times 108} = 97.6 \text{ mc} \approx 98 \text{ mc}. \qquad (7.8)$$

The normalized cut-off frequency is:

$$\text{High Side: } \overline{\omega}_{bp} = 2|\omega_o - \omega_1|/\omega_c = 2|98 - 150|/(108 - 88)$$
$$= 2 \times 52/20 = 5.2$$
$$\text{Low Side: } \overline{\omega}_{bp} = 2|98 - 50|/20 = 2 \times 48/20 = 4.8.$$

Table 7.2
PHYSICAL REALIZABILITY OF A BAND-PASS FILTER

Band-Pass Filter Prototype		f_o = 1 kc									f_o = 10 kc								
		Q_L = 5			Q_L = 15			Q_L = 50			Q_L = 5			Q_L = 15			Q_L = 50		
Type	Figure	50	500	10K	50	500	10K	50	500	10K	50	500	10K	50	500	10K	50	500	10K
1st	5.6	I	P	P	I	I	I	I	I	I	M	R	P	I	M	P	I	M	P
2nd	5.7	I	P	P	I	I	I	I	I	I	M	R	P	I	M	I	I	M	P
3rd	5.12	I	M	I	I	I	I	I	I	I	M	P	M	I	P	P	I	M	I
4th	5.13	I	M	P	I	I	P	I	I	M	M	P	P	I	P	P	I	M	P
5th	5.17	P	P	P	P	I	P	P	P	I	R	R	P	R	P	P	R	P	M
6th	5.18	P	P	I	P	P	I	P	P	I	R	R	P	R	P	P	R	P	M
7th	5.19	I	M	P	I	I	P	I	I	M	M	P	R	I	P	R	I	M	P
8th	5.20	M	P	I	M	P	I	M	P	I	P	R	P	P	P	P	P	P	M
9th	5.21	I	M	P	I	I	P	I	I	M	M	P	P	I	P	P	I	M	P
10th	5.28	M	P	M	P	R	P	R	R	P	P	R	P	R	R	R	R	R	R
11th	5.29	M	P	P	M	P	P	M	M	P	P	R	R	P	R	R	M	P	R

Band-Pass Filter Prototype		f_o = 100 kc									f_o = 1 mc								
		Q_L = 5			Q_L = 15			Q_L = 50			Q_L = 5			Q_L = 15			Q_L = 50		
Type	Figure	50	500	10K	50	500	10K	50	500	10K	50	500	10K	50	500	10K	50	500	10K
1st	5.6	P	R	R	P	P	I	M	M	I	P	R	P	P	P	I	M	P	I
2nd	5.7	P	R	R	P	P	I	M	M	I	P	R	P	P	P	I	M	M	I
3rd	5.12	P	R	P	P	R	P	M	P	P	R	R	P	R	R	R	M	P	I
4th	5.13	P	R	R	P	R	R	M	P	R	R	R	R	P	R	R	M	P	R
5th	5.17	R	R	P	R	R	P	R	R	P	R	R	P	R	R	M	R	P	I
6th	5.18	R	R	P	R	R	P	R	P	P	R	R	P	R	R	M	R	P	I
7th	5.19	P	R	R	P	R	R	M	P	R	R	R	R	P	R	R	M	P	R
8th	5.20	R	R	P	R	R	P	R	R	P	R	R	P	R	R	M	R	P	I
9th	5.21	P	R	R	P	R	R	M	P	R	R	R	R	P	R	R	M	P	R
10th	5.28	R	R	R	R	R	P	R	R	P	R	R	P	R	R	M	R	R	M
11th	5.29	R	R	R	R	R	R	P	R	R	R	R	R	R	R	R	R	R	R

Band-Pass Filter Prototype		f_o = 10 mc									f_o = 100 mc								
		Q_L = 5			Q_L = 15			Q_L = 50			Q_L = 5			Q_L = 15			Q_L = 50		
Type	Figure	50	500	10K	50	500	10K	50	500	10K	50	500	10K	50	500	10K	50	500	10K
1st	5.6	M	P	M	I	P	I	I	I	I	I	I	I	I	I	I	I	I	I
2nd	5.7	M	P	M	I	P	I	I	I	I	I	I	I	I	I	I	I	I	I
3rd	5.12	P	R	M	R	P	I	I	M	I	I	M	I	I	I	I	I	I	I
4th	5.13	M	R	R	I	P	R	I	M	R	I	M	R	I	I	P	I	I	M
5th	5.17	P	R	M	M	P	I	P	M	I	M	M	I	I	I	I	M	I	I
6th	5.18	R	R	M	P	P	I	P	M	I	P	M	I	M	I	I	M	I	I
7th	5.19	M	R	P	I	P	P	I	P	P	I	P	M	I	I	I	I	M	I
8th	5.20	R	R	M	R	P	I	P	M	I	P	M	I	P	I	I	M	I	I
9th	5.21	M	R	R	I	P	R	I	M	R	I	M	R	I	I	P	I	I	M
10th	5.28	P	R	I	P	M	I	P	M	I	P	M	I	M	I	I	M	I	I
11th	5.29	M	R	M	M	P	M	I	P	M	I	M	I	I	M	I	I	I	I

The reason for calculating both the high and low side, ω_{bp}, is because it does not necessarily follow that the requirements will give an equal attenuation for symmetrically disposed frequencies. If the frequencies are not equally disposed geometrically, then compute $\overline{\omega}_{bp}$ as above and take the tighter (the smaller $\overline{\omega}_{bp}$) requirement of the two, or 4.8 in the example.

According to Fig. 4.5, for an $\overline{\omega}_{bp}$ of 4.8 and an L_{db} of 40 db, the number of stages n must equal 3. From Table 7.2 use f_o = 100 mc, Q_L = 5, and R = 500 ohms, all of which are closest to the requirements. Note that all filters score impractical (I) or marginal (M) with the exception of the Seventh Type (see Fig. 5.19) which scores practical (P).

The desired band-pass filter characteristics are:

$$R = 300\Omega$$
$$f_o = 97.6 \text{ mc}$$
$$f_c = f_L - f_h = 108 - 88 = 20 \text{ mc}$$
$$Q_L = f_o/f_c = 97.6/20 = 4.89$$
$$n = 3 \text{ Butterworth.}$$

The element values for this filter are obtained from Table 4.1 and Fig. 5.19:

$$C_1' = C_3' = \frac{C_1}{R\omega_c} = \frac{1.00}{300 \times 2\pi \times 20 \times 10^6} = 26.6\ \mu\mu f$$

$$\frac{M_{12}}{R} = \frac{M_{23}}{R} = \frac{1}{R\omega_o}\sqrt{\frac{C_1}{L_2}} = \frac{1}{300 \times 2\pi \times 97.6 \times 10^6}\sqrt{\frac{1.00}{2.00}} = 3.84\ \mu\mu f$$

$$\frac{C_1}{R\omega_c} - \frac{M_{12}}{R} = \frac{C_1}{R\omega_c} - \frac{M_{23}}{R} = 26.6 - 3.8 = 22.8\ \mu\mu f$$

$$\frac{C_1}{R\omega_c} - \frac{M_{12}}{R} - \frac{M_{23}}{R} = 26.6 - 3.84 - 3.84 = 18.9\ \mu\mu f$$

$$L_1' = L_2' = L_3' = \frac{R}{C_1 Q_L \omega_o} = \frac{300}{1.00 \times 4.89 \times 2\pi \times 97.6 \times 10^6} = 0.1\ \mu h.$$

Because a balanced twin line is being used, each M_{mn}/R series capacitors will be replaced by two, one of which is in the same position and the other is in the equivalent "ground" leg of the unbalanced ladder depicted in Fig. 5.29. Since these capacitors help determine the frequency of resonance at each node (cf., Eq. (5.32)) they are in series to yield the value of the replaced

capacitance. Hence, their value is $2M_{mn}/R$ or 7.68 $\mu\mu$f. The resulting filter is shown in Fig. 7.1 and its response is shown in Fig. 7.2. The response is not shown beyond 300 mc since the components are likely to self-resonate in this region and it is difficult to determine what the real response would be beyond this frequency.

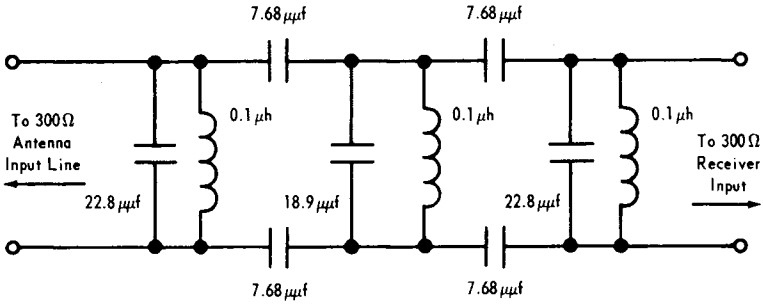

Figure 7.1. Band-Pass Filter Intended to Protect an FM Receiver from Heterodyning and Intermodulation

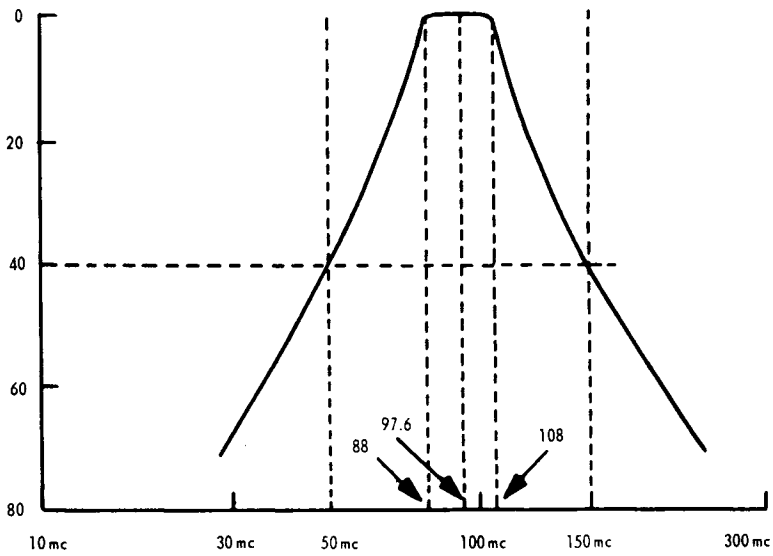

Figure 7.2. Frequency Response of Filter Depicted in Figure 7.1

CHAPTER 8

ALIGNMENT AND MEASUREMENT TECHNIQUES

The preceding chapters bring the filter from a theoretical design up to the fabricated unit. It now remains to discuss the methods of tuning the filter and measuring its performance. This is presented in this chapter.

8.1 MULTISTAGE FILTER TUNING TECHNIQUES[1]

This section on filter tuning applies mainly to band-pass filters having small percentage bandwidths; viz, $Q_L > 10$. Nodal-type networks are emphasized (cf., band-pass filter types No. 7, 9, and 11). Using the principle of duality and substituting the following words—loop for node, current for voltage, open circuit for short circuit, and the like—the alignment procedure applies similarly to loop networks (cf., band-pass filter types Nos. 6, 8, and 10).

8.1.1 Principles of Tuning

The underlying principle used in this section is that alignment is best accomplished by completely assembling a band-pass filter and then concentrating on the amplitude phenomena occurring in the first resonant circuit of a filter chain at the desired resonant frequency, f_o. Subsequently it will be shown that if all filter stages are first detuned and if they are resonated in numerical order, calling the input tuned circuit number 1, then all odd-numbered resonant circuits place an open circuit (high resistance) and all even-numbered resonant circuits place a short circuit (low resistance) across the input terminals of the generator source.

8.1.2 Alignment Procedure

The alignment procedure will be described using a five-stage, capacitively-coupled, band-pass filter (cf., Fig. 5.19) shown in Fig. 8.1 as an example. The following procedure is applicable to

[1]Much of this section was obtained from reference (8).

all coupled-resonant-circuit filters, whether they be low-frequency, constant-K configurations; medium-frequency coupled circuits; microwave quarter-wave-coupled, waveguide filters; or the like.

(1) Connect the generator to the first tuned circuit of the filter and the load to the last tuned circuit of the filter in exactly the same manner as they would be connected in actual use (see Fig. 8.1).

(2) Couple a nonresonant detector directly and loosely[1] to either the electric (voltage node) or magnetic (current loop) field of the first resonant circuit of the filter chain.

(3) Completely detune[2] all resonant circuits.

(4) Set the signal generator frequency to the desired mid-frequency of the filter, ω_o.

(5) Tune resonant circuit No. 1 for maximum voltage output indication on the detector. Lock the tuning adjustment (either the capacitor or coil or both can be tuned to give ω_o).

(6) Tune resonant circuit No. 2 for minimum voltage output indication on the detector. Lock the tuning adjustment.

(7) Tune resonant circuit No. 3 for maximum voltage output and lock the tuning adjustment.

(8) Tune resonant circuit No. 4 for minimum output and lock the tuning adjustment.

(9) Tune resonant circuit No. 5 for maximum output and lock the tuning adjustment.

The resonant circuit frequency alignment of the filter shown in Fig. 8.1 is now complete.

Regarding the ability to detune the resonant circuits, a sufficient dynamic range of the tunable elements (capacitors in Fig. 8.1) must exist. At resonances:

$$\omega_o^2 = \frac{1}{LC} \text{ or } C = \frac{1}{\omega_o^2 L} . \tag{8.1}$$

[1] A nonresonant detector (or generator) may be said to be loosely coupled when it lowers the unloaded Q_u of the resonator by less than about 5%.

[2] A resonant circuit is sufficiently detuned when its resonant frequency is at least 10 pass-band-widths (10 f_c) removed from the pass-band mid-frequency, f_o.

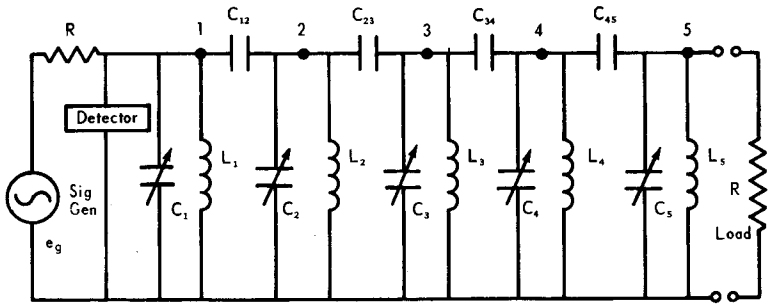

Figure 8.1. Five-Stage, Capacitively-Coupled, Band-Pass Filter Used to Demonstrate Alignment Procedure

At the detuned frequency, ω_d:

$$\omega_d \approx \omega_o \pm 10\,\omega_c \tag{8.2}$$

$$= \omega_o \pm 10\frac{\omega_c}{\omega_o}\omega_o = \omega_o\left(1 \pm \frac{10}{Q_L}\right). \tag{8.3}$$

To achieve the detuned frequency, the capacitance becomes:

$$C'|_{\omega=\omega_d} = C \mp \Delta C. \tag{8.4}$$

The change in capacitance, therefore, is:

$$\Delta C = |C - C'| = |C - (C \mp \Delta C)|. \tag{8.5}$$

Substituting Eqs. (8.1) and (8.3) into Eq. (8.5) yields:

$$\begin{aligned}\Delta C &= \frac{1}{\omega_o^2 L} - \frac{1}{\omega_o^2 L(1 \pm 10/Q_L)^2} \\ &= C\left[1 - \frac{1}{(1 \pm 10/Q_L)^2}\right].\end{aligned} \tag{8.6}$$

Thus the percentage change or tuning range required of C is:

$$\frac{\Delta C}{C} = 100\left[1 - \frac{Q_L{}^2}{(10 + Q_L)^2}\right]. \tag{8.7}$$

The tuning range requirements on C (or L) as a function of Q_L is tabulated from Eq. (8.7) in Table 8.1.

Table 8.1
TUNED-CIRCUIT TUNING RANGE REQUIREMENTS TO PERMIT EFFECTING A DETUNED CIRCUIT CONDITION

Q_L	Minimum Element Value Tunable Range (in percent)
1	100
3	95
10	75
30	44
100	17
300	6
1000	2

If it is impracticable to detune all the resonant circuits in a nodal network (see Table 8.1), a shorting jumper may be used to short-circuit the resonant circuit immediately following the one being tuned as this will remove the effect of all subsequent resonant circuits. It is important that this short circuit be effective at the center frequency, f_o. Since the alignment adjustments depend exclusively on the amplitude of the response at the resonant frequency f_o, a sweep-frequency generator is not required and all adjustments can be made with a single-frequency input.

Efficient filters with low internal losses, i.e., those using resonators having unloaded Q_u's very much greater than the loaded Q_L-factor, produce deep minimums when the even-numbered resonators are properly tuned. Therefore, it is important to use a large-amplitude signal input and a high detector gain so that the middle of the minimum can be tuned accurately to the mid-frequency. If the maximum generator input and detector gain still produce a broad null, the tuning adjustments should be set midway between two points of equal output on the detector.

8.1.3 Theory of Alignment

One way of showing that the above alignment procedure is correct is to consider the large-percentage-bandwidth filter chain, shown in Fig. 8.2, to which all small-percentage-bandwidth coupled-resonant-circuit filters are equivalent no matter what

type of coupling is used between adjacent resonant circuits (cf., Chap. 5 and accompanying discussion). Next consider the small-percentage-bandwidth nodal circuit shown in Fig. 8.1.

The reasoning applicable to the large percentage-bandwidth configuration of Fig. 8.2 requires previous knowledge of two simple facts.

(1) Complete detuning of all the resonant circuits means that all the series circuits are effectively open-circuited and all the shunt resonant circuits are effectively short-circuited.

(2) When correctly aligned, the resonant frequency, f_o, of each separate resonant circuit is identical.

Thus, when resonant circuit No. 1 is tuned to f_o (with resonant circuit No. 2 open-circuited), maximum voltage will appear across the high parallel internal resonant resistance of circuit No. 1. When resonant circuit No. 2 is tuned to f_o (with resonant circuit No. 3 short-circuited), the low series-resonant resistance of No. 2 will shunt the terminals of 1, thus dropping the voltage across resonant circuit No. 1 to a minimum. On tuning circuit No. 3 to f_o (with resonant circuit No. 4 open-circuited), the high parallel-resonant resistance of No. 3 will remove the low series-resonant resistance of No. 2 from across the terminals of No. 1 so that the voltage across No. 1 will again rise to a maximum. Thus, starting at the front end of the filter, all odd-numbered resonant circuits (parallel circuits) will produce a maximum voltage and all even-numbered resonant circuits (series circuits) will produce a minimum voltage across No. 1 terminals.

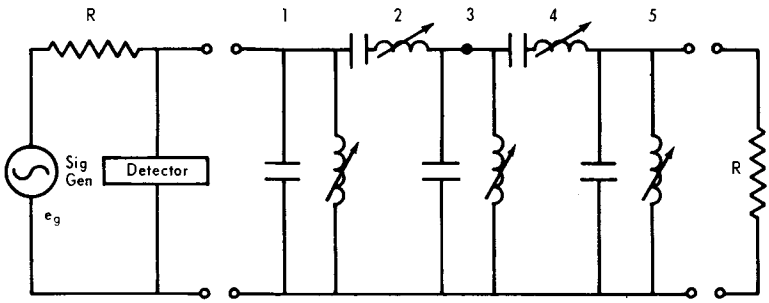

Figure 8.2. Five-Stage, Band-Pass Filter Used to Demonstrate Alignment Procedure

Now, the reasoning applicable to the small-percentage-bandwidth nodal network of Fig. 8.1 requires previous knowledge of three simple facts.

(1) Complete detuning of a resonator means that the node involved is effectively short-circuited.

(2) When correctly aligned, the resonant frequency of each node is identical, and the elements that resonate a node consist of every susceptance that touches the node. For example, node No. 2 of Fig. 8.1 is resonated by adjusting C_2 to resonate with the parallel combination of C_{12}, C_2, L_2, and C_{23}.

(3) If a group of reactances parallel-resonate together, then any one of the reactances also series-resonates with all the others in parallel. For example, C_{12} series-resonates with the parallel combination of C_2, L_2, and C_{23}.

Thus, when node No. 1 is tuned to f_0 and node No. 2 is short-circuited, the high parallel-resonant resistance of C_1, L_1, and C_{12} will produce a voltage maximum at f_0. When node No. 2 is tuned to f_0 and node No. 3 is short-circuited, C_{12} will series resonate with the parallel combination of C_2, L_2, and C_{23}. This effects a short circuit across node No. 1 and hence a voltage minimum. The process repeats as alignment proceeds, producing maximums for alignment of odd-numbered and minimums for even-numbered resonant circuits.

8.2 FILTER PERFORMANCE MEASUREMENTS

Compatible measurement techniques must be used to determine pertinent characteristics of filters after final fabrication and tuning. This section discusses various measurements necessary to determine the overall filter characteristics, techniques for performing such measurements, and some misunderstandings associated with such measurement procedures.

All filters should be subjected to insertion loss and relative attenuation measurements over the entire frequency spectrum of concern, which generally includes harmonic frequencies of bandpass filters. Load, source, and, in applicable situations, transmission line impedances must be selected to duplicate equivalent impedances of the network configuration in which the filter is to be used. All measurements on power filters should be made under rated load conditions.

8.2.1 Insertion Loss

The insertion loss, L_{db}, of a filter connected into a given transmission system is defined as the ratio of powers (before and after insertion) delivered to the output network immediately beyond the point of insertion at a given frequency; viz,

$$L_{db} = 10 \log_{10}\left(\frac{P_b}{P_a}\right) \text{db}. \tag{8.8}$$

Since both the powers existing before insertion (P_b) and after insertion (P_a) are terminated by the same network load, R_L, Eq. (8.8) becomes:

$$L_{db} = 10 \log_{10}\left[\frac{E_{bo}^2/R_L}{E_{ao}^2/R_L}\right] \tag{8.9}$$

$$L_{db} = 20 \log_{10}\frac{E_{bo}}{E_{ao}} \text{db} \tag{8.10}$$

where, E_b = output voltage at the load before filter insertion
E_a = output voltage at the load after filter insertion.

Fig. 8.3 illustrates one test circuit configuration for making insertion loss measurements under rated-load or simulated-output circuit conditions. The signal generator termination (R_{sg}) must be kept constant under test conditions. Similarly, the input termination (R_{Rx}) of the receiver must be preserved. Thus, impedance matching and isolation attenuators are generally required. When the rated filter source impedances $R_g = R_{sg}$ and the filter load impedance $R_L = R_{Rx}$, no impedance matching is required. In any event, isolation is generally used at the filter input and output terminals to minimize the effects of generator source impedance or receiver load impedance variation with frequency. A minimum of 10 db and usually, 20 db of isolation is considered good measurement practice.

Fig. 8.3 involves an insertion loss measurement set-up which may be used where several insertion loss measurements are to be made either at different pass-band frequencies or where several filters are to be tested, such as in a production run. When only a single measurement is required, as in most cases, or where more accurate insertion loss measurements are indicated, the test set-up

in Fig. 8.4 should be used. Here, the before and after effects of inserting the filter in the actual existing circuit are measured. This technique is also preferred when measuring the insertion loss of power filters because of the high power demands it would otherwise make on the signal generator and because of the possibility of varying load conditions, such as in power line applications.

8.2.2 Relative Attenuation and Transmission Loss

Relative attenuation is the attenuation offered by a filter at a specified frequency relative to the insertion loss provided at the pass-band signal test frequency. Thus, relative attenuation at the insertion-loss test frequency is zero.

The transmission loss of a filter is defined in the same manner as the insertion loss relation given in Eq. (8.10) except that the test frequency may assume any value rather than the signal frequency in the pass band. The transmission loss response is the only true and absolute filter attenuation frequency response description since it is defined in terms of the before and after effects of inserting the filter. It may not necessarily be equal to the sum of the insertion loss and relative attenuation measurements because of the manner in which the actual filter load (and power not realized due to mismatch) may change with frequency, especially in the rejection-band region. Notwithstanding this, relative attenuation measurements are convenient to make since the filter does not have to be inserted and removed at each test frequency.

Figs. 8.5 and 8.6 show two test methods for measuring the relative attenuation of a filter. The first is the classical point-by-point, frequency-amplitude method and the latter is the swept-frequency, scope-response method. The latter is generally less accurate and does not provide as wide a dynamic range of measurement of the amplitude response of the frequency covered, but is a considerably more rapid technique.

Transmission loss measurements (cf., Figs. 8.3 and 8.4) as mentioned above, are the most accurate method for determining absolute attenuation vs. frequency. Occasionally, none of the test arrangements discussed so far is adequate since the signal generator and receiver may require, for example, a 50-ohm output and input termination respectively to permit preserving calibration and the filter may be a power unit of very low input/output

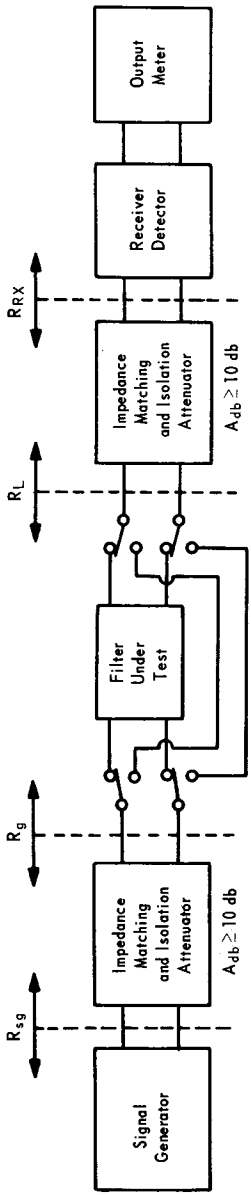

Figure 8.3. Test Circuit for Rapid Insertion Loss Measurements at Different Pass-Band Frequencies

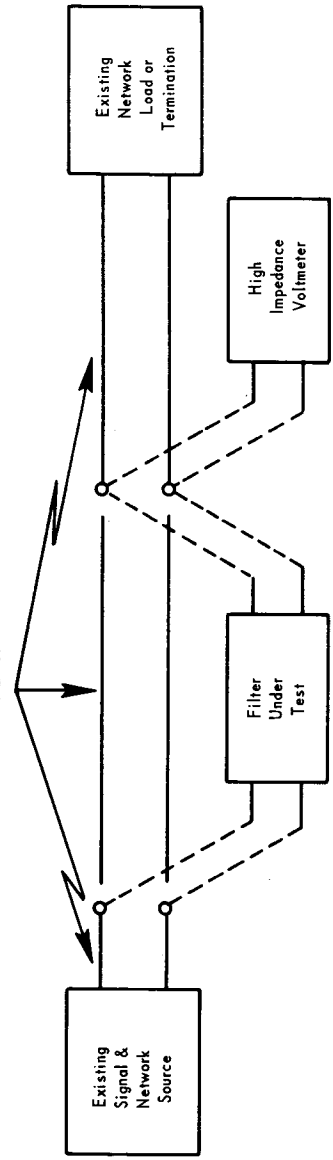

Figure 8.4. More Accurate Insertion Loss Measurement Set-Up than Figure 8.3

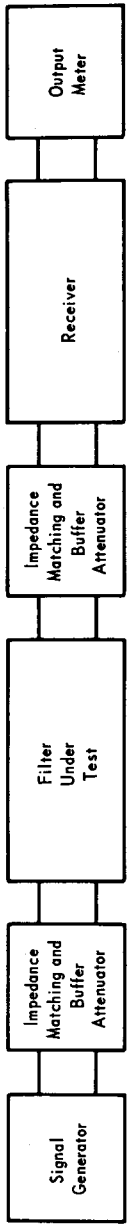

Figure 8.5. Classical Test Configuration for Making Point-by-Point, Relative Attenuation Measurements of Filter Frequency Response

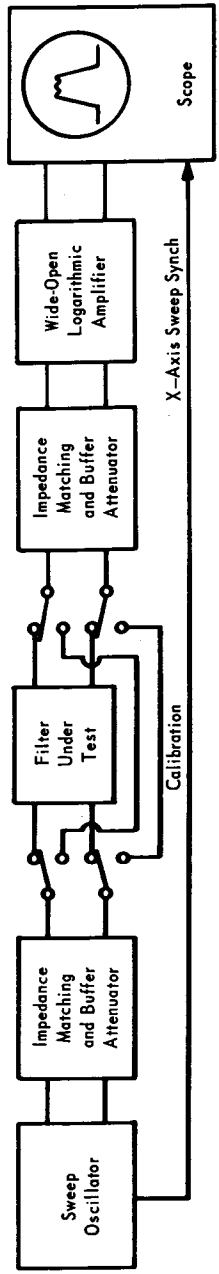

Figure 8.6. Test Configuration for Making Relative Attenuation Measurements of Filter Frequency Response by the Swept-Oscillator Method

impedance. Thus, an arrangement similar to that depicted in Fig. 8.7 is required to permit transmission loss measurements.

8.2.3 Filter Input Impedance and VSWR

Filter input impedance magnitude and phase and/or voltage standing wave ratio (VSWR) must often be determined in order to ensure compatible filter performance in specific circuit configurations. Required test instrumentation is dependent upon the frequency range and amplitude over which the complex impedances or VSWR is to be determined, and upon the desired accuracy of the measured data.

(1) *Transmission Loss Method*

It was shown in Chap. 4 that the transmission coefficient, $|t(j\omega)|^2$, (reciprocal of the transmission loss L) is related to the power reflection coefficient, $|p(j\omega)|^2$:

$$|p(j\omega)|^2 = 1 - |t(j\omega)|^2 = 1 - 1/L. \tag{8.11}$$

The input impedance, Z_{11} (see Chap. 4), is related to the voltage reflection coefficient:

$$Z_{11} = R_g \frac{1 - p}{1 + p} \tag{8.12}$$

or,

$$\frac{Z_{11}}{R_g} = \frac{1 - |p|e^{j\theta}}{1 + |p|e^{j\theta}} \tag{8.13}$$

where, θ is the phase angle of p.

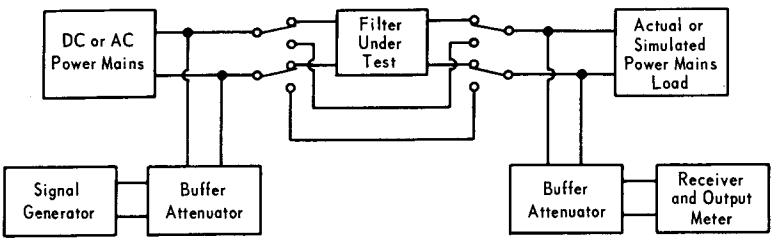

Figure 8.7. Test Configuration for Making Transmission Loss Measurements of Power Filters

Finally, the voltage standing-wave ratio, VSWR, is:

$$\text{VSWR} = \frac{1 + |\rho|}{1 - |\rho|}. \tag{8.14}$$

Substituting Eq. (8.11) into Eq. (8.14) yields:

$$\text{VSWR} = \frac{1 + \sqrt{1 - 1/L}}{1 - \sqrt{1 - 1/L}}. \tag{8.15}$$

Illustrative Example 8.1

Suppose the transmission loss of a filter at some frequency has been measured and found to be 7 db. Compute the VSWR. A 7-db loss corresponds to an L (power loss ratio) of 5.0 and $1 - 1/L = 1 - 0.2 = 0.8$. The magnitude of the voltage reflection coefficient is $|\rho| = \sqrt{1 - 1/L} = \sqrt{0.8} = 0.895$.

Thus, from Eq. (8.15), the VSWR is:

$$\text{VSWR} = \frac{1 + 0.895}{1 - 0.895} \approx 18.$$

For future reference, Eq. (8.15) is plotted in Fig. 8.8.

(2) *Lissajous Pattern Method*

Fig. 8.9 shows a test set-up that may be used below about 50 mc (lead length should be less than $\lambda/50$ or about 5°) to measure the input impedance, Z_{11}, by the Lissajous pattern method. The voltage, V_R, across R, which is applied directly to one set of oscilloscope deflection plates, is:

$$V_R = \frac{Re_g}{R + R_g + Z_{11}}. \tag{8.16}$$

The other voltage appearing across the filter input terminals, which is applied to the other deflection plates of the oscilloscope, is:

$$V_Z = \frac{Z_{11}e_g}{R + R_g + Z_{11}}. \tag{8.17}$$

Now, if R is changed in value until the inclination of the Lissajous ellipse is 45°, then $V_R = V_Z$ and $R = |Z_{11}|$. The phase

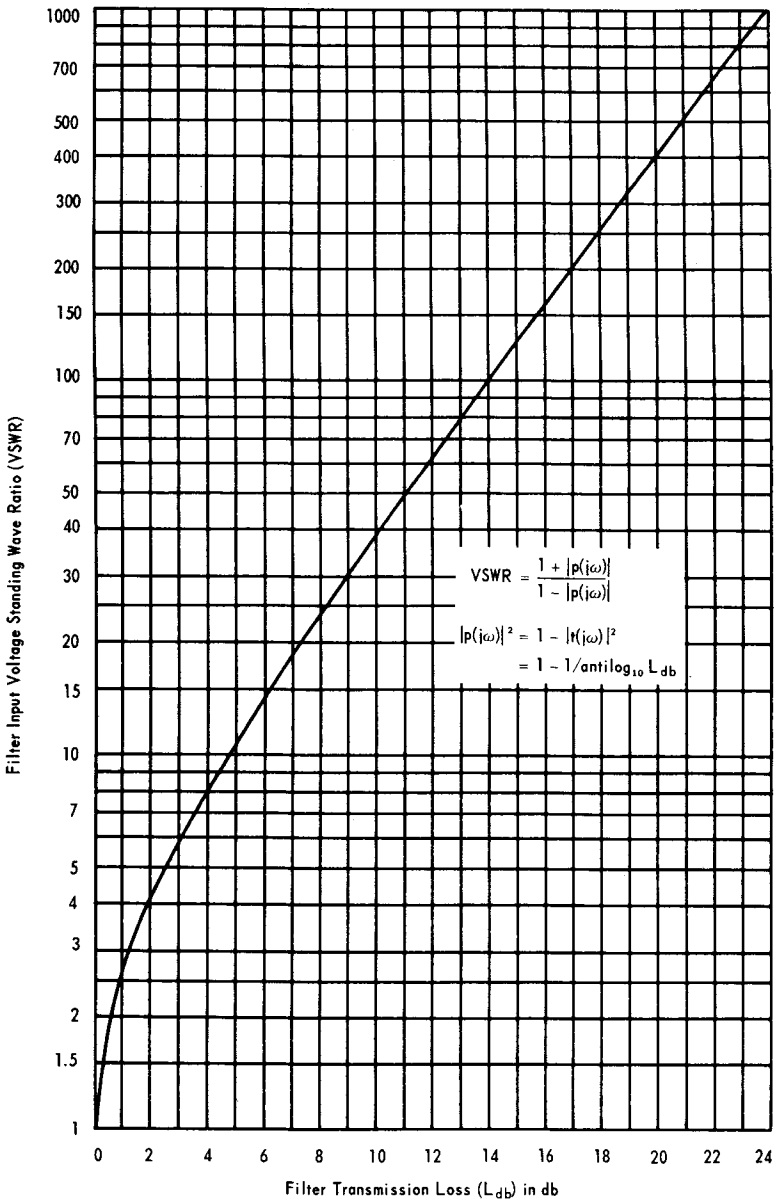

Figure 8.8. VSWR of Filter Input Terminals vs. Filter Transmission Loss for Zero Insertion Loss

angle of Z_{11} is determined by the quadrant inclination of the ellipse and the eccentricity in the normal Lissajous manner.

(3) *Impedance Bridge Method*

At frequencies from about 50 to 500 mc, the VHF/UHF impedance bridge method may be used to measure the magnitude and phase of the unknown filter input impedance. Instrumentation is available which is capable of yielding a resultant accuracy of approximately 2% in magnitude and 1° in phase angle. Fig. 8.10 illustrates the instrumentation required for the measurement of Z_{11} by the VHF/UHF impedance bridge method. The bridge is adjusted for a null and the magnitude and phase of the filter input impedance is read directly from the bridge.

(4) *Slotted Line Method*

Slotted lines are generally used for impedance or VSWR measurements at frequencies above about 500 mc. They are

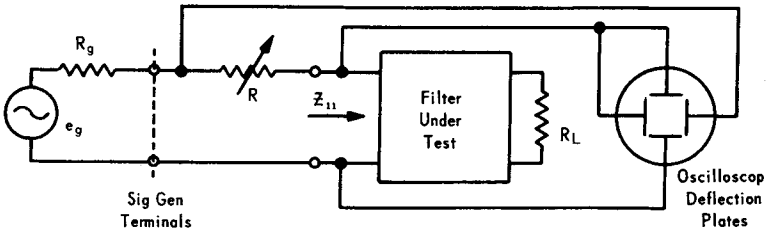

Figure 8.9. Lissajous Pattern Method of Measuring Filter Input Impedance, Z_{11}

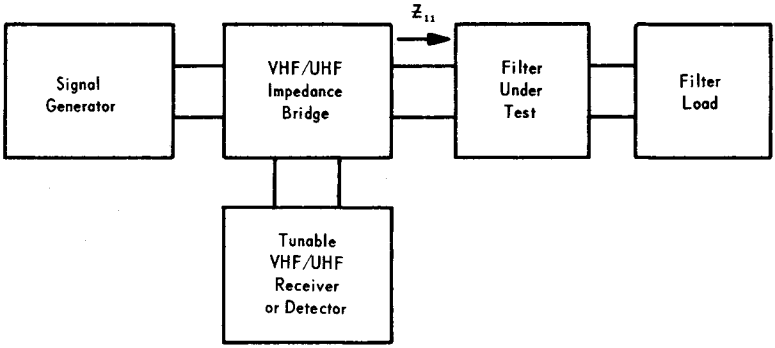

Figure 8.10. VHF/UHF Impedance Bridge Method of Measuring Filter Input Impedance, Z_{11}

driven by a buffered signal generator and terminated in the filter under test. For the most part, their use is very limited in the testing of lumped-element filters since slotted-line techniques cover only the upper frequency range of physically realizable lumped elements.

8.2.4 Transient Measurements

Filters should be subjected to transient and time delay testing when they are to be used in circuits which normally use pulses or may have transient type signals. One criterion for determining when to make transient measurements is if the filter bandwidth is less than about $3/\tau$ where τ is the rise time of an equivalent step function (transient) or the pulse duration of a pulse signal. Many techniques are available which are readily adaptable to measuring the time delay associated with a filter (see Sec. 4.1.3 and Sec. 4.2.3).

Fig. 8.11 illustrates one effective technique which may be used to determine the time delay associated with networks such as filters. The signal generator should be modulated with a similar type of signal expected in actual practice for a band-pass or band-rejection filter. Generally no carrier is used for low-pass filter testing unless it is a characteristic of the normally applied signal. Signals applied to the input and output terminals of the filter under test should drive separate channels of a dual-channel oscilloscope. Impedance matching networks are connected in series with the filter terminals in order to simulate normal operating conditions. Time delay is determined directly by comparison of leading edges and/or maximums and minimums of the two traces appearing on the oscilloscope. Polaroid or equivalent cameras may be used to photograph the resultant traces if a permanent record is desired.

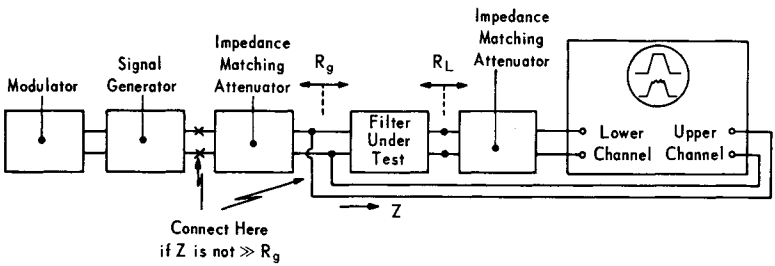

Figure 8.11. Typical Test Configuration for Measuring Filter Transient Response and Time Delay

8.3 REFERENCES

1. Blackburn, J. F., "Components Handbook," *Radiation Laboratory Series,* McGraw-Hill Book Co., Inc., M.I.T., 1949.
2. Cohn, S. B., "Direct-Coupled-Resonator Filters," *Proc. IRE,* 45, 2, pp. 187–196, February 1957.
3. Cohn, S. B., "Microwave Filter Design for Interference Suppression," *Proceedings of the Symposium Electromagnetic Interference,* Asbury Park, N. J., June 1958.
4. Dishal, M., "Alignment and Adjustment of Synchronously Tuned Multiple Resonant-Circuit Filters," *Proc. IRE,* 39, pp. 1448–1455, November 1951.
5. Dishal, M., "Design of Dissipative Band-Pass Filters Producing Desired Exact Amplitude Frequency Characteristics," *Proc. IRE,* Vol. 37, pp. 1050–1069, September 1949.
6. Ergul, "Miniaturized High-Efficiency R-F Filters," AD-43261, ASTIA Tab. U-79, p. 29.
7. Geza, Z., "Tunable Audio Filters," *Electronics,* pp. 173–175, November 1954.
8. Judge, W. L., "Spurious Emission Filter Design," *Tele-Tech,* p. 86, April 1956.
9. Karakash, J. J., "Transmission Lines and Filter Networks," The MacMillan Co., N. Y., 1950.
10. Terman, F. E., *Radio Engineers' Handbook,* McGraw-Hill Book Company, Inc., 1943.
11. White Electromagnetics, Inc., "RF Delay-Line Filters," Final Report, under NOLC Contract No. N123(62738)-29779A, June 30, 1962.

GLOSSARY OF SYMBOLS

A_{db} = attenuation (transmission loss), in db
C = capacitance
C_g = average value of capacitances in the prototype filter
C_p = parallel capacitance
C_s = series capacitance
C_T = total series capacitance
e_g = generating or source voltage
e_L = voltage appearing across network terminating load
e_o = output voltage of circuit
E = physical voltage
E_i = input voltage of circuit
f = real frequency, cycles per second (cps)
f_c = 3-db bandwidth of a filter, cycles/seconds
f_o = mean center frequency in a band-pass filter
f_L = lower 3-db cut-off frequency of a band-pass filter
f_H = upper 3-db cut-off frequency of a band-pass filter
$F(s)$ = Laplace transform
$g_L(t)$ = low-pass prototype transient response to impulse driving function
$h_L(t)$ = low-pass prototype transient response to step driving function
I = physical current
I_g = current from generator into network
j = $\sqrt{-1}$
k = coupling coefficient
K = dielectric constant
L = inductance
L_g = average value of inductances in the prototype filter
L_p = parallel inductance
L_s = series inductance
L_{mn} = coupling inductance of band-pass derived network
L_T = total series inductance
m_c = ratio of capacitive to inductive "Q" of circuit
M_{mn} = mutual inductance of band-pass derived network

n = number of reactive components (stages) in a network
$p(j\omega)$ = voltage reflection coefficient of a network
$|p(j\omega)|^2$ = power reflection coefficient of a network
P_a = power available from a generator
P_L = power delivered to a load
PF = power factor
P_o = transmitted power at resonant frequency f_o
Q_o = Q-factor associated with conductor losses
Q_c = capacitive Q of circuit
Q_d = Q-factor associated with dielectric losses
Q_L = loaded "Q" of a filter
Q_l = inductive "Q" of a circuit
Q_u = unloaded "Q" filter
R = resistance
$\overline{R}$ = ratio of filter source to load resistances or its reciprocal so that $\overline{R} \leq 1$
R_g = generator or source resistance
R_L = terminating or load resistance
R_T = total shunt resistance in a network
s = complex frequency variable = $\sigma + j\omega$
s_{pm} = "m" th pole of a rational function or polynomial
s_{zm} = "m" th zero of a rational function or polynomial
S = area of capacitor plates
t = time
$|t(j\omega)|^2$ = network transfer function
$|t_B(j\omega)|^2$ = transfer function of Butterworth network
$|t_T(j\omega)|^2$ = transfer function of Tchebycheff network
$T_n(\omega)$ = "n" th degree Tchebycheff polynomial
X_c = capacitive reactance
X_L = inductive reactance
X_{mn} = mutual reactance between stages of band-pass prototype network
Y_{11} = driving-point (input) admittance function
Y_{12} = transfer admittance function
Z = impedance function
Z_{mn} = mutual impedance function between "m" th & "n" th stages (branches) of a network or a circuit
Z_T = transfer impedance of network
Z_{11} = driving-point (input) impedance

Z_{12} = transfer impedance function

α_{db} = coaxial cable line attenuation in db/wavelength

λ_g = wavelength of transmission line

ϵ^2 = ripple tolerance in passband of Tchebycheff filter

ϵ_{db} = Tchebycheff ripple tolerance in db: $\epsilon_{db} = 10 \log_{10}(1 + \epsilon^2)$

δ = skin effect factor

σ = real component of complex frequency, $s = \sigma + j\omega$

$\sigma_n(\epsilon)$ = semi-minor axis of Tchebycheff ellipse, as a function of db ripple (ϵ) and number of stages (n)

τ_d = time-delay of network

ω = real frequency, radians per second = $2\pi f$

ω_{br} = frequency transformation variable for band-rejection network

$\overline{\omega}_{br}$ = normalized ratio of frequencies in the band-rejection network

$\overline{\omega}$ = normalized ratio of frequencies

ω_{bp} = frequency transformation variable for a band-pass network

$\overline{\omega}_{bp}$ = normalized ratio of frequencies for a band-pass network

ω_c = 3-db bandwidth of a filter, radians/second

ω_{lp} = normalized ratio of frequencies in low-pass network

ω_n = bandwidth of an n stage, constant k network, radians/second

$\omega_n(\epsilon)$ = semi-major axis of Tchebycheff ellipse as a function of db-ripple (ϵ) and number of stages (n)

ω_h = frequency transformation variable for a high-pass network

ω_o = center-frequency of a band-pass or band-rejection filter, radians/second

ω_∞ = frequency of high attenuation in an m-derived network, radians/second

ω_1 = frequency at which specified transmission loss, A_{db}, is desired

APPENDIX A

DECIBEL CONVERSION TABLE

For positive (+) values of the decibel–both voltage and power ratios are greater than unity–use the two right-hand columns.

For negative (–) values of the decibel–both voltage and power ratios are less than unity–use the two left-hand columns.

Example. Given: ± 9.1 db. Find:

	Power Ratio	Voltage Ratio
+9.1 db	8.128	2.851
–9.1 db	0.1230	0.3508

Voltage Ratio	Power Ratio	← db →	Voltage Ratio	Power Ratio
1.0000	1.0000	0	1.000	1.000
.9886	.9772	.1	1.012	1.023
.9772	.9550	.2	1.023	1.047
.9661	.9333	.3	1.035	1.072
.9550	.9120	.4	1.047	1.096
.9441	.8913	.5	1.059	1.122
.9333	.8710	.6	1.072	1.148
.9226	.8511	.7	1.084	1.175
.9120	.8318	.8	1.096	1.202
.9016	.8128	.9	1.109	1.230
.8913	.7943	1.0	1.122	1.259
.8810	.7762	1.1	1.135	1.288
.8710	.7586	1.2	1.148	1.318
.8610	.7413	1.3	1.161	1.349
.8511	.7244	1.4	1.175	1.380
.8414	.7079	1.5	1.189	1.413
.8318	.6918	1.6	1.202	1.445
.8222	.6761	1.7	1.216	1.479
.8128	.6607	1.8	1.230	1.514
.8035	.6457	1.9	1.245	1.549

Voltage Ratio	Power Ratio	← db →	Voltage Ratio	Power Ratio
.7943	.6310	2.0	1.259	1.585
.7852	.6166	2.1	1.274	1.622
.7762	.6026	2.2	1.288	1.660
.7674	.5888	2.3	1.303	1.698
.7586	.5754	2.4	1.318	1.738
.7499	.5623	2.5	1.334	1.778
.7413	.5495	2.6	1.349	1.820
.7328	.5370	2.7	1.365	1.862
.7244	.5248	2.8	1.380	1.905
.7161	.5129	2.9	1.396	1.950
.7079	.5012	3.0	1.413	1.995
.6998	.4898	3.1	1.429	2.042
.6918	.4786	3.2	1.445	2.089
.6839	.4677	3.3	1.462	2.138
.6761	.4571	3.4	1.479	2.188
.6683	.4467	3.5	1.496	2.239
.6607	.4365	3.6	1.514	2.291
.6531	.4266	3.7	1.531	2.344
.6457	.4169	3.8	1.549	2.399
.6383	.4074	3.9	1.567	2.455
.6310	.3981	4.0	1.585	2.512
.6237	.3890	4.1	1.603	2.570
.6166	.3802	4.2	1.622	2.630
.6095	.3715	4.3	1.641	2.692
.6026	.3631	4.4	1.660	2.754
.5957	.3548	4.5	1.679	2.818
.5888	.3467	4.6	1.698	2.884
.5821	.3388	4.7	1.718	2.951
.5754	.3311	4.8	1.738	3.020
.5689	.3236	4.9	1.758	3.090
.5623	.3162	5.0	1.778	3.162
.5559	.3090	5.1	1.799	3.236
.5495	.3020	5.2	1.820	3.311
.5433	.2951	5.3	1.841	3.388
.5370	.2884	5.4	1.862	3.467
.5309	.2818	5.5	1.884	3.548
.5248	.2754	5.6	1.905	3.631
.5188	.2692	5.7	1.928	3.715
.5129	.2630	5.8	1.950	3.802
.5070	.2570	5.9	1.972	3.890

Voltage Ratio	Power Ratio	←db→	Voltage Ratio	Power Ratio
.5012	.2512	6.0	1.995	3.981
.4955	.2455	6.1	2.018	4.074
.4898	.2399	6.2	2.042	4.169
.4842	.2344	6.3	2.065	4.266
.4786	.2291	6.4	2.089	4.365
.4732	.2239	6.5	2.113	4.467
.4677	.2188	6.6	2.138	4.571
.4624	.2138	6.7	2.163	4.677
.4571	.2089	6.8	2.188	4.786
.4519	.2042	6.9	2.213	4.898
.4467	.1995	7.0	2.239	5.012
.4416	.1950	7.1	2.265	5.129
.4365	.1905	7.2	2.291	5.248
.4315	.1862	7.3	2.317	5.370
.4266	.1820	7.4	2.344	5.495
.4217	.1778	7.5	2.371	5.623
.4169	.1738	7.6	2.399	5.754
.4121	.1698	7.7	2.427	5.888
.4074	.1660	7.8	2.455	6.026
.4027	.1622	7.9	2.483	6.166
.3981	.1585	8.0	2.512	6.310
.3936	.1549	8.1	2.541	6.457
.3890	.1514	8.2	2.570	6.607
.3846	.1479	8.3	2.600	6.761
.3802	.1445	8.4	2.630	6.918
.3758	.1413	8.5	2.661	7.079
.3715	.1380	8.6	2.692	7.244
.3673	.1349	8.7	2.723	7.413
.3631	.1318	8.8	2.754	7.586
.3589	.1288	8.9	2.786	7.762
.3548	.1259	9.0	2.818	7.943
.3508	.1230	9.1	2.851	8.128
.3467	.1202	9.2	2.884	8.318
.3428	.1175	9.3	2.917	8.511
.3388	.1148	9.4	2.951	8.710
.3350	.1122	9.5	2.985	8.913
.3311	.1096	9.6	3.020	9.120
.3273	.1072	9.7	3.055	9.333
.3236	.1047	9.8	3.090	9.550
.3199	.1023	9.9	3.126	9.772

Voltage Ratio	Power Ratio	←db→	Voltage Ratio	Power Ratio
.3162	.1000	10.0	3.162	10.000
.3126	.09772	10.1	3.199	10.23
.3090	.09550	10.2	3.236	10.47
.3055	.09333	10.3	3.273	10.72
.3020	.09120	10.4	3.311	10.96
.2985	.08913	10.5	3.350	11.22
.2951	.08710	10.6	3.388	11.48
.2917	.08511	10.7	3.428	11.75
.2884	.08318	10.8	3.467	12.02
.2851	.08128	10.9	3.508	12.30
.2818	.07943	11.0	3.548	12.59
.2786	.07762	11.1	3.589	12.88
.2754	.07586	11.2	3.631	13.18
.2723	.07413	11.3	3.673	13.49
.2692	.07244	11.4	3.715	13.80
.2661	.07079	11.5	3.758	14.13
.2630	.06918	11.6	3.802	14.45
.2600	.06761	11.7	3.846	14.79
.2570	.06607	11.8	3.890	15.14
.2451	.06457	11.9	3.936	15.49
.2512	.06310	12.0	3.981	15.85
.2483	.06166	12.1	4.027	16.22
.2455	.06026	12.2	4.074	16.60
.2427	.05888	12.3	4.121	16.98
.2399	.05754	12.4	4.169	17.38
.2371	.05623	12.5	4.217	17.78
.2344	.05495	12.6	4.266	18.20
.2317	.05370	12.7	4.315	18.62
.2291	.05248	12.8	4.365	19.05
.2265	.05129	12.9	4.416	19.50
.2239	.05012	13.0	4.467	19.95
.2213	.04898	13.1	4.519	20.42
.2188	.04786	13.2	4.571	20.89
.2163	.04677	13.3	4.624	21.38
.2138	.04571	13.4	4.677	21.88
.2113	.04467	13.5	4.732	22.39
.2089	.04365	13.6	4.786	22.91
.2065	.04266	13.7	4.842	23.44
.2042	.04169	13.8	4.898	23.99
.2018	.04074	13.9	4.955	24.55

Voltage Ratio	Power Ratio	←db→	Voltage Ratio	Power Ratio
.1995	.03981	14.0	5.012	25.12
.1972	.03890	14.1	5.070	25.70
.1950	.03802	14.2	5.129	26.30
.1928	.03715	14.3	5.188	26.92
.1905	.03631	14.4	5.248	27.54
.1884	.03548	14.5	5.309	28.18
.1862	.03467	14.6	5.370	28.84
.1841	.03388	14.7	5.433	29.51
.1820	.03311	14.8	5.495	30.20
.1799	.03236	14.9	5.559	30.90
.1778	.03162	15.0	5.623	31.62
.1758	.03090	15.1	5.689	32.36
.1738	.03020	15.2	5.754	33.11
.1718	.02951	15.3	5.821	33.88
.1698	.02884	15.4	5.888	34.67
.1679	.02818	15.5	5.957	35.48
.1660	.02754	15.6	6.026	36.31
.1641	.02692	15.7	6.095	37.15
.1622	.02630	15.8	6.166	38.02
.1603	.02570	15.9	6.237	38.90
.1585	.02512	16.0	6.310	39.81
.1567	.02455	16.1	6.383	40.74
.1549	.02399	16.2	6.457	41.69
.1531	.02344	16.3	6.531	42.66
		16.4		
.1496	.02239	16.5	6.683	44.67
.1479	.02188	16.6	6.761	45.71
.1462	.02138	16.7	6.839	46.77
.1445	.02089	16.8	6.918	47.86
.1429	.02042	16.9	6.998	48.98
.1413	.01995	17.0	7.097	50.12
.1396	.01950	17.1	7.161	51.29
.1380	.01905	17.2	7.244	52.48
.1365	.01862	17.3	7.328	53.70
.1349	.01820	17.4	7.413	54.95
.1334	.01778	17.5	7.499	56.23
.1318	.01738	17.6	7.586	57.54
.1303	.01698	17.7	7.674	58.88
.1288	.01660	17.8	7.762	60.26
.1274	.01622	17.9	7.852	61.66

Voltage Ratio	Power Ratio	←db→	Voltage Ratio	Power Ratio
.1259	.01585	18.0	7.943	63.10
.1245	.01549	18.1	8.035	64.57
.1230	.01514	18.2	8.128	66.07
.1216	.01479	18.3	8.222	67.61
.1202	.01445	18.4	8.318	69.18
.1189	.01413	18.5	8.414	70.79
.1175	.01380	18.6	8.511	72.44
.1161	.01349	18.7	8.610	74.13
.1148	.01318	18.8	8.710	75.86
.1135	.01288	18.9	8.811	77.62
.1122	.01259	19.0	8.913	79.43
.1109	.01230	19.1	9.016	81.28
.1096	.01202	19.2	9.120	83.18
.1084	.01175	19.3	9.226	85.11
.1072	.01148	19.4	9.333	87.10
.1059	.01122	19.5	9.441	89.13
.1047	.01096	19.6	9.550	91.20
.1035	.01072	19.7	9.661	93.33
.1023	.01047	19.8	9.772	95.50
.1012	.01023	19.9	9.886	97.72
.1000	.01000	20.0	10.000	100.00

APPENDIX B

LISTED SOURCES OF FILTER MANUFACTURERS

Filter Classifications

Type	Description
A	A-F
B	Automotive Noise Suppression
C	Antenna
D	Filters, Band Elimination
E	Filters, Band-Pass
F	Coaxial
G	High Pass
H	I-F
I	Interference
J	Line
K	Low Pass
L	Microwave
M	R-F
N	Single Sideband
O	UHF & VHF
P	Video
Q	Waveguide

Company Address	Filter Types
AC Electronics, Inc. 11725 Mississippi Ave. Los Angeles, Calif.	A, C, D, E, G, H, K, M
Adams-Russell Co., Inc. 200 6th St. Cambridge, Mass.	C, D, E, F, G, L, M, O, Q
ADC Products, Magnetic Controls Div. 6409 Cambridge St. Minneapolis, Minn.	A, D, E, G, H, J, K, M, N

Appendix B

Company Address	Filter Types
Ad-Yu Electronics Lab., Inc. 249 Terhune Ave. Passaic, N. J.	A, D, E, K
Airpax Electronics, Inc., Seminole Div. Box 8488 Ft. Lauderdale, Fla.	A, D, E, G, K
Airtron, Litton Industries Div. 200 E. Hanover Ave. Morris Plains, N. J.	C, D, E, G, K, L
Allison Laboratories, Inc. 11301 E. Ocean Ave. Lahabra, Calif.	A, D
American Electronics, Co. 178 Herricks Rd. Mineola, N. Y.	A, D, F, G, K
American Electronic Labs., Inc. Richardson Rd. Colmar, Pa.	D, E, G, K, L, Q
AMP, Inc., Capitron Div. 155 Park St. Elizabethtown, Pa.	A, D, E, G, I, J, K, M
Antenna Systems, Inc. Hingham, Mass.	C, D, E, K, L, M, O, Q
Applied Microwave Electronics, Inc. 6707 Whitestone Rd. Baltimore, Md.	C, D, E, F, G, K, L, M, O, Q
Applied Microwave Laboratory, Inc. 106 Abion St. Wakefield, Mass.	D, E, F, G, L
Applied Research, Inc. 76 South Bayles Ave. Port Washington, N. Y.	D, E, F, H, K, L, O
Ark Electronics Corp. 624 Davisville Rd. Willow Grove, Pa.	A, C, D, E, F, G, I, J, L, M, O

Company Address	Filter Types
ARRA Inc., Antenna & Radome Research Assoc. 27 Bond St. Westbury, N.Y.	D, E, F, G, K, L
Astron Corp. 255 Grant Ave. East Newark, N.J.	D, E, I, J, K, M
Barker & Williamson Bristol, Pa.	A, C, D, E, F, G, H, K, M, N, O
B&K Instruments, Inc. of Bruel & Kjaer 3024 W. 106th St. Cleveland, Ohio	D, E
Budelman Electronics Corp. 375 Fairfield Ave. Stanford, Conn.	D, E, G, K, L, M, O
Bulova Watch Co., Inc., Electronics Div. 61-10 Woodside Ave. Woodside, N.Y.	D, G, H, K, N
Bundy Electronics Corp. 171 Fabyan Pl. Newark, N.J.	D, E, G, K
Burnell & Co., Inc. 10 Pelham Pkwy. Pelham Manor, N.Y.	A, C, D, G, H, I, K, N
Carad Corp. Stanpard Industrial Pk. Palo Alto, Calif.	A, D, E, G
California Magnetic Control Co. 11922 Valerio St. North Hollywood, Calif.	D, O
Canadian Marconi Co. 2442 Trenton Ave. Montreal, Que, Canada	A, D, E, G, H, M, O
Centralized Data Control, Inc. 23 Skillman St. Roslyn, N.Y.	A, D, E

Appendix B

Company Address	Filter Types
C.E.S. Electronic Products, Inc. 5026 Newport Ave. San Diego, Calif.	A, D
Columbia Technical Corp. 24-30 Brooklyn-Queens Expwy. W. Woodside, N.Y.	D, K
Components Corp. 2857 N. Halsted St. Chicago, Ill.	D, E, G, K
Consolidated Microwave Corp. 850 Shepherd Ave. Brooklyn, N.Y.	D, G, K, L, M
Cornell-Dubilier 50 Paris St. Newark, N.J.	B, D, F, G, I, J, M, O
Daltronics, Inc. 100 Manton Ave. Providence, R.I.	D, E, G
Damon Engineering, Inc. 240 Highland Ave. Needham Hgts., Mass.	D, E, N
Datafilter Corp. 5921 Noble Ave. Van Nuys, Calif.	D, E, K
Decoursey Engrg. Lab. 11828 W. Jefferson Blvd. Culver City, Calif.	D, E, K, N
Dielectric Products Engrg. Co., Inc. Raymond, Maine	D, F, O
Dietz Design, Inc. Grandview, Mo.	A, D, F, G, H, I, K, M, N
Dorne & Margolin, Inc. 29 New York Ave. Westbury, N.Y.	C, D, G, K

Company Address	Filter Types
Double E. Products Co. 208 Standard St. El Segundo, Calif.	D, E, G, I, J, K, M
Drake, R. L. Co. 540 Richard St. Miamisburg, Ohio	C, D, E, G, H, I, K, O
Dytronics Co. 5485 N. High St. Columbus, Ohio	A, D, E, G, K
Electro Assemblies 4444 N. Kedzie Ave. Chicago, Ill.	C, D, G, H, I, J, K, M
Electrocon Industries 1105 N. Ironwood Dr. South Bend, Ind.	D, I
Electromagnetic Technology Corp. 1375 California Ave. Palo Alto, Calif.	D, E, F, I
Electronetics P. O. Box 862 Melborne, Fla.	A, D, E, G, H, K, N
Electronic Speciality Co. 5121 San Fernando Rd. Los Angeles, Calif.	A, D, E, F, H, K, L, M
Empire Devices, Inc. 37 Prospect St. Amsterdam, N. Y.	D, E, F, L, O
Erie Resistor Corp. 644 West 12th St. Erie, Pa.	D, I, K, M, O
Filtech Corp. 629 W. Washington Blvd. Chicago, Ill.	D, E, G, H, K, N
Forbes & Wagner, Inc. 345 Central Ave. Silver Creek, N. Y.	A, D, E, G, K, N

Appendix B

Company Address	Filter Types
Freed Transformer Co. 1795 Weirfield St. Brooklyn, Ridgewood, N.Y.	A, D, E, G, K
Frequency Engineering Labs. P.O. Box 504 Asbury Park, N.J.	C, D, E, F, K, L, Q
Fugle-Miller Labs., Inc. Central Ave. Clark, N.J.	A, C, D, E, G, H, I, K, M
FXR Div., Amphenol-Borg Electronics 33 E. Franklin Danbury, Conn.	D, L
General Electronic Labs., Inc. 18 Ames St. Cambridge, Mass.	C, D, E, H, L, M, N
General Magnetics, Inc. 2641 Louisiana Ave. Minneapolis, Minn.	A, C, D, E, G, K
General Microwave Corp. 155 Maine St. Farmingdale, N.Y.	D, E, F, G, K, L, M, O, Q
General Radio Company 22 Baker Ave. W. Concord, Mass.	A, D, E, F, G, K, M, O
Genistron, Inc. 2301 Federal Ave. Los Angeles, Calif.	B, D, E, G, I, K, M
Geotronic Labs., Inc. 1314 Cedar Hill Ave. Dallas, Tex.	A, D, E, G, J, K
Gombos Microwave, Inc. 48 Webro Rd. Clifton, N.J.	D, E, F, L
Hill Electronics, Inc. 300 N. Chestnut St. Mechanicsburg, Pa.	A, D, E, G, H, K, M, N

Company Address	Filter Types
Hisonic, Inc. Box 534 Shawnee, Kansas	A, D, E, G, H, J, K, M, N
Hy-Gain Antenna Products Corp. 1135 North 22nd St. Lincoln, Nebr.	C, D, E, F
Inductor Engrg., Inc. 117 Schley Ave. Lewes, Del.	D, E, G, K
Industrial Control Products, Inc. Caldwell Township, N. J.	D, E, G, K
Industrial Transformer Corp. Gouldsboro, Pa.	D, I, K
Kapitol Magnetic Corp. 2241 N. Knox Chicago, Ill.	D, E, G, K
Kenyon Transformer Co., Inc. 1057 Summit Ave. Jersey City, N. J.	A, D, E, G, K, O
Knights, James K., Co. 101 East Church St. Sandwich, Ill.	D, E, N
Krohn-Hite Corp. 500 Massachusetts Ave. Cambridge, Mass.	A, D, E, G, K
Leach Corp. 18435 Susana Rd. Compton, Calif.	C, D, E, G, H, I, K, M, O
Lockheed Aircraft Corp. P.O. Box 551 Burbank, Calif.	C, D, I, L, N, P, Q
Loral Electronics Corp. 825 Bronx River Ave. New York, N.Y.	D, L

Appendix B

Company Address	Filter Types
Lynch Communication Systems, Inc. 695 Bryant St. San Francisco, Calif.	D, E, G, K, N
Magnetic Systems Corp. 1897 U. S. #19 South Clearwater, Fla.	A, D, E, G, I, K
Magnetic Systems, Inc. 225 W. Duarte Rd. Monrovia, Calif.	A, D, E, G, I, K, M, N
Maury & Associates 10373 Mills Ave. Montclair, Calif.	D, E, F, G, K, L, M, Q
Meridian Metalcraft, Inc. 8739 S. Millergrove Dr. Whittier, Calif.	D, C, D, E, F, G, K, L
Metropolitan Telecommunications, Inc. Coil Winders Div. Ames Ct. Plainview, N. Y.	A, D, G, H, I, K, M
Microphase Corp. P. O. Box 1166 Greenwich, Conn.	C, D, E, F, G, H, M, O, Q
Microwave Technology, Inc. 235 High St. Waltham, Mass.	D, E, F, G, H, L, M, O, Q
Miller, J. W., Co. 5917 S. Main St. Los Angeles, Calif.	C, D, E, G, H, I, J, K, M
Narda Microwave Corp. Plainview, N. Y.	A, D, E, G, Q
Newton Co. 55 Elm St. Manchester, Conn.	D
North Hills Electronics, Inc. Alexander Pl. Glen Cove, N. Y.	A, D, E, G, H, I, J, K, M, N

Company Address	Filter Types
Ortho Industries, Inc. 7 Paterson St. Paterson, N. J.	D, E, G, K
Pacific Instrument Co. 4926 E. 12th St. Oakland, Calif.	A, D, E, G, K
Philco Corp., Government & Indl. Group 4700 Wissachickon Ave. Philadelphia, Pa.	D, E, H
Phoenix Transformer Co. 1818 Madison Phoenix, Ariz.	A, D, E, G, K
Polyphase Instrument Co. E. Fourth St. Bridgeport, Pa.	D, E, G, J, K
Pulse Engineering, Inc. 560 Robert Ave. Santa Clara, Calif.	A, E, G, K, M
Radio Engineering Laboratories, Inc. 29-01 Borden Ave. L.I.C., N.Y.	D, E
Railway Communications 9351 E. 59th St. Raytown, Mo.	D, G, J, K
Rantec Corp. Craftsman Center Calabases, Calif.	C, D, F, G, K, L, M, N, O, Q
Reed & Reese, Inc. 717 N. Lake Ave. Pasadena, Calif.	D, G, H, I, K
Relcoil Products Corp., Div. HIG. Inc., Dept 500 Rt. 75 and Spring St. Windsor Locks, Conn.	D, E, H, K
RHG Electronics Lab., Inc. 94 Milbar Blvd. Farmingdale, N.Y.	C, D, E, H, M

Appendix B

Company Address	Filter Types
Rixon Electronics, Inc. 2121 Industrial Pkwy. Silver Spring, Md.	A, D, E, F, K, M
Roberts, R.O., Co. Inc. 8338 S. Allport Ave. Santa Fe Springs, Calif.	A, C, D, E, L, Q
Rytron Co., Inc. 7305 Lankershim Blvd. N. Hollywood, Calif.	A, D, E, G, K
Sangamo Electric Electronic Products 1207 N. 11th Springfield, Ill.	A, D, E, G, I, J, K
Sartron Inc. 114 N. Main St. Newberg, Oreg.	D, G
Seg. Electronics Co., Inc. 12 Hillside St. Brooklyn, N.Y.	D, E, G, H, I, J, K, M, N, P
Serco Electronics Research Corp. 15735 Ambaum Blvd. Seattle, Wash.	C, D, E, F, G, L, Q
Sinclair Radio Laboratories, Ltd. P.O. Box 179 Downsview, Ont., Canada	C, D, E, F, G, K, L, M, O, Q
SkyBorne Electronics, Inc. 9841 Alburtis Ave. Sante Fe Springs, Calif.	A, C, D, E, G, H, I, K, M, N, O
Sparton Corp., Electronics Div. 2400 E. Ganson St. Jackson, Mich.	A, D, E, G, O
Spectran Electronics Corp. 146 Main St. Maynard, Mass.	D
Spectrum Instruments, Inc. Box 61 Steinway Station, L.I.C., N.Y.	D, E, K

Company Address	Filter Types
Sprague Electric Co. 481 Marshall St. N. Adams, Mass.	A, D, E, G, I, J, K, M
Systems, Inc. 2400 Diversified Way P. O. Box 7726 Orlando, Fla.	D, E, G, H, K, N, Q
Systems Research Labs., Fairborn Div. 500 Woods Dr. Dayton, Ohio	D, G, K, N
Telerad Div. Lionel Corp.	C, D, F, L, Q
Telex/Ballastran, Div., Telex 1701 North Calhoun Ft. Wayne, Ind.	A, D, E, G, I, J, K
Telex, Inc. Telex Park, Dept 1030 St. Paul, Minn.	A, D, E, G, I, J, K
Telex/Lumen P. O. Box 905 Joliet, Ill.	D, E, I, J, K
Thomson-Ramo-Wooldridge, Microwave Div. 8433 Fallbrook Canoga Park, Calif.	C, D, F, G, K, L, M, O, Q
Torotel, Inc. 5512 East 110th St. Kansas City, Mo.	D, E, G, J, K
Toroton Corp. 256 E. Third St. Mt. Vernon, N. Y.	A, D, E, G, H, K
Trak Microwave Corporation 5006 N. Coolidge Ave. Tampa, Fla.	D, E, G, L
Transformer Design, Inc. of Milwaukee 7377 N. 76 St. Milwaukee, Wisc.	A, D, E, G, H, K

Appendix B

Company Address	Filter Types
Transformers, Inc. 200 Stage Rd. Vestal, N. Y.	A, D, G, J, K
Transonic, Inc. P. O. Box 59 Bakersfield, Calif.	A, D, E, G, H, J K, N
T. T. Electronics, Inc. P. O. Box 180 Culver City, Calif.	D, E, G, I, J, K, N, P
United Transformer Corp. 150 Varick St. New York, N. Y.	A, D, E, G, H, I, J, K, M
United Transformer Corp., Pacific Div. 3630 Eastham Dr. Culver City, Calif.	A, D, E, H, I, J, K
Vanguard Electronics Co. 3384 Motor Ave. Los Angeles, Calif.	D, E, G, H, K, M
Wahlgren Magnetics 1900 Walker Ave. Monrovia, Calif.	D, I
Waveguide Inc. 851 West 18th St. Costa Mesa, Calif.	D, E, G, K, Q
Waveline, Inc. Box 718, W. Caldwell, N. J.	C, D, E, F, L, Q
Wells Electronics, Inc. 1702 South Main St. South Bend, Ind.	B, D, E, G, H, I, K, M, N
White Electromagnetics, Inc. 670 Lofstrand Lane Rockville, Md.	A, C, D, E, G, H, I, K, M, P
White Instrument Labs. Box 9006 Austin, Tex.	D, E, G, K

Company Address	Filter Types
Whitewater Electronics, Inc. 136 West Main St. Whitewater, Wisc.	C, D, E, G, H, I, K, M, N, O, P
Wilcox Magnetics 2800 East 14th St. Kansas City, Mo.	D, E, G, H, I, K, N

INDEX

C

D

E

F

H

I

K

L

M

N

P

Q

R

S

T

U

V

ERRATA

The following corrections should be made to your copy of "A Handbook on Electrical Filters--Synthesis, Design, and Applications," first edition 1963, by the Staff of WEI:

1. Page 80 and 81 - Table 4.3; Diagram (c) only:

   Change R_1 from $R_1 < 0.1\Omega$ to $R_1 > 10\Omega$

2. Pages 125 to 130 - Tables 4.11 to 4.16; Diagram (c) only:

   Change R_1 from $R_1 < 0.1\Omega$ to $R_1 > 10\Omega$

3. Page 149 under "Illustrative Example 5.1":

   Change the word "bandpass" to "high-pass."

4. Page 117 - Fig. 4.39, Re Capacitors:

   5450μμf should read 54.5 pf
   8100μμf should read 81 pf

5. Page 117 - Fig. 4.40, Re Capacitors:

   3920μμf should read 39.2 pf

6. Page 150 and 151 - all inductance values (including Figs. 5.1 and 5.2) are low by a factor of ten, viz:

   6.75μh should be 67.5μh
   4.94μh should be 49.4μh
   18.4μh should be 184μh

7. Page 156 -

   Change first part of equation $C_3^1 = \frac{C_3}{2\pi R F_o}$ to read

   $C_3^1 = \frac{C_3}{2\pi R F_c}$

8. Page 183 - mid-way on page, first sentence should read:

   "From Fig. 4.37 the intersection of $\overline{w_{br}} = 4.0$ and $A_{db} = 50$ db yields $N = 3.1$."